Hydrodynamics in Solid State Systems and the AdS/CFT correspondence

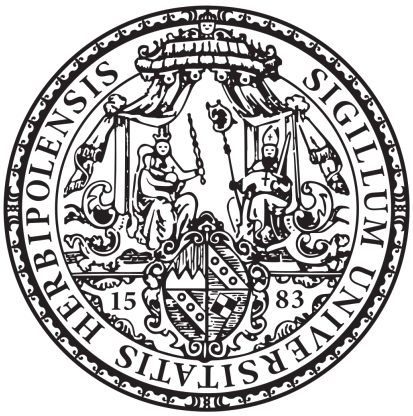

Dissertation zur Erlangung des
naturwissenschaftlichen Doktorgrades
der Julius-Maximilians-Universität Würzburg

vorgelegt von

Ioannis Matthaiakakis

aus Rethymno, Griechenland

Würzburg, 2021

Eingereicht am: 21.06.2021
bei der Fakultät für Physik und Astronomie

1. Gutachter: Prof. Dr. Erdmenger
2. Gutachter: Prof. Dr. Thomale
3. Gutachter: .....
der Dissertation

Vorsitzende(r): Prof. Dr. Höfling

1. Prüfer: Prof. Dr. Erdmenger
2. Prüfer: Prof. Dr. Thomale
3. Prüfer: Prof. Dr. Buhmann
im Promotionskolloquiums

Tag des Promotionskolloquiums: 31.08.2021

Doktorurkunde ausgehändigt am: .....

Abstract

We employ the AdS/CFT correspondence and hydrodynamics to analyze the transport properties of $2+1$ dimensional electron fluids. In this way, we use theoretical methods from both condensed matter and high-energy physics to derive tangible predictions that are directly verifiable in experiment.

The first research topic we consider is strongly-coupled electron fluids. Motivated by early results by Gurzhi on the transport properties of weakly coupled fluids, we consider whether similar properties are manifest in strongly coupled fluids. More specifically, we focus on the hydrodynamic tail of the *Gurzhi effect*: A decrease in fluid resistance with increasing temperature due to the formation of a Poiseuille flow of electrons in the sample. We show that the hydrodynamic tail of the Gurzhi effect is also realized in strongly coupled and fully relativistic fluids, but with modified quantitative features. Namely, strongly-coupled fluids always exhibit a smaller resistance than weakly coupled ones and are, thus, far more efficient conductors. We also suggest that the coupling dependence of the resistance can be used to measure the coupling strength of the fluid. In view of these measurements, we provide analytical results for the resistance as a function of the shear viscosity over entropy density η/s of the fluid. η/s is itself a known function of the coupling strength in the weak and infinite coupling limits.

In further analysis for strongly-coupled fluids, we propose a novel strongly coupled Dirac material based on a kagome lattice, Scandium-substituted Herbertsmithite (ScHb). The large coupling strength of this material, as well as its Dirac nature, provides us with theoretical and experimental access to non-perturbative relativistic and quantum critical physics. A highly suitable method for analyzing such a material's transport properties is the AdS/CFT correspondence. Concretely, using AdS/CFT we derive an estimate for ScHb's η/s and show that it takes a value much smaller than that observed in weakly coupled materials. In turn, the smallness of η/s implies that ScHb's Reynolds number, Re, is large. In fact, Re is large enough for *turbulence*, the most prevalent feature of fluids in nature, to make its appearance for the first time in electronic fluids.

Switching gears, we proceed to the second research topic considered in this thesis: Weakly coupled parity-breaking electron fluids. More precisely, we analyze the quantitative and qualitative changes to the classical Hall effect, for electrons propagating hydrodynamically in a lead. Apart from the Lorentz force, a parity-breaking fluid's motion is also impacted by the Hall-viscous force; the shear-stress force induced by the Hall-viscosity. We show that the interplay of these two forces leads to a hydrodynamic Hall voltage with *non-linear* dependence on the magnetic field. More importantly, the Lorentz and Hall-viscous forces become equal at a non-vanishing magnetic field, leading to a trivial hydrodynamic Hall voltage. Moreover, for small

magnetic fields we provide analytic results for the dependence of the hydrodynamic Hall voltage on all experimentally-tuned parameters of our simulations, such as temperature and density. These dependences, along with the zero of the hydrodynamic Hall voltage, are distinct features of hydrodynamic transport and can be used to verify our predictions in experiments.

Last but not least, we consider how a distinctly electronic property, spin, can be included into the hydrodynamic framework. In particular, we construct an effective action for non-dissipative spin hydrodynamics up to first order in a suitably defined derivative expansion. We also show that interesting spin-transport effects appear at second order in the derivative expansion. Namely, we show that the fluid's rotation polarizes its spin. This is the hydrodynamic manifestation of the Barnett effect and provides us with an example of hydrodynamic spintronics.

To conclude this thesis, we discuss several possible extensions of our research, as well as proposals for research in related directions.

All original research presented in this thesis is based on my publications

[1] J. Erdmenger, I. Matthaiakakis, R. Meyer, and D. Rodríguez Fernández, "Strongly coupled electron fluids in the Poiseuille regime," *Phys. Rev. B*, vol. 98, no. 19, p. 195143, 2018, discussed in chapter 4,

[2] D. Di Sante, J. Erdmenger, M. Greiter, I. Matthaiakakis, R. Meyer, D. Rodríguez Fernández, R. Thomale, E. van Loon, and T. Wehling, "Turbulent hydrodynamics in strongly correlated Kagome metals," *Nature Commun.*, vol. 11, no. 1, p. 3997, 2020, discussed in chapter 5,

[3] I. Matthaiakakis, D. Rodríguez Fernández, C. Tutschku, E. M. Hankiewicz, J. Erdmenger, and R. Meyer, "Functional dependence of Hall viscosity induced transverse voltage in two-dimensional Fermi liquids," *Phys. Rev. B*, vol. 101, no. 4, p. 045423, 2020, discussed in chapter 6,

as well as unpublished research presented in chapter 7.

Zusammenfassung

The author is grateful to Bastian Heß for assisting with the German translation of the abstract.

Wir verwenden die AdS/CFT-Korrespondenz und die Theorie der Hydrodynamik, um die Transporteigenschaften von $2+1$-dimensionalen Elektronisches Flüssigkeiten zu untersuchen. Somit nutzen wir sowohl theoretische Methoden der Festkörperphysik als auch der Hochenergiephysik, um konkrete Vorhersagen zu treffen, die unmittelbar in Experimenten verifiziert werden können.

Zunächst betrachten wir das Forschungsfeld der stark gekoppelten Elektronischen Flüssigkeiten. Motiviert durch die frühen Ergebnisse für die Transporteigenschaften schwach gekoppelter Flüssigkeiten von Gurzhi untersuchen wir, ob sich ähnliche Eigenschaften auch in stark gekoppelten Flüssigkeiten manifestieren. Dabei konzentrieren wir uns insbesondere auf den hydrodynamischen Teil des *Gurzhi-Effekts*, in welchem der Widerstand der Flüssigkeit mit steigender Temperatur sinkt, weil sich im untersuchten Material ein Poiseuillefluss von Elektronen bildet. Wir zeigen, dass dieser hydrodynamische Teil des Gurzhi-Effekts auch in stark gekoppelten und vollständig relativistischen Flüssigkeiten realisiert ist, einige Eigenschaften sich hierbei aber quantitativ unterscheiden. Insbesondere zeigen stark gekoppelte Flüssigkeiten immer kleinere Widerstände als schwach gekoppelte, und sind damit wesentlich effektivere Leiter. Wir schlagen darüber hinaus vor, die Abhängigkeit des Widerstands von der Kopplung zu nutzen, um die Kopplungsstärke der Flüssigkeit zu messen. Für diese Messungen stellen wir analytische Ergebnisse bereit, welche den Widerstand als Funktion des Quotienten aus Scherviskosität und Entropiedichte η/s der Flüssigkeit ausdrücken. Dabei ist η/s selbst eine bekannte Funktion der Kopplungsstärke in den Grenzfällen schwacher und unendlich starker Kopplung.

In einer weiteren Untersuchung stark gekoppelter Flüssigkeiten schlagen wir Scandium-substituiertes Herbertsmithit (ScHb) als neuartiges, stark gekoppeltes Diracmaterial vor, welches auf dem Kagome-Gitter basiert. Die hohe Kopplungsstärke und die Dirac-Eigenschaften dieses Materials vermitteln uns theoretischen und experimentellen Zugang zu nicht perturbativer relativistischer und quantenkritischer Physik. Um die Transporteigenschaften eines solchen Materials zu untersuchen, stellt die AdS/CFT-Korrespondenz eine hervorragend geeignete Methode dar. Konkret nutzen wir AdS/CFT, um eine Abschätzung von η/s in ScHb herzuleiten. Der so ermittelte Wert ist wesentlich kleiner als der entsprechende Messwert für schwach gekoppelte Materialien. Der kleine Wert von η/s wiederum impliziert, dass die Reynolds-Zahl Re in ScHb groß ist. Tatsächlich ist Re hinreichend groß, um

erstmals *Turbulenz* in Elektronisches Flüssigkeiten beobachten zu können, ein Effekt, der auch in viele anderen Flüssigkeiten in der Natur vorkommt.

Wir gehen zum zweiten Forschungsthema über, welches in der vorliegenden Arbeit besprochen wird: schwach gekoppelte, paritätsbrechende Elektronisches Flüssigkeiten. Wir betracthen die hydrodynamische Bewegung von Elektronen in einen zwei dimensionalen Kanal, und untersuchen die sich ergebenden quantitativen und qualitativen Änderungen gegenüber dem klassischen Hall-Effekt. Außer der Lorentzkraft ist die Bewegung einer paritätsbrechenden Flüss auch den Einflüssen der Hallviskositätskraft ausgesetzt, welche die von der Hall Viskosität induzierte Scherspannungskraft ist. Wir zeigen, dass das Wechselspiel dieser beiden Kräfte zu einer hydrodynamischen Hall-Spannung führt, die *nicht linear* vom magnetischen Feld abhängt. Noch wichtiger ist, dass Lorentz- sowie hallviskose Kraft für ein nicht verschwindendes Magnetfeld gleich werden und damit zu einer trivialen hydrodynamischen Hall-Spannung führen. Darüber hinaus geben wir für kleine Magnetfeldstärken analytische Ergebnisse an, die die Abhängigkeit der hydrodynamischen Hall-Spannung von allen experimentell festgelegten Parametern unserer Simulation, wie z.B. Temperatur und Dichte, beschreiben. Diese Abhängigkeiten sind zusammen mit der verschwindenden hydrodynamischen Hall-Spannung charakteristische Eigenschaften hydrodynamischen Transports und können daher verwendet werden, um unsere Vorhersagen experimentell zu verifizieren.

Zu guter Letzt untersuchen wir, wie eine charakteristische Eigenschaft von Elektronen, der Spin, in die hydrodynamische Theorie einbezogen werden kann. Dazu konstruieren wir eine effektive Wirkung, die nicht dissipative Spin-Hydrodynamik bis zur ersten Ordnung in einer geeigneten Ableitungsentwicklung beschreibt. Wir zeigen darüber hinaus, dass in zweiter Ordnung dieser Entwicklung interessante Spin-Transporteffekte auftreten. Dabei stellt sich heraus, dass die Rotation der Flüssigkeit seinen Spin polarisiert. Dies ist die hydrodynamische Manifestation des Barnett-Effekts, die als Beispiel für hydrodynamische Spintronics dient.

Zum Abschluss der vorliegenden Arbeit diskutieren wir mehrere mögliche Erweiterungen unserer Untersuchungen und unterbreiten Vorschläge für weitergehende Forschung in verschiedene Richtungen.

Sämtliche Forschung, die in der vorliegenden Arbeit behandelt wird, basiert auf meinen Veröffentlichungen

> [1] J. Erdmenger, I. Matthaiakakis, R. Meyer, und D. Rodríguez Fernández, "Strongly coupled electron fluids in the Poiseuille regime," *Phys. Rev. B*, vol. 98, no. 19, p. 195143, 2018, besprochen in Kapitel 4,
>
> [2] D. Di Sante, J. Erdmenger, M. Greiter, I. Matthaiakakis, R. Meyer, D. Rodríguez Fernández, R. Thomale, E. van Loon, und T. Weh-

ling, "Turbulent hydrodynamics in strongly correlated Kagome metals," *Nature Commun.*, vol. 11, no. 1, p. 3997, 2020, besprochen in Kapitel 5,

[3] I. Matthaiakakis, D. Rodríguez Fernández, C. Tutschku, E. M. Hankiewicz, J. Erdmenger, und R. Meyer, "Functional dependence of Hall viscosity induced transverse voltage in two-dimensional Fermi liquids," *Phys. Rev. B*, vol. 101, no. 4, p. 045423, 2020, besprochen in Kapitel 6,

sowie unveröffentlichter Forschungsarbeit, die in Kapitel 7 besprochen wird.

Contents

List of Figures

Chapter 1

Introduction

Water is evidently one of the most important fluids in the history of humanity. As a result, much interest has been directed towards understanding water's properties and behaviour. The first surviving written account of a theoretical exploration of water's mechanical properties comes to us from ancient Greece and Archimedes around 250 BC. Archimedes, with his law of buoyancy, inaugurated the field of research known as hydrostatics (hydro meaning water in ancient greek). Despite this relatively early formulation of the principles of hydrostatics, the dynamics of water and other fluids remained elusive until the 18th century [4][1]. This changed when Euler, among others, formulated his equations of hydrodynamics for a perfect and incompressible fluid moving in three-dimensional space [5]

$$\rho \frac{D\vec{v}}{dt} = -\nabla P + \vec{F} \quad , \quad \frac{D\rho}{dt} = 0 \ . \tag{1.1}$$

In Eq. (1.1), $\vec{v}$ is the fluid's velocity, P the internal pressure of a fluid with mass density ρ and $\vec{F}$ stands for any external force density acting on the fluid, e.g. due to gravity. The derivative acting on $\vec{v}$ and ρ is the material derivative, which describes their rate of change along the flow. It is defined as

$$\frac{D}{dt} = \partial_t + (\vec{v} \cdot \nabla) \ . \tag{1.2}$$

Despite Euler's success, solutions to his equations failed to describe the results of experiments. This discrepancy between theory and experiment can be summarized in D'Alembert's paradox [4]: An object moving within a perfect fluid feels no net drag force. To resolve this issue, Navier and independently Stokes introduced the concept of internal fluid friction, that

The style for the chapter headings used in this thesis is a modification of one of the styles found in Vincent Zoonekynd's latex website here.

[1] Note that this did not slow down engineers, who developed their own empirical rules for understanding the behaviour of fluids [4].

is friction between the molecules comprising the fluid. The strength of this internal friction is characterized by a so-called transport coefficient, the shear viscosity η. With the inclusion of η into hydrodynamics, the Euler equations gave their place to the Navier-Stokes equations

$$\rho \frac{D\vec{v}}{dt} = -\nabla P + \eta \nabla^2 \vec{v} + \vec{F} \quad , \quad \frac{D\rho}{dt} = 0 \; . \tag{1.3}$$

Mathematically, η changes the order of the hydrodynamic equations from first to second, allowing the fluid's momentum to diffuse. Through diffusion D'Alembert's paradox was resolved and the gap between theory and experiment was finally bridged. The importance of adding the viscosity term to the equations of hydrodynamics cannot be overstated: According to Lord Kelvin, "hydrodynamics is to be the root of all physical science, and is at present second to none in the beauty of its mathematics." [4]. An example of this importance is given by Maxwell's introduction of the concept of the electromagnetic field based on an analogy to hydrodynamics [6].

In recent years, additional transport coefficients analogous to η, have been argued to play an important role in the equations of hydrodynamics [7–9]. Then the following question naturally arises: If a single transport coefficient, η, alters dramatically the behaviour of a fluid, what drastic changes should we expect when additional transport coefficients are included? The purpose of this thesis is to identify some of these effects on the transport of fluids in $2+1$ space+time dimensions, and connect them to directly observable properties of solid state systems. At first glance, this statement seems self-contradictory; how can a solid behave hydrodynamically? Historically, the resolution of this contradiction is already hidden in the derivation of the equations of hydrodynamics by Navier and Stokes [4]. However, we choose to resolve this paradox below by employing a modern re-conceptualization of hydrodynamics, based on the advent of effective field theories (EFTs) in the 20th century (cf. [10] for a recent historical overview of EFTs).

Hydrodynamics as an EFT

We consider hydrodynamics to be an effective description of thermalized matter at length and time scales far larger than any microscopic length or time scale present in the system of interest[2]. Because of this hierarchy of scales, hydrodynamics should not be thought of as a theory for fluid transport, but rather as a framework for transport. The difference between framework and theory is that hydrodynamics provides the "scaffolding" for describing transport, in the same way that quantum field theory (QFT)

[2]Examples of these length scales are the eigenfrequencies of particle excitations in the system or particle-particle scattering times.

allows us to describe the dynamics of relativistic fields. Unlike QFT, hydrodynamics can give tangible predictions only through the use of additional information about the thermalized microscopic theory of interest. This can be seen more clearly by noting that the equations of motion of hydrodynamics (hEOM) can not be derived from microscopic information about the system, since we are considering length and time scales at which any transient microscopic effects become irrelevant for transport. Instead the hEOM use the only remaining information we have about the system, the conservation or quasi-conservation laws obeyed by the microscopic theory in thermal equilibrium. These conservation laws, according to Noether's theorem [11], take the same form for any system with the same underlying continuous symmetries. Hence the only way to differentiate between these systems is to include by hand some additional microscopic information into the hEOM.

It is exactly this generic framework nature of hydrodynamics that makes it so useful: The assumption of thermal equilibrium allows us to resolve the conserved charges of the system in terms of their conjugate thermodynamic variables. For example, a neutral fluid conserves energy and momentum. We can express these charges in terms of their conjugate variables, which are the temperature T and the velocity profile $\vec{v}$. The resulting expressions are the system's constitutive relations and take the same form for all systems with the same (discrete and continuous) symmetries, regardless if the system is macroscopically a solid or a fluid. Crucially though, the constitutive relations can be specified completely up to a few numerical coefficients, the transport coefficients. These transport coefficients are precisely the point where microscopic information about the system enters the hydrodynamic framework. This microscopic information is what allows us to differentiate between a solid and a typical fluid behaving hydrodynamically.

Our general discussion on hydrodynamics shows the practical usefulness of hydrodynamics in analyzing the transport properties of many systems. However, despite hydrodynamics being around for a few hundred years [5, 12], it was first applied to the problem of electronic transport in the 1960s [13, 14]. The most important reason for this time-gap is the following: It is difficult to achieve the conditions for electron hydrodynamics in condensed matter systems. The applicability of hydrodynamics depends on a microscopic length scale $\mathcal{K}$; hydrodynamics is a valid approximation only if $\mathcal{K}$ is much smaller than any other length scale relevant to the system of interest[3]. When it comes to electron hydrodynamics, $\mathcal{K}$ can be identified with the electron-electron mean free path l_{ee}. A "small" l_{ee} allows electrons to interact and achieve local thermodynamic equilibrium among themselves, enabling a hydrodynamic approach at low energies. The particular length scales l_{ee} has to compete against in a metal are the electron-phonon scat-

[3]Note that this is a necessary but not sufficient condition. For example, the physics of the quantum Hall effect can be described by a modification of the Euler equations [15].

tering length l_{ph}, the electron-impurity scattering length l_{imp} and any other geometric scale in the system, call it W. Hence, electron hydrodynamics is a valid description for an electronic system in local equilibrium when

$$l_{\text{ee}} \ll l_{\text{ph}},\ l_{\text{imp}}, W, \dots \ . \tag{1.4}$$

Typically, the scattering scales depend on temperature and, hence, condition (1.4) carves out a range of temperatures where electron hydrodynamics is a valid approximation [13]. To avoid phonon contributions, one usually freezes out the lattice vibrations by putting the system at a sufficiently low enough temperature[4]. Then, assuming W has been chosen appropriately, the only remaining obstacle to electron hydrodynamics is the impurity content of the system. The first instances of clean enough materials which satisfy Eq. (1.4) were made and examined both theoretically and experimentally nearly thirty years ago by Molenkamp and de Jong [16, 17][5]. This was a remarkable achievement for the field of electron hydrodynamics, especially if one notes that the second observation of electron hydrodynamics was made in 2016 [19]. Additional materials and direct observations of the electron flow followed suit shortly thereafter [20–23], thus establishing electron hydrodynamics as a fully fledged field of study.

Hydrodynamic transport coefficients

The relatively young age of this field implies that early research focused on areas closely connected with established methods and knowledge. In particular, early research on hydrodynamics focused on i) calculating the explicit form of transport coefficients for specific materials whose microscopic description is well-known, ii) re-deriving hydrodynamics for various novel symmetries enjoyed by condensed matter systems[6].

Concerning i), the microscopics of a given material are described in terms of a QFT. Therefore hydrodynamic transport coefficient calculations can generally be performed within the framework of QFT. In particular, these calculations are performed through Kubo's linear response formalism [24, 25], which relates the transport coefficient of interest to a particular retarded Green's function. For typical materials, then one calculates the corresponding Green's function through well-known perturbative QFT techniques. However, perturbation theory is useful only for weakly coupled fluids. If a fluid is strongly coupled (cf. chapter 5 for an example of a

[4] Note that l_{ee} also increases with decreasing temperature. Therefore, we cannot cool down the system at arbitrarily small temperatures.

[5] Note that [18] argues it was $1d$ diffusion of electrons that was observed by Molenkamp and de Jong and not a hydrodynamic flow.

[6] Novel meaning here that these symmetries are not enjoyed by typical fluids such as water.

strongly coupled material), perturbation theory fails and a new approach is necessary.

The approach we employ within this thesis comes under the name AdS/CFT correspondence or gauge/gravity duality. As we explain in more detail in chapter 2, the AdS/CFT correspondence in its weakest form is a duality between a gauge theory and a theory of gravity originally conjectured in string theory models [26, 27]. Notably, the gauge/gravity correspondence is a strong/weak form of duality, identifying a strongly coupled gauge theory with a weakly curved theory of gravity. This allows us to turn a non-perturbative QFT calculation into a textbook calculation within general relativity. In particular, one can calculate retarded Green's functions of operators and, hence, transport coefficients, by imposing appropriate boundary conditions on the black hole horizon of the gravitational dual. Naturally, one of the first transport coefficients calculated through AdS/CFT is the shear viscosity η. In particular, η has been shown to be proportional to the entropy density of the fluid s. Most importantly, the proportionality constant between η and s has been observed to take a universal value for all infinitely coupled Lorentz-invariant fluids near charge neutrality, i.e. at near vanishing fluid charge density,

$$\frac{\eta}{s} = \frac{\hbar}{4\pi k_{\mathrm{B}}}. \tag{1.5}$$

This particular value of η/s is directly connected to Planckian dissipation, i.e. to dissipation at time scales $\tau_{\mathrm{P}} \sim \hbar/k_{\mathrm{B}}T$, via $\eta/s \sim T\tau_{\mathrm{P}}$. Based on dimensional analysis, τ_{P} is expected to be the smallest dissipation time possible in nature [28]. This led the authors of [29] to conjecture that Eq. (1.5) is a lower bound for η/s for any viscous fluid found in nature. This minimal value is referred to as the KSS bound after the authors of [29], Kovtun, Son and Starinets. The KSS bound can rightfully be considered the most important prediction of the gauge/gravity duality so far. This is because it has also been put to the test in experiment. More precisely, η/s has been experimentally measured for the strongly coupled quark-gluon plasma at the LHC and RHIC accelerators, as well as for cold atom systems [30]. In both cases, the measured valued of η/s was of similar order to, but always bigger than, the KSS bound. Note, however, that violations do exist even in theory, as we discuss in section 2.4.1.

The gauge/gravity results for η/s in conjunction with its successful experimental confirmation prompted condensed matter theorists to examine whether similar results can be found in solids. To this end, η/s for weakly coupled solids with a relativistic spectrum was calculated. In particular, a value of the same order of magnitude for η/s was found in graphene [31–34]

$$\eta/s \simeq \frac{\hbar}{4\pi k_{\mathrm{B}}} \frac{1.7}{\alpha^2}\ , \tag{1.6}$$

with α graphene's coupling constant. Despite being the same order of magnitude, η/s for graphene is at least an order of magnitude larger than the KSS bound because of graphene's perturbative coupling strength, $\alpha < 1$. The perturbative results in conjunction with the gauge/gravity ones, indicate η/s is a monotonically decreasing function of the coupling strength and that the KSS bound is reached only deeply within the non-perturbative regime.

Apart from the shear viscosity, one additional transport coefficient of interest for conformal fluids is the quantum critical conductivity σ. In $3+1$ dimensions the quantum critical conductivity is a key transport coefficient. Its temperature dependence allows us to discern between Fermi-liquid behaviour, $\sigma \propto T^{-2}$, and non-Fermi liquid behaviour $\sigma \propto T^{-a}$, $a \neq 2$ [30]. Fortunately or unfortunately, the quantum critical conductivity is independent of temperature in $2+1$ dimensions[7]. However, similarly to η/s, σ takes a particular quantum critical value for a large class of gauge/gravity models $\sigma \sim e^2/\hbar$ [35]. In contrast, weakly coupled fluids exhibit a larger quantum critical conductivity because of their weak coupling [36]. Curiously, it was shown that the DC conductivity is inversely proportional to the entropy [37], suggesting a bound on the value of σ similar to the KSS bound. However, further inspection showed that σ is proportional to $1/s$ only for strong disorder [38].

The shear viscosity and the conductivity saturate the list of transport coefficients for conformally-invariant fluids[8]. Thankfully, here enters research-focus ii) mentioned above. Namely the multitude of symmetries realized in condensed matter systems, imply a similarly vast number of hydrodynamic equations differing in which transport coefficients appear in them. The first papers in this direction, considered how breaking parity-invariance alters hydrodynamics [8, 9]. Several additional transport coefficients appear in this case. One of the most important ones for the purposes of this thesis is the Hall-viscosity $\eta_{\rm H}$. Similarly to the shear viscosity, the Hall viscosity introduces (parity-breaking) stresses acting on the fluid to the Navier-Stokes equations

$$\rho \frac{D\vec{v}}{dt} = -\nabla P + \eta \nabla^2 \vec{v} + \eta_{\rm H} \nabla^2 (\vec{v} \times \mathbf{e}_{\rm z}) + \vec{F} \ , \tag{1.7}$$

with $\mathbf{e}_{\rm z}$ the unit vector in the direction normal to the fluid plane[9]. However, unlike η, $\eta_{\rm H}$ is not related to dissipation. In this respect, the Hall viscosity is for hydrodynamics, what the magnetic field is for the Lorentz force.

[7] Of course, if one deviates from quantum criticality, σ depends on temperature through the ratio μ/T.

[8] Note that conformal invariance for us also includes invariance under both parity- and time-reversal.

[9] The direction of $\mathbf{e}_{\rm z}$ is chosen so that the fluid is embedded in R^3 with a right-handed co-ordinate system.

Apart from realizing novel exact symmetries, condensed matter systems also exhibit anomalous symmetries [39]. Typically, one probes anomalies by weakly gauging the anomalous symmetry through the introduction of an external gauge field. The presence of the gauge field deforms the conservation law dual to the anomalous symmetry, thus explicitly invalidating it[10]. The most famous example of an anomaly is given by the $3+1$ dimensional U(1) triangle anomaly in the presence of external electric $\vec{E}$ and magnetic $\vec{B}$ fields

$$\partial_\mu J^\mu = C\vec{E}\cdot\vec{B}\ . \tag{1.8}$$

J^μ is the U(1) current, conserved in the absence of an anomaly, and C is the anomaly coefficient, which depends on the particular system we examine. The U(1) anomaly was first observed within the realm of high energy physics [40, 41]. A little more than a decade later, it also emerged in condensed matter systems with a relativistic low-energy spectrum, namely, Weyl semimetals [42]. As is expected, the modification of the conservation law of J^μ due to the U(1) anomaly, also modifies the hydrodynamics of the, now anomalous, fluid. In particular, the U(1) anomaly leads to novel transport coefficients [7], altering the fluid's conductivity in the presence of a magnetic field [39, 43, 44].

Returning to flatland [45] and the $2+1$ dimensional fluids of interest, we find the well-known parity anomaly [46–49]

$$J^\mu = \frac{e}{8\pi}\epsilon^{\mu\nu\rho}F_{\nu\rho}\ , \tag{1.9}$$

with e the electron charge and $F_{\nu\rho}$ Maxwell's field strength tensor. In contrast to the U(1) anomaly, the parity anomaly was predicted for high energy and condensed matter systems almost simultaneously. More precisely, the parity anomaly was shown in the 1980s to appear in a monolayer of graphite or, as we presently call it, graphene [49, 50](see also [51–54] for more recent work). Similarly to the U(1) anomaly, the breakdown of parity due to the parity anomaly (1.9) strongly affects the transport in a fluid. In particular, it endows the fluid with a non-vanishing Hall conductivity and Hall viscosity [9, 55] (see [56] for a review on the Hall viscosity).

Despite this large number of results on transport coefficients, theoretical methods on how to measure and distinguish between the effects induced by them are few and far between. This gap between transport coefficients and the transport effects they induce, is partly bridged by this thesis. In particular we are interested in two aspects of hydrodynamic transport: transport in strongly-coupled and in parity-breaking fluids. To see how our research fits into the existing literature, let us give a partial review of it. We will focus on particular examples that help, first, to present the distinct transport

[10] In the absence of external gauge fields, the anomaly appears in $n > 1$-point functions of the conserved current.

characteristics exhibited by a material due to its hydrodynamic behaviour and, second, to set the stage for understanding our research [1–3].

The Gurzhi effect and summary of results

Let us first review of the the Gurzhi effect, the first signature of hydrodynamic transport in electronic wires predicted by Gurzhi [13, 14] and confirmed by Molenkamp and de Jong in (Al,Ga)As wires [16, 17]. To describe the Gurzhi effect, let us consider a two-dimensional wire of width W and length $l \gg W$, see Fig. 1.1[11]. Assume we pump electrons through the wire via an applied electric field aligned along the channel. Gurzhi considered what happened to the resistance of such channels with varying temperature T. We assume the temperature is small enough such that electrons in the channel pass through it ballistically, $l_{\text{ee}} = l_{\text{ee}}(T) \gg W$.[12] In this case electrons pass through the channel like billiard balls, colliding only with the channel boundaries. In this ballistic regime, the resistance of the channel $\mathcal{R}_W$ can only depend on geometric parameters and hence it is constant in temperature. Next we increase the temperature of the channel, which in turn decreases $l_{\text{ee}} \gtrsim W$. In this temperature regime, electrons collide with the channel boundaries as well as with each other. As a consequence, the resistance of the channel will become larger than $\mathcal{R}_W$. Increasing the temperature further, we can reach the hydrodynamic regime for which $l_{\text{ee}} \ll W$. In this regime electrons collide mostly with each other and behave collectively. This allows them to drag each other along the channel within an enveloping flow profile, see Fig. 1.2. As a result, the resistance of the wire will start decreasing with increasing temperature until it reaches a minimum value. This increase and subsequent decrease of the resistance with temperature runs counter to the usual lore of transport in solids [57]. For this reason it was given a specific name, the Gurzhi effect, and it is a hallmark of hydrodynamic behaviour in electronic solids. If we increase the temperature further, phonon effects will start affecting transport in the system. As a consequence of electron-phonon collisions, the resistance of the channel will once more start to increase with temperature.

It is precisely this "anomalous" behaviour of the resistance as a function of temperature that was observed in [16], as shown in Fig.s 1.3a, 1.3b below. In these plots, the resistance dV/dI is plotted as a function of the current I flowing through the wire, instead of the temperature. This is because I is directly observable and depends on the temperature of the electron gas due to Joule heating, $T \sim I^2$.

It is important to remark here that our above discussion on the Gurzhi effect relied on the assumption of weak coupling, since we assumed the exis-

[11] We assume that electron-impurity scattering is irrelevant for this description, i.e. the channel is "clean".

[12] Recall l_{ee}, like all scattering scales, in general depends on T.

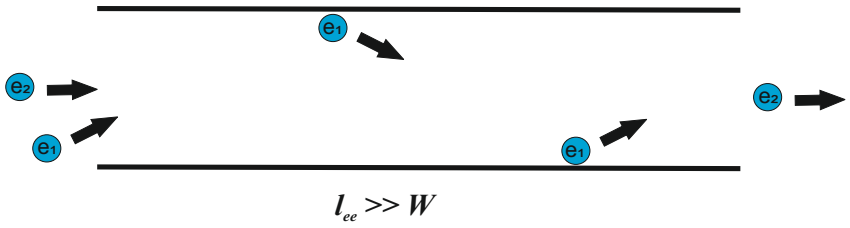

Figure 1.1: Channel of width W considered for the Gurzhi effect. Electrons at temperatures such that $l_{\mathrm{ee}} \gg W$ are pumped through the channel. They go through the channel ballistically, interacting only through the channels boundaries.

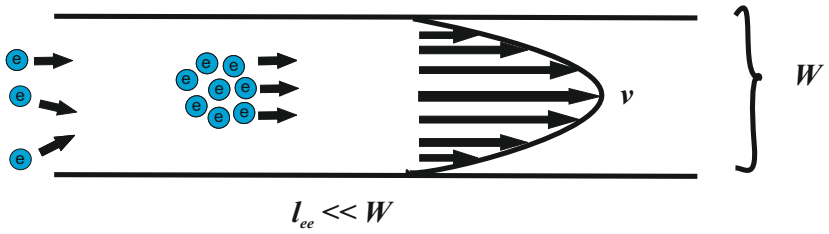

Figure 1.2: Channel of width W considered for the Gurzhi effect. Electrons at temperatures such that $l_{\mathrm{ee}} \ll W$ are pumped through the channel. As they move through the channel, they interact with each other thus forming a fluid with velocity $\mathbf{v}$.

tence of well-defined quasiparticles (the electrons) that propagate and interact with each other as they traverse the channel. However, in recent years moderately and strongly coupled materials have emerged, such as graphene around criticality [58, 59], where this assumption fails. The question then arises whether the Gurzhi effect can be realized in strongly coupled materials. We undertook the task of answering this question from the point of view of hydrodynamics in [1], as discussed in detail in chapter 4. In particular, we carried out a complete analysis of the hEOM for a relativistic fluid in a channel geometry. Crucially, we employed the gauge/gravity duality to supplement the hEOM with the thermodynamic parameters and transport coefficients of the fluid. In this way, we restricted ourselves to the non-perturbative regime and explored the hydrodynamic channel flow for fluids

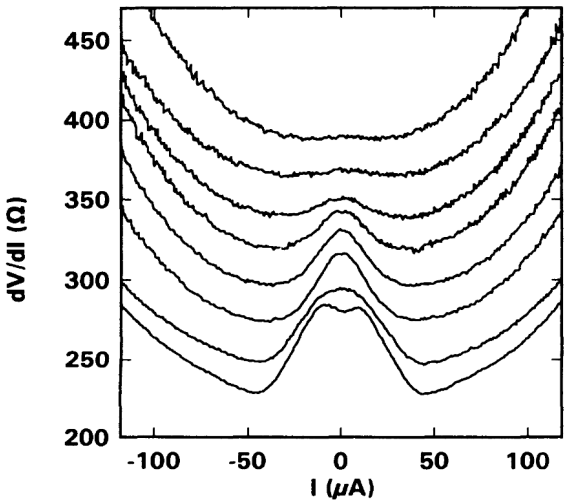

(a) Resistance of a wire with width $W = 3.9\mu$m and length $l = 20.2\mu$m as a function of the current passing through the wire for different lattice temperatures. From top to bottom $T = 24.7,\ 20.4,\ 17.3,\ 13.6,\ 10.4,\ 8.7,\ 4.4,\ 1.5$K. Reprinted from [16] with permission from APS.

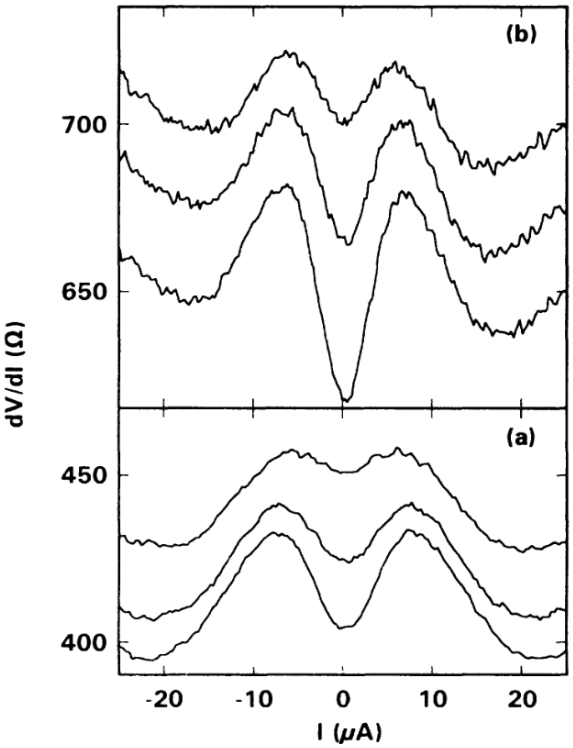

(b) Resistance of two wires with width $W = 4\mu$m and lengths $l = 63.7\mu$m (top panel) and $l = 127.3\mu$m (bottom panel) as a function of the current passing through the wire for different lattice temperatures. From top to bottom $T = 4.5,\ 3.1,\ 1.8$ K.. Reprinted from [16] with permission from APS.

whose η/s ratio is close to or even saturates the KSS bound. Our analysis shows that strongly-coupled fluids do exhibit the decrease in resistance predicted by Gurzhi at weak coupling, but with a relatively diminished resistance. This renders strongly coupled fluids more efficient conductors of electricity than their weakly coupled counterparts. Our research indicates, then, that the search for efficient conductors should not only focus on increasing the critical temperature of superconductors, but also on realizing strongly coupled materials.[13]

To showcase that this is a fruitful research direction, my collaborators and I have proposed a novel strongly coupled electronic system, Scandium-substituted Herbertsmithite (ScHb), in [2]. ScHb is a kagome metal constructed from copper oxide plaquettes. It exhibits a relativistic spectrum, similar to graphene, and a fine-structure constant of around 3. A fine-structure constant so large renders perturbation theory invalid and non-perturbative methods are necessary to understand the transport properties of ScHb. We used the gauge/gravity duality to estimate ScHb's η/s. The resulting estimate shows that ScHb can exhibit one of the hallmarks of hydrodynamic behaviour in nature, turbulence. Turbulence has never been observed in electronic fluids. In fact, it has even been suggested that a turbulent electron flow is nigh on impossible [58]. Our proposal for ScHb explicitly defies these expectations and paves the way towards bringing turbulence, strongly coupled electron fluids and the gauge/gravity duality within the reach of tabletop condensed matter experiments. Our detailed proposal for ScHb and its transport properties is presented in chapter 5.

Furthermore, in analogy to the Gurzhi effect, we explore how the Hall viscosity affects transport within a wire. In particular, we found in [3] that the Hall viscosity and hydrodynamic transport in general, alter the classical Hall effect present in $2+1$ dimensional materials under the combined influence of an in-plane external electric field and an out-of plane external magnetic field. We find that the hydrodynamic Hall effect is vastly different from the typical Hall effect in solids. Namely, while the standard Hall effect is linear in B, the Hall effect in fluids is a highly non-linear function of the external magnetic field. Even more importantly, the hydrodynamic Hall effect vanishes at a non-vanishing value of the magnetic field. This non-linearity and its vanishing are then distinct features of hydrodynamic transport in materials and can be used to clearly distinguish between ballistic and hydrodynamic transport! We presented in [3] a detailed analysis of the modified Hall effect and suggested ways it can be measured in experiment. We present this analysis in chapter 6.

Finally, we note that the above applications have considered only the transport of charge within electronic fluids. Recently, spintronics, devices us-

[13] Note that for us strongly coupled and strongly correlated are synonymous, in the sense that a perturbation theory approach to the problem is invalid.

ing the electron's spin to transfer information, have been heavily researched and developed [60]. It is interesting to understand how the properties of these devices change once they start behaving hydrodynamically. To do so, we need a theory of hydrodynamics which takes into account the macroscopically conserved electron spin. Such a theory, does not exist yet, which is why we take the first steps towards building it in chapter 7. The contents of chapter 7 are as of yet unpublished research I conducted during my PhD studies. In particular, we discuss some of the intricacies appearing in the construction of spin hydrodynamics and derive the effective action of spinfull fluids up to first order in the microscopic length scale $\mathcal{K}$. More importantly we show that once one includes $\mathcal{K}^2$ corrections, interesting spin transport phenomena emerge. An example of these includes the spontaneous magnetization of a rotating fluid, i.e. the Barnett effect [61].

The structure of this thesis is the following: In chapter 2 we present a short review of the AdS/CFT correspondence and its connection to transport and hydrodynamics. In particular, we show how holography allows us to specify the thermodynamics as well as the ratio η/s for a $2+1$ dimensional, charged relativistic fluid. We proceed in chapter 3 to give a review of the construction of the constitutive relations of hydrodynamics for parity-breaking fluids, using the methods of equilibrium partition functions as well as the second law of thermodynamics. Then, in chapters 4, 5 and 6, we apply hydrodynamics to derive the novel transport phenomena first appearing in [1, 2] and [3] respectively. We proceed in chapter 7 with our (partial) construction of spin hydrodynamics. Finally, we present our conclusions and suggestions for future research in chapter 8.

Chapter 2

The AdS/CFT correspondence

In the present chapter we review the AdS/CFT correspondence and its application to strongly coupled materials. We begin in section 2.1 by presenting the original conjecture for the AdS/CFT correspondence [26]. We also present the holographic dictionary [62, 63], which provides an explicit map between observables in the strongly coupled CFT and gravity fields.[1] Then, in section 2.2 we discuss how the correspondence can be extended to describe QFTs at finite temperature and charge density and use this extension to derive their thermodynamic properties. We proceed in section 2.3 with a short presentation of the linear response formalism within QFT and the AdS/CFT correspondence. Finally, we apply the results of section 2.3 in section 2.4 to calculate η/s for QFTs dual to the Einstein-Hilbert Lagrangian. This calculation leads to the well-known KSS lower bound on η/s (1.5) discussed in the introduction. Finally, we discuss how one can introduce coupling corrections to the KSS bound and whether these corrections violate the bound.

2.1 The AdS/CFT correspondence

We motivate the AdS/CFT or gauge/gravity correspondence through its original incarnation in string theory [26]. We base our account on several textbooks and lecture notes [30, 64–66], as well as on the original article by Maldacena [26].

To begin our discussion, let us present some general facts about type IIB string theory[2], for which Maldacena first proposed his conjecture. The excitations of Type IIB string theory consist of both open and closed (super)strings vibrating at a particular frequency while propagating in ten-

[1] We explain why this dictionary is holographic in nature below, see discussion below Eq. (2.9).

[2] The classification type IIB simply means that the low-energy string spectrum contains chiral fermions. In contrast type IIA string theory does not contain chiral matter.

dimensional spacetime. The open strings, like those of a guitar, necessarily have their endpoints fixed on $p+1$ dimensional hypersurfaces called Dp-branes. We can label the string endpoints and the D-brane they are fixed upon, by assigning to each string endpoint a *Chan-Paton factor*. At low energies, the Chan-Paton factors endow the string spectrum with a representation of a unitary group. Due to this, low-energy open-string excitations on the Dp-brane can be identified with the excitations of a gauge theory living on the Dp-brane. For example, low-energy open string excitations with their endpoints fixed on a single Dp-brane are described by a U(1) gauge theory in $p+1$ dimensions. On the other hand, closed strings are free to move anywhere in spacetime. That is, they can start or on a Dp-brane, or simply propagate in vacuum. Crucially, the low-energy excitations of a closed string, involve spin-2 modes which can be naturally interpreted as gravitons[3]. As a result, a closed string attached to Dp-brane can be thought of as a graviton emitting or absorbing process depending on the direction of time. Hence, we may think of Dp-branes as massive objects bending spacetime with their gravitational field.

As we can see, both open strings — giving rise to a gauge theory — and closed strings — giving rise to gravity — are closely related to Dp-branes. It is this connection between strings and Dp-branes that allows us to conjecture the gauge/gravity correspondence. To motivate a more precise form of the conjecture, consider a stack of N coincident $D3$-branes in flat $9+1$ dimensional Minkowski space, $M_{9,1}$. As already remarked, these branes are massive gravitating objects. Namely, they can be thought as gravitational solitons supported by their non-trivial Ricci curvature $R \sim 1/L^2$. The curvature radius L can be expressed in terms of N and the only free parameters in string theory, the string length l_s and the string-string interaction constant g_s. In particular,

$$\left(\frac{L}{l_s}\right)^4 = 4\pi g_s N \ . \tag{2.1}$$

To proceed, let us examine (2.1) in various limits. First, we assume $g_s N \ll 1$, i.e. $L \ll l_s$. In this case, the $D3$-branes are far smaller than any string propagating in the ambient spacetime. This implies a complete decoupling of the dynamics of the $D3$-branes from the closed strings of Type IIB theory, since no string is small enough to probe the branes or be sourced by them. This decoupling becomes exact in the low-energy limit of string theory, formally induced by taking $l_s \to 0$ [4]. In the same limit, the dynamics of the closed strings are given by a free-supergravity theory on $M_{9,1}$, while the dynamics

[3]Naturally means that the spin-2 string states satisfy all the gauge constraints as a graviton state.

[4]This is the low-energy limit of string theory because it implies we work at energy scales which cannot resolve the "stringy" structure of string theory.

of the $D3$-branes are given solely by the low-energy open-string vibrations, i.e by a $3+1$ dimensional gauge theory. In particular, the open string vibrations are described by a maximally supersymmetric, $\mathcal{N}=4$, super Yang-Mills (SYM) gauge theory with gauge group $SU(N)$. This is a (super)conformal gauge theory with a dimensionless coupling strength, $g_{\rm YM}$. Due to its string theoretic origin, $g_{\rm YM}$ can be expressed in terms of g_s as

$$g_{\rm YM}^2 = 4\pi g_s \ . \tag{2.2}$$

Let us now examine the opposite limit, where $g_s N \gg 1$ and $L \gg l_s$. In this limit, the $D3$-branes interact with the closed strings floating in spacetime, so a simple description of the dynamics in terms of open strings is not enough. Instead, since the branes are far larger than the strings, they always interact with each other. Therefore the branes are constantly emitting and absorbing gravitons, suggesting an effective description of their dynamics in terms of gravity is possible. Indeed, in the $L \gg l_s$ limit one can describe the $D3$-brane dynamics in terms of a Type IIB supergravity action, i.e. a supersymmetric theory of gravity with chiral fermions [67]. As all gravitational theories based on general relativity (GR), supergravity is non-renormalizable. Therefore for the supergravity action to be well-defined, we must suppress any quantum correction generating an infinite tower of higher derivative relevant operators. To achieve this tree-level limit of supergravity, we take $g_s \ll 1$. In this way, we find that the $D3$-brane dynamics are described by a well defined supergravity theory in the combined limit $g_s \ll 1$ and $N \gg 1$ such that $L \gg l_s$. Because we suppressed all quantum corrections, the effective supergravity action includes only the Einstein-Hilbert term ($\sim R$) plus the additional matter fields comprising the graviton supermultiplet [67]. Given this supergravity theory, we can now consider its low-energy limit. Similarly to the case $L \ll l_s$ a decoupling between degrees of freedom occurs. In particular, we find two decoupled supergravity theories: A free supergravity theory on $M_{9,1}$ and a supergravity theory on a product spacetime with line element

$$ds^2 = \frac{L^2}{z^2}\left(dz^2 + \eta_{\mu\nu}dx^\mu dx^\nu\right) + L^2 ds^2_{S^5} \ . \tag{2.3}$$

The first term on the right hand side (RHS) of Eq. (2.3) gives the line element of a five dimensional anti-De Sitter (AdS_5) spacetime with curvature radius L^2. The particular form of the AdS_5 metric used here, defines a foliaton of AdS_5 along the z-direction in terms of $3+1$ dimensional Minkowski spacetime with metric $\eta_{\mu\nu}$. The second term in Eq. (2.3) gives the line element of a five dimensional sphere of radius L. Thus, we can identify the product spacetime of the supergravity theory with $AdS_5 \times S^5$.

Let us summarize what we have seen so far. We started from Type IIB string theory and considered the two limiting cases $g_s N \ll 1$ and $g_s N \gg$

1. We argued that the low energy description of these limits is given by $\mathcal{N} = 4$ SYM times supergravity on $M_{9,1}$ on the one hand and supergravity on $AdS_5 \times S^5$ times supergravity on $M_{9,1}$ on the other. Now comes the crucial point: Due to supersymmetry, we can be certain that the $g_s N \ll 1$ limit of Type IIB string theory is adiabatically connected to the $g_s N \gg 1$ limit[5]. Assuming this adiabatic connection between the two limiting cases is inherited by their respective low energy theories, we can conjecture that

$$D = 3{+}1, \mathcal{N} = 4, SU(N) \text{ SYM gauge theory} \cong \text{ supergravity on } AdS_5 \times S^5 \ . \tag{2.4}$$

Further, one can consistently reduce the S^5 to fields propagating on AdS_5 via Kaluza Klein reduction [68, 69] (see also [70]). Hence, the equivalence Eq. (2.4) can also be expressed as

$$D = 3 + 1, \mathcal{N} = 4, SU(N) \text{ SYM gauge theory} \cong \text{ supergravity on } AdS_5 \ . \tag{2.5}$$

This is the AdS/CFT correspondence as was first proposed in [26]. It is a weak-strong coupling correspondence in the following sense: The supergravity theory is valid for $g_s N \gg 1$, with $N \gg 1$. Using Eq. (2.2) we can re-express this relation in terms of $g_{\rm YM}$ as

$$g_{\rm YM}^2 N = \lambda \gg 1 \ , \tag{2.6}$$

where we introduced the 't Hooft coupling λ. The 't Hooft coupling acts as the effective coupling strength of SYM in the large N limit. Therefore, supergravity on AdS_5 is an equivalent description of strongly coupled SYM[6]. This is the so called weakest form of the AdS/CFT correspondence. One can strengthen it by removing the requirement $\lambda \gg 1$, but still requiring $N \ll 1$. In this limit, SYM is conjectured to be equivalent to classical string theory since g_s must be perturbatively small. Clearly, one can strengthen the conjecture further by allowing g_s to take any value, not necessarily small. In this case, SYM is conjectured to be equivalent to the fully quantum Type IIB string theory. As a final comment we note that the construction qualitatively described above can be extended to include branes other than $D3$, leading to the equivalence of gauge and gravity theories in various dimensions and with various symmetries [30]. As a result, the AdS/CFT correspondence has also been dubbed the gauge/gravity correspondence.

[5] Supersymmetry is not necessary for this adiabatic connection between large and small $g_s N$. Instead, the necessary condition is that no phase transitions occur in the system as we move from one limit to the other [65].

[6] Because our conjecture is reflexive, we can also say that SYM is an equivalent description of sharply curved supergravity on $AdS_5 \times S^5$.

2.1.1 The holographic dictionary

To make practical use of the gauge/gravity correspondence, we must make precise how it relates physical observables between the two sides. The prescription for doing so is referred to as the holographic or GPKW dictionary, after Gubser, Polyakov and Klebanov [63] and Witten [62]. We present our version for the deduction of this prescription below[7].

The physical observables of a $d+1$ dimensional gauge theory consist of the correlation functions of local gauge-invariant operators $\mathcal{O}(x)$. These correlation functions can be calculated directly from the generating functional of the gauge theory, $\mathcal{Z}_{\text{gauge}}$, given by

$$\mathcal{Z}_{\text{gauge}} = \mathcal{Z}_{\text{gauge}}[J] = \left\langle \exp\left[i \int d^{d+1}x \; J(x) \circ \mathcal{O}(x) \right] \right\rangle \; , \tag{2.7}$$

where $J(x)$ is the source of the operator $\mathcal{O}(x)$, $\circ$ denotes the appropriate inner product such that $J(x) \circ \mathcal{O}(x)$ is a Lorentz scalar and the angled brackets denote averaging over the asymptotic vacuum state of the gauge theory and time-ordering.

On the other side of the correspondence, gravity does not have any well-defined local operators because of diffeomorphism invariance. Instead, theories of gravity are defined in terms of their dynamics, i.e. the gravitational action, as well as their boundary conditions. Let us denote the bulk fields of gravity and their boundary conditions by ϕ and ϕ_0 respectively. An example of a bulk field ϕ is the spacetime metric $g_{\mu\nu}$ of AdS_5 presented in Eq. (2.3). Its corresponding boundary condition is defined at the asymptotic boundary $z \to 0$ and is given by the Minkowski metric $\eta_{\mu\nu}$. Given ϕ and ϕ_0, all the physical properties of a theory of gravity are hidden in $S_{\text{grav}}[\phi_0]$, the on-shell gravitational action[8]. To arrive at $S_{\text{grav}}[\phi_0]$ one expresses ϕ in terms of ϕ_0 by solving ϕ's EOM and substitutes the solution back into $S_{\text{grav}}[\phi]$, hence the characterization on-shell. As in all QFTs, the exponential of $S_{\text{grav}}[\phi_0]$ defines the generating functional of gravity in the semiclassical limit [72]. In particular,

$$\mathcal{Z}_{\text{grav}} = \mathcal{Z}_{\text{grav}}[\phi_0] = \exp\left(i S_{\text{grav}}[\phi_0] \right) \; . \tag{2.8}$$

Let us apply now this general discussion to the special case of supergravity on AdS_{d+2}. In this case, the boundary fields ϕ_0 are defined on the $d+1$ dimensional boundary of AdS_{d+2}. This boundary can be identified up to a conformal transformation with $d+1$ dimensional Minkowski spacetime.

[7] No claim for the novelty of the following arguments is made. We just put textbook QFT, GR and classical mechanics lore to use.

[8] This is true for any classical field theory (cf. chapter 6 of [71]). Gravity is distinguished among these field theories, since boundary data are its only local invariants.

This suggests the identification, up to a conformal factor, of the boundary value ϕ_0 with the source $J(x)$ of the operator $\mathcal{O}(x)$ and, hence, leads to [9]

$$\mathcal{Z}_{\text{gauge}}[\phi_0] = \mathcal{Z}_{\text{grav}}[\phi_0] = \exp\left(iS_{\text{grav}}[\phi_0]\right) \ . \tag{2.9}$$

Equation (2.9) allows us to derive any and all correlation functions of the operator $\mathcal{O}(x)$ in a *strongly coupled* gauge theory, via the on-shell action of a theory of gravity. Thus the theory of gravity acts as an effective theory for the operators $\mathcal{O}(x)$ of interest. Equivalently, all physical information of a dynamical spacetime are given in terms of a gauge theory living on the spacetime's boundary. For this reason, the gauge/gravity correspondence is also called the holographic correspondence or holography for short. This holographic interpretation also allows us to give a physical meaning to the additional bulk spacetime dimension. Namely, the z co-ordinate in Eq. (2.3) can be interpreted as changing the energy of the dual QFT. That is, each hypersurface $z =$ constant can be identified with the boundary QFT, but at a different energy scale. In particular, the boundary $z = 0$ is interpreted as the UV limit of the dual QFT, while $z = \infty$ as the IR.

This concludes our very general introduction of holography, concerning QFTs at vanishing temperature and chemical potential. We can, however, extend the correspondence to field theories at finite temperature and away from charge neutrality. In particular, we argue in the following section that a thermal QFT at finite chemical potential is dual to a spacetime with a charged black hole residing in it. The temperature and total charge of the QFT are identified with the Hawking temperature and charge of the black hole.

2.2 Holographic thermodynamics

We now motivate and state the gauge/gravity correspondence for thermal QFTs at finite charge density. For this purpose, we first consider a QFT in thermal equilibrium at charge neutrality. The states of this thermal QFT are defined on R^3 and evolve in imaginary time τ. The imaginary time has the topology of a circle with perimeter β, playing the role of inverse temperature, meaning the QFT lives on the product manifold $S_1 \times R^3$. Therefore, the dual bulk geometry must be deformed at the boundary to exhibit the same topology. That is, we must compactify the time direction into a circle while leaving the spatial directions untouched. We can achieve this by introducing a black hole into the bulk *AdS* space, which warps the time and the non-QFT direction z. More precisely, consider an AdS_{d+2} black hole with the line element

[9] There are less hand-waving arguments for identifying ϕ_0 with $J(x)$. For detailed discussions from the string theory point of view see [64], while for discussions from the gauge theory point of view see [30].

$$ds^2 = \frac{L^2}{z^2}\left(\frac{dz^2}{f(z)} - f(z)dt^2 + d\mathbf{x}^2\right) \ . \tag{2.10}$$

In Eq. (2.10), $t, \mathbf{x}$ are the $d+1$ QFT co-ordinates, while z is the extra dimension of the bulk spacetime. The function $f(z)$ is the blackening factor with a simple zero at $z = z_h$, the position of the black hole horizon. Rotating t to imaginary time $t = i\tau$, we find the Euclidean AdS black hole with line element

$$ds^2 \equiv g_{\mu\nu}dx^\mu dx^\nu = \frac{L^2}{z^2}\left(\frac{dz^2}{f(z)} + f(z)d\tau^2 + d\mathbf{x}^2\right) \ . \tag{2.11}$$

Due to the blackening factor, the Euclidean black hole exhibits a conical singularity near the horizon. To avoid this singularity, we must compactify τ down to a circle with inverse period β^{-1} given by

$$\beta^{-1} = \frac{1}{4\pi}f'(z_h) \ . \tag{2.12}$$

Therefore after the compactification of τ, the boundary of AdS has the proper topology to harbour a thermal QFT with inverse temperature β. This makes it natural to identify a black hole spacetime with a thermal QFT. A further motivation to identify a spacetime with a black hole with a thermal QFT, is the energy interpretation of the bulk co-ordinate z. Viewed from this perspective, the black hole with its event horizon forbids the UV observer at $z = 0$ access to the IR degrees of freedom at $z = \infty$ [66]. This is exactly what placing a QFT at finite temperature does as well: Thermal fluctuations excite all IR degrees of freedom with energy smaller than β^{-1}. Of course, we can make our discussion more rigorous via a suitable modification of Maldacena's original argument. The interested reader can consult [30, 64] for details.

To go further and consider QFTs away from charge neutrality, we must also introduce a source for the charge density of the boundary QFT. The role of this source can be played both by a background Coulomb potential as well as a background chemical potential μ. Since the two are interchangeable, we choose μ as the charge density source. In particular, we have for the Euclidean partition function

$$\mathcal{Z}_{\text{gauge}} = \left\langle \exp\left[-\int d^{d+1}x \ \mu J^0\right]\right\rangle \ , \tag{2.13}$$

where J^0 is the charge density of the QFT. In a relativistic theory, this chemical potential must always appear as part of a $U(1)$ gauge field a_μ. To be more precise, we must write

$$\mathcal{Z}_{\text{gauge}} = \mathcal{Z}_{\text{gauge}}[a_\mu] = \left\langle \exp\left[-\int d^{d+1}x \ a_\mu J^\mu\right]\right\rangle \ . \tag{2.14}$$

The zeroth component a_0 gives the chemical potential, while the spatial components a_i source the current densities J^i in the boundary QFT. According to the holographic dictionary (2.9), the gauge field a_μ corresponds to the boundary value of a bulk gauge field A_μ [10]. That is, we can write

$$\mathcal{Z}_{\text{gauge}}[a_\mu] = \exp\left(-S_{\text{grav}}[A_\mu = A_\mu(a_\mu)]\right) \ , \tag{2.15}$$

with S_{grav} the gravitational action and A_μ expressed on-shell in terms of a_μ. To restrict the dual QFT to finite charge J^0 but vanishing current J^i, we must choose a_μ to be of the form

$$a_\mu = (a_t, a_i) = (\mu, 0) \tag{2.16}$$

and

$$A_M(z \to 0) = (A_z(z \to 0), A_\mu(z \to 0)) = (0, a_\mu) \ . \tag{2.17}$$

To summarize, in order for the dual QFT to be both at finite temperature and density, we must consider a gravitational action with a dynamical metric and gauge field. This action must be complex enough to accommodate both a black hole solution of the form Eq. (2.11) and a non-trivial solution for A_μ satisfying the boundary condition Eq. (2.17). The simplest action that meets these requirements is the Einstein-Maxwell Lagrangian, consisting of the Einstein-Hilbert term plus the Maxwell Lagrangian

$$S_{\text{EM}} = \int d^{d+2}x\sqrt{g}\left[\frac{-1}{2\kappa^2}\left(R - 2\Lambda\right) - \frac{1}{4g^2}F_{\mu\nu}F^{\mu\nu}\right] + S_{\text{GHY}} \ , \tag{2.18}$$

with g and R the determinant and Ricci scalar of the bulk metric $g_{\mu\nu}$, $\Lambda = -d(d+1)/(2L^2)$ the cosmological constant enforcing AdS_{d+2} as one of the solutions, and $F_{\mu\nu} = \partial_\mu A_\nu - \partial_\nu A_\mu$ is A_μ's field strength. The constants $\kappa = 8\pi G_{d+2}$ and g^2 are the gravitational and gauge couplings respectively, with G_{d+2} Newton's gravitational constant. Note that because of the asymptotic boundary of AdS space at $z \to 0$, we have also included the Gibbons-Hawking-York boundary term in the action [73, 74]

$$S_{\text{GHY}} = \frac{-1}{\kappa}\int d^{d+1}x\sqrt{\gamma}\ K \ . \tag{2.19}$$

In Eq. (2.19), γ is the determinant of the induced metric at the boundary and $K = \nabla_\mu n^\mu$ the boundary's extrinsic curvature with unit normal $n_\mu = L/(z\sqrt{f(z)})$.
A solution of S_{EM}'s EOM for A_μ is given by

[10] We will use the same notation for both bulk and boundary indices where no danger of confusion arises.

$$A_\mu = (0, A_t, 0) \quad , \quad A_t = \mu \left(1 - \left(\frac{z}{z_h} \right)^{d-1} \right) \ , \tag{2.20}$$

where z_h is the horizon of the black hole solution for $g_{\mu\nu}$. The solution for $g_{\mu\nu}$, A_μ is referred to as the Reissner-Nordström black hole in honour of, some of, its discoverers and has the form (2.11) with

$$f(z) = 1 - M \left(\frac{z}{z_h} \right)^{d+1} + Q^2 \left(\frac{z}{z_h} \right)^{2d} \ , \tag{2.21}$$

$$M = 1 + Q^2 \quad , \quad Q^2 = \frac{z_h^2 \mu^2}{\gamma^2} \quad , \quad \gamma^2 = \frac{dL^2 g^2}{(d-1)\kappa^2} \ . \tag{2.22}$$

The constants M and Q are the mass and charge of the black hole. From the point of view of the observer at infinity, they are the conserved mass and charge of the black hole. Since the observer at infinity is identified with the observer of a QFT, M and Q are also conserved quantities for the dual gauge theory. As expected, M and Q correspond to the conserved energy[11] $E \sim M$ and charge $q \sim Q$ of the thermal QFT.

More precisely, given the Reissner-Nordström solution, we can evaluate the gauge partition function $\mathcal{Z}_{\text{gauge}}$ via Eq. (2.9). Since we are working in Euclidean signature, $\mathcal{Z}_{\text{gauge}}$ gives the thermal partition function of the gauge theory. Furthermore, $\log \mathcal{Z}_{\text{gauge}} = -S_{\text{grav}}$ is proportional to the grand potential Ω of the grand canonical ensemble, since we are working in a homogeneous vacuum state characterized by constant β and μ [75]. Thus we may calculate any thermodynamic property of the dual QFT by calculating the on-shell gravitational action and its derivatives with respect to β and μ. To bring S_{grav} on-shell is a non-trivial task since the metric diverges as $z \to 0$. This divergence is akin to the UV divergences encountered in QFT and can be renormalized via similar approaches, e.g. by calculating the action on a cutoff surface $z = \epsilon \ll L$ instead of the boundary $z = 0$. After renormalization, the action is finite and can act as the grand potential Ω of the system. In particular we have for the Reissner-Norström solution [30]

$$\Omega = -\beta^{-1} \ln \mathcal{Z}_{\text{gauge}} = \beta^{-1} S_{\text{grav}} = -\frac{L^d M}{2\kappa^2 z_h^{d+1}} V_d \ , \tag{2.23}$$

with V_d the spatial volume of the boundary QFT.

Through Ω we can finally derive all of the thermodynamic properties of the dual QFT. Consider first the entropy of the dual QFT. It takes the form

$$S = \frac{A}{4G_{d+2}} = \frac{2\pi}{\kappa^2} \left(\frac{L}{z_h} \right)^d V_d \ , \tag{2.24}$$

[11] The speed of light is set to one.

where A is the area of the black hole horizon. This is a remarkable result: The entropy of the QFT, calculated via the gravitational action, is given by the Bekenstein-Hawking formula for the entropy of the black hole [76, 77]. This result acts as a further confirmation of the holographic principle: All the degrees of freedom of the gravity theory are encoded on a hypersurface with codimension one. However, we should mention that the QFT entropy is given by Eq. (2.24) only for gravitational actions involving up to two derivatives of the metric. For theories involving higher derivatives, additional curvature invariants of the black horizon enter the formula for S [78, 79].

Further, we can derive the charge density of the dual QFT and find

$$\rho = -\frac{L^d}{\kappa^2 z_h^{d+1}} Q^2 \ . \tag{2.25}$$

Using ρ, S and $\beta = T^{-1}$, we can also find the energy E and pressure P of the fluid via the usual thermodynamic relations[12]

$$\Omega = -PV_d = E - TS - \mu\rho V_d \ . \tag{2.26}$$

Finally, let us present below the thermodynamic variables for $2+1$ dimensional QFTs (to be used in chapter 4). To do so, we use a different parametrization for the metric, employed in [1] and chapter 4. More precisely, we define $z = L^2/r$ and rewrite the metric as

$$ds^2 = \frac{L^2}{r^2 f(r)} dr^2 + \frac{r^2}{L^2}\left(-f(r) v_{\rm F}^2 dt^2 + d\mathbf{x}^2\right) \ , \tag{2.27}$$

where we have also restored the speed of light $v_{\rm F}$ and $\mathbf{x} = (x, y)$ is a spatial vector. In this parametrization, the thermodynamics of the $2+1$ QFT are given by

$$\epsilon = \frac{L^2}{8\pi G_4} \hbar\, v_{\rm F} \frac{r_{\rm H}^3}{L^6}, \quad P = \frac{L^2}{16\pi G_4} \hbar\, v_{\rm F} \frac{r_{\rm H}^3}{L^6} \ , \tag{2.28}$$

$$\rho = \frac{L^2}{64\pi G_4} \left(\frac{r_{\rm H}}{L^2}\right) \frac{\mu}{\hbar v_{\rm F}}, \quad s = \frac{k_B L^2}{4 G_4} \frac{r_{\rm H}^2}{L^4} \ , \tag{2.29}$$

where G_4 the $3+1d$ gravitational constant and $r_{\rm H}$ the horizon radius. For later use, we also note that r_H is given in terms of the QFT's temperature and chemical potential via

$$\frac{r_H}{L^2} = \frac{1}{6} \frac{k_B T}{\hbar\, v_{\rm F}} \left(4\pi + \sqrt{16\pi^2 + \frac{3\mu^2}{k_B^2 T^2}}\right) \ , \tag{2.30}$$

with $T = \beta^{-1}$ and $k_{\rm B}$ Boltzmann's constant.

This concludes our derivation of a QFT's thermodynamic properties through holography.

[12] We work in units where charge is dimensionless.

2.3 Holographic transport

We proceed in the next section to describe how we can use holography to also derive a QFT's transport properties, i.e. its transport coefficients, following [30, 80]. To begin, let us define the notion of transport. Transport for us is defined as the change induced on the expectation value of an operator due to an external field. More precisely, consider a local bosonic operator $\mathcal{O}(x)$ perturbed by the external field $\phi(x)$[13]. We assume that the QFT Hamiltonian $\mathcal{H}$ is perturbed due to $\phi(x)$ as $\mathcal{H} \to \mathcal{H} + \delta\mathcal{H}$ with

$$\delta\mathcal{H} = -\int d^{d+1}x \ \phi(x) \circ \mathcal{O}(x) \ , \tag{2.31}$$

where $\circ$ was defined below (2.7). Let us assume that the state of the QFT is defined by a density matrix ρ. It satisfies the Liouville equation of motion

$$i\frac{d\rho}{dt} = [\mathcal{H} + \delta\mathcal{H}, \rho] \ . \tag{2.32}$$

Assuming $\delta\mathcal{H}$ is "small", (2.32) can be solved up to first order in $\delta\mathcal{H}$, by expanding $\rho = \rho_0 + \delta\rho$. The density matrix ρ_0 satisfies the unperturbed Liouville equation, while $\delta\rho$ satisfies

$$i\frac{d\delta\rho}{dt} \simeq [\mathcal{H}, \delta\rho] + [\delta\mathcal{H}, \rho] \ . \tag{2.33}$$

Equation (2.33) can be solved analytically for $\delta\rho$ [80]. The total density matrix ρ can then be used to calculate the expectation value of $\mathcal{O}(x)$ after the perturbation. This expectation value differs from its equilibrium value by an amount $\delta\langle\mathcal{O}(x)\rangle$,

$$\mathrm{Tr}\,[\rho\mathcal{O}(x)] - \mathrm{Tr}\,[\rho_0\mathcal{O}(x)] \equiv \delta\langle\mathcal{O}(x)\rangle \simeq \int d^{d+1}y \ G_R^{\mathcal{O},\mathcal{O}}(x,y) \circ \phi(y) \ , \tag{2.34}$$

where $G_R^{\mathcal{O},\mathcal{O}}(x,y)$ is the retarded Green's function between two $\mathcal{O}$ operators. More precisely, we have

$$G_R^{\mathcal{O},\mathcal{O}}(x,y) = \langle[\mathcal{O}(x), \mathcal{O}(y)]\rangle_R \ , \tag{2.35}$$

where the angled brackets denote averaging with respect to the equilibrium ρ_0 and the index R means $\mathcal{O}(x)$ is inserted at a time $x^0 > y^0$. This ensures the causal nature of the perturbation; $\mathcal{O}(x)$ changes only after it has been perturbed by $\phi(y)$. We can re-express (2.34) in terms of the Fourier transforms of the $\mathcal{O}$'s and ϕ's

$$\delta\langle\mathcal{O}(k)\rangle \simeq G_R^{\mathcal{O},\mathcal{O}}(k) \circ \phi(k) \ , \tag{2.36}$$

[13] Don't let the notation full you, $\mathcal{O}(x)$ and $\phi(x)$ are not necessarily scalar operators.

Equation (2.36) makes evident the physical meaning of the linear response calculation. In particular, it allows us to identify the retarded Green's function $G_R^{\mathcal{O},\mathcal{O}}(k)$ with a generalized susceptibility matrix, since it relates the perturbation ϕ to the induced response of the system $\delta\langle\mathcal{O}\rangle$ in a linear fashion.

As an example, let us consider a perturbation due to an external gauge field a_μ. The gauge field appears in the perturbation Hamiltonian $\delta\mathcal{H}$ contracted with the charge current of the QFT J^μ. So we may apply Eq. (2.36) with $\phi \to a_\mu$ and $\mathcal{O} \to J^\mu$ to find the induced current

$$\delta\langle J^\mu(k)\rangle \simeq G_R^{J^\mu,J^\nu}(k)a_\nu(k) \ . \tag{2.37}$$

To proceed, let us assume $a_\mu(k)$ depends only on the frequency ω. Such a frequency-dependent gauge field generates an electric field $E_\mu(\omega) = i\omega a_\mu(\omega)$. Thus, we can re-write Eq. (2.37) as

$$\delta\langle J^\mu(\omega)\rangle \simeq \frac{G_R^{J^\mu,J^\nu}(\omega)}{i\omega}E_\nu(k) \equiv \sigma_{\mu\nu}(\omega)E^\nu(\omega) \ . \tag{2.38}$$

Equation (2.38) is the well-known Ohm's law that relates the current flowing through a system to the external electric field which induced it. The matrix appearing in Ohm's law is of course the conductivity matrix $\sigma^{\mu\nu}$. Due to linear response theory we can now express $\sigma^{\mu\nu}$ in terms of a current-current Green's function

$$\sigma^{\mu\nu}(\omega) = \frac{G_R^{J^\mu,J^\nu}}{i\omega} \ . \tag{2.39}$$

Last but certainly not least, we note that Eq. (2.36) provides us with a simple recipe for calculating $G_R^{\mathcal{O},\mathcal{O}}$ through holography: The small perturbation (2.31) to $\mathcal{H}$ also perturbs the source of $\mathcal{O}$, call it Φ_0, by $\Phi_0 \to \Phi_0 + \phi$. This implies via the holographic dictionary, that Φ, the bulk field dual to $\mathcal{O}$, also gets perturbed. Because ϕ is considered a small perturbation, we can calculate its effect on boundary observables by keeping only the leading term in ϕ in the gravitational action. As a result, we no longer need to solve the fully non-linear supergravity equations to calculate expectation values. Instead, we need only to solve the *linearized* EOM for Φ and substitute the solution back to the gravitational action. We provide a specific example of this formalism in the next section, where we calculate the shear viscosity η in $3+1$ dimensions.

2.4 The shear viscosity to entropy density ratio

Let us apply the linear response formalism of the previous section to calculate the shear viscosity η of a $3+1$ dimensional fluid. Along the way, we shall encounter and address some subtleties appearing in the calculation of

retarded holographic Green's functions that are due to the black hole in the bulk. As we show, addressing these subtleties is necessary to ensure causality is not violated by the boundary QFT. Our analysis follows [30], as well as the original article on the matter at hand [81]. To begin our derivation, we note that η is given by the following Green's function (cf. chapter 3)

$$\eta = -\lim_{\omega\to 0}\frac{1}{\omega}\mathrm{Im}G_R^{T^{xy},T^{xy}}(\omega,0)\ , \tag{2.40}$$

with T^{xy} the shear stress component of the energy-momentum of the boundary QFT. Connecting to the notation of the previous section, T^{xy} plays the role of the operator $\mathcal{O}$. Furthermore, the source of $T^{\mu\nu}$ in the dual QFT is simply the QFT's metric. Hence, we can calculate $G_R^{T^{xy},T^{xy}}$ and η by perturbing the bulk metric $g_{\mu\nu}$ as

$$g_{xy} \to g_{xy} + h_{xy}\ , \tag{2.41}$$

with h_{xy} the metric perturbation. To make our discussion more precise, let us consider a gravitational action which contains only the Einstein-Hilbert term

$$S_{\text{grav}} = \frac{-1}{2\kappa^2}\int d^{d+2}x\sqrt{g}\left(R-2\Lambda\right)\ . \tag{2.42}$$

Under the perturbation (2.41), the action S_{grav} becomes to leading order in h_{xy}

$$S_{\text{grav}} \equiv S_h \simeq \frac{-1}{2\kappa^2}\int d^{d+2}x\sqrt{g}g^{\mu\nu}\partial_\mu h_{xy}\partial_\nu h_{xy}\ . \tag{2.43}$$

As we can see S_{grav} has simplified considerably compared to the fully non-linear Einstein-Hilbert action. Namely, S_h describes the dynamics of a massless scalar field propagating in a black hole background. Physically, the excitations of h_{xy} are part of the graviton degrees of freedom of the bulk metric.

To proceed with the calculation of η, we need to solve h_{xy}'s EOM and substitute the solution into S_h. For concreteness, we choose the bulk metric $g_{\mu\nu}$ to be that of five dimensional AdS-Schwarschild black hole

$$ds^2 = g_{\mu\nu}dx^\mu dx^\nu = \frac{L^2}{4u^2 f(u)}du^2 + \frac{(\pi TL)^2}{u}\left(-f(u)dt^2 + d\mathbf{x}^2\right)\ , \tag{2.44}$$

with $f(u) = 1-u^2$ and T the black hole temperature. The horizon is located at $u=1$, while the boundary is at $u=0$. We observe that $g_{\mu\nu}$ is translation invariant in the boundary co-ordinates $t, \mathbf{x}$. Therefore, we can simplify the EOM by Fourier transforming h_{xy} in the boundary directions

$$h_{xy}(u,x) = \int \frac{d^4k}{(2\pi)^4}\, e^{ik\cdot x} h_{xy}(u,k) \quad , \tag{2.45}$$

with $k \cdot x = \eta_{\mu\nu} k^\mu x^\nu = -\omega t + \mathbf{k}\cdot\mathbf{x}$. The Fourier transformed EOM in terms of $h_{xy}(u,k)$ then read

$$4u^3 \partial_u \left(\frac{f}{u} \partial_u h_{xy}(u,k) \right) + \frac{u}{(\pi T)^2 f} \left(\omega^2 - k^2 f \right) h_{xy}(u,k) = 0 \ . \tag{2.46}$$

As we can see the EOM of h_{xy} is second order in u, so it requires two boundary conditions to specify a unique solution. The first boundary condition comes from the holographic dictionary: The boundary value of h_{xy} is identified with the source of the perturbation h^0_{xy}, i.e. $h_{xy}(u=0,k) = h^0_{xy}$. The second boundary condition must be imposed at the horizon. To derive this boundary condition, we look for a regular solution of Eq. (2.46) around $u = 1$. There are two such regular solutions near the horizon

$$h_{xy}(u \to 1, k) \propto (1-u)^p \quad , \quad p = \pm \frac{i\omega}{4\pi T} \ . \tag{2.47}$$

Which solution we choose as the boundary condition for h_{xy} is crucial. It will define whether the Green's function we are calculating is a retarded or advanced one. To see this, let us substitute Eq. (2.47) back into the Fourier transform (2.45). We find

$$h_{x,y}(u,x) \sim \exp\left[-i\omega t + i\mathbf{k}\cdot\mathbf{x}\right](1-u)^p = \mathrm{e}^{i\mathbf{k}\cdot\mathbf{x}} \exp\left[-i\omega \left(t \mp \frac{\ln(1-u)}{4\pi T} \right) \right] \ . \tag{2.48}$$

Now redefine the bulk co-ordinate u to $U = \ln(1-u)/4\pi T$. After this redefinition, the horizon is located at $U \to -\infty$ and the boundary at $U = 0$. More importantly, the time dependence of the graviton field $h_{x,y}$ in Eq. (2.48) becomes that of a plane wave, $h_{x,y} \sim \mathrm{e}^{-i\omega(t \mp U)}$. The graviton moves away from the horizon for the positive branch of p, but towards the horizon for the negative branch. Clearly, a black hole (classically) emitting gravitons cannot be black. Therefore, while we do have two regular solutions near the horizon, only the infalling $p = -i\omega/4\pi T$ solution is physical. From the QFT point of view, the choice of the infalling branch makes sure that the poles of the Green's function appear in the lower-half of the complex frequency plane. A Green's function with such poles is by definition a retarded one and respects causality [80].

To recapitulate, in order to calculate the retarded Green's function for the transverse components of the stress tensor $T^{xy}x$, we linearized the equations of motion via the metric perturbation (2.41). Then we derived the appropriate boundary conditions for the EOM by solving them near the

asymptotic boundary and the black hole horizon. In particular, we identified h_{xy} with the source of T^{xy} at the boundary and chose infalling boundary conditions at the black hole horizon. To incorporate both of these boundary conditions, we can choose a product ansatz for h_{xy},

$$h_{x,y}(u,k) = h^0_{xy}(k)H(u,k),$$

with

$$H(u=0,k) = 1 \quad , \quad H(u\to 1,k) = (1-u)^{-i\omega/4\pi T}.$$

Assuming we can solve the EOM for $H(u,k)$, we must then substitute the solution back into S_h. The result is the following functional of the source $h^0_{xy}(k)$ on the boundary spacetime

$$S_h = \int \frac{d^4k}{(2\pi)^4} \;\; h^0_{xy}(-k)\mathcal{F}(k,u)h^0_{xy}(k)\big|^{u=1}_{u=0} \;\; , \tag{2.49}$$

with

$$\mathcal{F}(k,u) = \frac{-1}{2\kappa^2}\sqrt{-g}g^{uu}H^*(u,k)\partial_u H(u,k) \;\; , \tag{2.50}$$

and star denoting complex conjugation. Now the holographic dictionary, as formulated in Eq. (2.9), tells us that the Green's function for T^{xy} is given by the second variation of S_h with respect to h^0_{xy}, i.e.

$$G_R^{T^{xy},T^{xy}}(k) = [-\mathcal{F}(k,u) - \mathcal{F}(-k,u)]^{u=1}_{u=0} = -2Re\,[\mathcal{F}(k,u)]^{u=1}_{u=0} \;\; , \tag{2.51}$$

where the last equality follows from $\mathcal{F}^*(k,u) = \mathcal{F}(-k,u)$ which in turn is a consequence of S_h being a real functional. As we can see $G_R^{T^{xy},T^{xy}}(k)$ is a purely real function, contrary to the traditional lore of Green's functions which dictates Green's functions are in general complex functions of their arguments [80]. This is a result of working in *imaginary* time. However, the Green's function appearing in Kubo formulae and which dictates transport is necessarily a function of *real* time in order to enforce causality[14]. We may derive the required real time Green's function through the Euclidean result via analytical continuation [82].

We may also derive the Green's function in real time using the Schwinger-Keldysh formalism [84, 85]. This formalism is more involved than the approach presented above. This is because finite temperature QFT is not readily defined in Minkowski signature; a finite temperature QFT is in a mixed state meaning it has no adiabatically connected in and out asymptotic states [83]. Instead, to define a thermal QFT in real time one needs to use

[14]There are no light-cones and hence no concept of causality in Euclidean signature, unless one prescribes a universal time as in non-relativistic mechanics.

the in-in or out-out Schwinger-Keldysh formalism [84, 85]. The Schwinger-Keldysh formalism was introduced into the AdS/CFT correspondence in [86] (see also [87–90]) and, fortunately, it confirms the calculation we have presented so far. In fact, the result turns out simpler than expected. More precisely the retarded Green's function is given by

$$G_R^{T^{xy},T^{xy}}(k) = -2\mathcal{F}(k, u = 0) \ . \tag{2.52}$$

An intuitive explanation of this formula is the following: In the Schwinger-Keldysh formalism, correlation functions are calculated by using two copies of the same system. The only difference between the two copies is that while one propagates forward in time, the other propagates backwards (see Fig 2.1). Therefore, one can run the algorithm for calculating Green's functions above also in the Schwinger-Keldysh formalism, by applying it to each copy of the system. Extra care, however, must be taken when choosing the appropriate boundary conditions at the black hole horizons: The system propagating forward in time must employ the usual infalling boundary conditions. In contrast, the system propagating backwards in time must employ the outgoing boundary conditions, with $p = i\omega/4\pi T$. This way, we ensure that the black hole is indeed black for all observers. This difference in boundary conditions means that the infalling waves will cancel the contribution of the outgoing waves and, hence, the net effect of the black hole horizon on the Green's functions will be zero. Thus, we are left only with the Green's function contribution stemming from the asymptotic boundary. Assuming time-reversal invariance[15], these boundary contributions will be the same and give the result (2.52).

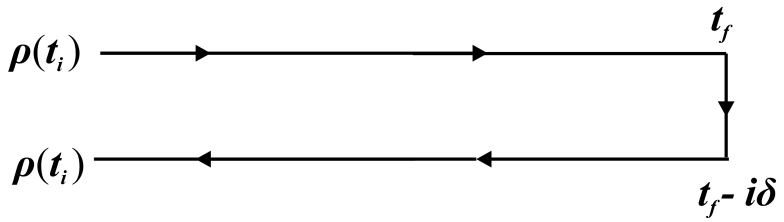

Figure 2.1: Schwinger Keldysh contour for out of equilibrium QFT. The initial state $\rho(t_i)$ of the system propagates from time t_i to time t_f along the real axis. Then the state propagates for an arbitrary imaginary time δ before returning to t_i and its initial state along the real axis.

After this long discussion, we are now ready to apply Eq. (2.52) and write down the two-point Green's function of T^{xy}. In particular, we have

[15] More precisely, we assume the QFT respects a symmetry involving time reversal, e.g. CPT invariance.

for $G_R^{T^{xy},T^{xy}}$ at zero wave-momentum [30]

$$G_R^{T^{xy},T^{xy}}(\omega,0) = -i\omega\frac{\pi^3\beta^{-3}L^3}{2\kappa^2} = -i\omega\frac{1}{2\kappa^2}\left(\frac{L}{z_h}\right)^3 \ , \tag{2.53}$$

where in the last equality we used $z_h = \beta/\pi$ stemming from Eq. (2.12). Therefore, the shear viscosity η finally reads

$$\eta = \frac{1}{2\kappa^2}\left(\frac{L}{z_h}\right)^3 \ . \tag{2.54}$$

Let us now combine the result for η with our result for the entropy density s, (2.24), for $d = 3$. Doing so, leads to the celebrated KSS bound for the ratio of η/s given by [29]

$$\frac{\eta}{s} = \frac{1}{2\kappa^2}\left(\frac{L}{z_h}\right)^3 \frac{\kappa^2}{2\pi}\left(\frac{L}{z_h}\right)^{-3} = \frac{1}{4\pi} \ . \tag{2.55}$$

This particular value for η/s is not simply a feature of the specific black hole solution we used. Rather, any rotationally invariant black hole solution of the Einstein-Hilbert action leads to exactly the same result for η/s for any spacetime dimension [91]. In this sense, the KSS bound is a universal feature of all infinitely-coupled rotationally invariant fluids. The question is, however, if going away from the infinite coupling limit, and towards more realistic QFTs, alters the value of η/s and how? We review the answer to this question in the following subsection.

2.4.1 Coupling corrections

The gravitational action contains every parameter of the boundary QFT. So in order to introduce coupling corrections to the KSS bound (2.55), we must understand how the coupling of the QFT enters the action. Clearly, the Einstein-Hilbert term $\sim R$ is coupling independent. Recall, however, Eq. (2.1)

$$\left(\frac{L}{l_s}\right)^4 = \lambda \ , \tag{2.56}$$

where λ is the 't Hooft coupling. Further note that, because L is the curvature radius of AdS space, $R \sim L^{-2}$ and we can write

$$l_s^2 R \sim \frac{1}{\sqrt{\lambda}} \ . \tag{2.57}$$

Therefore, coupling corrections to η/s can be introduced via the inclusion of curvature terms involving powers of R into the gravitational action. More precisely, if we are interested in coupling corrections up to order $\lambda^{-n/2}$, with n a positive integer, we must modify the Einstein-Hilbert action to

$$S_{\rm grav} = \frac{-1}{2\kappa^2}\int d^5x\sqrt{g}\ \left(R - 2\Lambda + \sum_{i=1}^{i=n} c_i l_s^{2i} R^{i+1}\right)\ . \tag{2.58}$$

Let us explain the notation in Eq. (2.58): The R^{i+1} curvature term contains all the contractions of the product of $i+1$ Riemann tensors. Similarly, the c_i are $\mathcal{O}(1)$ numbers multiplying each higher Riemann tensor contraction. For example, the action for $n=1$ reads

$$S_{\rm grav} = \frac{-1}{2\kappa^2}\int d^{d+2}x\sqrt{g}\ \left[R - 2\Lambda + l_s^2\left(c_{1,1}R^2 + c_{1,2}R_{\mu\nu}^2 + c_{1,3}R_{\mu\nu\rho\sigma}^2\right)\right]\ , \tag{2.59}$$

with $R_{\mu\nu}^2 = R_{\mu\nu}R^{\mu\nu}$, $R_{\mu\nu\rho\sigma}^2 = R_{\mu\nu\rho\sigma}R^{\mu\nu\rho\sigma}$. Note that in order to consistently truncate the series of corrections to a finite order n, we must assume that $l_s R \ll 1$, i.e. $1/\lambda$ acts as a perturbation parameter.

Apart from the Riemann tensor, coupling corrections to $S_{\rm grav}$ appear also due to higher derivative terms of matter fields. To see this recall that the matter fields on AdS_5 stem from the dimensional reduction of the metric on the S^5. Since the curvature radius of S^5 is also L^{-2}, we may schematically re-express Eq. (2.56) as

$$l_s^2\partial_\mu\partial^\mu\phi \sim \frac{1}{\sqrt{\lambda}}\ , \tag{2.60}$$

for any matter field ϕ on AdS_5. Hence, the inclusion of any higher derivative term in the gravitational action captures the effect of coupling corrections in the dual QFT.

Remarks:

• Our analysis of coupling corrections was based on the explicit $D3$-brane construction of [26]. However, a similar analysis holds for any gravitational dual based on a similar Dp-brane construction [92]. The only essential difference between the $p=3$ case and the rest is that the 't Hooft coupling $\lambda_{p\neq 3}$ is no longer dimensionless. Consequently, $\lambda_{p\neq 3}$ has in general a non-trivial RG flow that needs to be taken into account in the gravitational action. This can be achieved by the inclusion of a scalar field ϕ, the dilaton, into the gravitational action. The dilaton can be thought of as a deformation of the boundary QFT by a relevant scalar operator with coupling $\lambda_{p\neq 3}$. Furthermore, ϕ couples to gravity and can deform the bulk geometry. This deformation can be interpreted as the geometric realization of the RG flow [30, 64]. For our purposes, it is important to note that the dilaton also depends on $\lambda_{p\neq 3}$ and must be taken into account when discussing coupling corrections in $p\neq 3$. More precisely [92],

$$\mathrm{e}^{\phi} \sim \lambda_{p\neq 3}^{(7-p)/2}\ . \tag{2.61}$$

• Recall that higher derivative corrections in the gravitational action are naturally generated by quantum effects. These quantum effects were suppressed in our construction of the gauge/gravity correspondence by taking $g_s \ll 1$ and $N \gg 1$. This means that higher derivative corrections can also induce $1/N$ corrections, instead of coupling corrections, to η/s. To avoid mixing and matching $1/N$ corrections with $1/\lambda$ corrections, we must work in the tree-level approximation for the gravitational action. For example, one should not use QFT observables that stem purely from loop effects, such as anomalies, to match observables derived from a higher derivative $S_{\rm grav}$.

Finally, let us give a brief survey of the known coupling corrections to η/s, following [93] as well as the original publications mentioned below.

Quadratic Lagrangian: The quadratic curvature corrections take the form of (2.59) in general $d+2$ bulk dimensions

$$S_{\rm grav} = \frac{-1}{2\kappa^2}\int d^{d+2}x\sqrt{g}\ \left[R - 2\Lambda + l_s^2\left(c_{1,1}R^2 + c_{1,2}R_{\mu\nu}^2 + c_{1,3}R_{\mu\nu\rho\sigma}^2\right)\right]\ , \tag{2.62}$$

with $R_{\mu\nu}^2 = R_{\mu\nu}R^{\mu\nu}$, $R_{\mu\nu\rho\sigma}^2 = R_{\mu\nu\rho\sigma}R^{\mu\nu\rho\sigma}$. The coefficients $c_{1,i}$ are not uniquely defined: $S_{\rm grav}$ is defined only up to $\mathcal{O}(1/\sqrt{\lambda})$. Thus, any transformation of the metric that leaves the action invariant up to the same order in λ is a symmetry of the truncated theory. In particular, we can transform the metric $g_{\mu\nu} \to g_{\mu\nu} + \delta g_{\mu\nu}$ with

$$\delta g_{\mu\nu} = l_s^2 a R_{\mu\nu} + l_s^2 b R g_{\mu\nu}\ , \tag{2.63}$$

with a, b $\mathcal{O}(1)$ numbers. The effect of $\delta g_{\mu\nu}$ up to quadratic order in R is to shift the constants $c_{1,1}$ and $c_{1,2}$ as [94]

$$c_{1,1} \to c_{1,1} + \frac{1}{2}a + \frac{3}{2}b\ \ ,\ \ c_{1,2} \to c_{1,2} - a\ . \tag{2.64}$$

Clearly, we can set $c_{1,1} = 0 = c_{1,2}$ by choosing $a = c_{1,2}$ and $b = -2c_{1,1}/3 - c_{1,2}/3$. This shows that only $c_{1,3}$ leads to any physical change in η/s. Another useful choice for a and b is the following

$$a = c_{1,2} + 4c_{1,3}\ \ ,\ \ b = -\frac{2}{3}c_{1,3} - c_{1,1}\ . \tag{2.65}$$

Using Eq. (2.65), we can bring the quadratic corrections in $S_{\rm grav}$ into the topological Gauss-Bonnet (GB) form

$$S_{\rm grav} = \frac{-1}{2\kappa^2}\int d^{d+2}x\sqrt{g}\ \left[R - 2\Lambda + l_s^2 c_{1,3}\left(R^2 - 4R_{\mu\nu}R^{\mu\nu} + R_{\mu\nu\rho\sigma}R^{\mu\nu\rho\sigma}\right)\right]\ . \tag{2.66}$$

Bringing the R^2 coupling corrections to the GB form is useful for two reasons: First, despite the GB form being higher order, the EOM stemming from it

are second order. This means that quadratic or GB gravity avoids the usual Ostrogadski instabilities plaguing higher derivative theories [95, 96]. Equivalently, the propagating degrees of freedom of GB gravity are GR gravitons (with a modified propagator [97]). Second, the GB form is non-trivial only for $d+2 \geq 5$. As a result, the ratio η/s for QFTs living in $d = 2^{16}$ spatial dimensions does not receive any corrections at this order[17]. More precisely, following the same procedure as in section 2.4, we find for η/s equals the KSS bound for $d = 2$, while for $d \geq 3$ [97]

$$\begin{aligned} \frac{\eta}{s} &= \frac{1}{4\pi}\left(1 - 2(d+1)(d-2)c_{1,3}\frac{l_s^2}{L^2}\right) \\ &\overset{(2.56)}{=} \frac{1}{4\pi}\left(1 - \frac{2(d+1)(d-2)c_{1,3}}{\sqrt{\lambda}}\right). \end{aligned} \tag{2.67}$$

The resulting η/s scales with λ as expected from our general discussion on coupling corrections. We can now ask whether the coupling corrections violate the KSS bound. To do so, we must match the $c_{1,3}$ coefficient to some parameter of the boundary QFT. This was done in [98, 99] for a large class of superconformal theories. They found that η/s violates the KSS bound for several of these theories. Let us focus on the violation of the bound found in [99] for $\mathcal{N} = 2$ Sp(N) gauge theory

$$\frac{\eta}{s} = \frac{1}{4\pi}\left(1 - \frac{1}{2N}\right) . \tag{2.68}$$

Clearly this is a peculiar result, the coupling correction has turned out to be an $1/N$ correction. The reason for this is that both [98, 99] have used the conformal anomaly of superconformal theories to calculate $c_{1,3}$. Anomalies are fully quantum, loop effects. This violates our remark that only tree-level observables must be used for matching and has led to the transmutation of the coupling correction to an $1/N$ correction.

The question then becomes, can we identify $c_{1,3}$ with a tree-level QFT observable and does it lead to a violation of the bound? The answer was given in the negative in [100]. More precisely, the authors of [100] have shown that treating the action of quadratic gravity at tree-level leads to causality violation, since it allows for spacetimes with e.g. closed timelike curves. Although closed timelike curves are interesting for science-fiction[18],

[16] The shear viscosity is undefined in $d = 1$ since T^{xy} cannot exist.

[17] Note that the dilaton ϕ spoils this argument for $d = 2$. However, ϕ appears at least quadratically in the action [98] and, hence, leads to sub-leading $\lambda_{p\neq 3}^{-5/2}$ corrections.

[18] See "By His Bootstraps" by A. MacDonald for an example, highlighting the bootstrap paradox associated to closed timelike curves.

and maybe computer science [101], they are not a desirable feature of physical theories. Therefore, at tree level the $c_{1,i}$s must be set to zero and η/s equals again the KSS bound.

To close our discussion on quadratic gravity, let us consider what happens to η/s when additional matter fields are included. In particular, we consider QFTs away from charge neutrality by including a dynamical gauge field into the bulk gravitational action. The terms that can alter η/s have the schematic form RF^2. The coefficients multiplying these terms are again subject to change under field redefinitions. Using these field redefinitions, one can set to zero most of the coefficients and find the following "minimal" action [94]

$$S_{\text{grav}} = \frac{-1}{2\kappa^2}\int d^{d+2}x\sqrt{g}\ \left[(R-2\Lambda)+l_s^2 c_{RFF}R_{\mu\nu\rho\sigma}F^{\mu\nu}F^{\rho\sigma}\right]\ . \tag{2.69}$$

The coefficient c_{RFF} is the coupling constant of the bulk photon-graviton interaction. As such, it can generically take any value. However, in superconformal theories it necessarily takes the value $c_{RFF} = -c_{1,3}/2$ [94]. Therefore, for tree-level duals at a finite charge density, $c_{RFF} = 0$ and η/s is still given by the KSS bound. Despite this, let us quote the result for η/s for a generic c_{RFF} and $d = 3$ [94]

$$\frac{\eta}{s} = \frac{1}{4\pi}\left(1+\frac{32\bar{\mu}^2 c_{RFF}}{(1+\sqrt{1+2\bar{\mu}^2/3})^2}\frac{1}{\sqrt{\lambda}}\right)\ , \tag{2.70}$$

with $\bar{\mu} = \mu/T$. Equation (2.70) shows that for $c_{RFF} < 0$, the KSS bound is violated when we move away from charge neutrality.

Cubic gravity: We now consider gravitational actions containing cubic terms in the Ricci scalar. The discussion regarding cubic gravity is far shorter than that of quadratic gravity. This is because of early work on supergravity theories stemming as low-energy limits of superstring theory. In particular, it was shown in [102] that the kinematics of graviton-graviton scattering generated by cubic curvature terms are inconsistent with supersymmetry. Therefore, cubic terms cannot be generated by a parent string theory and hence cannot appear in the gravitational action. This means that η/s does not receive coupling corrections at order $1/\lambda$.

For those not fond of supersymmetry, note that the $1/\lambda$ corrections are absent even if we break supersymmetry explicitly. More precisely, [92] shows that cubic curvature corrections also lead to causality violation in the bulk geometry and, hence, must be dropped from the action. This result is again at tree level, hence the results of [92] leave open the question of $1/N$ corrections to η/s from cubic curvature corrections in non-supersymmetric QFTs.

Quartic gravity: Finally, let us discuss gravitational actions which include quartic curvature terms. Our general discussion on coupling correc-

tions, shows that the R^4 terms contribute to order $\lambda^{-3/2}$ in η/s [19]. A general analysis of the quartic corrections to η/s in any dimension does not exist. However, a comprehensive analysis for the original AdS_5 dual of $\mathcal{N}=4$ SYM does exist [103, 104]. In particular the 10-dimensional supergravity action relevant to the η/s calculations at quartic order is given by[20]

$$S_{10} = \frac{-1}{2\kappa_{10}^2}\int d^{10}x\sqrt{-G}\left[R + l_s^6\gamma W\right] \ , \tag{2.71}$$

with $\gamma = \zeta(3)/8$, $\zeta(3) \simeq 1.2$ is Apéry's constant and G the 10-dimensional metric, with Ricci scalar R defined by

$$ds_{10}^2 = G_{MN}dX^M dX^N = \mathrm{e}^{-10\nu/3}ds_5^2 + \mathrm{e}^{2\nu}ds_{S^5}^2 \ . \tag{2.72}$$

The line elements $ds_{S^5}^2$ is that of the unit 5-sphere, while ds_5^2 is a warped version of the metric (2.44)

$$ds_5^2 = \frac{L^2\mathrm{e}^b}{4u^2 f(u)}du^2 + \frac{(\pi TL)^2}{u}\left(-\mathrm{e}^a f(u)dt^2 + d\mathbf{x}^2\right) \ , \tag{2.73}$$

with

$$\begin{aligned} a(u) &= -15l_s^6\gamma\left(5u^2 + 5u^4 - 3u^6\right) \ , \\ b(u) &= 15l_s^6\gamma\left(5u^2 + 5u^4 - 19u^6\right) \ , \qquad (2.74) \\ \nu(u) &= \frac{15l_s^6\gamma}{32}u^4\left(1+u^2\right) \ . \qquad (2.75) \end{aligned}$$

Finally, W is a quartic polynomial of the Weyl tensor $C_{\mu\nu\rho\sigma}$, i.e. of the traceless part of the Riemann tensor

$$W = C^{\alpha\beta\gamma\delta}C_{\epsilon\beta\gamma\zeta}C^{\eta\kappa\epsilon}_{\ \ \alpha}C^{\zeta}_{\ \eta\kappa\delta} + \frac{1}{2}C^{\alpha\beta\gamma\delta}C_{\epsilon\zeta\gamma\delta}C^{\eta\kappa\epsilon}_{\ \ \alpha}C^{\zeta}_{\ \eta\kappa\beta} \ . \tag{2.76}$$

One can substitute the metric G_{MN} into the action S_{10} and consistently reduce the 10-dimensional action down to a 5-dimensional one. In particular [103] found

$$S_{\rm grav} = \frac{\pi^3}{2\kappa_{10}^2}\int d^5x\sqrt{-g}\left[R + 20\mathrm{e}^{-16/3\nu} - \frac{40}{3}(\partial_\mu\nu)^2 - 8\mathrm{e}^{-40\nu/3} + l_s^6\gamma w\right] \ , \tag{2.77}$$

with $w = 180u^8 + 1800u^8\nu + \mathcal{O}(\nu^2)$. With $S_{\rm grav}$ at hand, we can run the same algorithm for calculating η/s described in this section. In particular,

[19] Again, we note that the dilaton contributes sub-leading corrections.

[20] In writing Eq. (2.71), we have neglected the dilaton as well as additional gauge fields appearing in it.

[103] found that η/s, including quartic corrections, does not violate the KSS bound and is given by

$$\frac{\eta}{s} = \frac{1}{4\pi}\left(1 + \frac{15\zeta(3)}{\lambda^{3/2}}\right) = \frac{1}{4\pi}\left(1 + \frac{15N^{-3/2}\zeta(3)}{g_{\mathrm{YM}}^3}\right) , \tag{2.78}$$

Note that because our starting point was a parent string theory of our 5-dimensional action, we can be certain that the correction to η/s is indeed due to the coupling and not $1/N$. Note further that in the last equality we have expressed λ in terms of the Yang-Mills coupling of the dual gauge theory. We did so, because the final form of Eq. (2.78), allows us to apply our formula for η/s for abelian gauge theories. Namely, we can replace g_{YM}^2 with the fine structure constant α of the abelian theory to find

$$\frac{\eta}{s} = \frac{1}{4\pi}\left(1 + \frac{15N^{-3/2}\zeta(3)}{\alpha^{3/2}}\right) . \tag{2.79}$$

One issue with this application of Eq. (2.78) to abelian field theories, is the physical interpretation of N. In non-abelian gauge theories, N is the rank of the gauge group. In abelian gauge theories, however, the rank of the gauge group is by default unity, so we cannot use it as an avatar of N[21]. Instead it is expected that for abelian field theories N is a flavour index, i.e. N counts the number of electron species of the dual QFT.

This concludes our overview of holography in general and on the bound on η/s in particular. We have shown how a theory of gravity is related to a strongly coupled QFT and how to match the observables between the two sides. We used this matching between observables to show how we can derive, first, the thermodynamic properties of a strongly coupled QFT and, second, the QFT's retarded Green's functions. These Green's functions are related to the transport properties of the QFT via the appropriate linear response Kubo formulae. In particular, we showed how we can derive the KSS bound for the ratio η/s of strongly coupled QFTs and discussed the effect of coupling corrections on said bound. We shall apply these results in chapters 4 and 5 in order to define the thermodynamics and transport coefficients appearing in our hydrodynamic simulations. Doing so, will allow us to understand the dynamics of strongly coupled systems through hydrodynamics. However, before we proceed to solving the hEOM we first derive them in the chapter that follows.

[21] Recall $N \gg 1$.

Chapter 3

Hydrodynamics

In the present chapter we present a short review of hydrodynamics. In particular, we derive the hydrodynamic constitutive relations for parity-breaking, $2+1$ dimensional charged relativistic fluids. We begin our derivation by reviewing the construction of the hydrodynamic equilibrium effective action and constitutive relations of [105–108] in section 3.1. We apply this formalism in section 3.2 to derive the equilibrium constitutive relations. Then, we use a more general symmetry argument that allows us to describe diffusive effects in section 3.3, following [9]. Having written down the constitutive relations, we use them to derive Kubo formulae for the hydrodynamic transport coefficients in section 3.4. The final part of our review of hydrodynamics contains a short discussion on turbulence and its phenomenology in section 3.5.

3.1 Equilibrium partition function

We begin our journey towards the hydrodynamics of charged relativistic fluids by first recounting some basic facts regarding equilibrium partition functions, as found in [105, 106]. The starting point of the equilibrium partition function method is the fact that hydrodynamics is a framework for describing thermalized matter. Therefore the quantum state of a fluid in thermal equilibrium is described by a thermal density matrix of the form

$$\rho = \exp\left[-\sum_{i=1}^{n} \mu_i^a Q_a^i\right] = \exp\left[-\mu_i^a Q_a^i\right] \ , \tag{3.1}$$

with n the number of conserved charges of the system $\{Q_a^i\}$ and $\{\mu_i^a\}$ the corresponding conjugate thermodynamic variables/chemical potentials. The index a is a placeholder for any internal symmetry index carried by non-abelian charges.
Given ρ we can define the partition function of the system through the trace,

$$\mathcal{Z} = \mathcal{Z}[\mu_i^a] = \mathrm{Tr}\,[\rho] \equiv \exp(-W)\ , \tag{3.2}$$

where W is the effective action of the system[1].
The partition function $\mathcal{Z}$ (the effective action W) is extremely useful, because we can use it to derive the thermal average of the charges Q_a^i via

$$\langle Q_a^i \rangle = \frac{\mathrm{Tr}\left[\rho Q_a^i\right]}{\mathrm{Tr}\,[\rho]} = -\frac{\partial \log \mathcal{Z}}{\partial \mu_i^a} = \frac{\partial W}{\partial \mu_i^a}\ . \tag{3.3}$$

In fact one can go even further and define all possible connected correlation functions for say N charges in terms of W [75][2]

$$\langle Q_{a_1}^{i_1} Q_{a_2}^{i_2} ... Q_{a_N}^{i_N} \rangle_{\mathrm{conn}} = (-)^{N+1} \frac{\partial^N W}{\partial \mu_{i_1}^{a_1} \partial \mu_{i_2}^{a_2} ... \partial \mu_{i_N}^{a_N}}\ . \tag{3.4}$$

The thermal density matrix ρ as it stands in Eq. (3.1) can describe any possible system is in thermal equilibrium, as long as the charges are specified. To particularize ρ to the case of hydrodynamics, we will assume that the underlying system has a continuum description on a spacetime M with metric $g_{\mu\nu}$. Then, we can express the Q_a^i, as well as ρ in terms of the charge current densities $\mathcal{Q}_a^{i,\mu}$ viz.

$$Q_a^i = \int_V d\Sigma_\mu\ \mathcal{Q}_a^{i,\mu}\ , \tag{3.5}$$

$$\rho = \exp\left[-\int_\Sigma d\Sigma_\mu\ \mu_i^a \mathcal{Q}_a^{i,\mu}\right] = \exp\left[-\int_\Sigma d\Sigma\ \mu_i^a \mathcal{Q}_a^{i,\mu} n_\mu\right]\ , \tag{3.6}$$

where Σ is a spatial hypersurface of co-dimension one on M normal to n_μ and with volume element $d\Sigma$. Note that we pulled μ_a^i into the spatial integral, since it is a spacetime constant in equilibrium.

Now that we have included the $\mathcal{Q}_a^{i,\mu}$ into the theory, we may wonder whether we can derive its expectation value using an equation similar to (3.3). The answer is yes, but to show how we must first bring Eq. (3.6) into a more convenient form. To do that, we will assume the existence of a timelike Killing vector $V = N\partial_t$ on M. This timelike Killing vector can be thought of as the time-direction of the observer for which the system in thermal equilibrium. Given V, we can express the metric M and invariant volume element, dV, on M as [109]

$$ds^2 = -N^2 dt^2 + \gamma_{ij} dx^i dx^j \Rightarrow dV = N dt d\Sigma\ , \tag{3.7}$$

[1] If the system is described by the canonical ensemble, W equals the free energy over the temperature of the system.

[2] We restrict ourselves to connected diagrams, because these respect causality in "healthy" quantum field theories and, hence, are in principle well-defined observables [75].

with γ_{ij} the metric on Σ and $L \equiv \int N dt$ the length of the time dimension of M. Then

$$\begin{aligned}\mathcal{Z} &= \mathrm{Tr}\exp\left[-L^{-1}L\int_\Sigma d\Sigma\ \mu_i^a \mathcal{Q}_a^{i,\mu} n_\mu\right] \\ &= \mathrm{Tr}\exp\left[-\int_M dV\ \left(\mu_i^a n_\mu L^{-1}\right)\mathcal{Q}_a^{i,\mu}\right]\ ,\end{aligned} \tag{3.8}$$

where again we assume L to be constant in spacetime. Given $\mathcal{Z}$ as in Eq. (3.8), we can re-interpret it as a special case of the QFT generating functional for $\mathcal{Q}_a^{i,\mu}$ defined as

$$Z = Z[A_{i,\mu}^a] = \left\langle \exp\left[-\int_M dV A_{i,\mu}^a \mathcal{Q}_a^{i,\mu}\right]\right\rangle\ . \tag{3.9}$$

Clearly for a timelike $A_{i,\mu}^a \propto n_\mu$, we recover $\mathcal{Z}$. Using this similarity between Z and $\mathcal{Z}$, we see that we can write down a generating functional for all of the components of $\mathcal{Q}_a^{i,\mu}$ by introducing an external field $A_{i,\mu}^a$ into $\mathcal{Z}$ as

$$\mathcal{Z} = \mathcal{Z}[\mu_i^a, A_{i,\mu}^a] = \mathrm{Tr}\exp\left[-\int_M dV\ \left(\mu_i^a n_\mu L^{-1} + A_{i,\mu}^a\right)\mathcal{Q}_a^{i,\mu}\right]\ . \tag{3.10}$$

Note that the timelike part of $A_{i,\mu}^a$ alters the chemical potential μ_i^a and hence the value of the equilibrium charge Q_a^i [110]. In order to avoid this, we choose to absorb μ_i^a into $A_{i,\mu}^a$ and define the partition function as

$$\mathcal{Z} = \mathcal{Z}[A_{i,\mu}^a] = \mathrm{Tr}\exp\left[-\int_M dV\ A_{i,\mu}^a \mathcal{Q}_a^{i,\mu}\right]\quad ,\quad A_{i,\mu}^a n^\mu = -\mu_i^a L^{-1}\ . \tag{3.11}$$

Choosing the timelike component of $A_{i,\mu}^a$ to be proportional to μ_i^a defines the so-called thermodynamic frame of hydrodynamics. If one wants to work in a more general frame, they must then re-define the chemical potentials as

$$\Lambda_i^a + A_{i,\mu}^a n^\mu = -\mu_i^a L^{-1}\ , \tag{3.12}$$

where Λ_i^a can be thought of as a gauge-fixing element, similar to the Maurer-Cartan form in usual gauge theories [111, 112][3].
Equation (3.21) means we must fix the gauge where A_μ's is trivially zero. Finally, we can take variations of $\mathcal{Z}[A_{i,\mu}^a]$ to derive $\mathcal{Q}_a^{i,\mu}$, and their connected correlation functions i.e.[4]

[3] We clarify this statement with an explicit example in the following.

[4] We define the variation of W as $\delta W = \int dV \delta A_{i,\mu}^a \delta W/\delta A_{i,\mu}^a$. This definition, allows us to drop the usual metric determinant factor present in textbook definitions of Eq. (3.13) [112].

$$\langle \mathcal{Q}^{i_1,\mu_1}_{a_1} \mathcal{Q}^{i_2,\mu_2}_{a_2} ... \mathcal{Q}^{i_N,\mu_N}_{a_N} \rangle_{\text{conn}} = (-)^{N+1} \frac{\delta^N W}{\delta A^{a_1}_{i_1,\mu_1} \delta A^{a_2}_{i_2,\mu_2} ... \delta A^{a_N}_{i_N,\mu_N}} \Big|_{A^a_{i,\perp}=0} , \tag{3.13}$$

with $(A^a_{i,\perp})_\mu = A^a_{i,\mu} + A^a_{i,\mu} n^\mu$, the part of $A^a_{i,\mu}$ normal to n_μ.

We have seen that introducing $A^a_{i,\mu}$ into $\mathcal{Z}$ enables us to derive $\langle \mathcal{Q}^{i,\mu}_a \rangle$. But, if we are smart in the way we introduce $A^a_{i,\mu}$, we can also derive the conservation equations satisfied by $\mathcal{Q}^{i,\mu}_a$. To perform this derivation, consider an infinitesimal deformation of $A^a_{i,\mu}$ of the form

$$A^a_{i,\mu} \to A^a_{i,\mu} + \delta_\xi A^a_{i,\mu} \quad , \quad \delta_\xi A^a_{i,\mu} n^\mu = 0 \ , \tag{3.14}$$

where ξ is the deformation parameter[5] and we assumed the deformation is normal to n^μ in order to keep the value of the chemical potential fixed. Under the deformation Eq. (3.14), the partition function becomes

$$\begin{aligned} \mathcal{Z}[A^a_{i,\mu} + \delta_\xi A^a_{i,\mu}] &= \left\langle \exp\left[- \int_M dV \ \delta_\xi A^a_{i,\mu} \mathcal{Q}^{i,\mu}_a \right] \right\rangle \\ &\simeq \mathcal{Z}[A^a_{i,\mu}] - \int_M dV \ \delta_\xi A^a_{i,\mu} \langle \mathcal{Q}^{i,\mu}_a \rangle \ . \end{aligned} \tag{3.15}$$

Now comes the crux of the whole argument. We usually know the conservation law obeyed by $\mathcal{Q}^{i,\mu}$ through Noether's theorem [11]. So we can try fixing $\delta_\xi A_\mu$ such that the RHS of Eq. (3.15) is proportional to the conservation equation and vanished identically on-shell. Hence,

$$\delta_\xi \mathcal{Z} = \mathcal{Z}[A^a_{i,\mu} + \delta_\xi A^a_{i,\mu}] - \mathcal{Z}[A^a_{i,\mu}] = - \int_M dV \ \delta_\xi A^a_{i,\mu} \langle \mathcal{Q}^{i,\mu}_a \rangle = 0 \tag{3.16}$$

and $\mathcal{Z}$ is invariant under the deformation (3.14) of $A^a_{i,\mu}$. The reader might have noticed that this method of fixing the transformation law of external fields is exactly the Noether procedure for gauging a global symmetry [113]. Therefore we may think of $A^a_{i,\mu}$ as a non-dynamical gauge field, and $\mathcal{Z}[A^a_{i,\mu}]$ as a gauge invariant functional. Working the logic of our argument backwards, we can infer the conservation laws for a given set of charges by introducing their associated gauge fields into $\mathcal{Z}$ and enforcing Eq. (3.16).[6]

Remarks:

• The gauge invariance is with respect to the restricted or residual gauge transformations of Eq. (3.14) which keep the chemical potential fixed. This distinction is of nil importance for equilibrium partition functions, but becomes crucial when considering the out of equilibrium case [114].

[5] That is $\delta_{\xi=0} = 0$.

[6] We will see examples of this procedure in the following.

• We can incorporate any possible anomaly present in the equations of motion by loosening the assumption $\delta_\xi \mathcal{Z} = 0$ to

$$\delta_\xi \mathcal{Z} = \int dV G(\xi, A^a_{i,\mu}) \ , \tag{3.17}$$

where $G(\xi, A^a_{i,\mu})$ is the anomaly of the symmetry generating $\mathcal{Q}^{i,\mu}_a$.

Examples:

Global $U(1)$ conserved charge: Consider a conserved electromagnetic charge Q with charge current density J^μ. Then the external field generating correlation functions of J^μ is a co-vector field A_μ. Its timelike part defines the usual chemical potential via

$$Ln^\mu A_\mu = \mu/T,$$

with T the temperature of the system[7].

The conservation law for the current J^μ is simply

$$\partial_\mu J^\mu = \partial_i J^i = 0 \ . \tag{3.18}$$

The second equality holds because we are by assumption in a static equilibrium with $\partial_t = 0$. In order to generate the conservation law of Eq. (3.18) from Eq. (3.16), we choose the co-vector field to transform as

$$A_0 \to A_0 \quad , \quad A_i \to A_i + \partial_i \xi. \tag{3.19}$$

In a static equilibrium, we can rewrite Eq. (3.19) as

$$A_\mu \to A_\mu + \partial_\mu \xi \ . \tag{3.20}$$

Hence A_μ can be thought of as a $U(1)$ gauge field[8]. The gauge covariance of A_μ allows us to clarify the role of Λ^a_i in Eq. (3.12). Namely, the conservation of J^μ implies that we can relax the condition $\mathcal{L}_V A_\mu = 0$ to $\mathcal{L}_V A_\mu =$ pure gauge. That is, there exists a scalar function Λ such that

$$\mathcal{L}_V A_\mu + \partial_\mu \Lambda = 0 \ . \tag{3.21}$$

Because of (3.21), the chemical potential of (3.1) is no longer time-independent

$$\mathcal{L}_V (\mu/T) = -\mathcal{L}_V \Lambda \Leftrightarrow \mathcal{L}_V \left(\mu/T + \Lambda\right) = 0 \ . \tag{3.22}$$

The final equality, however, shows that the chemical potential shifted by Λ is a time-independent quantity and can be used to define thermal equilibrium.

[7]Note that we have absorbed a minus sign into μ compared to the definition Eq. (3.11). This was done to follow the usual convention for μ in thermodynamics.

[8]Note again the crucial role of static equilibrium for enlarging Eq. (3.19) to the full $U(1)$ gauge symmetry Eq. (3.19).

The above discussion shows that μ/T in our formalism is defined modulo the gauge transformation Λ which cancels A_μ's time-evolution. This is why Λ, and Λ_i^a in general, can be thought of as gauge-fixing parameters.

Energy-momentum conservation: As a final example, let us consider the case of a conserved energy E and momentum P^i. Since we are interested in relativistic hydrodynamics, we assume that these conserved quantities compile into a single Lorentz vector P^μ. The corresponding energy-momentum density is given by the energy-momentum tensor $T^{\mu\nu} = T^{\nu\mu}$. We call the respective external field that couples $T^{\mu\nu}$ by $g_{\mu\nu}$. Note that in this case, the generating functional is usually written with an extra factor of $1/2$

$$\mathcal{Z}[g_{\mu\nu}] = \mathrm{Tr}\exp\left[-\int_M dV\ \frac{1}{2}T^{\mu\nu}g_{\mu\nu}\right]\ , \tag{3.23}$$

and the counterpart of Eq. (3.13) with an extra factor of two.

The conjugate "chemical potential" is given by

$$Ln^\mu g_{\mu\nu} \equiv \beta_\nu\ . \tag{3.24}$$

The transformation law for $g_{\mu\nu}$ can be derived by observing that the conservation law for $T^{\mu\nu}$ is simply,

$$\nabla_\mu T^{\mu\nu} = 0.$$

with ∇_μ the covariant derivative on M. Hence, $g_{\mu\nu}$ transforms as[9]

$$g_{\mu\nu} \to g_{\mu\nu} - \nabla_{(\mu}\xi_{\nu)}. \tag{3.25}$$

The transformation law Eq. (3.25), allows us to identify $g_{\mu\nu}$ as the metric on M and ξ^μ as an infinitesimal diffeomorphism.

Finally, $g_{\mu\nu}$ being the metric implies

$$\beta_\mu = Ln_\mu\ . \tag{3.26}$$

Equation (3.26) allows us to give a physical meaning to L^{-1}. The quantum state corresponding to energy conservation is simply the Boltzmann distribution $\exp[-\beta H]$, with β the inverse temperature. In order for (3.23) to match the Boltzmann distribution, then $L = \beta$. For this reason, β_μ is also called the thermal vector.

Let us summarize what we have found out so far. We saw that a continuous system in a thermal state generated by the conserved charges $\{Q_a^i\}$ can be described by a generating functional $\mathcal{Z}[A_{i,\mu}^a]$ or an effective action W, which is gauge-invariant under the global symmetries that lead to the conservation of the $\{Q_a^i\}$. The timelike part of the external field $A_{i,\mu}^a$ can

[9] To be more precise, we should constrain ξ^ν to be spacelike and time independent, such that we do not change β_ν.

be identified with the chemical potential, μ_i^a, thermodynamically conjugate to Q_a^i. This way, the charged densities derived from W via Eq. (3.13) become functions of the chemical potentials. The expressions $\mathcal{Q}_a^{i,\mu} = \mathcal{Q}_a^{i,\mu}[\mu_i^a]$ are precisely the constitutive relations of hydrodynamics in global thermal equilibrium.

In order to deviate from global thermal equilibrium, we formally allow $A_{i,\mu}^a$ and hence μ_i^a to be functions in spacetime. However, we cannot allow $A_{i,\mu}^a$ to be generic functions on spacetime. This is because we relied on the time independence of μ_i^a in order to identify it with the timelike part of $A_{i,\mu}^a$ [10]. Therefore, we constrain the external gauge fields to be constant in the time direction by enforcing

$$\mathcal{L}_V A_{i,\mu}^a = 0 \quad , \quad V = N\partial_t \ , \tag{3.27}$$

where $\mathcal{L}_V$ is the Lie derivative in the direction of the timelike vector V [11]. Because of condition Eq. (3.27), W is also called the hydrostatic effective action.

On the practical side of things, in order to derive the constitutive relations we need to specify $\mathcal{Z}[A_{i,\mu}^a]$ or equivalently $W[A_{i,\mu}^a]$. To achieve this, we take a phenomenological approach and assume that W is the most general functional of $A_{i,\mu}^a$ that is consistent with the constraint Eq. (3.27) and the gauge symmetries of $\mathcal{Z}$, i.e. $\delta_\xi W = 0$ modulo anomalous terms. Of course, there are an infinite number of terms that are consistent with these two constraints and, hence, an infinite number of terms that enter the constitutive relations. This makes the problem of solving the hydrodynamic equations of motion (hEOM) intractable and so some approximations need to be made. The approximation usually employed is that of expanding W in powers of derivatives of $A_{i,\mu}^a$ as

$$W[A_{i,\mu}^a] = \int dV \ \left[P_0 + \mathcal{K} P_1 + \mathcal{K}^2 P_2 + ...\right] \ , \tag{3.28}$$

where P_0, P_1, P_2 depend on $A_{i,\mu}^a$, its first, and second derivatives respectively. The constant $\mathcal{K}$ is a length scale such that

$$\mathcal{K} \left| \frac{\partial_\mu A_{i,\nu}^a}{A_{i,\nu}^a} \right| \ll 1 \ . \tag{3.29}$$

Because of condition Eq. (3.29), we can truncate the expansion of W to some finite order in $\mathcal{K}$ and keep only a finite number of terms in the hEOM.

[10] A more fundamental reason is that the state of the system is given by a thermal density matrix only if the quantum analog of Liouville's theorem holds; ρ must be time-independent [110].

[11] In a system with a conserved symmetric energy-momentum tensor, as in Eq. (3.23), we may identify V^μ with the thermal vector β^μ.

Moreover, condition Eq. (3.29) implies that $A^a_{i,\mu}$ and hence $\mathcal{Q}^{i,\mu}$ vary significantly only in scales larger than $\mathcal{K}$ e.g. $\mathcal{Q}^{i,\mu}_a(x+a) \simeq \mathcal{Q}^{i,\mu}_a$ if $a \leq \mathcal{K}$. Therefore, we may think of the fluid as consisting of patches with size $\mathcal{K}$ which contain matter in thermal equilibrium "woven" together such that they can be described by continuous fields $A^a_{i,\mu}$. This physical picture also clarifies the physical meaning of $\mathcal{K}$: Thermal equilibrium is reached through the interaction between the constituents of a system. Hence, $\mathcal{K}$ maybe thought of as the maximum distance between fluid constituents that can interact with each other.

Concluding remark: Before we use the formalism laid above to derive the constitutive relations for charged relativistic fluids, let us remark on its existing extensions. We have seen that hydrodynamics is described by a classical effective action $W[A^a_{i,\mu}]$ that contains inside it all quantum effects. We can make this construction look "more quantum" by integrating in some new field degrees of freedom ϕ such that

$$\mathrm{e}^{-W[A^a_{i,\mu}]} \equiv \int D\phi \exp\left[-I[\phi, A^a_{i,\mu}]\right] \ . \tag{3.30}$$

The functional $I[\phi, A^a_{i,\mu}]$ defines the quantum action of the fields ϕ in the presence of external fields $A^a_{i,\mu}$. We choose $I[\phi, A^a_{i,\mu}]$, such that W is symmetric under the infinitesimal deformations δ_ξ and the equations of motion for ϕ are simply the hEOM. Both of these requirements can be satisfied by choosing ϕ to transform under δ_ξ and assuming that $I[\phi, A^a_{i,\mu}]$ is a functional of an invariant field combination schematically written as

$$B^a_{i,\mu} = M^{a,\nu}_{b,\mu}[\phi] A^b_{i,\nu} + C^a_{i,\mu}[\phi] \ . \tag{3.31}$$

The functionals $M^{a,\nu}_{b\mu}$ and $C^a_{i,\mu}$ are chosen such that $B^a_{i,\mu}$ is invariant under δ_ξ, $\delta_\xi B^a_{i,\mu} = 0$, and the equations of motion for ϕ are the $\mathcal{Q}^{i,\mu}_a$ conservation laws. For example, in the case of a $U(1)$ symmetry we can choose ϕ to be a compact scalar field ϕ such that

$$\delta_\xi \phi = -\xi \quad , \quad B_\mu = A_\mu + \partial_\mu \phi \ . \tag{3.32}$$

The physical reasons for introducing the ϕ field are the following: First, fixing the equations of motion of ϕ to be the conservation laws implies that ϕ constitutes the dynamical degrees of freedom of the fluid.[12] This allows us to include quantum, thermal and out-of-equilibrium fluctuations into hydrodynamics by applying on ϕ the in-in path integral or Schwinger-Keldysh formalism [83–85, 114, 115]. Second, as we can see from Eq. (3.32), ϕ generically appears in $B^a_{i,\mu}$ and, hence, in I only through its derivatives. Therefore ϕ enjoys a shift symmetry which renders it massless. Several

[12] For example, ϕ can be the Lagrangian co-ordinates of the fluid flow.

works on effective actions for hydrodynamics consider this massless field to be the Goldstone mode of the symmetry generating $\mathcal{Q}_a^{i,\mu}$ [114]. This allows us to apply all of the QFT machinery for writing down Goldstone boson effective actions [116, 117] in the realm of hydrodynamics [118].

We proceed with the derivation of the constitutive relations through the formalism laid out above in the following section.

3.2 Hydrostatic charged relativistic fluids

In this section, we will apply the formalism of [105,106] laid out in section 3.1 to the case of $2+1d$ parity-breaking relativistic hydrodynamics of charged fluids. The conserved charges for this case are the energy-momentum tensor and $U(1)$ current

$$\{\mathcal{Q}^a_{i,\mu}\} = \{T^{\mu\nu}, J^\mu\} \ . \tag{3.33}$$

The external fields that couple to $T^{\mu\nu}$, J^μ are the metric $g_{\mu\nu}$ and $U(1)$ gauge field, A_μ described in the previous section. The corresponding chemical potentials are the thermal vector $\beta_\mu = \beta n_\mu$ of Eq. (3.26) and chemical potential $\beta\mu = \beta^\mu A_\mu$. Since we are in static equilibrium, we assume the effective action W is invariant under diffeomorphisms and $U(1)$ gauge transformations under which $g_{\mu\nu}$ and A_μ transform as

$$\begin{aligned} x^\mu \to x'^\mu \ , \ g'_{\mu\nu}(x') = \frac{\partial x^a}{\partial x'^\mu}\frac{\partial x^b}{\partial x'^\nu} g_{ab}(x) \ , \\ A'_\mu(x') = \frac{\partial x^a}{\partial x'^\mu} A_a(x) \ , \ A'_\mu = A_\mu + \partial_\mu \lambda \ , \end{aligned} \tag{3.34}$$

with infinitesimal form

$$\begin{aligned} x'^\mu = x^\mu + \xi^\mu(x) \ , \ g'_{\mu\nu}(x') = g_{\mu\nu}(x) - \partial_{(\mu}\xi_{\nu)} \ , \\ A'\mu(x') = A_\mu(x) - A_a \partial_\mu \xi^a \ , A'_\mu = A_\mu + \partial_\mu \lambda \ . \end{aligned} \tag{3.35}$$

The infinitesimal transformations Eq. (3.35) lead to the field variations

$$\begin{aligned} \delta_\xi g_{\mu\nu} \equiv g'_{\mu\nu}(x) - g_{\mu\nu}(x) = -\mathcal{L}_\xi g_{\mu\nu} = -\nabla_{(\mu}\xi_{\nu)} \ , \\ \delta_\xi A_\mu = -\mathcal{L}_\xi A_\mu = -\xi^a F_{a\mu} - \partial_\mu(A_a \xi^a) \ , \delta_\lambda A_\mu = \partial_\mu \lambda \ . \end{aligned} \tag{3.36}$$

Using the variations in (3.36), we can translate the invariance of W into the conservation laws for energy-momentum and charge[13]

$$\nabla_\mu T^{\mu\nu} = -J_\mu F^{\mu\nu} + A^\nu \partial_\mu J^\mu = -J_\mu F^{\mu\nu} \ , \tag{3.37}$$

$$\partial_\mu J^\mu = 0 \ . \tag{3.38}$$

Because we are interested in parity breaking fluids, let us also note how $g_{\mu\nu}$, A_μ transform under parity. In $2+1$ dimensions we define parity as the diffeomorphism which inverts one spatial co-ordinate, say the y co-ordinate. Therefore, we define the parity operator $\mathcal{P}$

$$\mathcal{P} : x^\mu = (x^0, x, y) \to \mathcal{P}[x] = (x^0, x, -y) \ , \tag{3.39}$$

under which we find for $g_{\mu\nu}$, A_μ

$$\begin{gathered} A_\mu(x) \overset{\mathcal{P}}{\to} (A_0, A_1, -A_2)(\mathcal{P}[x]) \ , \\ g_{ay}(x) \overset{\mathcal{P}}{\to} -g_{ay}(\mathcal{P}[x]) \quad , \quad g_{yy}(x) \overset{\mathcal{P}}{\to} g_{yy}(\mathcal{P}[x]) \quad , \quad g_{ab}(x) \overset{\mathcal{P}}{\to} g_{ab}(\mathcal{P}[x]), \end{gathered} \tag{3.40}$$

with $a, b = x^0, \ x$.

Now that we have clarified the conserved charges and the conservation laws – Eq.s (3.37), (3.38) – for charged relativistic fluids, we need to resolve them in terms of β_μ and μ/T. To do so, we proceed with constructing the derivative expansion of W. We begin with the zeroth order in derivatives action. To zeroth order part of W consists only of the gauge and diffeomorphism invariant scalars, S_0, that can be constructed by the zeroth order data $g_{\mu\nu}$, A_μ and the thermal vector β_μ. If we are interested in breaking parity invariance we must also include the Levi-Civita tensor $\varepsilon_{\mu\nu\rho}$ into the list of data. Thus, the zeroth order scalars and effective action W_0 are simply

$$S_0 = \{\beta^2, \beta^\mu A_\mu\} \simeq \{T, \mu\} \ , \tag{3.41}$$

$$W_0 = \int dV P(S_0) = \int d^3x \sqrt{-g} \ P(T, \mu) \ , \tag{3.42}$$

where g is the metric determinant and both T and μ are assumed hydrostatic, i.e. the Lie derivative in the direction of β^μ vanishes identically, $\mathcal{L}_\beta = 0$[14].

Taking the variations of W with respect to $g_{\mu\nu}$ and A_μ, as shown in appendix B, we find the constitutive relations for $T^{\mu\nu}$ and J^μ

[13] Recall Eq.s (3.16) and (3.23).

[14] Being hydrostatic simply means that T and μ are time-independent. To see this, boost in a co-ordinate system where $\beta = \beta\partial_t$.

$$T^{\mu\nu} = \epsilon u^\mu u^\nu + P\Delta^{\mu\nu} \quad , \quad J^\mu = \rho u^\mu \ , \tag{3.43}$$

$$\epsilon = T\frac{\partial P}{\partial T} + \mu\rho - P \quad , \quad u^\mu = \frac{\beta^\mu}{\sqrt{-\beta^2}} \quad , \quad \Delta^{\mu\nu} = g^{\mu\nu} + u^\mu u^\nu \quad , \quad \rho = \frac{\partial P}{\partial \mu} \ . \tag{3.44}$$

The constitutive relations Eq. (3.43) alongside (3.44) define a perfect charged relativistic fluid in 2+1 dimensions with energy ϵ, pressure P, charge density ρ and velocity profile u^μ [9, 119, 120]. Note that the expression for the energy in Eq. (3.44) becomes the Gibbs-Duhem relation for charged matter in thermal equilibrium, when we identify the entropy density[15]

$$s = \frac{\partial P}{\partial T} \ .$$

Let us now go beyond the perfect fluid limit by including first order derivative corrections to W. Gauge invariance requires A_μ to appear in W only through μ/T or through the field strength[16]

$$F_{\mu\nu} = \partial_\mu A_\nu - \partial_\nu A_\mu = \partial_{[\mu} A_{\nu]} \ . \tag{3.45}$$

The remaining building blocks for the first order data are the gradients of temperature, chemical potential and velocity profile. To use these gradients though we must constrain them to be hydrostatic, $\mathcal{L}_\beta = 0$. Being hydrostatic allows us to resolve the aforementioned gradients into simpler first order data (see App. A)

$$\partial_\mu T = -T a_\mu \quad , \quad \partial_\nu \mu = -\mu a_\nu + E_\nu \quad , \quad \partial_\mu u_\nu = -u_\mu a_\nu + \omega_{\mu\nu} \quad . \tag{3.46}$$

where

$$a_\mu = u^\nu \partial_\nu u_\mu \ , \ E_\mu = F_{\mu\nu} u^\nu \ , \ \omega_{\mu\nu} = \Delta_{\mu a}\Delta_{b\nu}\partial^{[a} u^{b]}/2 \tag{3.47}$$

are the acceleration of the fluid, the electric field as seen in the rest frame of the fluid and the vorticity tensor of the fluid respectively. Equation (3.46) also teaches us that $G = \{u^\mu, a^\mu, E^\mu\}$ is an orthogonal co-ordinate system[17]. This implies that J^μ can be expanded in terms of G and its parity-odd counterpart $\tilde{G}$

[15] The Gibbs-Duhem relation can also be derived directly from the definition of entropy $S = -\mathrm{Tr}\,[\rho_N \log \rho_N]$ and the normalized thermal density matrix $\rho_N = \exp[-\beta(PV + H - \mu Q)]$.

[16] Recall μ/T has been gauge-fixed to a particular value, cf. discussion around Eq. (3.21).

[17] To show that $a_\mu E^\mu = 0$, perform the calculation in a co-ordinate system with $u^\mu = u\partial_t$. Then recall $a_\mu E^\mu$ is Lorentz invariant, when u^μ is also rotated along.

$$\tilde{G} = \{\epsilon_{\mu\nu\rho}u^\nu a^\rho, \epsilon_{\mu\nu\rho}u^\nu a^\rho\} \equiv \{(u\times a)_\mu, (u\times E)_\mu\} \ . \tag{3.48}$$

Having imposed the hydrodstatic constraints on the gradients of T, μ and u_μ we can now write down the most general first order scalars, S_1, that enter the effective action. We can generate S_1 somewhat algorithmically: We take the list of first order tensors, the gradients of T, μ and u_μ, and saturate them with the list of zeroth order vectors to produce scalars. Then we enforce (3.46) and keep the non-trivial results S_1. These are

$$S_1 = \frac{1}{2}\{\varepsilon_{\mu\nu\rho}u^\mu F^{\nu\rho}, \varepsilon_{\mu\nu\rho}u^\mu\omega^{\nu\rho}\} \equiv \{B,\omega\} \ , \tag{3.49}$$

where B is the external magnetic field and ω the vorticity of the fluid. Note that with our conventions, both B and ω are parity even — $\epsilon_{\mu\nu\rho}$, $\omega_{\mu\nu}$ and the spatial part of $F_{\mu\nu}$ are all parity odd. If, however, we consider A_μ and u_μ fixed external fields, then B, ω are parity odd and break the parity invariance of W.

Using S_1, we can write the effective action at first order in derivatives as[18]

$$W = \int d^dx\sqrt{-g}\,[\ P(T,\mu) + \alpha_1 B + \alpha_2\omega] \equiv \int d^dx\sqrt{-g}\mathcal{P} \ . \tag{3.50}$$

The variation of the first order W can be found in App. B. The resulting constitutive relations are

$$\begin{aligned} T^{\mu\nu} &= \mathcal{E}u^\mu u^\nu + \Pi\Delta^{\mu\nu} + \alpha_1(u\times E)^{(\mu}u^{\nu)} - \alpha_2(u\times a)^{(\mu}u^{\nu)} \ , \\ J^\mu &= Ru^\mu + c_a(u\times a)^\mu + c_E(u\times E)^\mu \ , \end{aligned} \tag{3.51}$$

with

$$\begin{aligned} \mathcal{E} &= T\frac{\partial\mathcal{P}}{\partial T} + \mu\frac{\partial\mathcal{P}}{\partial\mu} + \alpha_2\omega - \mathcal{P} \quad , \quad \Pi = \mathcal{P} - \alpha_1 B - \alpha_2\omega \\ R &= \frac{\partial\mathcal{P}}{\partial\mu} - \alpha_1\omega \quad , \quad c_a = T\frac{\partial\alpha_1}{\partial T} + \mu\frac{\partial a_1}{\partial\mu} - \alpha_1 \quad , \quad c_E = \frac{\partial\alpha_1}{\partial\mu} \end{aligned} \tag{3.52}$$

or in terms of the zeroth order energy, pressure and charge density found in Eq. (3.44)

[18]The coefficients α_1, α_2 were denoted $\mathcal{M}_B$ and $\mathcal{M}_\Omega$ in [9].

$$\mathcal{E} = \epsilon + c_a B + \left(T\frac{\partial \alpha_2}{\partial T} + \mu \frac{\partial \alpha_2}{\partial \mu} \right) \omega \quad , \quad \Pi = P$$
$$R = \rho + c_E B + \left(\frac{\partial \alpha_2}{\partial \mu} - \alpha_1 \right) \omega \quad , \quad c_a = T\frac{\partial \alpha_1}{\partial T} + \mu \frac{\partial a_1}{\partial \mu} - \alpha_1 \quad , \quad c_E = \frac{\partial \alpha_1}{\partial \mu} \ . \tag{3.53}$$

Equations (3.51) and (3.52) give the hydrostatic, first order constitutive relations for a parity-breaking $2+1d$ relativistic fluid. We see that the lack of parity invariance leads to the modification of the thermodynamics of the fluid — $\mathcal{E}$ and R — as well as heat and charge transport in the direction of the "parity-breaking" frame $\tilde{G}$. These effects are governed by the acceleration of and the electric field applied to the fluid and most importantly by the coefficients α_1 and α_2 and the conductivity-like coefficients c_a and c_E. However, these coefficients are not defined unambiguously. They are subject to change under an emergent symmetry-transformation of truncated hydrodynamics. This symmetry transformation, first discussed in [119, 121], is called a frame change and is the subject of the following subsection.

3.2.1 Frame Change

To see why the coefficients found in the constitutive relations are not uniquely defined, let us go back to the equilibrium partition function (3.11)

$$\mathcal{Z} = \mathcal{Z}[A^a_{i,\mu}] = \mathrm{Tr} \exp \left[- \int_M dV \ A^a_{i,\mu} \mathcal{Q}^{i,\mu}_a \right] \quad , \quad A^a_{i,\mu} n^\mu = -\mu^a_i L^{-1} \ . \tag{3.54}$$

To arrive at Eq. (3.54) we assumed that $A^a_{i,\mu}$ and, hence, μ^a_i are constant in spacetime. When constant, the μ^a_i are fixed by the thermal averages of the charges Q^i_μ [110]. Then we grew bolder and relaxed this assumption in order to describe systems in local thermal equilibrium. This step forward implies that we can no longer rely on Q^i_a in order to derive the value of μ^a_i. Instead we fixed the chemical potentials like any other field: We defined their value via the solution of a set of differential equations, the hEOM. Unfortunately, to make practical use of the hEOM we had to restrict to some particular derivative order of the chemical potentials. It is in this step that we introduced an ambiguity in the definition of the chemical potentials.

To make the above discussion more precise, let us go back to the constitutive relations Eq. (3.51). Let us explore what happens to the constitutive relations if the temperature, chemical potential and velocity profile all receive first order corrections

$$\mu \to \mu + \mu_{(1)} \quad , \quad T \to T + T_{(1)} \quad , \quad u^\mu \to u^\mu + u^\mu_{(1)} \ . \tag{3.55}$$

Equation Eq. (3.55) defines a special kind of transformation called the frame change. It can be thought of as the purely timelike version of the symmetry transformation for the external gauge fields, $g_{\mu\nu}$ and A_μ. It is precisely the kind of transformation we forbade in Eq. (3.14). Thus there is a priori no reason for a frame change to leave the constitutive relations unchanged. In fact under a frame change, we find for Eq. (3.51) up to first order in $\mathcal{K}$

$$\begin{aligned} T^{\mu\nu} \to T^{\mu\nu} = \mathcal{E}' u^\mu u^\nu + P' \Delta^{\mu\nu} \\ + u^{(\mu} \left[\epsilon u^{\nu)}_{(1)} + \alpha_1 (u \times E)^{\nu)} - \alpha_2 (u \times a)^{\nu)} \right] \quad , \end{aligned} \tag{3.56}$$

$$J^\mu \to J^\mu = R' u^\mu + \rho u^\mu_{(1)} + c_a (u \times a)^\mu + c_E (u \times E)^\mu \ , \tag{3.57}$$

with

$$\begin{aligned} \mathcal{E}' &= \mathcal{E} + \frac{\partial \epsilon}{\partial T} T_{(1)} + \frac{\partial \epsilon}{\partial \mu} \mu_{(1)} \ , \\ P' &= P + \frac{\partial P}{\partial T} T_{(1)} + \frac{\partial P}{\partial \mu} \mu_{(1)} \ , \\ R' &= R + \frac{\partial \rho}{\partial T} T_{(1)} + \frac{\partial \rho}{\partial \mu} \mu_{(1)} \ . \end{aligned} \tag{3.58}$$

Note that since $u^\mu_{(1)}$ is first order, it can be expanded like any vector in terms of the first order elements of the frames G and $\tilde{G}$, Eq. (3.48). However if we restrict $u^\mu_{(1)}$ to stem from a change of the effective action, $u^\mu_{(1)}$ must be parallel to $\tilde{G}$ alone[19]. That is, we may write

$$u^\mu_{(1)} = U_E (u \times E)^\mu + U_a (u \times a)^\mu \tag{3.59}$$

and

$$\begin{aligned} T^{\mu\nu} \to T^{\mu\nu} = \mathcal{E}' u^\mu u^\nu + P' \Delta^{\mu\nu} \\ + u^{(\mu} \left[(\epsilon U_E + \alpha_1) (u \times E)^{\nu)} + (\epsilon U_a - \alpha_2) (u \times a)^{\nu)} \right] \quad , \end{aligned} \tag{3.60}$$

$$J^\mu \to J^\mu = R' u^\mu + + (\rho U_a + c_a) (u \times a)^\mu + (\rho U_E + c_E) (u \times E)^\mu \ , \tag{3.61}$$

with U_E, U_a functions of μ, T.

[19] All first order terms in the action are parity-breaking.

We see then that under a frame change the hEOM remain invariant in form. Only the coefficients in Eq. (3.53) change. These coefficients, similarly to μ and T have no intrinsic physical meaning, but are defined from the solution of the hEOM themselves[20]. This means that we could equally well begin our discussion of hydrodynamics with the constitutive relations in a new frame, Eq.s (3.60) and (3.61), without changing the underlying *local* equilibrium physics. Therefore a frame change can be thought of as a symmetry of truncated hydrodynamics.

We can use the frame-symmetry of hydrodynamics to redefine parts of the constitutive relations to a form that we find more "physical" or convenient. More precisely, we can alter the thermodynamics of the fluid via Eq. (3.58), as well some of the parity-odd transport coefficients in $T^{\mu\nu}$ and J^{μ} through Eq. (3.59). A particularly physical choice for relativistic hydrodynamics is to choose the flow of energy parallel to the velocity profile, i.e. choose the frame for which

$$u_\mu T^{\mu\nu} = -\mathcal{E}' u^\nu \ , \tag{3.62}$$

This condition fixes the coefficients U_E and U_a in the $u^\mu_{(1)}$ expansion to

$$U_E = -\frac{\alpha_1}{\epsilon} \ \ , \ \ U_a = \frac{\alpha_2}{\epsilon} \ . \tag{3.63}$$

We deem this choice of frame for $T^{\mu\nu}$ physical, since it resembles the case of a perfect fluid where $u_\mu T^{\mu\nu} = -\epsilon u^\nu$. In fact, if we want we can go even further and use (3.58) and define $\mathcal{E}' = \epsilon$. There is an infinite number of frames which satisfy $\mathcal{E}' = \epsilon$. To restrict ourselves to a single frame, we may fix either P or R to their equilibrium values. Choosing $R = \rho$ then fixes our choice of frame completely to

$$T_{(1)} = \frac{\left(c_A \frac{\partial\rho}{\partial\mu} - c_E \frac{\partial\epsilon}{\partial\mu}\right) B + \left[\left(\alpha_1 - \frac{\partial\alpha_2}{\partial\mu}\right)\frac{\partial\epsilon}{\partial\mu} + \left(\mu\frac{\partial\alpha_2}{\partial\mu} + T\frac{\partial\alpha_2}{\partial T}\right)\frac{\partial\rho}{\partial\mu}\right]}{\frac{\partial\epsilon}{\partial\mu}\frac{\partial\rho}{\partial T} - \frac{\partial\epsilon}{\partial T}\frac{\partial\rho}{\partial\mu}} \tag{3.64}$$

$$\mu_{(1)} = \frac{\left(c_A \frac{\partial\rho}{\partial T} - c_E \frac{\partial\epsilon}{\partial T}\right) B + \left[\left(\alpha_1 - \frac{\partial\alpha_2}{\partial\mu}\right)\frac{\partial\epsilon}{\partial T} + \left(\mu\frac{\partial\alpha_2}{\partial\mu} + T\frac{\partial\alpha_2}{\partial T}\right)\frac{\partial\rho}{\partial T}\right]}{\frac{\partial\epsilon}{\partial T}\frac{\partial\rho}{\partial\mu} - \frac{\partial\epsilon}{\partial\mu}\frac{\partial\rho}{\partial T}} \ . \tag{3.65}$$

Thus our frame choice can be made unique via two covariant constraints for the energy-momentum tensor and current,

$$u_\mu T^{\mu\nu} = -\epsilon u^\nu \ \ , \ \ u_\mu J^\mu = -\rho \ , \tag{3.66}$$

[20]The "α"s are functions of μ, T and μ, T are specified from the hEOM solutions.

with ϵ and ρ the equilibrium energy and charge density respectively. This is the so-called *Landau frame*of hydrodynamics [119]. For the sake of completeness we mention another frequently used frame in the literature, the Eckart frame [121, 122] defined via

$$u_\mu T^{\mu\nu} u_\nu = \epsilon \quad , \quad J^\mu = \rho u^\mu \ . \tag{3.67}$$

In the sequel we restrict ourselves to the Landau frame.

As a final remark on frame changes, we note that in recent years the question of whether a frame change is a true symmetry of the theory is a hot topic of investigation. The current consensus seems to be that a frame change affects the stability of the theory under small perturbations of the hydrodynamic fields or a change of the initial conditions [123–125]. Therefore, it seems we are in anticipation of a new physical principle that either picks out a stable family of frames or clarifies why relativistic hydrodynamics is intrinsically not well-defined and a reformulation in terms of additional dynamical degrees of freedom is necessary, such as in Israel-Stewart theory [126–128].

To conclude our discussion of hydrostatic charged fluids, let us consider in the following subsection a feature of our construction hidden in plain sight: the second law of thermodynamics.

3.2.2 The second law of thermodynamics

The second law of thermodynamics postulates the existence of an entropy function $S = S(\mu, T)$ that never decreases with time [110]

$$\frac{\partial S}{\partial t} \geq 0 \ . \tag{3.68}$$

For relativistic fluids, we extend the second law to its local relativistic version

$$\partial_\mu s^\mu \geq 0 \ , \tag{3.69}$$

with s^μ the entropy density current. We can derive s^μ in equilibrium using the definition of the entropy in terms of the partition function $\mathcal{Z}$

$$S = \frac{\partial}{\partial T} \left(T \log \mathcal{Z} \right) = -\frac{\partial}{\partial T} \left(TW \right) = -\int d\Sigma \ \frac{\partial \mathcal{P}}{\partial T} = \int d\Sigma_\mu s^\mu \ , \tag{3.70}$$

with $s^\mu = \partial \mathcal{P} / \partial T u^\mu \equiv s u^\mu$. In the second to last equality above, we have first substituted the explicit form of W given by Eq. (3.50) and then used the time-independence of the action to write $W = T^{-1} \int dV \mathcal{P}$. Now we can explicitly calculate the divergence of the entropy current in equilibrium to find

$$\partial_\mu s^\mu = (\partial_\mu s)u^\mu + s\partial_\mu u^\mu = \frac{\partial s}{\partial T}u^\mu\partial_\mu T + \frac{\partial s}{\partial \mu}u^\nu\partial_\nu\mu + s\partial_\mu u^\mu = 0 \ , \quad (3.71)$$

where in the last equality we have made use of Eq. (3.46).

There is one additional way to derive the entropy current, which becomes quite useful when we try to go beyond the hydrostatic limit. So we will spend some time discussing it here. This second definition comes directly from the statistical definition of entropy via

$$s = -\mathrm{Tr}\left[\rho_N \log \rho_N\right] \ , \quad (3.72)$$

with ρ_N the normalized thermal density matrix[21]

$$\begin{aligned}\rho_N &= e^W \exp\left[\int d\Sigma_\mu \left(T^{\mu\nu}\beta_\nu + \beta\mu J^\mu\right)\right] \\ &= \exp\left[-\int d\Sigma_\mu \left(\mathcal{P}u^\mu - T^{\mu\nu}u_\nu - \mu J^\mu\right)\frac{1}{T}\right] \ . \end{aligned} \quad (3.73)$$

The definition of entropy Eq. (3.72) alongside Eq. (3.73) allows us to define what we call the canonical entropy current J_s^μ as

$$J_s^\mu = \left(\mathcal{P}u^\mu - T^{\mu\nu}u_\nu - \mu J^\mu\right)/T \ . \quad (3.74)$$

It is straightforward to show that J_s^μ also has vanishing divergence, if one uses the hEOM, Eq.s (3.37), (3.38), alongside the gradient expansion Eq. (3.46). So we will not present the full calculation here. However, we want to mention one particular part of the calculation that becomes of interest in fluids with non-vanishing angular momentum. This term stems from the derivative of the thermal vector β_ν in Eq. (3.74), which in static equilibrium takes the form

$$\partial_\mu J_s^\mu \supset -T^{\mu\nu}\left(a_{[\mu}u_{\nu]} + \omega_{\mu\nu}\right)/T \ . \quad (3.75)$$

The terms in the parenthesis are anti-symmetric under the exchange of μ and ν and, hence, vanish when contracted with the symmetric energy momentum tensor. This, however, seizes to be true when a fluid possesses a conserved angular momentum tensor. In that case, the energy momentum tensor is allowed to contain an anti-symmetric part that can be thought of as the source of spin-angular momentum. Then equilibrium can be achieved only if the vorticity of the fluid spans the same plane as the velocity profile and the acceleration [129], i.e. $\omega_{\mu\nu} = u_{[\mu}a_{\nu]}$. In simpler terms, a rotating fluid can be in thermal equilibrium if the rotation axis is normal both to the

[21] Recall $\mathrm{Tr}[\rho] = \mathcal{Z} = \exp(-W)$.

velocity and the acceleration of the fluid. An exemplary case of such a steady state is a fluid in a cylindrically symmetric vessel rotating with a constant angular frequency around its symmetry axis.

Note that this requirement for a rigidly-rotating equilibrium is impossible to satisfy in our case, since $\omega_{\mu\nu}$ is by definition normal to the time-direction u_μ(see Eq. (3.47)). This implies that we cannot define an inertial frame of reference with time parallel to the flow profile for a rotating fluid. The fundamental reason for this is the following: A purely rotating frame of reference is not connected to an inertial frame of reference via a Lorentz transformation [130, 131]. Recent work on hydrodynamics of rotating fluids [129] has side-tracked this difficulty by introducing torsion into the system. Torsion then alters the above condition such that u_μ can again play the role of time. We will see this in more detail in chapter 7.

In summary, we have seen that entropy production vanishes in equilibrium and the second law of thermodynamics is obeyed identically. Real-life fluids, however, are rarely in state of hydrostatic equilibrium and their entropy is ever-increasing until said equilibrium is reached. Therefore, any realistic hydrodynamic theory must go beyond the equilibrium partition function level and introduce diffusive, entropy-producing effects. There are at least two ways of doing this: The first follows a similar path to the above and describes hydrodynamics as an out-of-equilibrium field theory on a Schwinger-Keldysh time contour [114, 132–135], while the second works directly at the level of the conserved charges and constrains them using symmetries and the second law of thermodynamics [8,9,119,120]. We follow the second route to dissipation in the following subsection.

3.3 Dissipative charged relativistic fluids

In this section, we will construct the constitutive relations of first-order parity-breaking hydrodynamics, first established in [9]. The construction follows the symmetry analysis of Section 3.2: First we construct the energy-momentum tensor $T^{\mu\nu}$ and $U(1)$ current J^μ consistent with diffeomorphism and gauge invariance in subsection 3.3.1. Then we enforce the constraints stemming from the second law of thermodynamics in section 3.3.2.

3.3.1 Symmetry Analysis

We begin our symmetry analysis by recounting the symmetries of the problem, diffeomorphism and $U(1)$ gauge-invariance. Recall, that the diffeomorphism invariance we refer to leaves the velocity profile u^μ unchanged. For this reason, it is useful to decompose both $T^{\mu\nu}$ and J^μ in an orthonormal basis where the timelike direction is given by u^μ. Performing this decomposition, we find

$$T^{\mu\nu} = \mathcal{E}u^\mu u^\nu + q^{(\mu}u^{\nu)} + \Pi^{\mu\nu} \quad , \quad J^\mu = Ru^\mu + j^\mu \ , \tag{3.76}$$

with $q^\mu u_\mu = 0 = u_\mu \Pi^{\mu\nu} = \Pi^{\mu\nu} u_\nu$ and $j^\mu u_\mu = 0$. We can further split $\Pi^{\mu\nu}$ into its symmetric-traceless, $\pi^{\mu\nu}$, and trace, Π, parts and express $T^{\mu\nu}$ as

$$T^{\mu\nu} = \mathcal{E}u^\mu u^\nu + \Pi\Delta^{\mu\nu} + q^{(\mu}u^{\nu)} + \pi^{\mu\nu} \quad , \quad J^\mu = Ru^\mu + j^\mu \ . \tag{3.77}$$

Having split $T^{\mu\nu}$ and J^μ as in Eq. (3.77), the remaining task is to specify the functions $\mathcal{E}, \Pi$ and R as well as the vectors q^μ, j^μ and the tensor $\pi^{\mu\nu}$. Towards this end, we can employ the Landau-frame constraints Eq. (3.66) discussed in subsection 3.2.1. Doing so fixes $\mathcal{E}$ and R to their thermal equilibrium values and q^μ to vanish, thus leading to simpler constitutive relations

$$T^{\mu\nu} = \epsilon u^\mu u^\nu + \Pi\Delta^{\mu\nu} + \pi^{\mu\nu} \quad , \quad J^\mu = \rho u^\mu + j^\mu \ . \tag{3.78}$$

Apart from the choice of frame, there is an additional simplification that makes the construction of the constitutive relations simpler. The simplification stems from the fact that the constitutive relations are the on-shell expectation values the $T^{\mu\nu}$ and J^μ operators. On-shell means here that the fields of hydrodynamics – μ, T and u^μ – satisfy the hEOM. Since, the constitutive relations are valid only up to first order in the derivative expansion, we must enforce the hEOM only to first order as well. This means that we can restrict ourselves to constitutive relations for which u^μ, μ and T satisfy the first order equations of hydrodynamics. Let us see how this simplifies the analysis, by first constructing the transverse trace of $T^{\mu\nu}$, the function Π.

Constructing Π. In general, Π is a scalar under both diffeomorphisms and gauge transformations and contains both zeroth and first order terms. So we can construct Π in the same way we constructed the effective action W in Section 3.2. In fact, consistency with thermodynamics requires

$$\Pi = \mathcal{P} + \text{dissipative corrections} \ , \tag{3.79}$$

where $\mathcal{P}$ is the effective action density in the Landau frame defined through Eq.s (3.50), (3.58) and (3.64). The dissipative corrections in Π consist of the scalars that where set to zero due to the hydrostatic constraint $\mathcal{L}_\beta = 0$ (see Eq. (3.46) and App. A). There are three such scalars at first order in derivatives given by

$$S_D = \{u^\mu \partial_\mu T, u^\mu \partial_\mu \mu, \partial_\mu u^\mu\} \ . \tag{3.80}$$

Restricting S_D on-shell leaves us with only one dissipative scalar, say $\partial_\mu u^\mu$. This can be seen from the scalar part of the equations of motion for hydrodynamics restricted to first order in the derivative expansion,

$$\begin{aligned} u_\nu \partial_\mu T^{\mu\nu} &\simeq -\frac{\partial \epsilon}{\partial T} u^\mu \partial_\mu T - \frac{\partial \epsilon}{\partial \mu} u^\nu \partial_\nu \mu - \partial_\mu u^\mu = 0 \ , \\ \partial_\mu J^\mu &\simeq \frac{\partial \rho}{\partial T} u^\mu \partial_\mu T + \frac{\partial \rho}{\partial \mu} u^\nu \partial_\nu \mu + \rho \partial_\mu u^\mu = 0 \ . \end{aligned} \tag{3.81}$$

Therefore the first order, dissipative Π is given by[22]

$$\Pi = P' - \zeta \partial_\mu u^\mu = P + 2\chi_\omega \omega - \chi_B B - \zeta \partial_\mu u^\mu \ . \tag{3.82}$$

The new transport coefficient ζ we introduced in Π is called the bulk viscosity. Furthermore consistency with the hydrostatic result implies that P' is the Landau frame pressure given by Eq. (3.58) and Eq. (3.64).

Constructing $\pi^{\mu\nu}$. Stepping up the complexity slightly, we now look at the construction of the tensor part of $T^{\mu\nu}$. There are only two dissipative tensors at first order in derivatives (see App. A), the shear tensor $\sigma^{\mu\nu}$ and its parity-odd version $\tilde{\sigma}^{\mu\nu}$ defined as

$$\sigma_{\mu\nu} = \Delta_{\mu a} \left(\partial^a u^b + \partial^b u^a - g^{ab} \partial_\lambda u^\lambda \right) \Delta_{\nu b} \ , \tag{3.83}$$

$$\tilde{\sigma}_{\mu\nu} = \frac{1}{2} \left(\varepsilon_{\mu\alpha\beta} u^\alpha \sigma^\beta_\nu + \varepsilon_{\nu\alpha\beta} u^\alpha \sigma^\beta_\mu \right) \ . \tag{3.84}$$

In curved space, the partial derivatives in $\sigma_{\mu\nu}$, $\tilde{\sigma}_{\mu\nu}$ should be replaced by covariant derivatives. There are no tensor hEOM, so both $\sigma_{\mu\nu}$ and $\tilde{\sigma}_{\mu\nu}$ should appear in $\pi_{\mu\nu}$. Therefore, $\pi_{\mu\nu}$ to first order in derivatives is simply

$$\pi_{\mu\nu} = -\eta \sigma_{\mu\nu} - \eta_{\rm H} \tilde{\sigma}_{\mu\nu} \ , \tag{3.85}$$

with η and $\eta_{\rm H}$ the shear and Hall viscosities, which we will be concerned with for most of this thesis. We note again that the result for $\pi_{\mu\nu}$ vanishes in the hydrostatic limit once we impose $\mathcal{L}_\beta = 0$.

Constructing j^μ. Finally let us fix the transverse part of J^μ, j^μ. The most general transverse vector can be built out of the first order G and $\tilde{G}$ vectors, Eq. (3.48), alongside the gradients of temperature and chemical potential. Thus, the first order vector data are

$$V = \{ \Delta^{\mu\nu} \partial_\nu T, \Delta^{\mu\nu} \partial_\nu \mu, E^\mu, a_\mu \} \quad , \quad \tilde{V}^\mu = \varepsilon^{\mu\nu\rho} u_\nu V_\rho = (u \times V)^\mu \ . \tag{3.86}$$

[22] We have introduced a factor of -2 in front of ω to match the definition in [9].

To put the data in V, $\tilde{V}$ on-shell, we can use the first order transverse-vector hEOM, $\Delta_{\rho\nu}\partial_\mu T^{\mu\nu} = \Delta_{\rho\nu}F^{\nu\mu}J_\mu$ and its parity-odd counterpart $\varepsilon_{\rho\sigma\nu}u^\sigma\partial_\mu T^{\mu\nu} = \varepsilon_{\rho\sigma\nu}u^\sigma F^{\nu\mu}J_\mu$

$$(\epsilon+P)a_\rho + \frac{\partial P}{\partial T}\Delta_{\rho\nu}\partial^\nu T + \frac{\partial P}{\partial \mu}\Delta_{\rho\nu}\partial^\nu \mu = \rho E_\rho \ , \tag{3.87}$$

$$(\epsilon+P)(u\times a)_\rho + \frac{\partial P}{\partial T}(u\times\partial T)_\rho + \frac{\partial P}{\partial \mu}(u\times\partial\mu)_\rho = \rho(u\times E)_\rho \ . \tag{3.88}$$

The vector and pseudo-vector equations (3.87), (3.88) can be used to express one vector in V and one pseudo-vector in $\tilde{V}$ in terms of the rest of the data. We choose to drop the acceleration vector a_μ and its parity-odd partner from the constitutive relations. Thus, we can express j^μ as

$$\begin{aligned} j^\mu = {}& \chi_T\Delta^{\mu\nu}\partial_\nu T + \chi_M\Delta^{\mu\nu}\partial_\nu\mu + \chi_E E^\mu + \tilde{\chi}_T(u\times\partial T)^\mu \\ & + \tilde{\chi}_M(u\times\partial\mu)^\mu + \tilde{\chi}_E(u\times E)^\mu \ , \end{aligned} \tag{3.89}$$

Note that in this case j^μ does not reduce to the hydrostatic result of section 3.2, Eq. (3.51), even after a frame change. That means we need to constrain the χs and $\tilde{\chi}$s in order to recover the proper hydrostatic limit. Consequently, the electric field E^μ and the gradients of μ, T must appear only through a particular combination that vanishes in hydrostatic equilibrium. This combination is simply $U^\mu = E^\mu - T\Delta^{\mu\nu}\partial_\nu(\mu/T)$ and its parity-odd partner $u\times U$. In addition both $u\times E$ and $u\times\partial T$ are allowed in j^μ, since they have a well-defined hydrostatic limit, see(3.46). Thus, the current consistent with the hydrostatic constitutive relations simplifies down to

$$j^\mu = \sigma U^\mu + \tilde{\sigma}(u\times U)^\mu + \tilde{\chi}_T(u\times\partial T)^\mu + \tilde{\chi}_E(u\times E)^\mu \ . \tag{3.90}$$

In fact, consistency with the hydrostatic constitutive relations Eq. (3.51), also allows to specify the transport coefficients $\tilde{\chi}_T$ and $\tilde{\chi}_E$, in terms of the "conductivities" c_a and c_E in the Landau frame (see Eq.s (3.61) and (3.63))

$$T\tilde{\chi}_T = -c_a \ \ , \ \ \tilde{\chi}_E = c_E \ . \tag{3.91}$$

Herein lies the power of the hydrostatic analysis we spent two section building up. Instead of working with j^μ of Eq. (3.89) and its six independent coefficients, we can now work with j^μ of Eq. (3.90) and only two unspecified coefficients. Contrast this with the entropy analysis in [9] which spent a significant and non-trivial part of the calculation proving the expressions for $\mathcal{P}$, $\tilde{\chi}_T$ and $\tilde{\chi}_E$, Eq.s (3.82), (3.91).

Finally, we are ready to write down the most general form of the constitutive relations allowed by symmetry. To do so we apply Eq.s (3.82), (3.85) and (3.90) to (3.78) and find

$$T^{\mu\nu} = \epsilon u^\mu u^\nu + (\mathcal{P} - \zeta\partial_\mu u^\mu)\,\Delta^{\mu\nu} - \eta\sigma^{\mu\nu} - \eta_{\rm H}\tilde{\sigma}^{\mu\nu}\ , \tag{3.92}$$

$$J^\mu = \rho u^\mu + \sigma U^\mu + \tilde{\sigma}(u\times U)^\mu + \tilde{\chi}_T(u\times\partial T)^\mu + \tilde{\chi}_E(u\times E)^\mu\ . \tag{3.93}$$

However, equations (3.92) and (3.93) are not the end of the story. We must now make sure that our construction is consistent with the local second law of thermodynamics. We do this in the following subsection.

3.3.2 The second law of thermodynamics

In this subsection, we derive the constraints on the transport coefficients appearing in the constitutive relations (3.92) and (3.93) imposed by the second law of thermodynamics. To perform the calculation we follow references [119] and [9] closely.

We construct the entropy current following the inverse path than the one followed in the previous section. Instead of using symmetry arguments to derive the divergence of $T^{\mu\nu}$ and J^μ, we will use the divergence of $T^{\mu\nu}$ and J^μ to derive the entropy current. If this starting point seems peculiar, recall that the equations of motion, and their boundary conditions, hold all physical information for the system. Therefore, it must be possible to derive the entropy current directly from the equations of motion [119].

Let us call the entropy current J^μ_S. It must satisfy a scalar equation $\partial_\mu J^\mu_S \geq 0$. Thus for constructing the entropy current, we must use a combination of the scalar hEOM. A bit of foresight and dimensional analysis leads us to consider the following scalar combination

$$u_\mu\partial_\nu T^{\nu\mu} + u_\mu F^{\mu\nu}J_\nu + \mu\partial_\mu J^\mu = 0\ . \tag{3.94}$$

After a short calculation, we can re-express Eq. (3.94) as

$$\partial_\mu J^\mu_{\rm canon} = -\left[\partial_\nu\left(\frac{\mu}{T}\right) - \frac{E_\nu}{T}\right] j^\nu - \partial_\mu\left(\frac{u_\nu}{T}\right)\pi^{\mu\nu} + \Delta^{\mu\nu}\partial_\mu\left(\frac{u_\nu}{T}\right)(\zeta - 2\chi_\omega + \chi_B)\ , \tag{3.95}$$

with $J^\mu_{\rm canon}$ the canonical entropy current of section 3.2.2

$$J^\mu_{\rm canon} = (Pu^\mu - T^{\mu\nu}u_\nu - \mu J^\mu)/T\ . \tag{3.96}$$

To proceed further we split $\partial_\mu J^\mu_{\rm canon}$ into hydrostatic and dissipative terms by using Eq.s (3.85), (3.90) and the tensor expansion of $\partial_\mu u_\nu$ Eq. (19). The resulting expression is

$$\begin{aligned} T\partial_\mu J^\mu_{\text{canon}} &= U_\nu j^\nu - \sigma_{\mu\nu}\pi^{\mu\nu} + \partial_\mu u^\mu \left(\zeta - 2\chi_\omega + \chi_B\right) \\ &= \left[\sigma U^2 + \eta(\sigma_{\mu\nu})^2 + \zeta(\partial_\mu u^\mu)^2\right]_D \\ &+ \left[\tilde{\chi}_T U_\mu \left(u\times\partial T\right)^\mu + \tilde{\chi}_E U_\mu \left(u\times E\right)^\mu + \partial_\mu u^\mu\left(-2\chi_\omega + \chi_B\right)\right]_H \ . \end{aligned} \tag{3.97}$$

There are several things of note in Eq. (3.97): First, neither η_H nor $\tilde{\sigma}$ appear in it because $\tilde{\sigma}_{\mu\nu}\sigma^{\mu\nu} = 0 = U_\mu(u\times U)^\mu$. It follows that η_H and $\tilde{\sigma}$ remain unconstrained from the second law and can take any real value. Second, each term in $\partial_\mu J^\mu_{\text{canon}}$ is independent of the rest. Therefore, each one of them must be positive-definite in order to respect the second law. This implies that we must constrain the coefficients in front of the dissipative terms in the brackets labeled by D to be positive semi-definite, that is

$$\sigma \geq 0 \quad , \quad \eta \geq 0 \quad , \quad \zeta \geq 0 \ . \tag{3.98}$$

Finally, let us discuss the hydrostatic terms in the bracket labeled by H. The $\tilde{\chi}$s and χs as well as the scalars they multiply are not necessarily positive semi-definite and, hence, may disobey the second law of thermodynamics. This is of course unacceptable, so some modification to our entropy current construction must be made. To this end, we follow [7] and redefine the entropy current to

$$J^\mu_{\text{canon}} \to J^\mu_S = J^\mu_{\text{canon}} + \nu^\mu \ . \tag{3.99}$$

The current ν^μ will be chosen such that $\partial_\mu\nu^\mu$ cancels the hydrostatic terms in $\partial_\mu J^\mu_{\text{can}}$. Clearly, ν^μ must be parity odd. So going back to our symmetry analysis, we find it can in general take the following form

$$\nu^\mu = \tilde{\nu}_1(u\times\partial T)^\mu + \tilde{\nu}_2(u\times E)^\mu + \tilde{\nu}_3(u\times\partial\mu/T)^\mu + \frac{1}{2}\tilde{\nu}_4\varepsilon^{\mu\nu\rho}F_{\nu\rho} + \tilde{\nu}_5\varepsilon^{\mu\nu\rho}\partial_\nu u_\rho \ . \tag{3.100}$$

Also note that since we are interested in the divergence of ν^μ, we may redefine it at will by adding to it a divergenceless vector N^μ. This divergenceless vector can be expressed in the same basis as ν^μ as

$$N^\mu \equiv \varepsilon^{\mu\nu\rho}\partial_\nu(\tilde{\alpha}u_\rho) = -\frac{\partial\tilde{\alpha}}{\partial T}(u\times\partial T)^\mu - \frac{\partial\tilde{\alpha}}{\partial\mu/T}(u\times\partial\mu/T)^\mu + \tilde{\alpha}\varepsilon^{\mu\nu\rho}\partial_\nu u_\rho \ , \tag{3.101}$$

with $\tilde{\alpha}$ an arbitrary function of μ, T. As a result only two of the $\tilde{\nu}_1, \tilde{\nu}_3, \tilde{\nu}_5$ are independent. All that said, the remaining calculation involves taking the divergence of ν^μ and enforcing the second law for J^μ_S. The complete analysis can be found in [9]. Below we simply report the final result

$$\tilde{\nu}_2 = 0 \ , \ T\tilde{\nu}_4 = \alpha_1 \ , \ \frac{\partial\tilde{\nu}_5}{\partial\mu/T} + \tilde{\nu}_3 = \frac{1}{T}\frac{\partial\alpha_2}{\partial\mu/T} - \alpha_1 \ ,$$
$$T^2\left(\frac{\partial\tilde{\nu}_5}{\partial T} + \tilde{\nu}_1\right) = T\frac{\partial\alpha_2}{\partial T} - 2\alpha_2 + f_\omega(T) \ , \tag{3.102}$$

with $f_\omega(T)$ an arbitrary function of T.

Enforcing the second law of thermodynamics concludes our construction of parity-breaking hydrodynamics. Let us then write down the final result for the constitutive relations

$$T^{\mu\nu} = \epsilon u^\mu u^\nu + (\mathcal{P} - \zeta\partial_\mu u^\mu)\,\Delta^{\mu\nu} - \eta\sigma^{\mu\nu} - \eta_{\rm H}\tilde{\sigma}^{\mu\nu} \ , \tag{3.103}$$
$$J^\mu = \rho u^\mu + \sigma U^\mu + \tilde{\sigma}(u\times U)^\mu + \tilde{\chi}_T(u\times\partial T)^\mu + \tilde{\chi}_E(u\times E)^\mu \ , \tag{3.104}$$

alongside the entropy-constraints

$$\zeta \geq 0 \ , \ \eta \geq 0 \ , \ \sigma \geq 0 \ , \ \tilde{\sigma}, \ \eta_H \in \mathbb{R} \ . \tag{3.105}$$

As we mentioned in the introduction, the constitutive relations (3.103) and (3.104) take the same form for *every* $2+1$ dimensional parity-breaking relativistic fluid. The only thing which differentiates one fluid from another is the value of the transport coefficients appearing in those constitutive relations, such as η and η_H. One then wonders how can we know these values in order to make quantitative predictions using our constitutive relations. The answer, in a true EFT fashion, combines both the macroscopic constitutive relations and the microscopic behaviour of the fluid and comes under the name "response functions". These response functions will be the subject of the following section.

3.4 Response functions and transport coefficients

In this section, we consider the retarded two-point functions of the energy-momentum tensor and $U(1)$ current within parity-breaking hydrodynamics. This derivation was first presented in [9]. We also use the response function discussion found in [120]. We are interested in these 2-point functions because they can be shown to contain all the physical information regarding the fluid fluctuations and the fluid's response to a "small" external perturbation [24, 25, 136]. In particular, we use these 2-point functions to derive the spectrum of the fluid's fluctuations and derive Kubo formulae which define the transport coefficients such as η and η_H. These Kubo formulae can then be applied to any microscopic theory to calculate the transport coefficients and specify completely the constitutive relations for $T^{\mu\nu}$ and J^μ of a particular fluid.

We begin, then, by defining the 2-point functions of interest. Within the canonical approach to QFT, they take the following form [72]

$$G^{\mu\nu,\rho\sigma}_{TT}(x) = \langle [T^{\mu\nu}(x), T^{\rho\sigma}(0)] \rangle_R \ , \ G^{\mu,\nu}_{JJ}(x) = \langle [J^{\mu}(x), J^{\nu}(0)] \rangle_R$$
$$G^{\mu\nu,\rho}_{TJ}(x) = \langle [T^{\mu\nu}(x), J^{\rho}(0)] \rangle_R \ , \ G^{\mu,\rho\sigma}_{JT}(x) = \langle [J^{\mu}(x), T^{\rho\sigma}(0)] \rangle_R \ , \tag{3.106}$$

where the angled brackets denote a thermal average with the thermal density matrix ρ, Eq. (3.1), and the index means we have restricted $t > 0$. However, instead of the canonical approach we will use the variatonal approach discussed in section 3.1 (cf. Eq. (3.13)) [120])[23]. In this approach, the Green's function can be defined via the variations of the one-point functions, i.e. the constitutive relations[24]

$$\delta\left(\sqrt{-g}T^{\mu\nu}(0)\right) = -\int d^3x\sqrt{-g}\left[\frac{1}{2}G^{\mu\nu,\rho\sigma}_{TT}(x)\delta g_{\rho\sigma}(x) + G^{\mu\nu,\rho}_{TJ}(x)\delta A_{\rho}(x)\right] \ , \tag{3.107}$$

$$\delta\left(\sqrt{-g}J^{\mu}(0)\right) = -\int d^3x\sqrt{-g}\left[\frac{1}{2}G^{\mu,\rho\sigma}_{JT}(x)\delta g_{\rho\sigma}(x) + G^{\mu,\nu}_{JJ}(x)\delta A_{\nu}(x)\right] \ . \tag{3.108}$$

The canonical and variational definitions differ only by contact terms that stem from the variation of the metric determinant on the left-hand side of Eq.s (3.107) and (3.108). These contact terms are physically important, because they make consistent the Ward-Takahashi identities due to diffeomorphism and gauge-invariance [138].

Similarly to the constitutive relations, the 2-point functions are evaluated on-shell. The relevant equations of motion that need to be satisfied in this case are the hEOM up to second order in the derivative expansion. This is the only way dissipation effects will become apparent in the Green's function. We can use this on-shell constraint in order to calculate the Green's function directly through taking the variations of $T^{\mu\nu}$ and J^{μ}. To do this, we first introduce into the constitutive relations a metric and gauge field perturbation

$$g_{\mu\nu} \to g_{\mu\nu} + \delta g_{\mu\nu} \ \ , \ \ A_{\mu} \to A_{\mu} + \delta A_{\mu} \ . \tag{3.109}$$

[23] If you are wondering why we can use the equilibrium partition function for diffusive hydrodynamics, consult [137]. In this paper, the authors prove Eq.s (3.107) and (3.108) rigorously using as a starting point the Schwinger-Keldysh functional integral.

[24] Our definitions match those in [120] and differ with those in [9] by an overall minus sign.

Then we can use the hEOM in order to express $T^{\mu\nu}$ and J^{μ} in terms of $\delta g_{\mu\nu}$, δA_{μ} and simply read off the Green's functions directly from Eq.s (3.107), (3.108).

Clearly the recipe for calculating the Green's function is algorithmically simple. However, it is in general difficult to find an analytic solution to the hEOM. For this reason, we will make several simplifications in the following. First, we will assume a Minkowski background metric $\eta_{\mu\nu}$ and a vanishing background gauge field $A_{\mu} = 0$. Second, we ignore fluid-fluid interactions by linearizing the equations of motion. We choose to linearize the hEOM around the thermal equilibrium background by expanding the hydrodynamic fields as

$$T = T_0 + \delta T \ , \ \mu = \mu_0 + \delta\mu \ , \ u^{\mu} = u^{\mu}_{(0)} + \delta u^{\mu} \ , \tag{3.110}$$

where T_0, μ_0 are constant and $u^{\mu}_{(0)} = (1, 0, 0)$. Note that the normalization of u^{μ}, $u^2 = -1$, implies δu^{μ} is normal to u^{μ}. That is $\delta u^{\mu} = (0, \delta u^1, \delta u^2)$. The calculation of the linearised hEOM is straightforward, but tedious. So we have included in App. C the code we have used to automatize the derivation. Below we just quote the final result assuming $\partial_y = 0$ for simplicity

$$D\Phi = S \ , \tag{3.111}$$

With $\Phi = \left(\delta\mu, \delta T, \delta u^1, \delta u^2\right)$ the hydrodynamic fields vector, D the differential operator matrix

$$D = \begin{bmatrix} -\sigma\partial_x^2 + \frac{\partial\rho_0}{\partial\mu}\partial_t & \frac{\sigma\mu_0}{T_0}\partial_x^2 + \frac{\partial\rho_0}{\partial T} & \rho_0\partial_x & 0 \\ \frac{\partial\epsilon_0}{\partial\mu}\partial_t & \frac{\partial\epsilon_0}{\partial T}\partial_t & (\epsilon_0 + P_0)\partial_x & 0 \\ \rho_0\partial_x & s_0\partial_x & -(\eta+\zeta)\partial_x^2 + (\epsilon_0 + P_0)\partial_t & -(\chi_\omega + \eta_H)\partial_x^2 \\ 0 & 0 & \eta_H\partial_x^2 & -\eta\partial_x^2 + (\epsilon_0 + P_0)\partial_t \end{bmatrix} \tag{3.112}$$

and source S, which can be found in App. C.
Since the equations are linearized, they can be easily solved by going to Fourier space with frequency w and momentum k along the $x-$direction, where D becomes

$$D = \begin{bmatrix} \sigma k^2 - iw\frac{\partial\rho_0}{\partial\mu} & -k^2\frac{\sigma\mu_0}{T_0} - iw\frac{\partial\rho_0}{\partial T} & ik\rho_0 & 0 \\ -iw\frac{\partial\epsilon_0}{\partial\mu} & -iw\frac{\partial\epsilon_0}{\partial T} & ik(\epsilon_0 + P_0) & 0 \\ ik\rho_0 & iks_0 & k^2(\eta+\zeta) - iw(\epsilon_0 + P_0) & k^2(\chi_\omega + \eta_H) \\ 0 & 0 & -k^2\eta_H & k^2\eta - iw(\epsilon_0 + P_0) \end{bmatrix} . \tag{3.113}$$

We can solve Eq. (3.111) for Φ by inverting D. Imposing $\det[D] \neq 0$, we can then find Φ as a function of S by inverting D. Doing so, we can write down all Green's functions of the system. For the purposes of this thesis

we focus only on three of these Green's functions, $G_{TT}^{12,12}$, $G_{TT}^{12,11}$ and $G_{JJ}^{1,1}$. These three Green's functions can be used to define the corresponding three transport coefficients– η, η_H and σ – most relevant for the applications of hydrodynamics we have in mind. We have then [9]

$$\eta = \lim_{w\to 0} \frac{G_{TT}^{12,12}(w,k)}{iw} \quad , \quad \eta_H = \lim_{w\to 0} \frac{G_{TT}^{12,11}(w,k)}{iw} \quad , \quad \sigma = \lim_{w\to 0} \frac{G_{TT}^{1,1}(w,k)}{iw} \ . \tag{3.114}$$

The importance of the Kubo formulae Eq. (3.114) cannot be overstated. First, they provide us with the physical meaning of the shear and Hall viscosities as well as the conductivity as the proportionality constants between a disturbance acting on the fluid and the fluid's response. Second, they give us a method for calculating these transport coefficients, by calculating the right-hand sides of Eq. (3.114), the Green's functions, for a given microscopic theory. This is exactly what was done in Chapter 2 and section 2.4.

With this we conclude the present section. But there are a lot more to be said about Green's functions derived directly from hydrodynamics . Examples of these include, how the non-linear fluid-fluid interactions cause thermal fluctuations that break the validity assumptions of hydrodynamics [120], how one can constrain the spectrum of operators in CFTs directly from the hydrodynamic equations of motion [139] and how stochastic effects alter the behaviour of the fluid, even if no stochastic forces are present in the constitutive relations [140].

3.5 Turbulence

To close off this short introduction of ours to hydrodynamics, we wish to discuss the phenomenon of turbulence, which is a major motivator in one of my works during the completion of my PhD [2]. The present discussion of turbulence is brief and contains only the facts necessary for understanding [2] in chapter 5. We follow references [1, 141, 142], albeit we our exposition of turbulence has a somewhat different starting point than in these references.

To begin our discussion on turbulence, we state that the momentum-momentum density Green's function in real space takes the form [30]

$$G_{TT}^{0i,0i}(t,x) \sim \frac{1}{\sqrt{\gamma_\eta t}} \exp\left[-\frac{x^2}{4\gamma_\eta t}\right] \ , \gamma_\eta = \frac{\eta}{\epsilon + P} \ . \tag{3.115}$$

Because of the decaying exponential, Eq. (3.115) tells us that any momentum introduced into the system at point $(t,x) = 0$, will have diffused by the time one reaches point (t,x) by an exponential factor which depends on the kinematic viscosity γ_η. This urges us to define fluids with "large" γ_η as more

diffusive than fluids with a "small" one. However, this is not necessarily a helpful definition in practical situations. We could restrict fluids with a "large" kinematic viscosity to such a small region of space, that we never see any diffusion at all. To remedy this, and obtain a useful classification of fluids, we can introduce dimensionless variables in Eq. (3.115), i.e.

$$x \to \chi = \frac{x}{L} \ , \ t \to \tau = \frac{t}{\mathcal{T}} \ , \ U = \frac{L}{\mathcal{T}} \ , \tag{3.116}$$

where L, $\mathcal{T}$, U are typical *macroscopic* length, time and velocity scales characterizing the fluid. For example, L could be the dimension of a channel containing the moving fluid. In dimensionless units the momentum-momentum Green's functions becomes

$$G_{TT}^{0i,0i}(\tau,\chi) \sim \sqrt{\frac{Re}{\tau}} \exp\left[-Re\frac{\chi^2}{4\tau}\right] \ , \tag{3.117}$$

where we have defined the dimensionless Reynolds number of the fluid $Re = LU/\gamma_\eta$ [143, 144]. The inverse of the Reynolds number plays the role of the diffusion constant in these dimensionless units, and can hence function as a measure of how diffusive a fluid really is. More precisely, fluids with $Re \gg 1$ are less diffusive than fluids with $Re \ll 1$.

In the limit of infinite Re, momentum does not diffuse at all from its point of injection. This suggests that fluids with large Re subject to external forces, are vulnerable to instabilities due to the lack of diffusion. When these instabilities grow to encompass the majority of the flow, the fluid is called turbulent. For example, one may consider forcing an incompressible fluid through a channel constriction. The constriction will force part of the fluid to stop moving and part of it to move faster due to incompressibility. This will create a discontinuity of the velocity profile that can be smoothed out due to diffusion. However, if the constriction width is small enough such that $Re \gg 1$, this discontinuity cannot be remedied and the flow will stay discontinuous. This discontinuity is characteristic of turbulent behaviour.

At this point, we should note that the definition of the Reynolds number is a phenomenological one, and should not be taken as a precise measure of when turbulence sets in; for different flows, different Reynolds number definitions might be more physical. To see this let us consider the hEOM for parity-even fluids with the speed of light re-instated[25]. These are

$$\frac{1}{v_F^2}\frac{D\vec{u}}{Dt} = -\left(\frac{\vec{u}}{v_F^2}\frac{D}{Dt} + \nabla\right)\ln(\epsilon + P) - \frac{\eta}{\epsilon + P}\vec{\Sigma}, \tag{3.118}$$

with

[25] What follows first appeared in the appendix of my work [1].

$$\vec{\Sigma}^i \equiv \partial_\mu \sigma^{\mu i} i = 1, 2 \quad , \quad \frac{D}{Dt} \equiv u^\mu \partial_\mu \tag{3.119}$$

and $v_{\rm F}$ is the speed of light in the fluid. To read off the Reynolds number from Eq. (3.118), we need to express it in terms of dimensionless variables, as in Eq. (3.116) . The hEOM in dimensionless form then read

$$\frac{D\vec{u}}{D\tau} = -\left[\vec{u}\frac{D}{D\tau} + \left(\frac{v_F}{U}\right)^2 \nabla\right] ln(\epsilon + p) - \left(\frac{v_F}{U}\right)^2 \frac{\eta U}{L(\epsilon+p)}\vec{\tilde{\Sigma}} \tag{3.120}$$

with $\tilde{\Sigma}$ the dimensionless form of Σ.

Now to read of the Reynolds number from Eq. (3.120), we need to bring it into the diffusion equation form. Then the Green's function of the hEOM becomes that of Eq. (3.117). To do this, we simply need to assume that ϵ and P are constant in spacetime. Then the Reynolds number is simply the dimensionless number multiplying the second derivatives of the velocity profile on the right-hand side of Eq. (3.120). Fortunately or unfortunately, there is no unique dimensionless number that does the job. This is because of $\vec{\tilde{\Sigma}}$, since it contains terms proportional to $(U/v_F)^a$, $a = 0, 2, 4$.
Thus in the case of relativistic hydrodynamics, there are more than one relevant definitions for the Reynolds number. These definitions depend on how large the ratio of U/v_F becomes. Let us focus on two of these definitions, the non-relativistic(NR) and the ultra-relativistic(UR) limits of Eq. (3.120).

- **NR limit:** In this case $v_F/U >> 1$, and Re may be defined

$$Re_{NR} = \frac{(\epsilon + P)L}{\eta U}\left(\frac{U}{v_F}\right)^2 = \frac{LU}{\gamma_\eta}\left(\frac{U}{v_F}\right)^2 = Re\left(\frac{U}{v_F}\right)^2 . \tag{3.121}$$

- **UR limit:** In this case we keep the terms proportional to $(U/v_F)^4$ in $\vec{\tilde{\Sigma}}$ and obtain

$$Re_{UR} = \frac{(\epsilon + P)L}{\eta U}\left(\frac{v_F}{U}\right)^2 = \frac{LU}{\gamma_\eta}\frac{v_F^2}{U^4} = Re\frac{v_F^2}{U^4} . \tag{3.122}$$

The important distinction between the non-relativistic and the ultra-relativistic Reynolds numbers, which makes them worthy of a definition, is that in general $Re_{UR} \gg Re_{NR}$. This indicates that fluids with a velocity approximating the speed of light are inherently more prone to the emergence of turbulent instabilities, than non-relativistic fluids. A final useful formula for Re, which we use in the sequel is

$$Re = \frac{LU(\epsilon + P)}{\eta} = \frac{LU(\mu\rho + Ts)}{\eta} \sim TLU\frac{s}{\eta} . \tag{3.123}$$

In the second equality we used the Gibbs-Duhem relation $\epsilon + P = \mu\rho + Ts$ for parity-even fluids, while in the last equality we considered the charge neutrality limit with $\rho \sim 0$. The relevance of this limit will become obvious in upcoming chapters, where we discuss holographic fluids which, has been conjectured, exhibit the smallest possible value for η/s .

At this point, we deem it useful to summarize what we have seen so far regarding relativistic hydrodynamics, in preparation of applying the hEOM to electronic fluids. First, we considered hydrostatic fluids where the constraint of staticity allowed us to use the method of thermal equilibrium partition functions to write down the hydrodynamic constitutive relations for parity-breaking hydrodynamics in $2 + 1d$. These manifested new transport phenomena compared to parity-even fluids, due to the existence of static parity-odd transport coefficients. Then we used symmetry and the second law of thermodynamics to derive the complete constitutive relations for dissipative relativistic fluids. In these constitutive relations, appeared the transport coefficients which we focus on in the rest of this thesis. These transport coefficients are the parity-even shear and parity-odd Hall viscosities η and η_H respectively. Having written down the constitutive relations, we used them to derive Kubo formulae for η and η_H, which allow the microscopic derivation of these quantities, as seen in chapter 2 and chapters 4, 6 below. Finally, we introduced the notion of turbulence as an instability of a given flow against small fluctuations and gave a phenomenological requirement for when turbulent behaviour is expected to arise: The Reynolds number Re of the flow must be much larger than 1.

Following this review of hydrodynamics, we proceed in the following chapters to apply hydrodynamics to parity-even as well as parity-odd electronic systems, following my research on electron hydrodynamics as published in [1–3]. First, we describe in chapter 4 how we used holography and hydrodynamics to confirm the existence of the hydrodynamic tail of the Gurzhi effect in strongly coupled electronic fluids and its consequences for electronic transport in $2d$ channels [1].

Chapter 4

Poiseuille flow of strongly coupled fluids and the Gurzhi effect

The purpose of this chapter is to review our paper [1], which explores the hydrodynamic tail of the Gurzhi effect for strongly coupled electronic systems. In particular, we find a monotonic decrease of the resistance as a function of the current through a wire in the hydrodynamic regime. To do so, we consider the Gurzhi setup consisting of a $2+1$ dimensional channel of width W and length $l \gg W$, see Fig. 4.1. We assume the electrons move hydrodynamically along the channel in the presence of the Lorentz force generated by a constant electric field $\vec{E} = (E_x, 0)$.

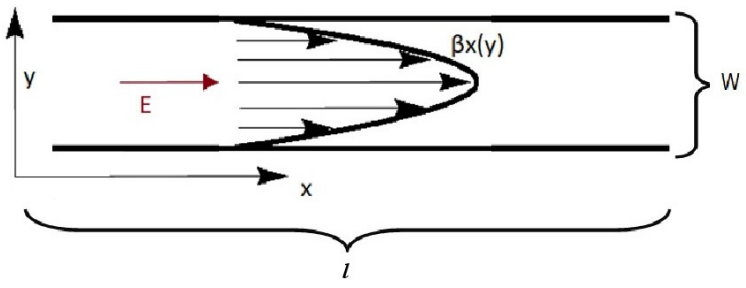

Figure 4.1: The channel setup examined in the main text. The channel is aligned with the x-axis, and has a width W and length l. The electrons move through the wire with a velocity $\beta_x(y)$ under the influence of the electric field E_x. Reprinted from [1] with permission from APS.

Our goal, then, is to explore the decrease in resistance predicted by Gurzhi, by solving the hEOM in the channel setup of Fig. 4.1 and derive the resistance of the channel as a function of the current moving through the wire. The assumption of strong coupling will enter through the thermo-

dynamics and transport coefficients of the fluid, as will be explained in due time. For the moment, though, we will keep our analysis as general as we can when possible. In the spirit of this generality, note that we are considering the fully relativistic hEOM, thus including materials with a relativistic spectrum such as graphene.

In order to make precise quantitative predictions for electronic systems, we need to re-express the constitutive relations in SI units. To transform into SI units, we introduce v_{F}, the Fermi velocity and e the electron charge into the constitutive relations as

$$T^{\mu\nu} = \epsilon \frac{u^\mu u^\nu}{v_{\mathrm{F}}^2} + P\Delta^{\mu\nu} - \eta\sigma^{\mu\nu} \ , \tag{4.1}$$

$$J^\mu = e\rho u^\mu + \sigma\left[E^\mu - \frac{1}{e}T\Delta^{\mu\nu}\partial_\nu\left(\frac{\mu}{T}\right)\right] \ . \tag{4.2}$$

with $u^\mu u_\mu = -v_{\mathrm{F}}^2$, and $\Delta_{\mu\nu} = \eta_{\mu\nu} + u_\mu u_\nu / v_{\mathrm{F}}^2$. Note that here v_{F} plays the role of the speed of light in the system.

In addition, we can take into account the bound currents present in any electronic material. We accomplish this by expressing the electric field acting on the system in terms of the electric displacement tensor [145]

$$D^{\mu\nu} = e\begin{bmatrix} 0 & E_x/\epsilon_m v_{\mathrm{F}} & 0 \\ -E_x/\epsilon_m v_{\mathrm{F}} & 0 & 0 \\ 0 & 0 & 0 \end{bmatrix} \ , \tag{4.3}$$

where ϵ_m is the electric permittivity of the material, which is proportional to the vacuum one, ϵ_0, $\epsilon_m = \epsilon_0\epsilon_r$. The inclusion of the displacement tensor into our framework allows us to express the hEOM in terms of $D^{\mu\nu}$ and the free currents in the material j^μ. In particular we have for the hEOM and the free current

$$\partial_\mu T^{\mu\nu} = \frac{h}{e^3 v_{\mathrm{F}}} D^{\nu\mu} j_\mu \ \ , \ \ \partial_\mu j^\mu = 0 \ . \tag{4.4}$$

$$j^\mu = e\rho u^\mu + \sigma\left[E^\mu - \frac{1}{e}T\Delta^{\mu\nu}\partial_\nu\left(\frac{\mu}{T}\right)\right] \ \ , \ \ E^\mu = \frac{h}{e^3 v_{\mathrm{F}}} D^{\mu\nu} u_\nu \ . \tag{4.5}$$

To approximate the conditions in real materials even closer, we will also consider the effects of impurities on the system. To do so we introduce a Drude-like dissipation term into the momentum-conservation equation. That is we take

$$\Delta_{\rho\nu}\partial_\mu T^{\mu\nu} = \frac{h}{e^3 v_{\mathrm{F}}} D^{\nu\mu} j_\mu - \frac{1}{v_{\mathrm{F}}\tau_{\mathrm{imp}}}\Delta_{\rho\nu} T^{t\nu} \ , \tag{4.6}$$

with $\tau_{\rm imp} = l_{\rm imp}/v_{\rm F}$ the electron-impurity scattering time. Note that the introduction of $\tau_{\rm imp}$ implies the breaking of translation symmetry, since momentum is no longer conserved. We consider the breaking of the symmetry to be soft, in the sense that we assume impurities do not deform the thermodynamics of homogeneous fluids presented in chapters 3.2 and 2. An *a posteriori* justification of this assumption is presented in the sequel.

To solve the hEOM we make use of the emergent translation symmetry of the channel in the x-direction[1] and consider the following ansatz for the velocity profile

$$u^\mu = \gamma(v_{\rm F}, \beta_x(y), 0), \quad \gamma = \left[1 - \left(\beta_x^2/v_{\rm F}\right)^2\right]^{-1/2} \ . \tag{4.7}$$

$\beta_x(y)$ is the non-relativistic velocity of the fluid, which depends only on the y co-ordinate, while γ is the usual Lorentz factor. We also assume that T and μ are simply constant in the channel. We will justify this assumption in more detail in section 6. Under these assumptions, the current conservation equation is satisfied by default, while the momentum equations read

$$\beta_x'' + \frac{2\gamma^2}{v_{\rm F}^2}\beta_x\beta_x'^2 = -\frac{\rho E_x h v_{\rm F}\epsilon_m}{e\gamma^2\eta} + \frac{\epsilon + P}{\eta\tau_{\rm imp}\gamma}\frac{\beta_x}{v_{\rm F}^2} \ , \tag{4.8}$$

$$P' = \frac{\eta}{\tau_{\rm imp}v_{\rm F}^2}\gamma^3\beta_x\beta_x' = \frac{\eta}{\tau_{\rm imp}v_{\rm F}^2}\gamma' \ , \tag{4.9}$$

where $' = \partial_y$. We supplement these equations with no-slip boundary conditions for u^μ and fix the pressure to take its equilibrium value at the boundary

$$u_x(y=0) = 0 = u_x(y=W) \quad , \quad P(y=0) = p \ . \tag{4.10}$$

with $p = p(\mu, T)$ the equilibrium pressure. Before discussing the solution for β_x, we note that the pressure equation (4.9) can be integrated directly to give

$$P = p + \frac{\eta}{\tau_{\rm imp}v_{\rm F}^2}\left[\gamma(y) - 1\right] \ . \tag{4.11}$$

We observe that the pressure deviates from its translationally-invariant value, p, by a constant shift and a spatially-modulating function of the velocity profile. Recall that the constant shift was fixed by the boundary conditions Eq. (4.10). If we wish, we could redefine the shift to any other constant value. This phenomenological deformation of the equilibrium pressure is enough to account for the change of thermodynamics due to the "soft" breaking of translation invariance due to impurities [146]. This justifies our assumption of homogeneous equilibrium for our fluid. A further justification

[1] Due to $l \gg W$, we expect $\partial_x u^\mu \sim u^\mu/l \ll u^\mu/W \sim \partial_y u^\mu$. Therefore, we can neglect the x-gradients of u^μ.

of this assumption stems from the ultra-relativistic limit of Eq. (4.11). In that case, $\gamma \to \infty$ and overshadows any constant contribution in P.

Apart from the constant shift due to impurities, the pressure becomes in general a function of the y co-ordinate due to the flow. This can in principle lead to an observable voltage difference across the channel, which is sourced directly from the hydrodynamic flow of electrons. For the moment we will focus our attention only on the Gurzhi effect in the channel and leave further details on the properties of this voltage difference for section 6.

Next we turn our attention to the solution of the hEOM for β_x. We are interested in this solution, because we can substitute it into the current j^μ and extract the resistance $\mathcal{R}$ of the channel via using Ohm's law[2]

$$\mathcal{R} = \frac{dV}{dI} = l\frac{dE_x}{dI} \quad , \quad I = \int_0^W dy\ j_x = \int_0^W dy\ \left(e\rho\gamma\beta_x + \sigma E_x\right) \ . \tag{4.12}$$

To find $\mathcal{R}$ as a function of I, we need to first solve for β_x as a function of E_x. Then, we can calculate I directly as a function of E_x. Finally, we can invert this relation to find $E_x = E_x(I)$ and use Eq. (4.12) to find $\mathcal{R}$. This short discussion shows that $\mathcal{R}$ can be a non-constant function of the current only if the velocity profile depends non-linearly on E_x. Since E_x appears as a source for β_x, this implies that the non-linear, relativistic correction terms in the equation for β_x are crucial for obtaining a non-constant $\mathcal{R}$. A physical way to state this result is that a fast velocity profile, induced by a "large" electric field, induces a fast fluid and non-trivial current dependence. This non-trivial current dependence will by default appear for "large" currents I.

As a consequence of the above discussion, restricting ourselves to the non-relativistic limit of the hEOM allows us to derive the behaviour of $\mathcal{R}$ around $I = 0$. According to Fig. 1.3a, this allows us to estimate the maximum value of $\mathcal{R}$. Let us derive this maximum of $\mathcal{R}$ in the following section, in order to see how the above algorithm works and confirm our intuition.

4.1 Non-relativistic limit

The non-relativistic limit of the equation for β_x is found by taking $\beta_x \ll v_{\mathrm{F}}^2$, $\gamma \sim 1$ in Eq. (4.8)

$$\beta_x'' = -\frac{\rho E_x h v_{\mathrm{F}} \epsilon_m}{e\eta} + \frac{\epsilon + P}{\eta\tau_{\mathrm{imp}}}\frac{\beta_x}{v_{\mathrm{F}}^2} \ . \tag{4.13}$$

The solution to Eq. (4.13) can be found by standard methods and reads

[2]Recall $\eta_{\mu\nu} = \mathrm{diag}(-1, 1, 1)$ and $j_x = j^x$.

$$\beta_x = \frac{\rho E_x v_{\rm F} h \epsilon_m \lambda_G^2}{e\eta} \left[1 - \cosh(y/\lambda_G) + \sinh(y/\lambda_G)\tanh(W/2\lambda_G)\right] \ , \quad (4.14)$$

with $\lambda_G = \sqrt{\eta v_{\rm F}^2 \tau_{\rm imp}/(\epsilon + p)}$ the Gurzhi length, quantifying the relative strength of viscous to impurity effects on the flow. More precisely, taking $\lambda_G \to \infty$ leads to a Poiseuille flow in the absence of impurities , while taking $\lambda_G \to = 0$ leads to an Ohmic flow with a constant β_x. Given β_x, we can easily calculate the current to find

$$I = E_x v_{\rm F} \epsilon_m \left[\frac{\sigma W}{e^2} + \frac{\rho^2 \lambda_G^3}{\eta}\left(\frac{W}{\lambda_G} - 2\tanh(W/2\lambda_G)\right)\right] \ . \quad (4.15)$$

We see that I is linear in E_x, so $\mathcal{R}$ is clearly independent of I. In particular

$$\mathcal{R} = \frac{l}{v_{\rm F}\epsilon_m}\left[\frac{\sigma W}{e^2} + \frac{\rho^2 \lambda_G^3}{\eta}\left(\frac{W}{\lambda_G} - 2\tanh(W/2\lambda_G)\right)\right]^{-1} \ . \quad (4.16)$$

The calculated resistance $\mathcal{R}$ might be boring when it comes to the Gurzhi effect, since it does not depend on the I,[3], but it holds a few interesting lessons regarding charge transport in electron fluids. The first lesson is that we *cannot* disentangle shear-induced resistance and impurity induced resistance. To see this, we expand $\mathcal{R}^{-1}$ at the limit of $\tau_{\rm imp} \to \infty$. The resulting expression is

$$\mathcal{R}^{-1} = \frac{h\epsilon_m v_{\rm F} W}{l}\left(\frac{\sigma}{e^2} + \frac{\rho^2 W^2}{12\eta}\right) - \frac{h\epsilon_m(\epsilon + P)\rho^2 W^5}{120\eta^2 l_{\rm imp} l} \ . \quad (4.17)$$

Equation (4.17) tells us that any small amount of impurities in the system will necessarily entangle shear and impurity effects. This can be seen directly from the equations of motion in Fourier space, where the β_x propagator, G_β depends on η and $\tau_{\rm imp}$ only through λ_G, $G_\beta = (k^2 + 1/\lambda_G^2)^{-1}$.

Another lesson to be gleaned from $\mathcal{R}$ is that quantum critical effects to the conductivity are completely independent from viscosity effects. This can be seen from the fact that $\mathcal{R}^{-1}$ can be written as a sum of resistors in parallel

$$\mathcal{R}^{-1} = \mathcal{R}_\sigma^{-1} + \mathcal{R}_\eta^{-1} \ , \quad (4.18)$$

with

[3]Note that $\mathcal{R}$ depends on temperature in this case as well. However, we chose to consider an experiment where only I and $\mathcal{R}$ can be measured directly.

$$\mathcal{R}_\sigma^{-1} = \frac{l}{v_{\rm F}\epsilon_m}\frac{\sigma W}{e^2} \ , \tag{4.19}$$

$$\mathcal{R}_\eta^{-1} = \frac{\rho^2\lambda_G^3}{\eta}\left(\frac{W}{\lambda_G} - 2\tanh(W/2\lambda_G)\right) \ . \tag{4.20}$$

Note that this picture of parallel resistors is atypical for electronic materials. In fact for typical materials, the total resistance is the sum of the resistivities arising from different scattering mechanisms[4]. In standard nomenclature, we say that hydrodynamic resistivities obey an inverse Matthiessen rule.

To conclude this section, let us also consider the limit where impurities dominate the flow. In this case, the Navier-Stokes equations become algebraic

$$\beta_x = \frac{h\epsilon_m\rho v_{\rm F}^3\tau_{\rm imp}}{e(\epsilon+P)}E_x \ . \tag{4.21}$$

It is useful to consider the conductivity for this particular regime, which is defined as $\sigma = j_x/E_x$ and has the following form

$$\sigma_{\rm tot} = \sigma + \sigma_D \quad , \quad \sigma_D = \frac{h\epsilon_m v_{\rm F}^3}{e(\epsilon+P)}\rho^2\tau_{\rm imp} \ . \tag{4.22}$$

The conductivity σ_D is the Drude conductivity of the channel. The form of $\sigma_{\rm tot}$ begs a comparison of the two terms that comprise it in order to check which, if any, dominates over the other. To do so, we must consider a particular fluid for which $\sigma \neq 0$ and fix its thermodynamics and transport coefficients. Let us do so below.

Our particular choice of fluid, for the comparison of conductivities is motivated by our goal to analyze the Gurzhi effect for strongly coupled fluids. We choose to restrict ourselves to the strongly coupled regime by using holography to prescribe particular values to the thermodynamics and transport coefficients of the fluid. This allows us to study not just a single particular fluid, but a whole class of fluids described by holography.

The relevant analysis for the transport coefficients and thermodynamics of holographic fluids has been discussed in chapter 2. Here, we quote only the final results we will employ. As a reminder, we mention that the holographic setup we use is an AdS Reissner-Nordström (AdS-RN) black hole in Einstein-Maxwell theory with no higher derivative corrections, see Eq. (2.18). The thermodynamics of AdS-RN are

[4]We implicitly used this result in our description of the Gurzhi effect. Recall that we asserted the resistance becomes larger when phonon effects kick in.

$$\epsilon = \frac{L^2}{8\pi G_4}\hbar\, v_{\rm F}\frac{r_{\rm H}^3}{L^6}, \quad P = \frac{L^2}{16\pi G_4}\hbar\, v_{\rm F}\frac{r_{\rm H}^3}{L^6}\ , \tag{4.23}$$

$$\rho = \frac{L^2}{64\pi G_4}\left(\frac{r_{\rm H}}{L^2}\right)\frac{\mu}{\hbar v_{\rm F}}, \quad s = \frac{k_B L^2}{4G_4}\frac{r_{\rm H}^2}{L^4}\ , \tag{4.24}$$

where L is the AdS radius, G_4 the $3+1$ dimensional gravitational constant and $r_{\rm H}$ the event horizon radius, which is related to the fluid's temperature and chemical potential via

$$\frac{r_H}{L^2} = \frac{1}{6}\frac{k_B T}{\hbar\, v_{\rm F}}\left(4\pi + \sqrt{16\pi^2 + \frac{3\mu^2}{k_B^2 T^2}}\right). \tag{4.25}$$

To make practical use of these equations, we must fix the ratio L^2/G_4. We do so through a phenomenological matching of the charge density to typical charge densities in experiments, $\rho \sim 10^{11}{\rm cm}^{-2}$ for temperature $T = 2$K and $\mu = 4.5$meV [16]. Doing so yields

$$\frac{L^2}{G_4} = 64\sqrt{3}\ . \tag{4.26}$$

Having fixed the thermodynamics of the fluid, we proceed to its transport coefficients. The two transport coefficients relevant for our purposes are σ and η. The conductivity σ takes its quantum critical value [147–149]

$$\sigma = \frac{L^2}{G_4}\left(\frac{sT}{\epsilon + P}\right)^2\frac{e^2}{2h} = 32\sqrt{3}\left(\frac{sT}{\epsilon + P}\right)^2\frac{e^2}{h}\ . \tag{4.27}$$

Although unnecessary for the comparison of conductivities, let us also comment on the value of η. In this work, we shall not use a single value for η. Instead, we will vary η as a function of s starting from the KSS bound $(\eta/s)_{\rm KSS} = \hbar/4\pi k_{\rm B}$, up to a maximum value of twenty times the bound. This way, we "scan" the space of couplings from stronger to weaker ones respectively.

Finally, we fix $\epsilon_m = 5\epsilon_0$, $v_{\rm F} = 10^5$m/s and $\tau_{\rm imp} = 10^{-12}s$. These are typical values found in weakly coupled metals and in particular HgTe [150]. We expect ϵ_m, $v_{\rm F}$ and $\tau_{\rm imp}$ of strongly coupled fluids to take similar values (see e.g. chapter 5). Putting everything together we find for the ratio of the Drude to the quantum critical conductivity

$$\frac{\sigma_D}{\sigma} \simeq 0.84\ . \tag{4.28}$$

This shows that both conductivities play an important role in the total conductivity of a *strongly coupled* channel with an Ohmic flow given by Eq. (4.21). This is in stark contrast to the case of weakly coupled relativistic

electronic fluids. In these system the conductivity ratio goes to zero, since σ scales as $1/\alpha^2$ with the coupling strength $\alpha \ll 1$ [36].

This concludes what we wanted to mention on the non-relativistic limit of the relativistic Navier-Stokes equations. To summarize, we found that i) impurity and shear effects are entangled with one-another, ii) the "hydrodynamic" resistance obeys an inverse Matthiessen rule contrary to a typical metallic resistance, iii) in strongly coupled systems the Drude and quantum critical conductivity are of the same order of magnitude, unlike for weakly coupled systems where the quantum critical conductivity dominates. To proceed with our derivation of the hydrodynamic part of the Gurzhi effect, we examine the fully relativistic equations in the next section.

4.2 Relativistic flows

Our approach for the derivation of the resistance in this section will be fully numerical, since the non-linearities in the Navier-Stokes equations precludes us from finding an analytical solution. In addition, we assume $\tau_{\rm imp} \to \infty$ in this section in order to focus purely on shear effects, i.e. coupling effects, on the resistance. To perform the numerical analysis, we first make the Navier-Stokes equation Eq. (4.8) dimensionless via the introduction of dimensionless parameters

$$u = \frac{k_{\rm B}T}{hv_{\rm F}}y \quad , \quad \mathcal{E}_x = \frac{h^2\epsilon_m v_{\rm F}^2}{ek_{\rm B}^2}E_x \quad , \quad w = \frac{k_{\rm B}T}{hv_{\rm F}}W \ . \tag{4.29}$$

In terms of dimensionless parameters, the Navier-Stokes equation for β_x becomes

$$\frac{\eta}{s}\left(\ddot{\beta}_x + \frac{2\gamma^2}{v_F^2}\beta_x\dot{\beta}_x{}^2\right) + h\frac{v_F\mathcal{E}^x}{\gamma^2}\frac{\rho}{s} = 0, \qquad \dot{\beta}_x = \frac{\partial\beta_x}{\partial u}, \tag{4.30}$$

where we made explicit the dependence of the equation on η/s by dividing the whole equation with s. Now, the flow profile depends on $\{\mathcal{E}_x, \mu/T, \eta/s\}$ directly through the Navier-Stokes equations and on w implicitly through the no-slip boundary conditions (4.10). Thus the set $\{\mathcal{E}_x, \mu/T, \eta/s, w\}$ are the input parameters for our numerical analysis. To begin with, let us plot below the velocity profile solving Eq. (4.30) each time varying a different input parameter.

We observe that the velocity of the fluid in the channel is a monotonically increasing function of $w, \mathcal{E}_x$ and $\mu/k_{\rm B}T$, while it is a monotonically decreasing function of η/s. Recalling that η/s decreases with increasing coupling strength, this means β_x is a monotonically increasing function of the coupling strength of the system as well.

This behaviour of β_x as a function of each input parameter has a simple physical explanation. For example, consider the dependence on $\mathcal{E}_x$ shown

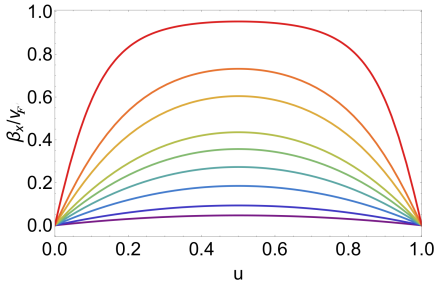

(a) Velocity profile as a function of u at different values of $\mathcal{E}_x$. From top to bottom: $\mathcal{E}_x = 50, 20, 15, 10, 8, 6, 4, 2, 1$ corresponding to $E_x \in [75, 1.5]\text{mV}/\mu\text{m}$ respectively. The rest of the input parameters are $w = 1$, corresponding to $W \sim 5\mu$m, $\mu/k_\text{B}T = 1$ and $\eta/s = (\eta/s)_\text{KSS}$. Reprinted from [1]with permission from APS

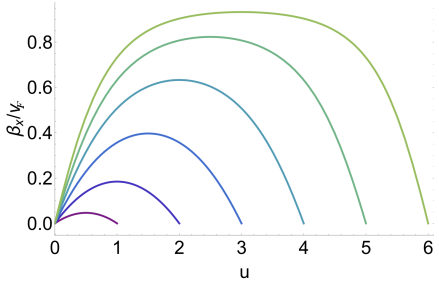

(c) Velocity profile as a function of u at varying values of w. A value of $w = 1$ corresponds to $W \simeq 5\mu$m and similarly for larger w. The rest of the input parameters have been fixed at $\mathcal{E}_x = 1$, $\eta/s = (\eta/s)_{KSS}$, $\mu/k_\text{B}T = 1$. Reprinted from [1]with permission from APS.

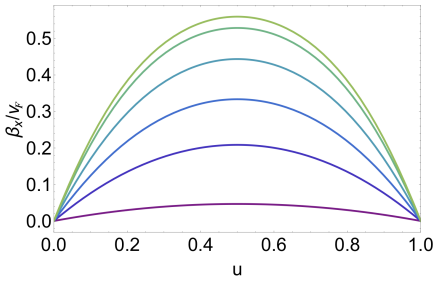

(b) Velocity profile as a function of u at varying values of $\mu/k_\text{B}T$. From top to bottom: $\mu/k_BT = 100, 50, 20, 10, 5, 1$. The rest of the parameters have been fixed to $\mathcal{E}_x = 1$, $w = 1$, $\eta/s = (\eta/s)_\text{KSS}$. Reprinted from [1]with permission from APS.

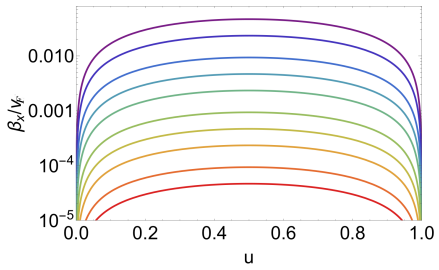

(d) Velocity profile as a function of u at varying η/s. From top to bottom: $\eta/s = 1, 2, 5, 10, 20, 50, 100, 200, 500, 100$ in units where the KSS bound equals one. The rest of the input parameters have been fixed at $\mathcal{E}_x = 1$, $w = 1$, $\mu/k_\text{B}T = 1$. Reprinted from [1]with permission from APS.

in Fig.4.2a. As we increase $\mathcal{E}_x$, we also increase the external Lorentz force due to the electric field acting on the fluid, thus accelerating the fluid to larger and larger velocities. Similarly, the external force is proportional to the charge density of the fluid. In turn the charge density is a monotonically increasing function of $\mu/k_{\rm B}T$. Hence, the behaviour observed in Fig. 4.2b where we plot β_x for various values of $\mu/k_{\rm B}T$. We also observe in Fig. 4.2c that as w increases, so does β_x. This is a consequence of the external electric field and the reflection symmetry along the middle of the channel. Because the external force always points in the same direction, the fluid can be zero only at the boundaries of the channel. Then, the boundary conditions and the reflection symmetry of the channel implies the existence of global maximum of the flow in the middle of the channel. Put another the way, the flow speed will increase from zero at $y = 0$ up to some maximum value at $y = W/2$ and decrease again to zero at $y = W$. Since it must do that in a continuous and monotonic way, the maximum of the flow will become larger as we increase W.

Finally, we observe that the stronger the coupling strength in the system, i.e. the smaller η/s becomes, the faster the fluid becomes. To see this is the expected physical behaviour, recall that η/s affects the local momentum transfer per degree of freedom of the fluid. Thus, keeping other input parameter fixed, more strongly coupled fluids will lose momentum towards the boundaries more slowly than strongly coupled ones. This allows strongly coupled fluids to absorb more of the momentum imparted to them by the external electric field, since they do not need to lose as much of it to the boundaries of the channel.

The inhibition of momentum dissipation for strongly coupled fluids also means that strongly coupled fluids can become relativistic much more easily than weakly coupled ones. To confirm this, we plot in Fig. 4.3 the maximum of the velocity profile with $\eta/s = (\eta/s)_{\rm KSS}$ as a function of $\mu/k_{\rm B}T$ at different values of $\mathcal{E}_x$. From this figure we see that a relatively small electric field $E_x \simeq 7.5{\rm mV}/\mu{\rm m}$ and $\mu/k_{\rm B}T \simeq 5$ is enough to achieve almost luminal speeds of propagation $\beta_x \simeq v_{\rm F}$.

Proceeding now to the resistance of the channel, notice that we can calculate it using the same algorithm as in section 4.1 for the numerical solutions presented above. We plot the results of our calculation of $\mathcal{R}$ in Fig.4.4 below. We can clearly observe the expected drop of the resistance with increasing current I, similar to the hydrodynamic part of the experimental results presented in Fig.s 1.3a and 1.3b. More importantly, we also observe a strong dependence of $\mathcal{R}$ on the value of η/s. This is important for two reasons: First, it shows that strongly coupled fluids exhibit a smaller resistance than their weakly coupled counterparts and are hence better conductors of electricity. Second, this strong dependence on η/s, means that the we can experimentally identify the value of η/s just by measuring the resistance of the channel. This approach presumes that there exists at least one material

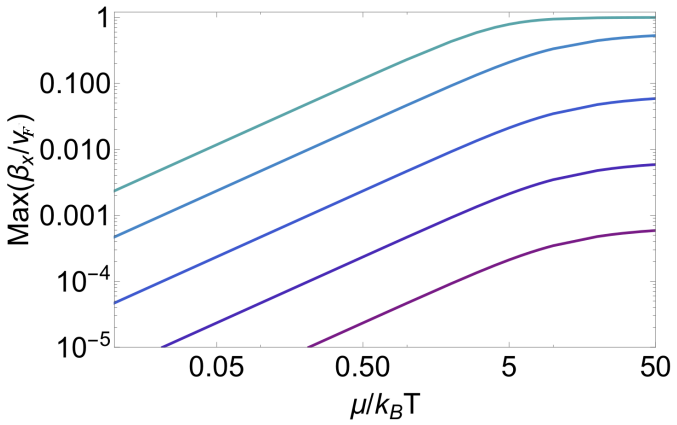

Figure 4.3: Maximum of the velocity profile as a function of $\mu/k_{\rm B}T$ at different values of $\mathcal{E}_x$. From top to bottom: $\mathcal{E}_x = 5, 1, 0.1, 0.01, 10^{-3}$. For illustration purposes, we have set $w = 1$. As mentioned in the main text, $\eta/s = (\eta/s)_{\rm KSS}$.Reprinted from [1] with permission from APS.

whose value for η/s has been measured independently of its resistance. An example of such a material is graphene with a value of $\eta/s \simeq 4 - 8$ times the KSS bound [23].

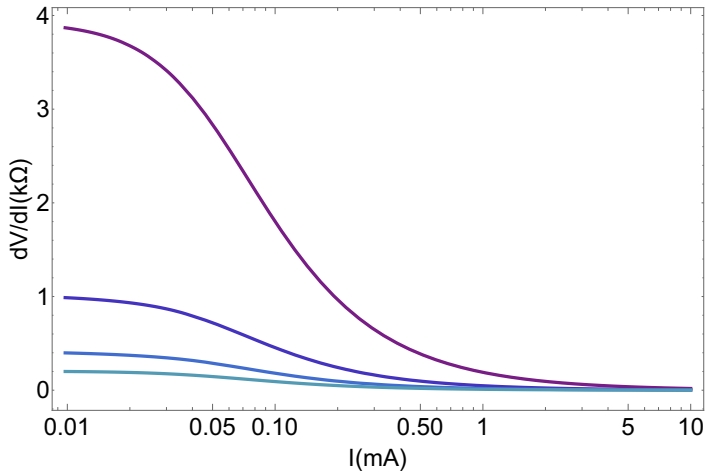

Figure 4.4: Resistance as a function of the current I at different values of η/s. From top to bottom: $\eta/s = 20, 5, 2, 1$ times the KSS bound. Reprinted from [1] with permission from APS.

Let us summarize our results. First, we have shown that the velocity profile for *fully relativistic* fluids increases monotonically with the channel's width, the external electric field and the ratio $\mu/k_{\rm B}T$. We have also shown

that the velocity profile increases with decreasing η/s, interpreted as an increasing coupling strength. Using these velocity profiles, we calculated the explicit form of the resistance $\mathcal{R}$ of the channel as a function of the current flowing through the channel. We have shown $\mathcal{R}$ takes the typical form expected from the hydrodynamic part of the Gurzhi effect found in experiments. In addition, we have shown that impurity and shear effects cannot be disentangled within $\mathcal{R}$. However, shear and quantum critical effects can be separated via the inverse Matthiesen rule satisfied by $\mathcal{R}$. Finally, we have shown that strongly coupled fluids are better conductors of electricity than weakly coupled ones, since they exhibit a smaller resistance and can reach almost luminal speeds for typical values of the input parameters.

This ease of reaching luminal speeds at strong coupling leads us to think of the possibility of turbulence in electronic channel setups. To this end we apply equations (3.121) and (3.122) to our flows. Unfortunately, the resulting value for $Re \leq 50$ far smaller than the $\mathcal{O}(1000)$ value of Re necessary to observe turbulence in $2+1d$ fluids. This value can be enhanced to $Re = \mathcal{O}(100)$ if we impose a constriction on the channel or obstruct the flow with a large compared to the channel obstacle, as in the graphene channel setup of [151]. This value of Re is still not large enough to achieve turbulence. It does, however, urges us to think of other materials where the fluid parameters are such that an order of magnitude enhancement of Re is achieved. In fact, my collaborators and I have proposed such a material where an even larger enhancement can be observed [2]. This material goes by the name Scandium-substituted Herbertsmithite or ScHb for short and is the subject of the following chapter.

Chapter 5

Turbulent hydrodynamics in kagome metals

In what follows we suggest the material Scandium-substituted Herbertsmithite (ScHb) as a suitable candidate for strongly-coupled, relativistic electron-hydrodynamics, following our publication [2]. There are a multitude of reasons which motivate our proposal in particular and the search for strongly coupled materials in general. The most relevant one for our purposes is the fact that strongly coupled materials are expected to exhibit transport properties that are way more exotic than the ones of weakly coupled fluids. Examples of these are quantum critical phases of matter [28,66], such as some models for high T_c superconductors and the quark gluon plasma [30]. The transport properties of interest to us are those related to hydrodynamics. We have already seen in chapter 4 that strongly coupled fluids constitute more efficient electric conductors than weakly coupled ones. Here we also argue that strongly coupled fluids are better suited for exploring turbulent hydrodynamics in electron materials. To see this, we recall the Reynolds number for fluids around charge neutrality given in Eq. (3.123)

$$Re \sim TWU\frac{s}{\eta} \,, \tag{5.1}$$

where T is the temperature of the fluid, W, U are typical length and velocity scales characterizing the flow and the equality becomes exact only at vanishing charge density. (5.1) is written in natural units. We bring it to SI units by multiplying it with the appropriate factors of k_{B}, $\hbar$ and v_{F} to find

$$Re \sim \frac{k_{\mathrm{B}}T}{\hbar v_{\mathrm{F}}}\frac{U}{v_{\mathrm{F}}}W\,\left(\frac{\eta k_{\mathrm{B}}}{s\hbar}\right)^{-1} \,. \tag{5.2}$$

Almost every term in Eq. (5.2) depends on the coupling. In particular, the Fermi velocity v_{F} depends on the electron-electron coupling. Indeed, the effective fine structure constant for QED in electronic systems is given by [152]

$$\alpha_{\text{eff}} = \frac{e^2}{\epsilon_m \hbar v_{\text{F}}} \;\Leftrightarrow\; v_{\text{F}} = \frac{e^2}{\epsilon_m \hbar \alpha_{\text{eff}}} \,, \tag{5.3}$$

where e is the electron charge and ϵ_m the electric permittivity of the material. Second, the Reynolds number depends on the coupling via the coupling dependence of η/s. More precisely, for weakly coupled fluids [31]

$$\eta/s \simeq \frac{\hbar}{k_{\text{B}}} \frac{0.04\pi}{\alpha_{\text{eff}}^2} \,. \tag{5.4}$$

while for strongly coupled $2+1d$ fluids around charge neutrality, we argue in section 5.2 that it takes the form

$$\eta/s \simeq \frac{\hbar}{4\pi k_{\text{B}}} \left(1 + \frac{\mathcal{C}}{\alpha^{3/2}}\right) \,, \tag{5.5}$$

with $\mathcal{C}$ a phenomenological constant that we fix shortly. Finally, the typical velocity U also depends implicitly on the coupling strength. To see this recall Fig. 4.2d in section 4.2. This figure shows that the smaller η/s becomes, i.e. the large the coupling becomes, the faster the fluid flows. Putting everything together, we see that the Reynolds number is a monotonically increasing function of the coupling strength. Hence, strongly coupled materials are the ideal candidate for observing turbulent electronic flows.

A further motivation for the search of strongly coupled materials for my collaborators and myself, is the prospect of using such materials to experimentally test the predictions of holography and to postdict new holographic phenomena seen in experiments.

In the next section we make precise our proposal for a strongly coupled material, ScHb, by deriving its electron and phonon spectra, and most importantly its effective coupling strength α_{ScHb}. We find a non-perturbatively large value $\alpha_{\text{ScHb}} \simeq 3$, implying the AdS/CFT correspondence can be used to derive its transport properties. We focus on the ratio of shear viscosity to entropy density η/s in section 5.2 where we use the AdS/CFT correspondence to derive an estimate for η/s of the ScHb fluid. This estimate, when substituted into the Reynolds number of the fluid, suggests that ScHb is one of the first strongly-coupled materials proposed that can host a fully turbulent flow.

5.1 Overview of ScHb and some of its essential properties

The strongly coupled material we propose is based on a kagome lattice. Kagome lattices are lattices that resemble a Jpanese basket-weaving pattern, see Fig. 5.1a [153, 154].

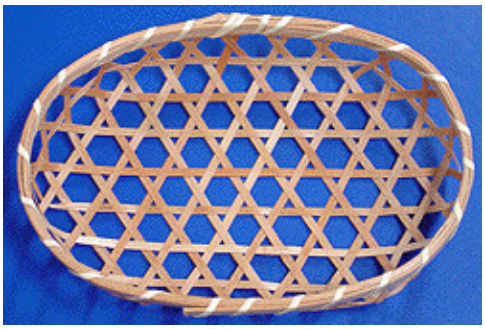

(a) Example of a basket woven in kagome-style. Source: `http://www.hfmphysics.com/2006/motif.html`.

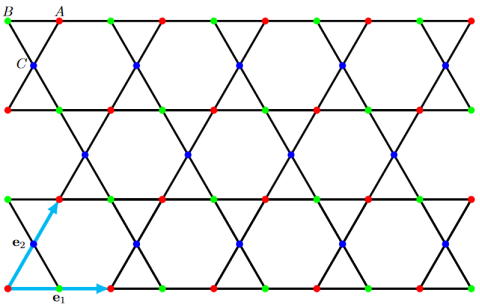

(b) Kagome lattice. The red, blue and green points denote the occupied points of the lattice, while $\mathbf{e}_1$, $\mathbf{e}_2$ are a particular choice of the lattice basis which spans the unit cell. Reprinted from [155] with permission from APS.

The use of such a lattice is crucial, since its tri-hexagonal symmetry ensures the existence of a Dirac point in the spectrum [156]. However, whether we have access to Dirac physics at low energies depends on how we populate the kagome lattice points. To pin the Fermi level directly on the Dirac point, we choose to construct the kagome lattice using CuO_4 plaquettes. This way, we can *in principle* generate the ScHb lattice, or in chemical notation $ScCu_3(OH)_6Cl_2$, see Fig. 5.2. Due the Scandium substitution, the copper atoms tend to hybridize in terms of $d_{x^2-y^2}$ orbitals. This has two important consequences: First, d-orbital hybridization implies that electrons travelling in the lattice tend to spend more time around a single copper atom than propagating around all of them. As a result the effective speed of propagation of low-energy electrons, the Fermi velocity v_F will tend to be smaller than materials which hybridize in terms of less-correlated orbitals, such as graphene and its p-orbitals. We find[1]

$$v_{\text{ScHb}} = 1.0 \text{ eV Å} \quad , \quad v_{\text{Gr}} = 6.6 \text{ eV Å} .^{2} \tag{5.6}$$

The relatively small Fermi velocity implies that ScHb is expected to be more strongly coupled than graphene, following the discussion around Eq. (5.3). Second, the Scandium substitution allows us to reach the Dirac point at a filling fraction $n = 4/3$. This implies that ScHb is expected to be robust against magnetic instabilities and the dissolution of the Dirac point [157–159]. Therefore, the effective Dirac-fermion low-energy description of ScHb necessary for relativistic hydrodynamics is expected to be present for typical experimental conditions.

[1] To see exactly how the Fermi velocities were calculated, consult the supplemental of [2]. See also Fig. 5.2.

[2] For reference, the speed of light in the vacuum is $c = 2 \times 10^3$eV Å.

This does not mean, however, that ScHb will necessarily exhibit hydrodynamic behaviour. Recall that for hydrodynamics to be a valid description of the system, we have to ensure that electron-electron interactions dominate over electron-phonon and electron-impurity interactions. Ab initio calculations of the electron-phonon coupling show that electron-phonon interactions are negligible for temperatures $T < T_{\text{ph}} = 80\text{K}$ (see Fig. 5.2 and the supplemental of [2]). Unfortunately we cannot know whether impurity effects are negligible, since the amount of impurities present in ScHb depends strongly on the precise chemical process used for its synthesis. We can, however, say that the complete Scandium substitution necessary to construct ScHb implies that disorder due to vacant lattice sites will not appear in ScHb. It is implicitly assumed in what follows that a clean enough sample can be constructed.

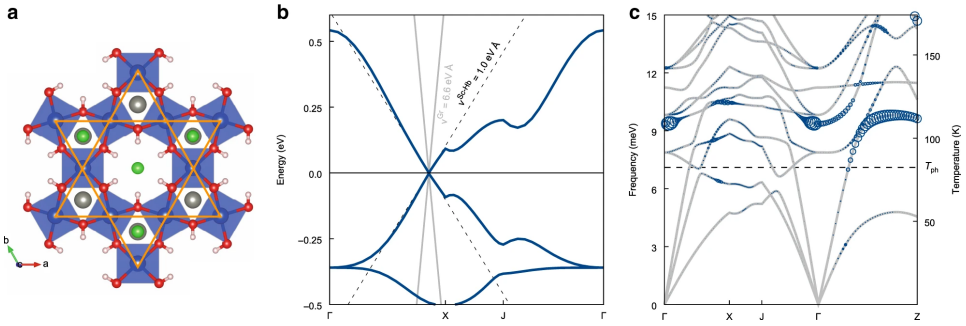

Figure 5.2: **a** Crystal structure of ScHb as seen from the top. The kagome lattice formed by the CuO_4 plaquettes is drawn in orange. **b** Band structure of the low-energy manifold of Sc-Herbertsmithite along the high-symmetry directions of the Brillouin zone [160]. The Fermi velocity of ScHb is calculated via linear fit of the band structure around the Dirac point (dashed black lines). For comparison, we have also plotted with solid gray lines the corresponding linear fit for graphene. **c** Phonon spectrum for ScHb (gray lines) and relative distribution of the electron-phonon coupling strengths (blue circles). The horizontal dashed line denotes the temperature T_{ph} above which phonons with a sizeable coupling are thermally activated.

Finally let us focus on the main point of constructing ScHb, its coupling strength. To calculate α_{eff} for ScHb, we use Eq. (5.3). To do so, we also need to compute ϵ_m. We calculate ϵ_m directly from the calculated band structure shown in Fig. 5.2 and find $\epsilon_m = (5 \pm 0.5)\epsilon_0$. Putting everything together, we find that the effective fine structure constant for ScHb is

$$\alpha_{\text{ScHb}} = 2.9 \pm 0.3 \ . \tag{5.7}$$

For reference, let us compare $\alpha_{\rm ScHb}$ with the current state of the art in electronic hydrodynamics, hBN-encapsulated graphene. The fine structure constant for graphene, within the same calculation scheme used to calculate $\alpha_{\rm ScHb}$, is [2]

$$\alpha_{\rm Gr} = 0.5 \ - \ 1.0 \ . \tag{5.8}$$

We observe that even if we take a representative value for $\alpha_{\rm Gr}$ closer to the upper limit of our computational error, say $\alpha_{\rm Gr} = 0.9$, we may still use perturbation theory to describe the properties of graphene. On the other hand, it is clear that ScHb is a strongly coupled material, whose transport properties perturbation theory fails to capture even in principle. On the contrary, holography is perfectly suited to describe the transport properties of strongly coupled materials, such as ScHb. We apply holography to ScHb in the next section, with a particular focus on η/s.

5.2 Holographic estimate for η/s and turbulence

Here we derive an estimate for the η/s ratio of ScHb and check whether it leads to a large enough Re for turbulence to set in. To derive this estimate we resort to the use of holography, since perturbation theory breaks down at $\alpha_{\rm ScHb}$. We cannot, however, use holography with a pure Einstein-Hilbert term, since the dual QFTs described by this term exhibit an infinite structure constant as we saw in 2. While $\alpha_{\rm ScHb}$ is certainly non-perturbatively large is nowhere near infinity. So the model we are going to use must involve higher-derivative corrections as discussed in section 2.4.1. For $2+1$ dimensional charged fluids, this higher-derivative model exists in $3+1$ dimensional bulk dimensions and consists of the Einstein-Maxwell Lagrangian as well as all higher derivative contractions of the Riemann and Maxwell tensors. For our purposes, however, the Maxwell tensor can be neglected without loss of generality. This is due to the fact that we are interested in η/s around the Dirac point, where the charge density of the system is approximately zero. In this limit, any corrections to η/s from the chemical potential vanish and only the pure gravity terms remain relevant [161]. This follows from recalling that η/s is calculated via the graviton propagator in the background geometry; if the total charge of the background is vanishingly small, the corrections to η/s due to the charge are negligible. Then, the bulk action can be written schematically as

$$S_{\rm bulk} = \frac{1}{16\pi G_{\rm N}} \int d^4x\sqrt{-g}\left[R - 2\Lambda + c_2 R^2 + c_3 R^3 + c_4 R^4\right] \ , \tag{5.9}$$

where R^n contains all possible contractions of n Riemann tensors and c_n are coefficients of order $\mathcal{O}(\lambda^{(1-n)/2}) \simeq \mathcal{O}(\alpha_{\rm eff}^{(1-n)/2})$.

Then we may use $S_{\rm bulk}$ to derive η/s as a function of the effective fine structure. This task can be simplified considerably using the following observations. First, recall that since the action $S_{\rm bulk}$ is considered to be a truncated higher-derivative expansion, it is subject to an emergent symmetry transformation akin to a frame change. That is, we can deform the metric by higher derivative terms without changing the underlying physics. We exploit this symmetry to bring the quadratic terms in $S_{\rm bulk}$ to the Gauss-Bonnet form

$$R^2 \to R^2_{\mu\nu\rho\sigma} - 4R^2_{\mu\nu} + R^2 \ . \tag{5.10}$$

This deformation is advantageous since the Gauss-Bonnet form is a topological invariant of $3+1$ dimensional metric manifolds. As a result, the quadratic terms in $S_{\rm bulk}$ do not contribute the graviton equations of motion, nor its propagator[3]. Hence, as shown explicitly in [97], the corrections to η/s due to the R^2 terms vanish and we may set c_2 to zero. The resulting action is then simply

$$S_{\rm bulk} = \frac{1}{16\pi G_{\rm N}} \int d^4x\sqrt{-g}\left[R - 2\Lambda + c_3 R^3 + c_4 R^4\right] \ . \tag{5.11}$$

However, our action can be simplified even further. In particular, we may set c_3 to zero as well. There are two justifications for this: First, recall that if we can assume that our action stems from a well-defined Type IIB string-theoretical action, then $c_3 = 0$ by default [102]. Second, we choose to work only at tree level in the gravitational action, in order to focus only only on coupling, and not $1/N$, corrections. This means that we can use the results of [100] discussed in section 2.4.1. According to [100] we can set $c_3 = 0$, if we are to avoid acausal graviton-graviton scattering and closed time-loops in the bulk[4]. Thus we are left with a significantly simpler action than the original one, containing only quartic corrections of the Riemann tensor

$$S_{\rm bulk} = \frac{1}{16\pi G_{\rm N}} \int d^4x\sqrt{-g}\left[R - 2\Lambda + c_4 R^4\right] \ . \tag{5.12}$$

Then using Eq. (5.12) to calculate η/s we find [103, 104]

$$\eta/s \simeq \frac{\hbar}{4\pi k_{\rm B}}\left(1 + \frac{\mathcal{C}}{\alpha_{\rm eff}^{3/2}}\right) \ . \tag{5.13}$$

The phenomenological constant $\mathcal{C}$ depends on all the coefficients, denoted schematically as c_4, appearing in front of the quartic terms in $S_{\rm bulk}$ and

[3] A bulk topological invariant cannot contribute to a boundary action.

[4] Another way to avoid these pathologies is to include particles with spin larger than 2, as discussed in [100]. String theory with its infinite number of higher spin states, is an example of such a non-pathologic theory.

therefore is model dependent. To fix $\mathcal{C}$ we need to calculate it from a top-down holographic model. However, constructing such a model and matching it directly to ScHb is highly non-trivial if not impossible. So we will follow a phenomenological approach and vary $\mathcal{C}$ over four order of magnitude, $\mathcal{C} \in [5 \times 10^{-4}, 5]$. This range was motivated from a well-known top-down holographic construction for $\mathcal{N} = 4$ SYM [103]. Within this model, the range of $\mathcal{C}$ corresponds to varying the rank of the SYM gauge group from $N = 10^3$ to $N = 2$.

The resulting estimate for η/s is shown in Fig. 5.3, as the blue band generated by varying $\mathcal{C}$. We observe in this figure that the estimate for ScHb has a far smaller variance than the estimate for graphene. This provides more credence to our assertion that holographic methods are reliable for extracting the transport properties of materials at finite but large coupling strengths. We should also mention that the holographic estimate for η/s for graphene matches with experimental data from direct observations of hydrodynamic flow in graphene around charge neutrality [23], unlike the weak-coupling result drawn as black fading curve in Fig. 5.3.

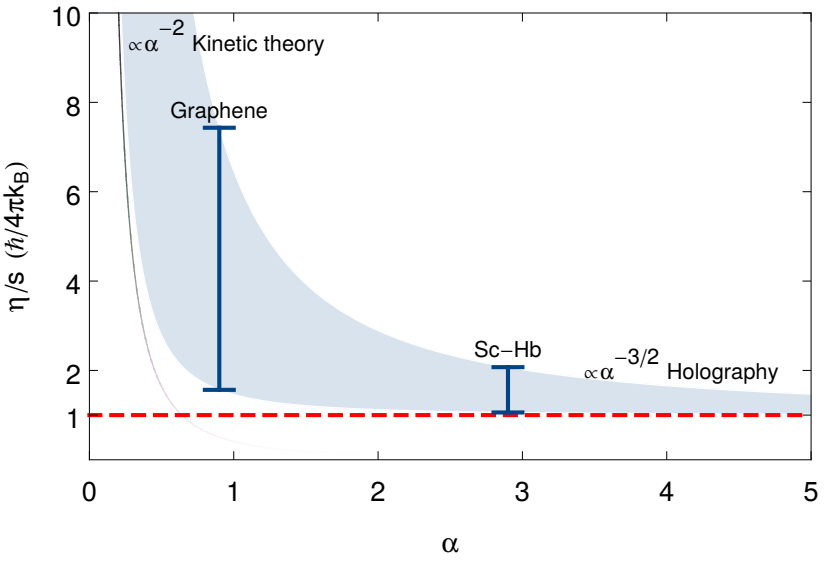

Figure 5.3: The blue band gives the ratio η/s of Eq. (5.13) for $\mathcal{C} \in [5 \times 10^{-4}, 5]$. The black fading line in the figure is the weakcoupling prediction for η/s of Eq. (5.4). The red dashed line corresponds to the KSS bound, $\eta/s = \hbar/4\pi k_B$. The blue vertical bars give the estimates of η/s for graphene at $\alpha_{Gr} = 0.9$ and for ScHb at $\alpha_{ScHb} = 2.9$. Figure reprinted from [2].

With the estimates for η/s at hand, we can now derive the Reynolds number for a hydrodynamic flow in ScHb. We choose to present our estimate

for Re_{ScHb} in terms of Re_{Gr} for reasons which will be clear presently. So, assuming that the typical velocity scales for ScHb and graphene are equal, $U_{\mathrm{ScHb}} = U_{\mathrm{Gr}}$, we find

$$Re_{\mathrm{ScHb}} = (63 - 156) Re_{\mathrm{Gr}} \ . \tag{5.14}$$

The ratio of Reynolds number in Eq. (5.14) should be considered as a lower bound. This is because we expect from Fig. 4.2d $U_{\mathrm{ScHb}} > U_{\mathrm{Gr}}$ for the same input parameters. Thus we observe that the Reynolds number for ScHb is at least two orders magnitude larger than the Reynolds number in graphene. This enhancement is enough to reach the turbulent flow regime as we now explain. To observe fully developed turbulence, a Reynolds number larger than 1000 is necessary [162]. Several works for graphene and electron hydrodynamics in general, have shown that typical Reynolds numbers for electronic flows range from $Re = \mathcal{O}(10) - \mathcal{O}(100)$ [1, 151, 163]. Hence, $Re_{\mathrm{ScHb}} = \mathcal{O}(1000) - \mathcal{O}(10000)$ which is certainly large enough for fully developed turbulence to be directly observable in ScHb flows.

Let us summarize the findings of this chapter. First, we gave a proposal for a strongly coupled electronic system with a relativistic spectrum, ScHb. We confirmed that this material is indeed strongly coupled by deriving its coupling strength to be $\alpha_{\mathrm{ScHb}} \simeq 2.9$. We argued that this material, when synthesized, is expected to host electron hydrodynamic flows, since instabilities of the Dirac cone and large electron-phonon interactions are absent at $T < 80$ K. We also argued that ScHb is a material where holographic methods can be applied, by calculating a ratio η/s which is close to what is expected in experiments. We also used this ratio to find a large Reynolds number for ScHb, which gives us for the first time access to the turbulent flow regime.

The discussion of both chapters 4 and 5 assumed parity is not broken. In the following chapter we discuss parity-breaking effects by considering how the Hall viscosity η_{H} alters hydrodynamic transport following [3].

Chapter 6

Hydrodynamic Hall effect in Fermi liquids

In this chapter, we explore the effect of the Hall viscosity $\eta_{\rm H}$ to hydrodynamic transport of weakly-coupled Fermi liquids in a channel, first presented in [3] by my collaborators and myself. In particular, we are interested in the strain induced on the fluid due to the Hall viscosity. This strain, as seen in the introduction and section 3.4, acts similarly to the Lorentz force in the sense that its normal to the fluid motion. We expect then that the Hall-viscous strain applied on a fluid within a channel will generate an analog of the usual Hall effect by pushing electrons to the sides of the sample, see Fig. 6.1.

We choose to break the parity-invariance of our system by introducing an external constant magnetic field B[1]. This has the effect of generating a non-trivial Hall viscosity $\eta_{\rm H}$, as well as altering the shear viscosity η of the fluid. In particular, in this chapter we focus on weakly-coupled Fermi liquids for which [164, 165]

$$\eta = \frac{\eta_0}{1+(2l_{\rm ee}/r_c)^2} \quad , \quad \eta_{\rm H} = \frac{2{\rm sgn}(B)\eta_0 l_{\rm ee}/r_c}{1+(2l_{\rm ee}/r_c)^2} \ . \tag{6.1}$$

In Eq. (6.1), $l_{\rm ee}$ is the electron-electron interaction length and $r_c = m_{\rm eff}v_{\rm F}/|eB|$ is the cyclotron radius of electron with effective mass $m_{\rm eff}$ and charge e. The shear viscosity at $B = 0$ is also fixed in terms of the thermodynamics of the Fermi liquid to

$$\eta_0 = \frac{1}{4} m_{\rm eff}\rho_0 v_{\rm F} l_{\rm ee} \ , \tag{6.2}$$

with ρ_0 the equilibrium *number* density of the fluid.

Within this setup, we can write down the precise form of the total Hall force $F_{\rm tot}$ after fixing our velocity profile ansatz. We choose to use the velocity profile of chapter 4, that is

[1] Recall B is a pseudoscalar and not a pseudovector in $2+1d$.

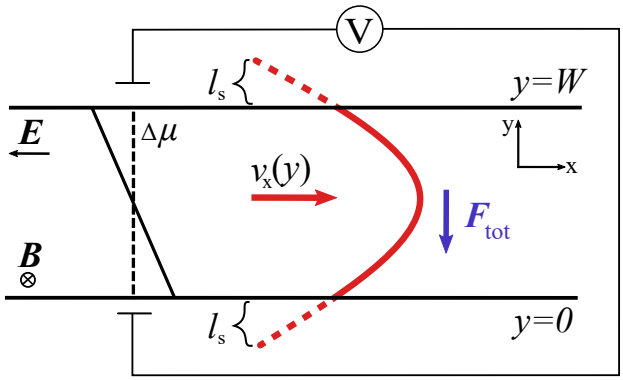

Figure 6.1: Channel setup of interest in this chapter. An electron fluid is forced to flow within a channel due to an external electric field E_x. In addition, an external magnetic field B generates $F_{\rm tot}$, the sum of the Lorentz and Hall-viscous forces, on the fluid pushing it towards the boundaries. This generates a finite chemical potential difference $\Delta\mu$ across the channel, shown as the slanted black line. The velocity profile is drawn in solid red, while the dashed red line denotes the profile's extrapolation which defines the slip length l_s. Figure reprinted from [3] with permission from APS.

$$v^\mu = \gamma(v_{\rm F}, \beta_x(y), 0), \quad \gamma = \left[1 - \left(\beta_x^2/v_{\rm F}\right)^2\right]^{-1/2} . \tag{6.3}$$

For the purposes of our investigation, let us also focus on the non-relativistic limit. This allows us to focus on the effects due to $\eta_{\rm H}$ alone without the extra contributions from relativistic effects[2]. Then $\gamma \simeq 1$ and the velocity profile reads

$$v^\mu = (v_{\rm F}, v_x(y), 0) . \tag{6.4}$$

With the above velocity profile, we find that the transverse force $F_{\rm tot}$ acting on the fluid has the form

$$F_{\rm tot} = eB\rho v_{\rm x} - \eta_{\rm H}\partial_y^2 v_x \equiv F_B + F_{\eta_H} . \tag{6.5}$$

Crucially, the Lorentz force F_B has the opposite sign as the Hall-viscous force F_{η_H}. This implies a *diminution* of the classical Hall effect in metals within the regime of applicability of hydrodynamics, compared to typical, ballistic transport in metals.

[2]Furthermore, weakly-coupled fluids are expected to be non-relativistic for typical experiments, cf. discussion around Fig. 4.3.

In the rest of this chapter, we derive the quantitative consequences of the above discussion. To do so, we first set up our hEOM in section 6.1 for the channel setup presented in Fig. 6.1. Then, in section 6.2 we solve the hEOM for the velocity profile v_x, derive the total Hall voltage ΔV_{tot} and explore their dependence on external parameters.

6.1 Hydrodynamic equations of motion

To derive the hEOM, we start with our hydrodynamic expansion of the energy-momentum and current presented in Eq.s (3.103), (3.104). In these equations, several transport and thermodynamic parameters appear, e.g. $\eta, \eta_{\text{H}}, \zeta, \tilde{\chi}_T$. Of these, we take into account only η and η_{H}. The reason we can do so varies from parameter to parameter. For example, ζ is irrelevant because our ansatz for the velocity profile satisfies $\partial_\mu v^\mu = 0$ by default. On the other hand, the quantum critical conductivity is generated only through the counter-propagation of electrons and holes around the charge neutrality point. As a result it becomes irrelevant in the Fermi liquid regime. Unfortunately, we have no sufficient explanation why $\tilde{\sigma}, \tilde{\chi}_T, \tilde{\chi}_E, \chi_\omega$ or χ_B can be neglected. So this assumption must be justified aposteriori through experiments.

With these assumptions in mind, the most general form of the hEOM is the following

$$(\partial_t + \mathbf{v}\cdot\nabla)\,\rho = -\rho\nabla\cdot\mathbf{v}, \tag{6.6}$$

$$\begin{aligned}\rho\,(\partial_t + \mathbf{v}\cdot\nabla)\,\mathbf{v} = &-\nabla P + \eta\nabla^2\mathbf{v} + \eta_{\text{H}}\nabla^2(\mathbf{v}\times\mathbf{e}_{\text{z}}) \\ &+ \text{e}\rho(\mathbf{E} + \mathbf{v}\times\mathbf{B}) - \frac{\rho v_{\text{F}} m_{\text{eff}}}{l_{\text{imp}}}\mathbf{v}\ ,\end{aligned} \tag{6.7}$$

with $\mathbf{v} = (v_x, v_y)$, l_{imp} the electron-impurity scattering length and $\mathbf{e}_{\text{z}}$ is normal to the plane defined by the channel[3].

Next let us restrict ourselves to the flow ansatz of Eq. (6.4) and choose $\mathbf{E} = -E_x\mathbf{e}_{\text{x}}$, $B = -B\mathbf{e}_{\text{z}}$ [4]. Then the charge conservation equation (6.6) is satisfied by default and the momentum conservation equations simplify down to

$$\eta\partial_y^2 v_x = e\rho E_x + \frac{\rho m_{\text{eff}} v_{\text{F}}}{l_{\text{imp}}} v_x\ , \tag{6.8}$$

$$\partial_y P = e\rho B v_x - \eta_{\text{H}}\partial_y^2 v_x\ . \tag{6.9}$$

[3] We assume the system is embedded in 3D space to accommodate experimentalists in our setup.

[4] There signs of $\mathbf{E}$, $\mathbf{B}$ were chosen in order to present the hEOM in what we consider a more aesthetically pleasing form. Our results hold for any choice of signs.

To proceed, we recall that the independent degrees of freedom of hydrodynamics are the velocity profile, the chemical potential μ and the temperature T. Hence, we can re-express $\partial_y P$ as

$$\partial_y P = \frac{\partial P}{\partial \mu}\partial_y \mu + \frac{\partial P}{\partial T}\partial_y T = \rho \partial_y \mu + s\partial_y T \ . \tag{6.10}$$

Expressing P in terms of μ and T, we see that the fluid is described by a total of three degrees of freedom, while we have only two equations of motion that can fix them. To proceed then, we must either extend our ansatz and solve a more complicated set of equations or examine whether we can fix one of the degrees of freedom apriori. We choose the second route and examine whether μ or T can be fixed to its respective equilibrium value. To this effect, we focus on the only term appearing in the hEOM which involves derivatives of μ and T, $\partial_y P$ and Eq. (6.10). Equation (6.10) can be re-written as

$$\partial_y P = \rho\mu_0 \partial_y(\mu/\mu_0) + sT_0\partial_y(T/T_0) \ , \tag{6.11}$$

where μ_0 and T_0 are the equilibrium chemical potential and temperature respectively. We introduced μ_0 and T_0 since we expect

$$\frac{\mu}{\mu_0} \simeq \frac{T}{T_0} \ . \tag{6.12}$$

As a result the relative strength of the chemical potential and temperature terms in $\partial_y P$ is quantified by the dimensionless ratio

$$\mathcal{U} = \frac{\rho\mu_0}{sT_0} \ . \tag{6.13}$$

If $\mathcal{U} \gg 1$ we may neglect the temperature contribution, and vice-versa for $\mathcal{U} \ll 1$. Substituting in the parameters for a typical Fermi liquid, such as GaAs, i.e. $\mu_0 = \mathcal{O}(50 \text{ meV})$ and $T = \mathcal{O}(1 \text{ K})$ we find $\mathcal{U} \simeq 10^{16}$. Thus, temperature gradient effects are certainly irrelevant for our analysis and $\partial_y P$ becomes

$$\partial_y P = \rho \partial_y \mu \ . \tag{6.14}$$

Then our hEOM become a closed system of equations for v_x and μ

$$\eta\partial_y^2 v_x = e\rho E_x + \frac{\rho m_{\text{eff}} v_{\text{F}}}{l_{\text{imp}}} v_x \ , \tag{6.15}$$

$$\rho\partial_y \mu = e\rho B v_x - \eta_{\text{H}}\partial_y^2 v_x \ . \tag{6.16}$$

However, further examination of the equations of motion reveals a further issue. We observe that the number density ρ being a function of μ, introduces a non-linear coupling between μ and the electric field. This is an issue

because experiments on electron hydrodynamics typically operate within the linear-response regime. Otherwise the backreaction of the electric field, for example to the energy of the fluid, must be taken into account. To evade this problem, we expand μ in terms of a fluctuation field around equilibrium. Therefore,

$$\mu \simeq \mu_0 + \delta\mu \quad , \quad |\delta\mu| \ll |\mu_0| \ . \tag{6.17}$$

Up to first order in $\delta\mu$ our hEOM, then read

$$\eta\partial_y^2 v_x = \left(\rho_0 + \frac{\partial\rho_0}{\partial\mu}\delta\mu\right) eE_x + \frac{\rho_0 v_{\mathrm{F}} m_{\mathrm{eff}}}{l_{\mathrm{imp}}} v_x, \tag{6.18}$$

$$\rho_0\partial_y\delta\mu = \left(eB\rho_0 - \eta_{\mathrm{H}}\partial_y^2\right) v_x \ . \tag{6.19}$$

Note that we have dropped a term $\propto E_x v_x$ from the expanded hEOM. This is because a direct solution of the equations including this term led again to non-linear effects in E_x. The same can be said for the term $\propto \delta\mu E_x$ in Eq. (6.17). However, we have chosen to leave this term in the hEOM, because it allows some insight into the non-linear corrections due to E_x without too much extra effort.

Given now the EOM for $\delta\mu$, we can define the voltage drop across the channel in terms of the velocity profile. In particular, we write

$$\Delta V_{\mathrm{tot}} = \left[\delta\mu(0) - \delta\mu(W)\right]/e \equiv \Delta V_B + \Delta V_{\eta_H} \ . \tag{6.20}$$

where due to Eq. (6.19)

$$\Delta V_B = -B\int_0^W dy\ v_x \quad , \quad \Delta V_{\eta_H} = \frac{\eta_H}{e\rho_0}\partial_y v_x\Big|_{y=0}^{y=W} \ . \tag{6.21}$$

With ΔV_B the classical Hall or Lorentz voltage[5] and ΔV_{η_H}, what we call, the Hall viscous voltage.

The definitions of the voltages are quite formal, but still hold a useful lesson in them. We observe that if the fluid moves fast enough, the Lorentz voltage will dominate over the Hall viscous voltage. This is simply because the area under the velocity profile curve grows faster than the area of its curvature, which in the absence of impurities is simply a constant. However, we may imagine a value of the input parameters where the Hall viscous voltage dominates. We shall derive these values in the next section and argue they are within experimental reach and the domain of validity of hydrodynamics.

To complete our discussion of our hEOM, we need to supplement them with appropriate boundary conditions. We choose

[5]To verify that ΔV_B is the classical Hall voltage, one can simply set v_x = constant.

$$v_x(y=-l_s)=0=v_x(y=W+l_s) \quad , \quad \delta\mu(y=0)=-\delta\mu(y=W)\ . \tag{6.22}$$

The boundary conditions for v_x generalize our no-slip boundary conditions used in section 4, via the introduction of the slip length l_s. A non-zero value of l_s implies that the channel boundaries are not completely diffusive and allow the fluid to slip on them with a finite drift velocity. Note that these are not the typical no-slip boundary conditions used in the literature [166], but they can be mapped to the typical ones one-to-one (cf. the supplemental of [3]). Finally, the boundary condition for $\delta\mu$ tries to capture our intuition behind the classical Hall effect. That is we expect the charge accumulated to one boundary to have come from the other. However, note that the boundary condition for $\delta\mu$ can be neglected all together, since only differences in $\delta\mu$ are measurable[6].

Let us then consider in the following section, the solution of the hEOM (6.18), (6.19) with the boundary conditions (6.22).

6.2 Velocity profile and Hall response

In this section, we solve analytically and numerically the hEOM (6.18), (6.19) for v_x and $\delta\mu$. We then use the solutions to calculate the voltages ΔV_B, ΔV_{η_H} and $\Delta V_{\rm tot}$. The dependence of these voltages on all of the external parameters, such as the density, temperature and the slip length, constitutes the novel research output of the work of my collaborators and myself in [3].

To begin with our derivation of the voltages, we note that the system of equations we plan to solve is linear and therefore can be solved directly via Fourier transform. However, the solution is not that illuminating with regards to the physical effects induced by $\eta_{\rm H}$. For this reason, we will solve the hEOM analytically only in the limit of "small" and "large" magnetic fields, while we consider the numerical solution of the hEOM for intermediate magnetic fields. The magnitude of the magnetic field is considered small in the limit of $r_c \gg l_G$, where l_G is the Gurzhi length defined below Eq. (4.14). For a material such as GaAs, the condition $r_c \gg l_G$ translates to $B \ll 100$ mT.

Solution for weak magnetic fields: To carry out the analysis of the hEOM for weak magnetic fields, we introduce a power counting parameter ϵ and assume

$$B\to\epsilon B\ ,\ \eta_{\rm H}\to\epsilon\eta_{\rm H}\ ,\ \delta\mu\to\epsilon\delta\mu\ ,\ v_x=v_x^0+\epsilon v_x^1\ . \tag{6.23}$$

[6]The absolute value of μ_0 will always overshadow the absolute value of $\delta\mu$.

Using ϵ as a perturbation parameter results in the following equations up to first order in ϵ

$$\eta\partial_y^2 v_x^0 - \frac{m_{\rm eff} v_{\rm F}\rho_0}{l_{\rm imp}} v_x^0 = e\rho_0 E_x \ , \tag{6.24}$$

$$\rho_0\partial_y\delta\mu = \left(eB\rho_0 - \eta_{\rm H}\partial_y^2\right) v_x^0 \ , \tag{6.25}$$

$$\eta\partial_y^2 v_x^1 - \frac{m_{\rm eff} v_{\rm F}\rho_0}{l_{\rm imp}} v_x^1 = e\frac{\partial\rho_0}{\partial\mu}\delta\mu E_x \ . \tag{6.26}$$

The solution to the perturbative equations above, can be solved sequentially. First we solve Eq. (6.24) for v_x^0, which is nothing other than the Poiseuille flow in the presence of impurities of section cf. Eq. (4.14). Then, we use v_X^0 as a source of the chemical potential $\delta\mu$. Finally, we use $\delta\mu$ as a source for v_x^1 and solve Eq. (6.26).

Let us focus for the moment to the solution of Eq. (6.25) for $\delta\mu$, which is the main new result of our approach. The solution reads

$$\delta\mu(y) = \frac{el_{\rm imp}E_x}{m_{\rm eff}v_{\rm F}}\left[l_G\left(\frac{m_{\rm eff}v_{\rm F}\eta_{\rm H}}{\eta l_{\rm imp}} - eB\right)\left(A_1\sinh[y/l_G] + A_2\cosh[y/l_G]\right) - eBy\right] + \Gamma \ , \tag{6.27}$$

with

$$A_1 = -\cosh\left(\frac{W}{2l_G}\right)\operatorname{sech}\left(\frac{2l_s+W}{2l_G}\right) \ ,$$

$$A_2 = \sinh\left(\frac{W}{2l_G}\right)\operatorname{sech}\left(\frac{2l_s+W}{2l_G}\right) \ ,$$

$$\Gamma = -\frac{el_{\rm imp}E_x}{2m_{\rm eff}v_{\rm F}}\left[l_G\left(\frac{m_{\rm eff}v_{\rm F}\eta_{\rm H}}{\eta l_{\rm imp}} - eB\right)\left(A_1\sinh[W/l_G] + A_2\cosh[W/l_G] + 1\right) - eBW\right] \ . \tag{6.28}$$

Equation Eq. (6.27) defines the total Hall voltage across the channel boundaries via

$$\Delta V_{\rm tot} = \left[\delta\mu(0) - \delta\mu(W)\right]/e \ . \tag{6.29}$$

To make clear the novel physical effects hidden within $\Delta V_{\rm tot}$, we will expand it in powers of $W/l_{\rm G} \ll 1$[7]. We call this the clean channel limit, since for

[7]For a typical Fermi liquid we find $l_G \simeq 6\mu$m, while typical channels range from $W = 1 - 5\mu$m.

$W \ll l_G$ the shear effects dominate over the impurity ones. The resulting expression $\Delta V_{\rm tot}$ accurate up to third order in W/l_G are

$$\Delta V_{\rm tot} \equiv \Delta V_B + \Delta V_{\eta_H}, \tag{6.30}$$

with

$$\Delta V_{\eta_H} = \frac{\eta_{\rm H} E_x}{\eta}\left[W - \frac{1}{12 l_G^2}\left(W^3 + 6 l_s W^2 + 6 l_s^2 W\right)\right] \ , \tag{6.31}$$

$$\Delta V_B = -\frac{{\rm sgn}(B) E_x}{3 r_c l_{\rm ee}}\left(W^3 + 6 l_s W^2 + 6 l_s^2 W\right) \ . \tag{6.32}$$

Equation (6.30) shows that the Hall viscosity generates a non-trivial Hall-viscous voltage. The question is, however, whether we can measure it in experiment. The simplest way to measure ΔV_{η_H} would be to restrict ourselves in a regime where $|\Delta V_{\eta_H}| \gg |\Delta V_B|$. To see whether this is possible, we calculate the ratio of the Hall-viscous to the Lorentz voltage using Eq.s (6.31),(6.32) and (6.1). We find

$$\frac{|\Delta V_{\eta_H}|}{|\Delta V_B|} = \frac{6 l_{\rm ee}^2}{W^2 + l_s W + l_s^2} + 2\frac{l_{\rm ee}}{l_{\rm imp}} \simeq \frac{6 l_{\rm ee}^2}{W^2 + l_s W + l_s^2} \ . \tag{6.33}$$

We dropped the impurity term in (6.33) because $l_{\rm ee} \ll l_{\rm imp}$ due to hydrodynamics. From the remaining term, we observe that an increasing slip-length will always decrease the ratio of the two voltages. This is physically intuitive, since a non-zero l_s allows a non-vanishing velocity near the boundaries, thus increasing the area under v_x and in turn ΔV_B (see Eq. (6.21)). Hence to observe a dominant Hall-viscous voltage, we must engineer the channel boundaries to diffuse momentum as efficiently as possible, such that $l_s = 0$. Methods (theoretical ones) on how to achieve this are described in [167]. Let us then restrict ourselves to the case of no-slip boundary conditions and write the ratio of voltages as

$$\frac{|\Delta V_{\eta_H}|}{|\Delta V_B|} = 6\left(\frac{l_{\rm ee}}{W}\right)^2 \ll 6 \ , \tag{6.34}$$

where the last inequality follows from the assumption of hydrodynamics. Therefore, the Hall-viscous voltage ΔV_{η_H} can at most be of the same order of magnitude as the Lorentz one ΔV_B. To see this more clearly, we have plotted in Fig. 6.2 the absolute value of the two voltages varying all lengths scales appearing in Eq. (6.33). In this figure, we clearly see that $\Delta V_{\eta_{\rm H}}$ can become larger than ΔV_B, but not large enough for ΔV_B be negligible within the regime of applicability of hydrodynamics.

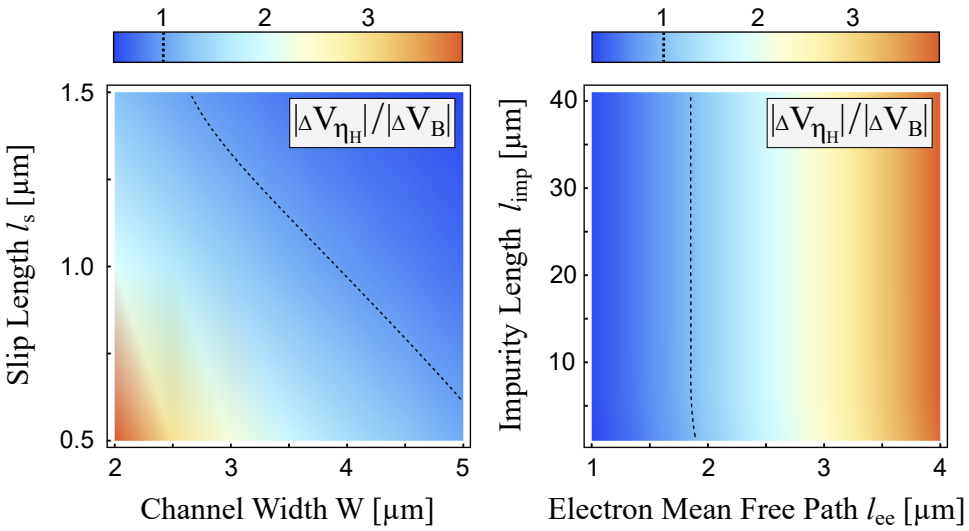

Figure 6.2: Absolute value of the ratio of the Hall-viscous ΔV_{η_H} to the Lorentz voltage ΔV_B, with varying l_s, W, l_{ee} and l_{imp}. For the parameters not varied in each figure, we choose $l_s = 0.5\mu\mathrm{m}$, $W = 3\mu\mathrm{m}$, $\rho_0 = 9.1 \times 10^{11}\mathrm{cm}^{-2}$, $T = 1.4\mathrm{K}$, $\eta_0 = 1.7 \times 10^{-16}\mathrm{Js/m}^2$ and $l_{\mathrm{imp}} = 40\mu\mathrm{m}$. The dashed lines correspond to $|\Delta V_{\eta_H}| = |\Delta V_B|$. Reprinted from [3] with permission from APS.

To summarize, we have found so far that the ratio of the viscous to Lorentz voltage increases with increasing l_{ee}, while it decreases with increasing l_s, W and l_{imp}. These parameters can be chosen such that the Hall-viscous voltage is larger than the Lorentz one, but not negligible. Moving forward, let us also examine whether the density and temperature dependence of the voltages can be used to distinguish between the two contributions.

The temperature and density dependence of the Hall-viscous and Lorentz voltages is built into the shear and Hall viscosities, as well as the length scales l_{ee} and l_G. However, since only the ratio $\eta_{\mathrm{H}}/\eta = 2l_{\mathrm{ee}}/r_c$ appears in our expressions for the voltages, we only need to specify l_{ee} and l_G as functions of ρ_0 and T. The electron-electron scattering length is given by [164, 168–170]

$$l_{\mathrm{ee}} = \frac{6v_{\mathrm{F}}\hbar^3}{F_\pi^2 m_{\mathrm{eff}} k_{\mathrm{B}}^2 T^2} \ln^2\left(\frac{\hbar^2\pi\rho_0}{m_{\mathrm{eff}} k_{\mathrm{B}} T}\right)\rho_0 \ , \tag{6.35}$$

with F_π a kinematic factor characterizing electron-electron collisions. To specify l_G as well, we need to know how l_{imp} depends on ρ_0 and T. We assume the impurities in the system are pointlike with scattering strength ν_0, density n_{imp} and impurity-electron scattering length [171]

$$l_{\rm imp} = \frac{v_{\rm F}\hbar^3}{\rho_0 m_{\rm eff}\nu_0^2 n_{\rm imp}} \ . \tag{6.36}$$

Using $l_{\rm imp}$, $l_{\rm ee}$ and Eq. (6.2) for the shear viscosity, we find for l_G

$$l_G^2 \simeq \frac{1}{4} l_{\rm imp} l_{\rm ee} = \frac{3}{2n_{\rm imp}} \left[\frac{v_{\rm F}^2 \hbar^3 \ln\left(\frac{\hbar^2\pi\rho_0}{m_{\rm eff}k_{\rm B}T}\right)}{F_\pi m_{\rm eff}\nu_0 k_{\rm B}T} \right]^2 \ . \tag{6.37}$$

The approximate equality in Eq. (6.37) stems from our approximating $\eta \simeq \eta_0$ for weak magnetic fields.

Putting everything together, we find for the density and temperature dependence of the voltages (6.31), (6.32)

$$\begin{aligned} \Delta V_{\eta_{\rm H}} = & \frac{13\hbar^3 E_x W|e|B}{F_\pi^2 m_{\rm eff}^2} \ln^2\left(\frac{\hbar^2\pi\rho_0}{m_{\rm eff}k_{\rm B}T}\right) \frac{\rho_0}{(k_{\rm B}T)^2} \\ & - \frac{|e|Bm_{\rm eff}^2\nu_0^2 E_x \left(W^3 + 6l_s W^2 + l_s^3\right)}{3\pi\hbar^5} n_{\rm imp} \ , \end{aligned} \tag{6.38}$$

$$\Delta V_B = \frac{|e|BE_x F_\pi^2 m_{\rm eff}}{36\pi\hbar^5} \frac{(k_{\rm B}T)^2}{\rho_0^2 \ln^2\left(\frac{\hbar^2\pi\rho_0}{m_{\rm eff}k_{\rm B}T}\right)} \ . \tag{6.39}$$

Equations (6.38) and (6.39) show that the Hall-viscous contribution to the total Hall voltage may be enhanced relative to the Lorentz one, by working at large densities and smaller temperatures. More importantly, (6.38) and (6.39) provide us with precise scaling laws with respect to temperature and density which can be used in the simple experiment setup of Fig. 6.1 to distinguish between the two contributions.

To conclude the discussion of our analytic results, let us discuss the local values of the voltage as we cross the channel. These local values are of interest since recent experiments have been able to measure them directly [22, 23]. We find for the voltages as a function of the transverse co-ordinate y

$$\Delta V_{\eta_H} = \frac{\eta_{\rm H}}{\eta} E_x \left[y - \frac{1}{12 l_{\rm G}^2} \left[6l_s(l_s + W) + y(3W - 2y) \right] y \right] \ , \tag{6.40}$$

$$\Delta V_B = -\frac{{\rm sgn}(B) E_x}{3 r_c l_{\rm ee}} \left[6l_s(l_s + W) + y(3W - 2y) \right] y \ . \tag{6.41}$$

There are two important features of Eq.s (6.40) and (6.41). The first one is the directly observable curvature κ of the Hall-field $E_y = -\partial_y \Delta V_{\rm tot}$. For a large $l_{\rm imp}$ it has the form

$$\kappa = -\frac{4E_x}{l_{\rm ee}}\left[\frac{\mathrm{sgn}(B)}{r_c} + \frac{\eta_H}{\eta l_{\rm imp}}\right] . \tag{6.42}$$

Unfortunately, κ is dominated by the $1/r_c$ contribution, due to the hydrodynamic assumption $l_{\rm ee}/l_{\rm imp} \ll 1$, and hence κ is not immediately useful for observing Hall-viscous transport. However, the value of the Hall field at the boundaries is immediately useful since it depends strongly on the Hall-viscosity,

$$E_y(0) = E_x\left[\frac{2l_s(l_s+W)}{sgn(B)r_c l_{\rm ee}} - \left(1 - \frac{2l_s(l_s+W)}{l_{\rm imp}l_{\rm ee}}\right)\frac{\eta_H}{\eta}\right] \overset{l_s\to 0}{=} -\frac{\eta_H}{\eta}E_x . \tag{6.43}$$

Clearly a Hall-field measurement near the boundaries of a highly diffusive channel, allows a direct measurement of η_H (in units of $\eta = 1$).[8]

Numerical analysis. We have seen analytically, the Hall-viscous voltage can be at most the same order of magnitude as the Lorentz voltage. This can seem disheartening for observing Hall-viscous transport, however, the two-voltages being equal leads to a distinctive imprint of hydrodynamics to the Hall effect. That is the vanishing of the total Hall voltage $\Delta V_{\rm tot}$ at $B = B_c \neq 0$. This feature is not captured by our analytic calculations, so a fully numerical solution of the hEOM is imperative. We plot this solution for the velocity profile at various values of the magnetic field in Fig. 6.3. The important features of the velocity profiles plotted in 6.3 are the following: As we increase the magnetic field strength i) the flow becomes faster, ii) the flow profile becomes flatter. This implies, due to (6.21), that the Hall-viscous voltage will be the principal part of the total Hall-voltage for small magnetic fields, while the Lorentz voltage will dominate for larger ones. As a consequence, there exists a critical magnetic field strength $B = B_c \neq 0$ where we crossover from $|\Delta V_{\eta_H}| > |\Delta V_B|$ to $|\Delta V_{\eta_H}| < |\Delta V_B|$. Exactly at $B = B_c$ the total Hall voltage must vanish, because of the opposite sign of the two contributions. We confirm this intuition by plotting in Fig. 6.4 the voltages for GaAs as a function of the magnetic field and with varying l_s. We observe that the critical magnetic field appears to be of order 10mT and its precise value can be shifted by varying the sample's length scales. For example, a larger l_s will push B_c to smaller values. This is due to the dependence of the voltage ratio on the sample's length scales, cf. Eq. (6.33) and Fig. 6.2.

We conclude the discussion of our work [3] by summarizing our results. We examined the modifications to classical Hall transport in a channel, due to hydrodynamics. In particular, we found that the classical Hall voltage

[8] Note that such a boundary measurement is not that easy to perform. The reason is that present measurement techniques depend on induced currents and voltages on the sample and probe. These can become discontinuous as the voltage probe approaches the boundaries of the samples, and hence can bury the signal inside the surrounding noise.

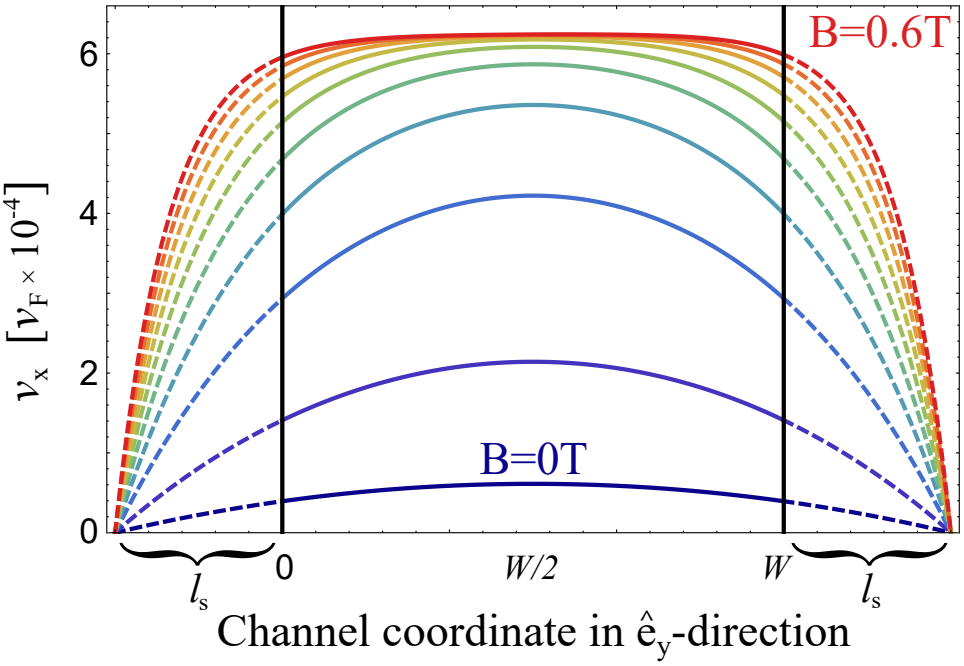

Figure 6.3: Velocity profile as a function of the transverse channel coordinate for various magnetic field strengths, $B \in [0, 0.6]$T. The input parameters are $\rho_0 = 9.1 \times 10^{11}\text{cm}^{-2}$, $T = 1.4$K, $\eta_0 = 1.7 \times 10^{-16}\text{Js/m}^2$ and $l_{\text{imp}} = 40\mu$m. Figure reprinted from [3] with permission from APS.

gains an additional contribution due to the Hall viscosity and becomes nonlinear in the magnetic field strength. We have for the first time derived the dependence of the Hall-viscous voltage to all external parameters and found that it increases with increasing density, l_{ee} and decreasing temperature, while it decreases for increasing l_s, W and l_{imp}. We also presented precise scaling laws for the temperature and density of the total Hall voltage and shown how the Hall-field at the boundaries is directly related to the Hall viscosity. Finally, we have derived a smoking-gun feature of hydrodynamic transport in a channel, the vanishing of the total Hall voltage at a non-vanishing magnetic field strength of order 10mT. Clearly, our results show how hydrodynamic behaviour can make exotic even textbook examples of transport such as the classical Hall effect and provide a multitude of ways for identifying and quantifying this exotic behaviour.

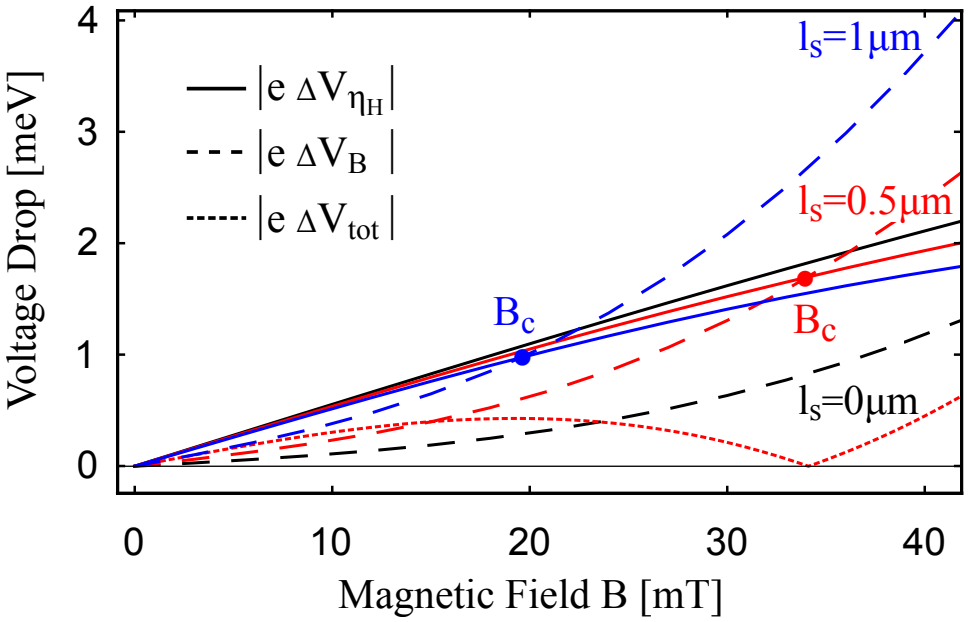

Figure 6.4: Plots of the Hall-viscous ΔV_{η_H}, Lorentz ΔV_B and total ΔV_{tot} voltages in GaAs as a function of the magnetic field B and $l_s = 0, 0.5, 1.0$ μm. The parameters fixed for this plot are $T = 1.4$ K, $W = 3\mu$m, $\rho_0 = 9.1 \times 10^{11}\text{cm}^{-2}$, $\eta_0 = 1.7 \times 10^{-16}\text{Js/m}^2$ and $l_{\text{imp}} = 40\mu$m. The critical magnetic field, $B_c = \mathcal{O}(10\text{mT})$, is defined by the bounce of $\Delta V_{\text{tot}} = 0$. The Hall-viscous contribution dominates for $B < B_c$. Figure reprinted from [3] with permission from APS

Chapter 7

Spinning-fluid hydrodynamics

In the present chapter, we present our construction of the hydrostatics of a fluid whose thermal state includes a conserved orbital and spin angular momentum. To begin, we discuss the intricacies with defining the thermal state of a charged rotating relativistic fluid in thermal equilibrium and recount some of its thermodynamic properties in section 7.1. Based on this discussion, we present in the same section two possible ways for constructing the hydrostatic effective action for a spinning fluid. Finally, in section 7.2 we derive the hydrostatic effective action and constitutive relations of a spinning fluid up to first order in the derivative expansion. We also comment on the novel spin-transport effects arising at second order in the derivative expansion.

Note: The paper [172] discussing spin hydrodynamics appeared while we were working on the spin-fluid derivative expansion. Some of the results appearing in said paper overlap with the results presented in the following.

7.1 Spinning fluid in thermal (quasi) equilibrium

In the present section we derive and discuss some of the properties of a charged spinning fluid in thermal equilibrium.

As remarked in chapter 3, the thermal equilibrium state of a system is defined in terms of the conserved charges of the system and their conjugate thermodynamic variables entering the Boltzmann distribution. In our case, the conserved charges are the energy-momentum, P^μ, the electromagnetic charge, Q, and the total angular momentum $\mathcal{J}^{\mu\nu}$[1]. Thus we define the state of a spinning fluid in global thermal equilibrium as

$$\rho_G = \exp\left[-\beta_\mu P^\mu - \zeta Q - \omega_{\mu\nu}\mathcal{J}^{\mu\nu}\right], \tag{7.1}$$

[1]Recall that the angular momentum is represented by an anti-symmetric tensor in special relativity [72].

where G stands for global, β_μ is the thermal vector, and ζ, $\omega_{\mu\nu}$ are the charge and spin chemical potential over temperature of the system respectively. We proceed as in chapter 3 and decompose the conserved charges in terms of their respective tensor densities as

$$\begin{aligned} P^\mu &= \int_\Sigma d\Sigma_\nu \; T^{\mu\nu}, \\ Q &= \int_\Sigma d\Sigma_\mu J^\mu, \\ \mathcal{J}^{\mu\nu} &= \int_\Sigma d\Sigma_\rho \left[x^\mu T^{\rho\nu} - x^\nu T^{\rho\mu} + S^{\rho\mu\nu} \right]. \end{aligned} \tag{7.2}$$

In the above equations, Σ is a spatial surface with volume element $d\Sigma_\mu$, and $T^{\mu\nu}$, J^μ are the energy-momentum tensor and U(1) current respectively. More importantly, the angular momentum density has been decomposed into two parts: The first, proportional to $T^{\mu\nu}$, corresponds to the fluid's orbital angular momentum density, while the second, $S^{\rho\mu\nu}$, to its spin-angular momentum. Note that $S^{\rho\mu\nu}$ inherits an anti-symmetry under $\mu \leftrightarrow \nu$ from the anti-symmetry of $\mathcal{J}^{\mu\nu}$.

In terms of the tensor densities, the density matrix now becomes

$$\rho_L = \exp\left[- \int_\Sigma d\Sigma_a \; T^{a\mu} b_\mu + \zeta J^a + \frac{1}{2} \omega_{\mu\nu} S^{a\mu\nu} \right], \tag{7.3}$$

where L stands for local and $b_\mu = \beta_\mu - \omega_{\mu\nu} x^\nu$. Let us compare the density matrix of Eq. (7.3) with that of Eq. (7.1). In Eq. (7.1), the conserved charges are clearly, P^μ, Q and $\mathcal{J}^{\mu\nu}$. However, in Eq. (7.3) the conserved quantities seem to be P^μ, Q and $S^{\rho\mu\nu}$. Clearly, this is physically impossible unless the orbital angular momentum vanishes identically. However, we have not made any such assumption. So how can Eq. (7.3) be equivalent to Eq. (7.1)? The answer is the following: The difference between ρ_G and ρ_L is that the momentum conserved under ρ_G is different from the momentum conserved in ρ_L. Namely, ρ_G conserves the global momentum of the system in the direction of the thermal vector β_μ, while the momentum in ρ_L is, at most, only locally conserved in the direction of the thermo-orbital vector b_μ.

Let us explain why the momentum in ρ_L is only locally conserved: Note that because of Lorentz invariance we can rotate β_μ to align with the time direction, $\beta_\mu \propto \delta^t_\mu \partial_t$. Then, the Boltzmann distribution takes its usual form $\rho_G \propto \mathrm{e}^{-\beta E}$ with $\beta = |\beta_\mu|$, E the inverse temperature and energy of the fluid respectively. We can also try to align b_μ with the time direction. Note, however, that b_μ is not just a random vector in spacetime. In fact, b_μ is the vector generated by β_μ after a local rotation with the "angular velocity" matrix $\omega_{\mu\nu}$ (cf. chapter 8 of [71][2]). Hence for a general $\omega_{\mu\nu}$, b_μ

[2] In [71] the authors work with the rotation group, but their approach generalizes directly to the Lorentz group.

defines a non-inertial frame of reference and so lies outside of any orbit of the global Lorentz group. It does, however, lie in the orbit of a local Lorentz transformation. So if we gauge Lorentz invariance, i.e. if we make diffeomorphism invariance a symmetry of the fluid, we can identify a non-inertial frame with an inertial one in the presence of a gravitational field and define the conserved momentum of the system. That is, we can deform the metric of the system from the Minkowski one and define the conserved momentum in terms of b_μ.

Unfortunately, this is again not in general possible for a rotating fluid. In order for b_μ to play the role of the direction of conserved momentum, it must also be a timelike Killing vector of the metric. Being a timelike Killing vector, b_μ defines a foliation of spacetime and allows us to apply the formalism of chapter 3 by splitting the spacetime volume element into a temporal and spatial part (as in e.g. Eq. (3.7)). In general, however, b_μ cannot define a smooth foliation of spacetime in terms of spatial surfaces. The condition for such a foliation to exist is the vanishing of Cartan's second structure equation

$$b \wedge db = b \wedge \omega = 0, \tag{7.4}$$

where $b = b_\mu dx^\mu$, $\omega = \omega_{\mu\nu} dx^\mu \wedge dx^\nu$, $d = dx^\mu \partial_\mu$ and $\wedge$ the anti-symmetric product between forms. Physically we must impose Eq. (7.4) on b_μ, because if this condition fails to hold it is possible for observers in spacetime to time-travel via regular space-travel on a particular hypersurface, see Fig.7.1c. This is problematic since it implies that an extended body, such as a fluid, can exist simultaneously in several different moments in time[3]. Clearly, Eq. (7.4) is satisfied trivially when angular momentum is not conserved because $\omega_{\mu\nu} = 0$ (see Fig. 7.1a). Another, non-trivial, solution is a "pure boost" in the plane defined by b_μ and, say, the x-direction, with $\omega_{\mu\nu} = b_{[\mu}\delta^x_{\nu]}$ (see Fig. 7.1b)[4].

Despite these solutions, it is expected that no solution of Eq. (7.4) exist for a general spin chemical potential $\omega_{\mu\nu}$. The reason is that b_μ ceases to be timelike for large enough values of the spatial components of ω. To see this, consider a purely spatial $\omega_{\mu\nu}$ given by

$$\omega = \Omega d\mathbf{x} \wedge d\mathbf{x} \ , \tag{7.5}$$

with "angular frequency" Ω. In this case, b_μ becomes spacelike for $|\mathbf{x}| > r_\Omega \equiv |\beta|/|\Omega|$. The existence of r_Ω means that the co-ordinate system attached to b_μ contains a horizon. Namely, r_Ω defines a spacetime region similar to the ergosphere of a rotating black hole. This is a region of spacetime, where worldlines change from timelike to spacelike. More importantly,

[3]Two events in spacetime are simultaneous if they happen on the same spatial hypersurface.

[4]In this case, $(b \wedge \omega)_{\mu\nu\rho} \propto b_{[\mu} b_\nu \delta^x_{\nu]} = 0$.

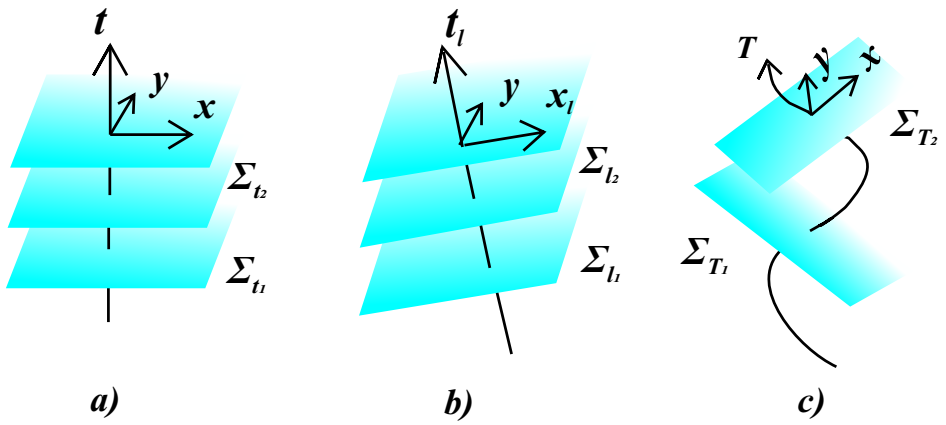

Figure 7.1: Hypersurfaces of simultaneity for $2+1$ dimensional observers defined by **a)** a stationary observer with $b_\mu = \beta_\mu$ parallel to the t-axis. In particular, the hypersurfaces Σ_{t_1}, Σ_{t_2} are defined by $t = t_1$, $t = t_2$ respectively. In **b)**, the hypersurfaces of simultaneity are defined through an observer boosted in the x-direction with respect to observer **a)**. The t_l co-ordinate is parallel to b_μ, related to β_μ via the Lorentz boost $\omega_{\mu\nu} = b_{[\mu}\delta^x_{\nu]}$, and x_l is the boosted x co-ordinate. Similarly to **a)**, Σ_{l_1}, Σ_{l_2} are defined by $t_l = l_1$, $t_l = l_2$ respectively. In **c)** we sketch an example of an observer whose b_μ vector, parallel to the T-axis, does not satisfy Eq. (7.4). In this case, the planes of simultaneity Σ_{T_1} and Σ_{T2} intersect at least at one common point p. Any object at p, then, exists at both time $T = T_1$ and $T = T_2$.

a fluid within the ergosphere can appear static to observers outside the ergosphere only if it moves faster than the speed of light. Therefore, if the fluid lies within the ergosphere, b_μ cannot define a foliation with which the momentum of the fluid can be considered conserved or even well-defined.

On a more general note, the existence of a well-defined timelike thermo-orbital vector b_μ has been studied in the past, as an attempt to extend the Unruh effect [173–175] to rotationally accelerating systems. In particular, it has been found that a timelike Killing vector cannot be defined for all values of the acceleration and angular rotation frequency of the observer moving parallel to b_μ [176]. This means that there is in general no single timelike Killing vector we can use to define a thermal state with zero orbital angular momentum, but non-zero spin angular momentum. However, it has been suggested that a family of timelike Killing vectors rotating at different

frequencies (as seen by an inertial observer) can in principle be used to circumvent this issue [177].

So what is the relevance of this discussion to writing down spinning-fluid hydrodynamics? It shows us that we can use two different methods for constructing the effective action of spinning hydrodynamics: One where the total angular momentum is conserved and one where spin angular momentum is conserved. We refer to these cases as the metric and vielbein approaches for reasons that become clear below.

Note: The orbital angular momentum appears in a conservation law in both the metric and vielbein approach (see Eq. (7.14) below). However, this is not obvious directly from the thermal density matrix of the vielbein approach, because the orbital angular momentum is hidden inside the energy-momentum of the system. To see this, consider for example the Hamiltonian of a rotating observer H_r. It can be expressed as

$$H_r = H + \omega_{\mu\nu}\left(x^\mu P^\nu - P^\mu x^\nu\right) \ , \tag{7.6}$$

with H, P^μ the Hamiltonian, momentum of the inertial observer.

Metric approach: First we consider the metric approach to spin-hydrodynamics. In this approach, we consider as conserved quantities the energy-momentum, charge and total angular momentum of the system. To enforce the conservation of $T^{\mu\nu}$ and J^μ we introduce the corresponding gauge fields, the metric $g_{\mu\nu}$ and the U(1) gauge field A_μ respectively. We must also introduce one additional tensor field to enforce the conservation of the total angular momentum of the system, call it $\Gamma^\rho_{\mu\nu}$. If we assume $\Gamma^\rho_{\mu\nu}$ is completely independent from $g_{\mu\nu}$, then the angular momentum $\mathcal{J}_{\mu\nu}$ would be completely independent from the energy-momentum P^μ. This is clearly wrong and must be corrected. To do so, we can either add additional Lagrange multiplier fields in the effective action, or impose additional constraints directly on $\Gamma^\rho_{\mu\nu}$. The second approach was considered in the absence of spin-angular momentum in [111]. The authors of [111] have shown that $\Gamma^\rho_{\mu\nu}$ is completely fixed in terms of the metric. In particular, $\Gamma^\rho_{\mu\nu}$ must take the form of the Christoffel connection

$$\Gamma^\rho_{\mu\nu} \to \mathring{\Gamma}^\rho_{\mu\nu} = \frac{1}{2} g^{\rho a}\left(\partial_\mu g_{\nu a} + \partial_\nu g_{\mu a} - \partial_a g_{\mu\nu}\right) \ . \tag{7.7}$$

In the absence of spin angular momentum and when $\Gamma^\rho_{\mu\nu}$ is given by the Christoffel connection, we can redefine the energy-momentum such that the orbital angular momentum tensor is identically conserved. More precisely, instead of the canonical energy-momentum tensor $T^{\mu\nu}$, we can work with the symmetric Belinfante energy-momentum tensor $T^{\mu\nu}_B$ [111,178]. Working with the Belinfante energy-momentum tensor means that $\omega_{\mu\nu}$ can be set to zero without loss of generality, since angular momentum conservation is always satisfied by construction. As a result, the thermal state of the fluid

is defined only through the fluid's energy-momentum and charge or equivalently the fluid's thermal vector β_μ and chemical potential. It follows from this discussion, that spin-angular momentum conservation is encoded by a metric independent, non-Christoffel part to $\Gamma^\rho_{\mu\nu}$. That is, we can decompose $\Gamma^\rho_{\mu\nu}$ as

$$\Gamma^\rho_{\mu\nu} = \mathring{\Gamma}^\rho_{\mu\nu} + K^\rho_{\mu\nu} \ . \tag{7.8}$$

The tensor $K^\rho_{\mu\nu}$ is the so-called con-torsion tensor and is anti-symmetric with respect to $\mu \leftrightarrow \nu$ [5]. With the inclusion of $K^\rho_{\mu\nu}$ into our setup, we can now derive the constitutive relations for $T^{\mu\nu}$, J^μ and $S^{\mu\nu\rho}$ by writing down the most general diffeomorphism and gauge invariant functional $W = W[g_{\mu\nu}, A_\mu, K^\rho_{\mu\nu}]$ and using Eq. (3.13). The chemical potentials necessary for this derivation are defined in terms of $g_{\mu\nu}$, A_μ and $K^\rho_{\mu\nu}$ via Eq. (3.11) or more precisely,

$$Ln^\mu g_{\mu\nu} \equiv \beta_\nu \ \ , \ \ Ln^\mu A_\mu = -\zeta = \mu/T \ \ , \ \ Ln^\rho K_{\mu\nu\rho} = -\omega_{\mu\nu} \equiv \mu^S_{\mu\nu}/T \ , \tag{7.9}$$

with $L = \sqrt{-\beta^2}$ the length of the compactified time direction of $g_{\mu\nu}$, parallel to n^μ, and $\mu^S_{\mu\nu}$ the spin chemical potential.

We wish to remark that $K^\rho_{\mu\nu}$, apart from a Lagrange multiplier, also has a geometric interpretation. Namely, the con-torsion tensor turns $\Gamma^\rho_{\mu\nu}$ into a torsionfull affine connection. More precisely, we can express the contorsion tensor in terms of the torsion tensor $T^\rho_{\mu\nu}$ as

$$K_{\mu\nu\rho} = \frac{1}{2}\left(T_{\mu\nu\rho} + T_{\nu\rho\mu} - T_{\rho\mu\nu}\right) \ . \tag{7.10}$$

The non-trivial torsion tensor turns the metric geometry of our spacetime into an Einstein-Cartan geometry [180, 181]. Geometrically, a non-trivial torsion tensor alters the relative angle between hypersurfaces (spacelike or timelike) defined by a non-inertial observer moving in spacetime, as in Fig. 7.1c [182]. In fact, the condition (7.4) can be written in terms of the torsion tensor as

$$b_\mu T^\mu_{\kappa\lambda} \Delta^\kappa_{b,\nu} \Delta^\lambda_{b,\rho} = 0 \ , \tag{7.11}$$

with $\Delta^\mu_{b,\nu}$ the projector in a direction normal to b_μ, i.e. $\Delta^\mu_{b,\nu} b^\nu = 0$. Physically, the torsion tensor is to the spin tensor, what the metric is to the energy-momentum tensor. In particular, in a dynamical theory of torsion the spin tensor acts as the source of torsion in the same way that $T^{\mu\nu}$ acts as a source to $g_{\mu\nu}$. We discuss the importance of this observation within the context of the gauge/gravity duality in chapter 8.

[5] Note that one can also choose a general asymmetric tensor in the place of $K^\rho_{\mu\nu}$. However, this asymmetric tensor leads to further conserved charges not considered here. See [179] and chapter 8 for more details.

Vielbein approach: The starting point for the vielbein approach is the density matrix ρ_L given by Eq. (7.3). We can bring ρ_L into an effective action form (recall (3.8)) by specifying equilibrium in terms of a timelike vector n^μ parallel to β^μ. More precisely, we define

$$\begin{aligned} &g_{\mu\nu} = \gamma_{\mu\nu} + n_\mu n_\nu, \quad n_\mu = -N\partial_\mu t \ , \\ &ds^2 = -N^2 dt^2 + \gamma_{ij} dx^i dx^j, \quad N = \sqrt{-\beta^2} \ , \end{aligned} \tag{7.12}$$

with γ_{ij} the metric on the hypersurface Σ. Given $g_{\mu\nu}$, we have then for ρ_L

$$\rho = \exp\left[-\beta^{-1}\int_M d^D x\sqrt{g}\ n^a T_a^\mu b_\mu + \zeta n^a J_a + \frac{1}{2} n^a \omega_{\mu\nu} S_a^{\mu\nu}\right]. \tag{7.13}$$

At this point in chapter 3, we introduced external sources coupling to the conserved charges. We know that these sources for J^μ and $S^{\mu\nu\rho}$ are A_μ and $\Gamma_{\mu\nu\rho}$ respectively. We can, however, no longer choose the metric as the source for $T^{\mu\nu}$, since in general we cannot take n_μ to be parallel to b_μ. Therefore, we need to introduce a new field that will source $T^{\mu\nu}$. To derive this source field, we can use the Noether procedure. That is, we can introduce a two-tensor field e_μ^a and assume it transforms under the symmetries which lead to the conservation of energy-momentum, charge and angular momentum

$$e_\mu^a \to e^{'a}_\mu = e_\mu^a + \delta e_\mu^a.$$

Then we fix δe_μ^a such that it enforces the conservation laws. To be more precise, the conservation laws for for a spinning fluid take the form

$$\partial_\mu T_a^\mu = F^{a\mu} J_\mu \quad , \quad \partial_\mu J^\mu = 0 \quad , \quad \partial_\rho S^\rho_{\mu\nu} = -T_{[\mu\nu]} \ . \tag{7.14}$$

These transformation laws stem from local translation invariance, U(1) gauge invariance and local Lorentz invariance. Since $T_{\mu\nu}$ appears in the energy-momentum and angular-momentum conservation equations, we see that e_μ^a must transform both under local translations as well as local Lorentz rotations, but be inert under U(1) gauge transformations. With some hindsight involved, it is quite simple to derive the appropriate transformation laws. Namely, we have

$$e_\mu^a \to e_\mu^a + \mathcal{L}_\xi e_\mu^a \quad , \quad e_\mu^a \to e_\mu^a + \Omega_b^a(x) e_\mu^b. \tag{7.15}$$

where ξ is an infinitesimal diffeomorphism and $\Omega_b^a(x)$ an anti-symmetric matrix parametrizing an infinitesimal local Lorentz transformation. The transformation rules (7.15) provide e_μ^a with a geometric interpretation. In

particular, e^a_μ is what in differential geometry is referred to as the vielbein field. The inclusion of e^a_μ into our formulation, generically turns the spacetime into a torsionfull metric spacetime. More precisely, the field strength of e^a_μ provides us with the torsion tensor as

$$T^a_{\mu\nu} = \nabla_{[\mu} e^a_{\nu]} = \partial_{[\mu} e^a_{\nu]} + \left(\Gamma^\rho_{\mu\nu} - \Gamma^\rho_{\nu\mu}\right) e^a_\rho \ . \tag{7.16}$$

Furthermore, e^a_μ can be considered an isomorphism between the spacetime tangent space and the Minkowski spacetime tangent space. In this sense e^a_μ provides us with the local mapping, suggested by [177], of the non-inertial co-ordinate system, based on b_μ, with an inertial one, thus allowing us to define the conserved momentum in the direction of b_μ [6]. This isomorphism between the inertial and non-inertial systems, also allows us to define the metric of the spacetime by pulling back the Minkowski tangent space metric to the spacetime

$$g_{\mu\nu} = \eta_{ab} e^a_\mu e^b_\nu \ . \tag{7.17}$$

It is also important to note that in this approach, the connection $\Gamma^a_{\mu b}$ is a spacetime tangent space vector, but transforms as a connection under a local Lorentz transformation L^a_c as

$$\Gamma^a_{\mu b} \to L^a_c \Gamma^c_{\mu d} (L^{-1})^d_b + L^a_c \mathrm{d}(L^{-1})^c_b. \tag{7.18}$$

Note that the transformation for the connection in the vielbein approach is different than the transformation of the connection $\Gamma^\rho_{\mu\nu}$ in the metric approach. In particular, the connection in the metric approach transforms as a connection under spacetime diffeomorphisms and not under Minkowski spacetime Lorentz transformations. However, the two connections are related to each other via the vielbein postulate [67][7]

$$\tilde{\nabla}_\mu e^a_\nu = \partial_\mu e^a_\nu + \Gamma^a_{\mu b} e^b_\nu - \Gamma^\rho_{\mu\nu} e^a_\rho = 0 \ .^{8} \tag{7.19}$$

With the inclusion of e^a_μ into our set of fields, we can now define the effective action for spinning fluids as a diffeomorphism, U(1) gauge and local Lorentz transformation invariant functional $W = W[e^a_\mu, A_\mu, \Gamma^a_{\mu b}]$. The remaining detail to be fixed before we can use W, is the choice of thermal state as in (7.9). We choose

$$\beta_a e^a_\mu \equiv b_\mu \quad , \quad L_n A_\mu = -\zeta = \frac{\mu}{T} \quad , \quad L_n \Gamma^a_{\rho b} = -\omega^a_b \equiv \frac{\mu^{S\ a}_b}{T} \ . \tag{7.20}$$

[6] In the following, greek indices denote non-inertial co-ordinates and latin indices denote inertial co-ordinates.

[7] Note that the vielbein postulate can also be thought of as a gauge transformation of $\Gamma^a_{\mu b}$ with parameter e^a_μ. The gauge group in this case is the general linear group over the real numbers [183].

[8] $\tilde{\nabla}_\mu$ is the connection on both the Minkowski and spacetime tangent spaces.

Again $L = \sqrt{-\beta^2}$ is the length of the thermal circle.

Our definitions in Eq. (7.20) are the standard ones presented in Eq. (3.11). Let us, however, give some comments regarding the condition $\beta_a e^a_\mu = b_\mu$. We claim that our frame choice for e^a_μ is a rule for translating thermodynamic quantities, such as temperature, between the rotating observers moving with the fluid (parallel to b_μ) and non-rotating observers moving in time (parallel to β_μ). Or in other words, our frame choice for e^a_μ defines an Euler observer that can measure the properties of the fluid at each point in spacetime even though there is no globally defined Euler observer. For example consider the temperature of the system $\beta^a\beta_a$

$$\beta^a\beta_a = (e^a_\mu b^\mu)(e^\nu_a b_\nu) = e^a_\mu e^\nu_a b^\mu b_\nu = \delta^\nu_\mu b^\mu b_\nu = b^\mu b_\mu. \tag{7.21}$$

In the above derivation we introduced the inverse frame e^μ_a and used several identities derivable directly from our frame choice for e^a_μ.

We have thus shown that the observer co-moving with the fluid measures the same local temperature as the global observer. Similarly, both observers measure the same values for the local charge and spin chemical potentials. Moreover, because the mapping from b_μ to β_μ preserves their magnitudes, we can identify $\omega_{\mu\nu}$ with the transformation parameter for the local Lorentz transformation connecting β_μ to b_μ. As a final remark, note that because e^a_μ is not symmetric under exchange of its indices, the same holds for T^μ_a. Contrast this with the energy momentum tensor $T^{\mu\nu}$ in the metric approach which is by construction symmetric under $\mu \leftrightarrow \nu$.

This concludes our exposition of the routes we can take to construct the effective action for spinning fluids. We have shown there are two equivalent such roots, depending on if we choose the metric or the vielbein field as the source of the energy-momentum tensor. These two approaches are equivalent to each other via the mappings (7.17), (7.19), so one can choose either one to construct the spinning fluid constitutive relations. We choose in the following to use e^a_μ as the independent field and construct the effective action $W[e^a_\mu, A_\mu, \Gamma^a_{\mu b}]$. The reason for this choice is the important role played by the vielbein field in the description of gravitational and torsional anomalies[9](see e.g. [55, 112]). We expect that modifying W to incorporate these anomalies will be easier than modifying the equivalent functional $W = W[g_{\mu\nu}, A_\mu, \Gamma^\rho_{\mu\nu}]$. Before we proceed to writing down the effective action of a spinning fluid, let us first use the Boltzmann distribution to derive some of the thermodynamic properties of a spinning fluid, which will also appear in the constitutive relations.

[9]Fermions couple directly to e^a_μ and not $g_{\mu\nu}$.

Equilibrium entropy current and the Gibbs-Duhem relation for spinning fluids

As an application of our general discussion on spinning-fluid thermodynamics, we derive in this subsection the equilibrium entropy current and the Gibbs-Duhem relation for fluids with angular momentum. To do that, we define the normalized density matrix

$$\rho_N = \exp\left[\beta_\mu \Omega^\mu\right] \exp\left[-\beta_\mu P^\mu - \zeta Q - \frac{1}{2}\omega_{\mu\nu}\mathcal{J}^{\mu\nu}\right], \tag{7.22}$$

$$\mathrm{e}^{-\beta_\mu \Omega^\mu} = \mathrm{Tr}[\rho_G] = \mathrm{Tr}\left[\exp\left[-\beta_\mu P^\mu - \zeta Q - \frac{1}{2}\omega_{\mu\nu}\mathcal{J}^{\mu\nu}\right]\right]. \tag{7.23}$$

Given ρ_N, the entropy of the system is defined as usual:

$$S = -\mathrm{Tr}\left[\rho_N \log \rho_N\right] = \beta_\mu \Omega^\mu + \beta_\mu \langle P^\mu \rangle + \zeta \langle Q \rangle + \frac{1}{2}\omega_{\mu\nu}\langle \mathcal{J}^{\mu\nu}\rangle. \tag{7.24}$$

Now we may introduce a local entropy density for S and the grand potential Ω^μ as

$$S = \int_\Sigma d\Sigma^a s_a \quad , \quad \Omega^\mu = \int_\Sigma d\Sigma^a \Phi^\mu_a \, . \tag{7.25}$$

Using Eq. (7.25), we can then express the entropy current in terms of the conserved tensor densities of the spinning fluid (7.2)

$$s_a = \beta_\mu \Phi^\mu_a + b_\mu \langle T^\mu_a \rangle + \zeta \langle J_a \rangle + \frac{1}{2}\omega_{\mu\nu}\langle S^{\mu\nu}_a \rangle. \tag{7.26}$$

If we assume that the partition function of the system, $\mathcal{Z}$, is properly normalized on-shell (os), then $\Phi^\mu_a = 0$ and we find for the on-shell entropy current

$$s_a \overset{\text{os}}{=} b_\mu \langle T^\mu_a \rangle + \zeta \langle J_a \rangle + \frac{1}{2}\omega_{\mu\nu}\langle S^{\mu\nu}_a \rangle. \tag{7.27}$$

As expected, for $\omega_{\mu\nu} = 0$, Eq. (7.27) reduces to the well-known expressions for the entropy current in charged relativistic fluids (see e.g. [9]).

Next, we derive the Gibbs-Duhem relation for spinning fluids. To do that, assume $\beta_\mu = \beta(1,0,0)$ and $\Omega^0 = -PV$, where P is the pressure and V the volume of the system. With these assumptions we obtain from Eq. (7.24)

$$S = \beta P V + \beta E + \zeta N + \frac{1}{2}\omega_{\mu\nu}\langle \mathcal{J}^{\mu\nu}\rangle.$$

We then introduce the global densities for entropy, $s = S/V$, energy $\epsilon = E/V$, charge density $\rho = N/V$ and angular momentum $j^{\mu\nu} = \langle \mathcal{J}^{\mu\nu} \rangle / V$ into the equation and re-arrange it a bit to find

$$P + \epsilon = sT - T\zeta\rho - \frac{1}{2} T \omega_{\mu\nu} j^{\mu\nu}.$$

The last equation is quite familiar and can become even more so by introducing the number and spin chemical potentials $\zeta T = -\mu$ and $\omega_{\mu\nu} T = -\mu^S_{\mu\nu}$. With the chemical potentials in place we finally arrive at the Gibbs-Duhem relation for spinning fluids

$$\epsilon + P = sT + \mu\rho + \frac{1}{2} \mu^S_{\mu\nu} j^{\mu\nu}. \tag{7.28}$$

Again, Eq. (7.28) reduces to the familiar case of the charged fluid when $\mu^S_{\mu\nu} = 0$.

7.2 Equilibrium effective action

In the present section, we shall write down the equilibrium or hydrostatic effective action of spinning fluids and their corresponding constitutive relations to zeroth and first order in the derivative expansion. We shall also comment on some of the transport effects generated from second order derivative terms. Unless stated otherwise we work in a general spacetime dimension D. We begin our construction at zeroth order in the derivative expansion, i.e. the expansion in powers of $\mathcal{K}$ [10], in the following subsection.

Equilibrium effective action at $\mathcal{O}(\mathcal{K}^0)$

As mentioned in the previous section, we construct the effective action using as the sources the fields e^a_μ, A_μ and $\Gamma^a_{\mu b}$. Consequently, the effective action is constructed by the scalars we can build up out of the thermodynamic data $\{b_\mu, \mu, \mu^S_{ab}\}$. In order to connect to the notation of chapter 3, we choose to split b_μ into two distinct zeroth order data. These are its magnitude $T = 1/\sqrt{-b^2}$ and its direction $u^\mu = T b^\mu$. As the notation suggests, we identify T with the temperature of the system and u^μ with the fluid's velocity profile. Apart from $\{T, u_\mu, \mu, \mu^S_{ab}\}$, we have one additional zeroth order datum we need to consider, the direction of time n^μ. We have to consider n^μ because it defines the time-direction of our system, i.e. it defines equilibrium. Finally, note that we are assuming μ^S_{ab} to be a zeroth order term.

Now we are ready to construct the zeroth order scalars for a spinning fluid. In order to compactify our results, we choose to change the notation

[10] Recall the discussion around (3.28).

a bit. Namely, we suppress index contractions and instead use quantum-mechanical matrix notation, e.g. $u^\mu \mu^S_{\mu\nu} n^\nu$ will be written as $(u|\mu^S|n)$. Similarly, products of the spin chemical potential will be interpreted as a product of matrices, e.g. $(\mu^S)^2_{\mu\nu} = \mu^S_{\mu a}\mu^{Sa}_\nu$. With this notation at hand, the zeroth order scalars for general dimension D are

$$S_0 = \left\{T,\ \mu/T, (u|n),\ (u+n|(\mu^S)^k|u+n),\ \mathrm{Tr}\left[(\mu^S)^{2k}\right]\right\}, \tag{7.29}$$

where k is a positive integer and the trace is defined as usual, i.e as the contraction of the free indices of $(\mu^S)^{2k}$. We note that the anti-symmetry of μ^S implies that the diagonal components of $(\mu^S)^k$ vanish if k is odd. For example, $(u|\mu^S|u) = (n|\mu^S|n) = 0 = (u|(\mu^S)^3|u)$, etc.

If we restrict ourselves to $D = 2+1$, we can construct additional zeroth order scalars by using the Levi-Civita tensor $\epsilon_{\mu\nu\rho}$ [11]. The addition of the Levi-Civita tensor adds two vectors and two anti-symmetric tensors into the list of zeroth order data. These are

$$\tilde{\epsilon}_\mu = \epsilon_{\mu\nu\rho}u^\nu n^\rho,\ \ \tilde{\mu}^{S,\mu} = \frac{1}{2}\epsilon^{\mu\nu\rho}\mu^S_{\nu\rho},\ \ \tilde{u}_{\mu\nu} = \epsilon_{\mu\nu\rho}u^\rho \ \text{ and } \ \tilde{n}_{\mu\nu} = \epsilon_{\mu\nu\rho}n^\rho. \tag{7.30}$$

We can use the vectors in Eq. (7.30) to construct scalars as in Eq. (7.29). However, not of all of these new scalars are independent of S_0. For example

$$\tilde{\epsilon}^2 = 1 - (u|n)^2 \ \ , \ \ (\mu^S|\mu^S) = 2\mathrm{Tr}\left[(\mu^S)^2\right] \ \ , \ \ \tilde{u}^2 = P_u \ \ , \ \ \tilde{n}^2 = P_n,$$

where P_x is the projector in the direction of $|x)$.

Using identities similar to the ones above, we end up with the extended list of zeroth order scalars below

$$S_0 = \left\{T,\ \mu/T,\ (u|n),\ (x_i + \tilde{\mu}^S|\prod_i (\mu^S)^{k_i} X_i|x_j + \tilde{\mu}^S),\ \mathrm{Tr}[\prod_i (\mu^S)^{k_i} X_i],\right\} \tag{7.31}$$

where $|x_i) = |u), |n), |\tilde{\epsilon})$, $X_i = 1, \tilde{u}, \tilde{n}, P_u, P_n$, and k_i are positive integers.

"Small" spin chemical potentials

Clearly, the list of zeroth order scalars S_0 contains an infinite number of terms. Therefore, the respective constitutive relations will also contain an infinite number of terms. We doubt that such an expansion can ever be practically useful, unless certain simplifications are made. In this subsection, we

[11] For $D > 3$, one must use the corresponding Levi-Civita tensor.

explore what happens to the constitutive relations when the spin-chemical potential is assumed to be small, i.e. $\mathcal{O}(\mathcal{K})$.

The small chemical potential regime, we believe, includes experimentally interesting and available materials. For example, we know that graphene can be in a regime where it exhibits spin transport (spin-Hall effect [184]) or in a regime where it exhibit hydrodynamic behaviour. If we assume that the transition from the spin transport regime to the hydrodynamic regime is continuous, then there is necessarily a regime where graphene exhibits spin-hydrodynamic transport with a small spin chemical potential. We assume the last assertion to be true and leave its verification to experimentalists.

Furthermore, we can make a formal argument for why we may assume the chemical potential to be $\mathcal{O}(\mathcal{K})$. Due to our frame choice (7.20), if $\mu^S_{\mu\nu}$ is $\mathcal{O}(\mathcal{K})$, then $\Gamma^a_{\mu\nu}$ is also $\mathcal{O}(\mathcal{K})$. Consequently, its field strength is $\mathcal{O}(\mathcal{K}^2)$. The field strength of $\Gamma^a_{\mu\nu}$ is given by the Riemann tensor of our spacetime, which is usually assumed second order in the derivative expansion. Hence, the order counting of the Riemann tensor enforces $\mu^S_{\mu\nu} = \mathcal{O}(\mathcal{K})$.

With the above motivation, we proceed with the effective action construction and assume that $\mu^S = \mathcal{O}(\mathcal{K})$. The minimal list of scalars containing μ^S splits into zeroth and first order scalars denoted by S_0 and S_1 respectively. These are

$$S_0 = \{T,\ \mu/T,\ (u|n)\}\ \ ,\ \ S_1 = \left\{\mathrm{Tr}\left[(\tilde{u}+\tilde{n})\mu^S\right],\ (u+n+\tilde{\epsilon}|\mu^S|u+n+\tilde{\epsilon})\right\}. \tag{7.32}$$

Recall that μ^S is an anti-symmetric matrix and, hence, has vanishing diagonal elements in any basis.

A further simplification follows if we recall that $|n)$ is defined in the observer's rest frame, while $|u)$ is defined in the fluid's frame. If we were to define them both in the rest frame, then these two vectors are identical because of our frame choice (7.20), see Fig. 7.2. Therefore, $|u)$, $|n)$ are not independent and $|\tilde{\epsilon}) = 0$.

Thus, we are finally led to the final list of scalars[12]

$$S_0 = \{T,\ \mu/T\}\ \ ,\ \ S_1 = \left\{\mathrm{Tr}\left[\tilde{u}\mu^S\right]\right\}. \tag{7.33}$$

Now we are ready to write down the effective action using S_0 and S_1. It takes the form

$$W = \int d^3x\ e\left(P(S_0)\ +\ \alpha(S_0)\mathrm{Tr}\left[\tilde{u}\mu^S\right]\right), \tag{7.34}$$

with e the determinant of e^a_μ, and $\alpha(S_0)$ an arbitrary function of S_0.

If we compare W with the spinless fluid equilibrium effective action, we see that P defines the pressure of the fluid and under variation gives

[12]Technically, S_1 is an incomplete list, but we consider it here since it leads to an equilibrium spin tensor.

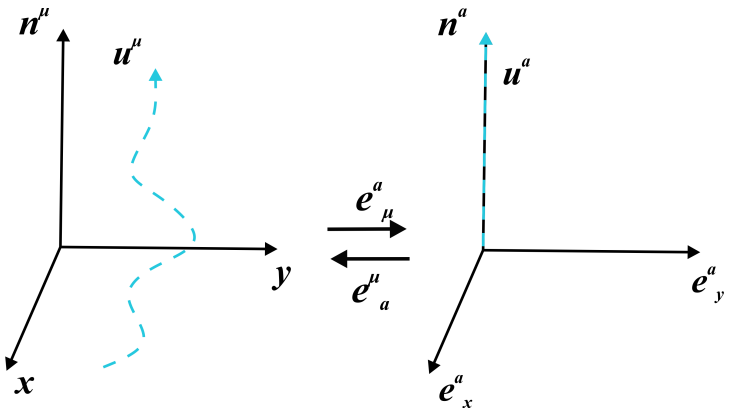

Figure 7.2: Mapping between the inertial(left) and non-inertial(right) rest frames of $2+1$ dimensional observers. On the left, the inertial observer moves tangent to n^μ, while they see the fluid move in spacetime with velocity u^μ. We transform the inertial coordinate system to the non-inertial one shown on the right using e^a_μ. Because of our fluid frame choice (7.20), n^a is parallel to u^a. In fact, since e^a_μ preserves their magnitude and both vectors have unit magnitude, they are actually equal.

the usual ideal energy-momentum tensor and charge current for the system. However, the extra term proportional to μ^S will alter all of these constitutive relations. Let us first present the conserved current of the system. Following the variation formulae presented in App. B, we find it is given by

$$\begin{aligned} J^\mu \equiv \frac{1}{e}\frac{\delta W}{\delta A_\mu}\Big|_{\text{Sources}\,=\,0} &= \left(\frac{\partial P}{\partial \mu} + \frac{\partial \alpha}{\partial \mu}\text{Tr}\left[\tilde{u}\mu^S\right]\right) u^\mu \\ &= \left(\rho + \frac{\partial \alpha}{\partial \mu}\epsilon^{\kappa\lambda\rho}u_\rho \mu^S_{\lambda\kappa}\right) u^\mu, \end{aligned} \tag{7.35}$$

where $\rho \equiv \partial P/\partial\mu$ is the usual charge density of the fluid in the absence of spin. The extra term in Eq. (7.35), proportional to μ^S, generates an additional contribution to the charge density of the system. To see the physical meaning of this extra term, let us assume that we can bring u^μ to the form $u^\mu = (1,0,0)$. Then the extra term contributes to the charge density only if $\mu^S_{12} \neq 0$. If $\mu^S_{12} \neq 0$, then the equilibrium density matrix of Eq. (7.13) tells us that $S^{12}_0 \neq 0$. Running the logic backwards, if the fluid has a non-vanishing and conserved spin in the out-of plane fluid direction, then the charge density of the fluid is altered when compared to a spinless fluid. Of course the above discussion is only valid if $\partial\alpha/\partial\mu \neq 0$. Unfortunately since both ρ and $\partial\alpha/\partial\mu$ change the charge density of the system, it is not easy to dis-

entangle the two just by calculating the current 1-point function.[13] Finally, note that the constitutive relation of the current implies that the pressure of the fluid is altered in the presence of spin from P to $P+\alpha \mathrm{Tr}\left[\tilde{u}\mu^{S}\right]$. This expectation shall act as a consistency check below, when we write down the energy-momentum tensor of the fluid.

We move on to the conserved spin tensor of the system which takes the form

$$S^{\mu\nu}_{\rho} \equiv \frac{1}{e}\frac{\delta W}{\delta \Gamma^{\rho}_{\mu\nu}}\Big|_{\text{Sources }=0} = \alpha \tilde{u}^{\mu\nu}u_{\rho}. \tag{7.36}$$

Note that $S^{\mu\nu}_{\rho}$ is anti-symmetric in its two upper indices, as expected from the general arguments given in the previous sections. More importantly, $S^{\mu\nu}_{\rho}$ is $\mathcal{O}(\mathcal{K}^0)$ even though the effective action used for its derivation is $\mathcal{O}(\mathcal{K})$. This implies that we can have a non-vanishing spin in the system even if $\mu^S = 0$. When $\mu^s = 0$, the constitutive relations for the current and energy-momentum tensor take the form of an ideal spinless fluid. Therefore, the spin tensor decouples from the energy-momentum and charge transport of the system. As a result, spin acts as an additional, independent mode of transport one can use in technological applications of electron hydrodynamics.

Finally, the constitutive relations (7.36) for $S^{\mu\nu}_{\rho}$ allows us to elucidate the physical meaning of α. To this end, assume that u^{μ} can be brought to the form $u^{\mu} = (1,0,0)$ and consider the spin density tensor $S^{\mu\nu}_{0} = \alpha\tilde{u}^{\mu\nu}$. We can dualize the spin density tensor to a spin density current via a contraction with the Levi-Civita tensor. We find

$$\tilde{S}_{\mu} \equiv \frac{1}{2}\epsilon_{\mu\nu\rho}S^{\nu\rho}_{0} = \frac{1}{2}\alpha\epsilon_{\mu\nu\rho}\tilde{u}^{\nu\rho} = \alpha u_{\mu}. \tag{7.37}$$

The dual $\tilde{S}_{\mu}$ is the spin current density, in the sense that its integral over a spatial hypersurface gives the spin of the fluid. Hence, Eq. (7.37) shows that α, in analogy to ρ, is the spin density of the system. Moreover, we now have an easy way to calculate α fix completely the effective action (7.34): Calculate the 1-point function of the spin current for a microscopic theory and read of α as a function of T and μ. Note that when α and ρ are constant, then charge conservation implies spin-current conservation. Therefore, the left-hand side of angular momentum conservation (7.14) vanishes identically. In turn, this means the anti-symmetric part of the energy momentum tensor vanishes identically at this order in the derivative expansion. This can be also be gleaned directly from Eq. (7.14) without any computation. According to Eq. (7.14), the anti-symmetric part of T^{μ}_{a} is $\mathcal{O}(\mathcal{K}S^{\mu\nu}_{\rho})$. Since $S^{\mu\nu}_{\rho}$ is

[13] It is interesting to understand whether higher-point functions could allow for disambiguating between the two contributions. We will not pursue this problem in the present thesis.

$\mathcal{O}(\mathcal{K}^0)$, the anti-symmetric part of T^μ_a is at least $\mathcal{O}(\mathcal{K})$ and hence vanishes identically at $\mathcal{O}(\mathcal{K}^0)$. This is another consistency check for the constitutive relation for T^μ_a derived below.

Finally, let us write down the constitutive relations for the energy-momentum tensor T^μ_a. To do that we need to derive the variation of the determinant of e^a_μ, e. For this derivation, we will use the formula relating e^a_μ and the spacetime metric

$$g_{\mu\nu} = \eta_{ab} e^a_\mu e^b_\nu \Rightarrow e = \sqrt{g}, \tag{7.38}$$

where g is the metric determinant. Taking the variation of the second equality we find

$$\delta e = \frac{1}{2}\sqrt{g} g^{\mu\nu}\delta g_{\mu\nu} = \frac{1}{2} e g^{\mu\nu}\left(\eta_{ab}\delta e^a_\mu e^b_\nu + \eta_{ab} e^a_\mu \delta e^b_\nu\right) = e e^\mu_a \delta e^a_\mu. \tag{7.39}$$

The remaining variations are similar to those found in App. B. We find then for the energy-momentum tensor

$$T^\mu_a = -\frac{1}{e}\frac{\delta W}{\delta e^a_\mu}\Big|_{\text{Sources }=0} = -T\frac{\partial p}{\partial T} u^\mu n_a + p\ e^\mu_a. \tag{7.40}$$

The term proportional to e^μ_a gives the pressure p of the fluid. We see that p is indeed altered by the spin chemical potential from P to $p = P + \alpha \text{Tr}\left[\tilde{u}\mu^S\right]$ as anticipated.

To recap the constitutive relations for an ideal spinning relativistic fluid are

$$J^\mu = \rho u^\mu \quad , \quad S^{\mu\nu}_\rho = \alpha \tilde{u}^{\mu\nu} u_\rho \quad , \quad T^\mu_a = (\epsilon + p) u^\mu n_a + \ p e^\mu_a, \tag{7.41}$$

with

$$p = P + \alpha \text{Tr}\left[\tilde{u}\mu^S\right] \quad , \quad \rho = \frac{\partial p}{\partial \mu} \quad , \quad \epsilon + p = -T\frac{\partial p}{\partial T} = Ts + \mu\rho + \frac{1}{2}\alpha\tilde{u}^{\mu\nu}\mu^S_{\mu\nu}, \tag{7.42}$$

the thermodynamic pressure, charge and energy density of the fluid respectively. To arrive at the final equality in Eq. (7.42), we used

$$\frac{\partial p}{\partial T} = \left(\frac{\partial p}{\partial T}\right)_{\mu,\mu^S} + \left(\frac{\partial p}{\partial \mu/T}\right)_{T,\mu^S}\frac{\partial(\mu/T)}{\partial T} + \left(\frac{\partial p}{\partial \mu^S_{\kappa\lambda}/T}\right)_{T,\mu}\frac{\partial(\mu^S_{\kappa\lambda}/T)}{\partial T}, \tag{7.43}$$

and the standard definitions of the derivatives of the pressure in the grand canonical ensemble [110].

We can also express α as a derivative of p, viz.

$$\alpha = \frac{\partial p}{\partial \mu^S_{\mu\nu}} \tilde{u}_{\mu\nu}. \tag{7.44}$$

This last formula implies that the spin tensor density of the fluid is $\rho_S^{\mu\nu} = \alpha \tilde{u}^{\mu\nu}$, meaning we can write for the constitutive relations

$$J^\mu = \rho u^\mu \quad , \quad S^{\mu\nu}_\rho = \rho_S^{\mu\nu} u_\rho \quad , \quad T^\mu_a = (\epsilon + p) u^\mu n_a + \ p e^\mu_a, \tag{7.45}$$

In their final form, (7.45), the constitutive relations at $\mathcal{O}(\mathcal{K}^0)$ are as expected those of a perfect spinning fluid – also called a Weyssenhof fluid (see e.g. [185]). Additional comments regarding the constitutive relations (7.41) were given below Eq.s (7.35), (7.36) and (7.40).

We wish to make one final remark on the construction of this section: We started with a zeroth order effective action with an infinite number of terms. Then, to make calculations useful, we restricted to a finite subset of those arguments. This had as a consequence the addition of first order terms in the effective action. However, the resulting constitutive relations for the spin tensor still turned out to be zeroth order and, thus, describing an equilibrium configuration. Therefore, we see that the order of the effective action and the order of the constitutive relations do not match. This phenomenon of "order transmutation" seems puzzling to us, since it seems to break down the fundamental assumptions of effective field theory; Higher order corrections do not change the leading order contribution to physical observables. In a sense, we could say that the addition of spin induces a UV/IR mixing of the degrees of freedom.

One naive way out of this apparent breakdown of EFT is the following: The inclusion of angular momentum introduces into our setup an additional length scale call it l, e.g. the distance from the axis of rotation of a fluid-particle dipole. If we restrict ourselves to distances $\mathcal{K} \gg l$, then we wont be able to measure any angular momentum since the fluid particles have merged[14]. As we start separating the fluid particles, we can resolve the angular momentum of the system and we can check whether it is conserved or not, see Fig. 7.3. In other words, the EFT expansion we have written down is not an expansion in $\mathcal{K}$ alone, but contains corrections in $l/\mathcal{K}$. A self-consistent microscopic derivation of spin-hydrodynamics should be carried out to check the validity of this assertion[15].

[14] There is no center of rotation.

[15] On a completely unrelated note, a similar expansion in terms of two scales appears in neural network effective theories [186]. In this case the two scales are the depth and width of the neural network.

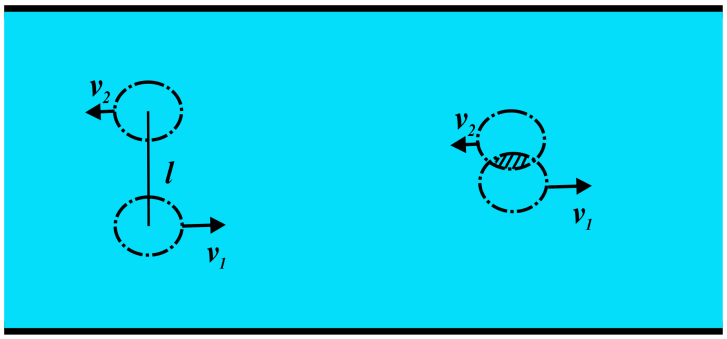

Figure 7.3: Channel (black borders) hosting a hydrodynamic flow (blue filling). Pictured as dashed circles are two pairs of fluid-particles, i.e. regions of the fluid of size $\mathcal{K}$ with constant temperature, chemical potentials and velocity, rotating around each other. The length l is twice the distance between each fluid particle and the center of rotation. When $l \gg \mathcal{K}$ (left fluid-particle pair), the rotation is observable and the fluid has a non-trivial angular momentum. When $l \ll \mathcal{K}$ (right fluid-particle pair) the fluid-particles merge partially and their angular momentum with respect to the center of rotation is ill-defined.

Equilibrium effective action at $\mathcal{O}(\mathcal{K})$

In this section we calculate the effective action and the constitutive relations at first order in derivatives. Part of the answer is obvious from symmetry arguments even in the non-dissipative case. For example, the current J^μ will be just a generalization of the usual current in parity-breaking $2+1$ hydrodynamics [9]. The generalization consists of considering the spin chemical potential as an anti-symmetric first order tensor on the same footing as the Maxwell tensor $F_{\mu\nu}$. That is, we can define "spin electromagnetic" fields and include them into the current in the same way as the usual electromagnetic fields. One aspect of this recipe can already be seen from the results of the previous section, where the pressure gets altered by a term proportional to the spatial components of μ^S. This is similar to what happens with the magnetic field in $2+1$ dimensions(see Eq.s (1.2a) and (1.3a) of [9]). Following the above, we can just write down the constitutive relation for the *dissipative* current of a spinning fluid at first order in derivatives. It reads(in matrix notation for simplicity

$$\begin{aligned}|J) = \rho|u) + \sigma\left[F|u) - TP_u|\partial\mu/T)\right] + \tilde{\sigma}\tilde{u}\left[F|u) - TP_u|\partial\mu/T)\right] \\ + \tilde{\chi}_E\tilde{u}F|u) + \left(F \to \mu^S\right).\end{aligned} \tag{7.46}$$

Notation reminder: $|x) = x^\mu$, $\forall$ vector x^μ, while $A|x)$ and AB denote the usual multiplication between matrices and vectors/matrices respectively.

Also $\tilde{u} = u^{\mu\nu} = \epsilon^{\mu\nu\rho}u_\rho$ and P_u is the projector in the direction of u^μ. Besides $F, \tilde{u}$ and P_u, all other factors multiplying the vectors in Eq. (7.46) are scalar functions of μ and T, i.e. transport coefficients. Note that Eq. (7.46) is written in the Landau frame, where $\rho = \partial P/\partial\mu$ and not equal to $\partial p/\partial\mu$. Also note that not all of the vector data appear in the charged fluid constitutive relation. The reason is that angular momentum conservation provides a vector constraint that we can use to reduce the number of vector data by one, as in section 3.3.1. Unfortunately the current $|J)$ is valid only off-shell, because we cannot know how the second law of thermodynamics affects the transport coefficients in $|J)$ without constructing the fully dissipative T^μ_a and $S^{\mu\nu}_\rho$.

Let us, however, forget the above speculative arguments and proceed with the equilibrium effective action expansion. To this order in the expansion, we get an additional vector to generate scalars, the partial derivative ∂_μ. This means that all of the scalars in the previous section are now considered functions in spacetime. However, to remain in equilibrium we will assume that these functions are constant in time. In covariant terms, we will assume that all the scalars are Lie transported along u^μ, $\mathcal{L}_u = 0$.

At this order in the expansion, the scalars will be build out of

$$\{T, \mu, \mu^S_{ab}, u^\mu, \epsilon_{\mu\nu\rho}, F_{\mu\nu}\}$$

and their derivatives. If we focus on the first order scalars, then we can take the building blocks for the scalars to be

$$\{\partial_\mu T, \partial_\mu\mu, \mu^S_{ab}, \epsilon_{\mu\nu\rho}, \partial_\mu u^\nu, F_{\mu\nu}\}\ .$$

Using these data and $\mathcal{L}_u = 0$, we construct the following list of scalars at most $\mathcal{O}(\mathcal{K})$.

$$S = \left\{T, \mu, \mathrm{Tr}\left[\tilde{u}(\mu^S + F + \nabla u)\right]\right\}, \tag{7.47}$$

with $\nabla u = \nabla_\mu u_\nu = \partial_\mu u_\nu - \Gamma^\rho_{\nu\mu}u_\rho$. Using the above list, we can construct the effective action for a spinning fluid at $\mathcal{O}(\mathcal{K})$. We find

$$W = \int d^3x e\left(P(S_0) + \mathrm{Tr}\left[\tilde{u}\left(\alpha(S_0)\mu^S + \beta(S_0)F + \gamma(S_0)\nabla u\right)\right]\right), \tag{7.48}$$

where $S_0 = \{T, \mu/T\}$ and $\nabla = \nabla_\mu$ the covariant derivative. First things first, the thermodynamic pressure density of the fluid is obviously given by

$$p = P + \mathrm{Tr}\left[\tilde{u}\left(\alpha\mu^S + \beta F + \gamma\partial u\right)\right]. \tag{7.49}$$

This is the standard result found for parity-breaking fluids in [9] and Eq. (3.50), but in a slightly different notation and with $P \to p = P + \alpha\mathrm{Tr}\left[\tilde{u}\mu^S\right]$. In

particular $\beta = \alpha_1/2$, $\gamma = \alpha_2/2$. Therefore, the equilibrium U(1) current and energy-momentum tensor for spinning fluids are given by (3.51) with $\mathcal{P} \to \mathcal{P} + \alpha \mathrm{Tr}\left[\tilde{u}\mu^S\right]$. Despite the lack of new terms in the constitutive relations for J^μ and T^μ_a, our re-writing of the effective action in matrix notation, suggests a particular interpretation of the terms proportional to F. More precisely, the term proportional to F is a so-called topological BF term [187]. Therefore, its corresponding contribution to the current can be thought of as the source of vortex flux.

We proceed now to the derivation of the spin-density tensor. It takes the Weyssenhof fluid form with a modified spin density

$$S^{\mu\nu}_\rho = (\alpha + \gamma)\, \tilde{u}^{\mu\nu} u_\rho. \tag{7.50}$$

We may think of γ as the spin density induced by the rotation of the velocity profile of the fluid. However, since the spin density of the fluid can be modified under a frame change, we can choose the spin tensor density to take its perfect fluid form as in (7.45).

This concludes our discussion of spin-effective actions at $\mathcal{O}(\mathcal{K})$. We saw that this case is not much different than the $\mathcal{O}(\mathcal{K}^0)$ one. Indeed, we found once again the constitutive relations for a perfect spin fluid. We proceed in the next section to discuss the corrections at $\mathcal{O}(\mathcal{K}^2)$ and provide some simple examples showcasing their contribution to spin transport.

A glimpse at the equilibrium effective action at $\mathcal{O}(\mathcal{K}^2)$

We have seen that the spin tensor does not contain any new physically non-trivial terms at first order in the effective action expansion. We expect this to change in the next order of the expansion. To see, let us Taylor expand our effective action up to first order in the connection. We have

$$\begin{aligned} W &= W[\Gamma^\rho_{\mu\nu} = 0] + \int d^3x \left(\Gamma^\rho_{\mu\nu} \frac{\delta W}{\delta \Gamma^\rho_{\mu\nu}}\Big|_{\text{Sources} \,=\, 0} \Gamma^\rho_{\mu\nu} + \mathcal{O}(\Gamma^2) \right) \\ &\simeq W[0] + \int d^3x e\; S^{\mu\nu}_\rho \Gamma^\rho_{\mu\nu} \equiv W[0] + W^{(1)}_\Gamma. \end{aligned} \tag{7.51}$$

In the second equality of Eq. (7.51), we used the definition of the spin tensor in terms of a derivative of W (see e.g. Eq. (7.36)). We now expand the spin tensor in $\mathcal{K}$ as

$$S^{\mu\nu}_\rho = S^{\mu\nu}_{(0)\rho} + S^{\mu\nu}_{(1)\rho} + \mathcal{O}(\mathcal{K}^2), \tag{7.52}$$

with $S^{\mu\nu}_{(i)\rho}$ being of ith order in $\mathcal{K}$. We substitute Eq. (7.52) into $W^{(1)}_\Gamma$ of Eq. (7.51) to find

$$W \simeq \int d^3x e \left(S^{\mu\nu}_{(0)\rho} \Gamma^\rho_{\mu\nu} + S^{\mu\nu}_{(1)\rho} \Gamma^\rho_{\mu\nu} \right). \tag{7.53}$$

Now recall that we assume $\Gamma^{\rho}_{\mu\nu} = \mathcal{O}(\mathcal{K})$. This means that the first and second term on the right hand side of Eq. (7.53) are $\mathcal{O}(\mathcal{K})$ and $\mathcal{O}(\mathcal{K}^2)$ respectively. This implies that if we want to observe $\mathcal{K}$ effects in the spin tensor, we must expand W to second order in $\mathcal{K}$. Similarly, in order to see $\mathcal{O}(\mathcal{K}^i)$ we must expand W up to $\mathcal{O}(\mathcal{K}^{i+1})$. Therefore, the anti-symmetric part of T^{μ}_{a}, which we argued is $\mathcal{O}(\mathcal{K})$ can be generated by a $\mathcal{O}(\mathcal{K}^2)$ effective action.

The full analysis of the second order corrections, is beyond the scope of this thesis. However, to conclude this chapter, we shall discuss one particular second order term that contributes to spin transport. This term leads to the so called Barnett effect in $3+1$ dimensions and a variant of it in $2+1$ dimensions. The Barnett effect for $3+1$ dimensional spin hydrodynamics was first derived using the AdS/CFT correspondence in [129]. We noticed, however, that the same effect can be recovered from the following effective action

$$S = \int d^4x \ |e|(\nabla_{[\mu}u_{\nu]})\nabla^{[\mu}u^{\nu]}. \tag{7.54}$$

To calculate the spin tensor from Eq. (7.54), we just expand S up to first order in $\Gamma^{\lambda}_{\mu\nu}$. To calculate said expansion, we recall that $\nabla_{\mu}u_{\nu} = \partial_{\mu}u_{\nu} - \Gamma^{\lambda}_{\mu\nu}u_{\lambda}$ and, hence, the action S of Eq. (7.54) is a polynomial in the connection. Explicitly, we have

$$S = \int d^4x|e| \left[(\partial u)^2 - 2(\partial^{[\mu}u^{\nu]})u_{\rho}\Gamma^{\rho}_{[\mu\nu]} + \mathcal{O}(\Gamma^2)\right]. \tag{7.55}$$

The linear in Γ term in the action of Eq. (7.55) is by definition the first derivative of S with respect to the connection, evaluated at $\Gamma = 0$ and gives us the spin tensor $S^{\mu\nu}_{\rho}$. Let us focus on the completely anti-symmetric part of $S^{\mu\nu}_{\rho}$. It takes the form

$$S^{\mu\nu\rho} = -2u^{[\mu}\partial^{\nu}u^{\rho]}. \tag{7.56}$$

Note that the anti-symmetrization is over all indices in Eq. (7.56). In $3+1$ dimensions, we can dualize the spin-tensor to a spin current via $\tilde{S}_{\mu} = \epsilon_{\mu\nu\rho\sigma}S^{\nu\rho\sigma}$. We find

$$\tilde{S}_{\mu} = -2\epsilon_{\mu\nu\rho\sigma}u^{[\nu}\partial^{\rho}u^{\sigma]} = -2\epsilon_{\mu\nu\rho\sigma}u^{\nu}\partial^{\rho}u^{\sigma} = -2\omega_{\mu}, \tag{7.57}$$

With ω_{μ} the vorticity of the fluid. Note that the dualization works in reverse as well and so we can write[16]

$$S^{\mu\nu\rho} = \epsilon^{\mu\nu\rho\sigma}\tilde{S}_{\sigma} = -2\epsilon^{\mu\nu\rho\sigma}\omega_{\sigma}. \tag{7.58}$$

[16] One can also check that Eq. (7.58) agrees with Eq. (7.56) by using the definition of ω_{μ} and the properties of the ϵ symbol under contractions with another ϵ symbol.

Equation (7.58) shows that a spinning fluid can exhibit the Barnett effect [61], namely it states that fluid rotation leads to the polarization of the spin of the fluid in the direction parallel to ω_μ. The Barnett effect can also be generated in $2+1$ dimensions by an action of the form [188]

$$S = \int d^3x |e| \mu^S_{\mu\nu} \nabla^{[\mu} u^{\nu]} \ . \tag{7.59}$$

Namely, the fully anti-symmetric part of the spin tensor derived from Eq. (7.59) is given by

$$S^{\mu\nu\rho} = -\frac{1}{6} \epsilon^{\mu\nu\rho} \omega \ , \tag{7.60}$$

with $\omega = \epsilon_{\mu\nu\rho} u^\mu \partial^\nu u^\rho$ the vorticity of the fluid.

Clearly, the Barnett effect is a directly observable effect in spin hydrodynamics. For example, one can measure the spin of the fluid by measuring the induced magnetic field due to the fluid's polarization. However, estimating the magnitude of this effect requires us to know all the terms appearing in the spin tensor and its backreaction to the magnetic field. This goes beyond the scope of this thesis, but we discuss it in more detail in the following and final chapter of the thesis.

Chapter 8

Conclusions and Outlook

8.1 Summary of main results

In this thesis, we explored how transport behaviour in a solid is altered when electrons propagate hydrodynamically within it. More precisely, chapters 4 and 5 focused on quantitative and qualitative changes in transport induced by increasing the coupling strength of a material to non-perturbatively large values. In particular, in chapter 4, the Poiseuille flow behaviour and resistance of a strongly coupled fluid were derived and analyzed. Crucial to this analysis was the use of the AdS/CFT correspondence, described in chapter 2, which allowed us to perform a fully non-perturbative calculation for the thermodynamic variables of the fluid. Furthermore, the AdS/CFT correspondence provided us with the single transport coefficient employed as a parameter in our simulations, the ratio of shear viscosity to entropy density η/s. Using these results, we solved for the first time the fully relativistic equations for a viscous fluid moving in a channel under the influence of an electric field. Through these flow solutions, we showed that strongly coupled fluids exhibit the hydrodynamic part of the Gurzhi effect, first predicted in weakly coupled materials. Importantly, the resistance of strongly coupled materials was shown to be always smaller than the resistance of a weakly coupled material at roughly equal input parameters. This showcases that strongly coupled materials constitute efficient conductors. Moreover, we derived analytic solutions for our channel flows and used them to derive the analytic dependence of the resistance on η/s. Since η/s depends on the coupling constant, α, of the fluid, our formulae can be used to experimentally identify α through a simple resistance measurement. Finally, we estimated the Reynolds number of our flows and showed that they stay laminar.

On the other hand, in chapter 5, we explored whether a turbulent flow can be achieved in another electronic material. We saw that weakly coupled materials cannot, in general, become turbulent. This, however, ceases to be true for strongly coupled materials. In particular, we presented a precise

proposal for a strongly-coupled material where this assertion can be tested. More precisely, we proposed a Dirac material, ScHb, based on a kagome lattice populated by copper-oxide plaquettes. These plaquettes hybridize in terms of d-orbital because of the replacement of zinc with scandium in Hb. As a result, the Sc substitution makes the material strongly coupled with a fine structure constant $\alpha \simeq 3$ and puts its Fermi level around charge neutrality. This implies that low-energy excitations of ScHb are quantum critical Dirac fermions, similar to graphene. Due to ScHb's large coupling strength, we cannot use perturbation theory to analyze its properties. Instead, we used the AdS/CFT correspondence to understand ScHb's transport properties and, in particular, η/s. We estimated η/s at finite coupling by using a higher-derivative bulk theory of gravity. According to the GPKW dictionary, these higher derivative corrections encode $1/\alpha^{3/2}$ corrections to η/s. The error of the resulting estimate is small when compared to the error of a similar η/s estimate for the moderately coupled graphene. This suggests higher derivative gravity is an accurate way to capture the essential properties of non-perturbative materials. Finally, we used the derived estimate for ScHb's η/s, to show that ScHb exhibits a Reynolds number far larger than 1000. Such a large value for the Reynolds number shows that ScHb is the *first* proposed Dirac material that can exhibit a fully turbulent flow.

Furthermore, in chapter 6 we focused on a trademark of solid state transport, the Hall effect in the presence of a non-quantizing external magnetic field. In particular, we examined modifications of the Hall effect for Fermi liquids in the hydrodynamic regime. We have shown that the hydrodynamic Hall effect is vastly different than the classical Hall effect. Namely, the hydrodynamic Hall voltage is a highly non-linear function of the magnetic field. More importantly, this non-linear dependence makes the Hall voltage a non-monotonic function of the magnetic field. This non-monotonicity leads to a distinctly hydrodynamic in nature transport feature, a zero of the Hall voltage at *non-vanishing* magnetic fields. In addition, we derived analytic formulae for the hydrodynamic Hall voltage for small ($\sim \mathcal{O}(10\text{mT})$) values of the magnetic field. We have used these formulae to understand the dependence of the Hall voltage and its corresponding Hall field on all experimentally relevant parameters, such as the fluid's temperature and density. These dependences along with the aforementioned features of the Hall voltage allow for the explicit experimental verification of our theoretical predictions. We have also shown that there already exists partial experimental confirmation of our results in [22].

Finally, in chapter 7 we took the first step at extending electron hydrodynamics to include a macroscopically-conserved spin and orbital angular momentum density. In particular, we have given a general discussion of the thermodynamics of a spinning fluid and showed they can be described in terms of either an inertial or non-inertial co-ordinate system in spacetime. These distinct descriptions suggest two different approaches of generating

the effective action of spinning fluids, differing in the operator generating the energy-momentum tensor. One approach uses the metric, while the other the vielbein field as the source. We have chosen the second, vielbein, approach and constructed the effective action of the spinning fluid. We have shown that interesting new features related to spin transport can appear at order $\mathcal{O}(\mathcal{K}^2)$ or higher in the derivative expansion because angular momentum introduces an additional length scale into the system. To conclude the chapter, we presented two examples of spin transport effects, namely the Barnett effect appearing in both $3+1$ and $2+1$ dimensional spinning fluids.

To conclude, let us summarize below our main results

[1] Poiseuille flow of strongly coupled fluids and the Gurzhi effect.

- We solved for the first time the fully relativistic hEOM of an electron fluid forced by a constant external electric field to move along an infinitely long wire.
- We presented the dependence of these solutions to all external parameters, i.e. the electric field, the wire width, the fluid's chemical potential over temperature ratio, as well as the fluid's coupling strength. In particular, we showed that the maximum speed of the flow is a monotonically increasing function of all of these parameters.
- We derived the resistance of the fluid and showed that it takes the form predicted by Gurzhi in the hydrodynamic regime, even at non-perturbatively large coupling strengths. In addition, we showed the resistance is a monotonically decreasing function of the coupling strength.
- We analyzed the effects of impurities on the resistance of a fully relativistic fluid. We showed that the Drude contribution to the conductivity at typical impurity densities is of the same order of magnitude as the contributions due to quantum critical transport. Furthermore, we showed that viscous and impurity effects cannot be disentangled as long as the fluid flow is hydrodynamic and not ohmic.
- We showed that strongly coupled fluids can reach relativistic speeds more easily than weakly coupled ones, but this does not lead to the development of turbulence.

[2] Turbulent hydrodynamics in kagome metals.

- We proposed a novel strongly coupled kagome material, ScHb. Apart from its strong coupling, $\alpha = 3$, ScHb's Fermi level is pinned exactly at the Dirac point, thus giving us access to relativistic and quantum critical physics around charge neutrality.

- We used the AdS/CFT correspondence and a higher-derivative theory of gravity to derive ScHb's shear viscosity to entropy density ratio at finite coupling.
- The derived estimate is close to the KSS bound for a large range of the phenomenological parameter entering the gravity model. This implies that the Reynolds number of ScHb takes on values which allow us to reach for the first time the turbulent flow regime in electron fluids.

[3] Hydrodynamic Hall effect in Fermi liquids.

- We solved both numerically and analytically the hEOM for a parity-breaking electron fluid flowing in a wire under the combined influence of constant external electric and magnetic fields.
- We derived the hydrodynamic Hall voltage for a large range of non-quantizing magnetic fields and other externally set parameters, i.e. temperature, density, electric field, wire width and slip length.
- We showed that the hydrodynamic Hall voltage can be decomposed into two contributions of *opposite sign* stemming from the Lorentz force and the Hall viscosity respectively. This sign difference leads to a zero of the Hall voltage at non-zero values of the magnetic field. Moreover, we showed the two contributions have different dependences on the external parameters, which can be used to disentangle them in experiment.
- We also derived the Hall voltage as a function of the transverse coordinate of the channel. Using this local Hall voltage we showed that the corresponding Hall field in the channel depends strongly on the Hall viscosity in the case of vanishing slip length.

[4] Spin-fluid hydrodynamics.

- We discussed the different approaches one can use to construct spin-fluid hydrodynamics and their physical interpretation in terms of inertial and non-inertial observers.
- We constructed the effective action for non-dissipative fluids up to first order in the derivative expansion and showed it takes the perfect spin (or Weyssenhof) fluid form.
- We showed that interesting spin transport phenomena appear at second order in the derivative expansion through the construction of the effective action leading to the Barnett effect.

Below, we present possible extensions of the research presented in this thesis, as well as additional ideas for further research.

8.2 Outlook to further research

To begin with, let us discuss possible extensions of the research presented in this thesis. First, we note that all of our hydrodynamic simulations in chapters 4 and 6 were performed in a channel geometry. The reason for this is the high symmetry of this setup, as well as the ease of performing experiments in channel geometries. However, this is not the unique geometry available in experiments. For example, channels with a Hall-bar or a Corbino disk geometry [189] can be created. Moreover, it is possible to glue together channels to create sharp corners or constrictions the fluid has to navigate past. All of these geometries have lower symmetry than our channel geometry, which generically leads to flows more complicated than the Poiseuille one. Using these geometries one can explore the effect of having both velocity components be non-trivial. This in turn will generically make the charge conservation equation and, thus, charge transport non-trivial. Finally, the geometries with sharp corners or constrictions are perfect for understanding the effects of the shear viscosity on the fluid's properties. This is because the viscosity is the only coefficient in our setups that can provide the friction necessary for the fluid to turn around a sharp corner. Therefore, a small enough viscosity, or η/s, may lead to a detachment between the flow and the channel boundary. But since a fluid by definition fills all of the volume available to it, this channel-fluid vacuum will have to be filled in, leading to the creation of turbulent wakes (see Fig. 8.1).

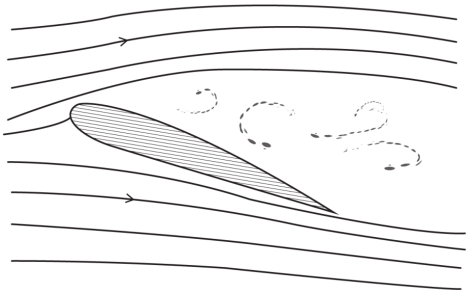

Figure 8.1: A familiar example of a turbulent wake generated by the inability of the fluid to "stick" to the surface of an airplane wing. Image reprinted from [142].

Apart from different channel geometries, a further possible extension of our previous work is to consider different electronic fluids. For example, the research presented in chapter 6 was performed in the Fermi liquid limit $\mu \gg T$. This assumption allowed us to neglect any temperature fluctuations in the system, as these were suppressed compared to the chemical potential fluctuations. However, the opposite limit $\mu \ll T$ is also of interest. Namely for graphene, $\mu \ll T$ gives us access to the Dirac dynamics of electrons

around charge neutrality. Apart from examining relativistic physics, taking $\mu \ll T$ also implies that temperature fluctuations can no longer be neglected. Therefore, besides the modified Hall response, we expect the generation of a heat gradient in the channel. This is nothing more than the manifestation of the inverse Nernst effect [190] in hydrodynamic systems. Given the large qualitative differences between the hydrodynamic and classical Hall effect, we expect similar enlightening differences between the hydrodynamic and ballistic inverse Nernst effect. Research in this direction is currently under way.

Finally, let us discuss possible extensions of the research on strongly coupled materials presented in chapter 5. One avenue of further research comes from the material science side of our work. Namely, we may ask whether additional strongly coupled materials can be built based on kagome or other lattices. The answer to this question is positive, as some of our collaborators in [2] have already confirmed. Namely, in [191], the $2+1$ dimensional Cu-dicyanoanthracene (Cu-DCA), an organometallic system was presented. In the same paper, the coupling strength of Cu-DCA was calculated and found to be $\alpha \simeq 13$.

Certainly, then, more strongly coupled materials exist and their dynamics should be analyzed. As was argued in chapter 5, holography is an excellent way to achieve this. In particular, more research should be done on the emergence of turbulence from the gravity side. Present research in this direction has already reproduced some of the important features of turbulence, such as the Kolmogorov scaling of the flow power-spectrum [192–194]. It is interesting, though, to understand the onset of turbulence by analyzing the flow fluctuations making the fluid unstable directly though holography.

Jet quenching

One further extension of the work presented in this thesis includes jet quenching. Jet quenching refers to the phenomenon of energy loss of a probe particle traveling within a medium. It has been investigated at length in the realm of high-energy physics, and more precisely for heavy ion collisions at the LHC and RHIC (see [195] for a review). More precisely, moments after the heavy ion collision, a quark-gluon plasma (QGP) is formed in addition to one or more secondary particle jets. These jets consist of highly energetic particles trying to make their way out of the viscous QGP and (hopefully) into a particle detector. Clearly, whether the particles make it into the detector depends on the jet-plasma interaction, i.e. if the QCD coupling constant is large enough, no particle will make it to the detector and the jet has been quenched.

One important phenomenological parameter describing jet quenching is, unsurprisingly, the jet quenching parameter $\hat{q}$. Given a jet particle moving through the QGP, $\hat{q}$ measures how fast its momentum transverse to the QGP

is diffused in the medium. In particular, $\hat{q}$ is phenomenologically defined as

$$\hat{q} = \frac{\langle p_\perp^2 \rangle}{\sqrt{2}L^-} \ , \tag{8.1}$$

with $p_\perp$ the momentum of the probe particle normal to the QGP and L^- the elapsed light-cone time the particle has been within the QGP. Complementary to the definition (8.1), there exists a definition of $\hat{q}$ in terms of a Wilson line of a quark-antiquark pair within the QGP(see [196] for a derivation)

$$W(C) = \exp\left[-\frac{1}{4\sqrt{2}}\hat{q}L^-L^2\right] \ . \tag{8.2}$$

C is the parallelogram with sides L^- and L. The length scale L is conjugate to the transverse momentum $p_\perp$ and can be thought of as the quark-antiquark distance in the transverse direction.

Both of the above formulae can be used to calculate the jet quenching parameter in perturbation theory, as well as holography: In perturbation theory, one can use kinetic theory and calculate the momentum lost within the QGP [195]. In holography, one can do one of two things: First, introduce a probe particle at the boundary. The particle, similar to holographic fields, gets extended into the boundary in the form of a string with one endpoint fixed on the boundary. One then can use the Nambu-Goto action for a string moving in the bulk spacetime and show it satisfies Newton's law in the presence of a drag force [197] $\dot{p}_\perp \propto -p_\perp$. We can then solve Newton's equations and use (8.1) to find $\hat{q}$. In a similar fashion, one can calculate the Wilson loop by considering a string with both of its endpoints fixed on the boundary [196]. The resulting expression for $\hat{q}$ in super Yang-Mills (SYM) theory is to leading order in λ is [196][1]

$$\hat{q} = \frac{\pi^{3/2}\Gamma(3/4)}{\Gamma(5/4)}\sqrt{\lambda}T^3 \ , \tag{8.3}$$

with $\Gamma(x)$ the gamma function.

We see that $\hat{q}$ acts as a direct probe of the coupling constant of SYM. For this reason, we want to extend the SYM calculations to the case of electronic flows in channels, thus providing an additional measure of the fine structure constant of a material, apart from the resistance mentioned in chapter 4. We cannot perform the Wilson line calculation, since Wilson lines in the AdS/CFT correspondence are not defined for abelian gauge theories[2]. Therefore, we have to extend the drag-force calculation of [197] to include particles charged only under a U(1) gauge theory and not the full SU(N) group of QCD. One possible way to achieve this, is within the $AdS_5 \times S_5$ gravity dual of SYM. In particular, one can introduce additional

[1] As far as we are aware, both methods lead to the same result.

[2] The rank of the gauge group $N \gg 1$ by assumption.

D-branes into the bulk spacetime, whose excitations will be charged only under a U(1) symmetry. Clearly, for the D-brane excitations to be dual to particles, we must employ $D1$-branes. Furthermore in order to enforce the U(1) symmetry, the $D1$ brane strings must not attach to the stack of N $D3$-branes in the bulk. This suggests that the $D1$-brane must be localized on the S_5. If this construction is possible, then dimensional reduction down to AdS_5 will provide us with the effective electron-string action and, hence, the starting point for the drag force calculation.

Spinning fluid hydrodynamics

A further extension of our work involves spinful hydrodynamics. Clearly, in order to understand spin hydrodynamics we need the complete list of constitutive relations for $T^{\mu\nu}, J^{\mu}$ and most importantly $S^{\mu\nu\rho}$. There are several ways of writing down this decomposition, presented in 3. We used one of these approaches to write down the constitutive relations up to first order in the derivative expansion. However, due to the reasons elaborated in chapter 7, interesting spin transport effects start appearing at second order. Therefore, the complete effective action to second order in the derivative expansion must be constructed. This is a non-trivial task because of the large number of terms appearing at second order in the derivative expansion.

To aid in keeping track of all the terms at second order, we propose a re-arranging of the source fields in spin-hydrodynamics. In particular, consider the vielbein formulation of the effective action. The source fields for this formulation, the vielbein field e^a_μ and the connection $\Gamma^a_{\mu b}$, are both related to spacetime gauge symmetries; Roughly speaking, e^a_μ is the gauge field of translation invariance, while $\Gamma^a_{\mu b}$ is the gauge field of Lorentz invariance [183]. Our suggestion is then to combine both e^a_μ and $\Gamma^a_{\mu b}$ into a *single* gauge field A_M for translations and Lorentz rotations

$$A_M = e^a_\mu P_a + \Gamma^a_{\mu b}\mathcal{J}^b_a \ , \tag{8.4}$$

with $P_a, \mathcal{J}^b_a$ the generators of translation and Lorenz transformations respectively. Mathematically, A_M is a Cartan-Ehresmann connection [198]. Physically, the decomposition of A_M as in the RHS of Eq. (8.4) means that, consistent parallel transport of vectors from one tangent space to another, described by e^a_μ, also requires a rotation of the vector. In brief, A_M describes how to roll a tangent space on spacetime without slipping.

Using A_M, we can now see that the spinning fluid effective action is nothing more than a functional invariant under a non-abelian gauge group. We expect that the resulting action will be much simpler than the action constructed in our vielbein formalism. As a justification of this statement, we note that A_M has already been used as a means to *solve* 2+1 dimensional quantum gravity [199,200], as well as to construct higher-spin theories [201],

and torsion-matter interactions in Einstein-Cartan gravity [202, 203][3].

Note that even after the construction of the effective action, we won't have a complete theory of hydrodynamics. That is because the effective action can only capture non-dissipative phenomena. So in order to resolve this problem, we should construct dissipative spin hydrodynamics using either the Schwinger-Keldysh effective action or the entropy current approach discussed in chapter 3.

Finally, once spin-hydrodynamics has been constructed one should derive its predictions for electronic systems. This can be done in the simple channel setup used in chapters 4 and 6. In particular, an analysis of the spin-Hall effect in metals [184] behaving hydrodynamically should be carried out.

Metric affine gravity and the gauge/gravity duality

The next research idea we wish to discuss is an extension of spin-fluid hydrodynamics. Recall, that in the case of spin-fluid hydrodynamics, the spacetime geometry was an Einstein-Cartan one. That is, besides non-trivial curvature, spacetime also hosted non-trivial torsion. We can generalize this geometry further by endowing the spacetime with non-metricity $Q_{\mu\nu\rho}$. Non-metricity, as the name suggests is related to the metric and more precisely to the incompatibility of the metric with the connection

$$Q_{\mu\nu\rho} = \nabla_\mu g_{\nu\rho} \ . \tag{8.5}$$

In metric-compatible spacetimes, as in conventional general relativity, the non-metricity tensor $Q_{\mu\nu\rho}$ vanishes by construction. However, there exist connections such that $Q_{\mu\nu\rho}$ as well as torsion are non-zero. The corresponding spacetime is then a metric affine one [183]. A non-vanishing $Q_{\mu\nu\rho}$ means that the inner-product between vectors changes even if the vectors are constant in spacetime. As a result, the causal structure of spacetime is different at different points.

Like curvature and torsion, we can consider a dynamical $Q_{\mu\nu\rho}$ tensor. Doing so introduces an additional conserved current into the spacetime, acting as a the source of $Q_{\mu\nu\rho}$. This source is the symmetric part of the hyper-momentum tensor $\Delta_{\mu\nu}$. In particular, the trace of Δ leads to an overall change in volume of a spacetime region, while the traceless part shears the light-cone structure of spacetime.

An interesting avenue for research is the derivation of the constitutive relations for the currents of a metric affine spacetime directly through holography. To achieve this we can use the fluid/gravity correspondence, which we now explain(see [204] for a review). In the fluid/gravity framework, the

[3]To this list, we should also add the philosophical advantage of using A_M; the unification of the conservation laws for energy-momentum and angular momentum This unification might also be useful for unifying the inertial and non-inertial descriptions of thermal equilibrium for a spinning fluid.

black hole in the bulk describing the thermodynamics of the QFT gets distorted. In particular, a neutral black hole is given a finite velocity in a timelike direction u^μ. When this velocity is constant, the distorted black hole is still a solution of the Einstein equations of motion. However, when u^μ as well as the black hole temperature β become spacetime fields, this ceases to be true. Despite this, it is still possible to find an approximate solution to the Einstein equations by assuming $\beta^\mu = u^\mu \beta$ is a slowly varying field in spacetime and expanding in its derivatives. This approach should be familiar. We did precisely the same thing in chapter 3, when we went from global thermal equilibrium to a local one and from that to hydrodynamics. This is not a coincidence. To see this note that the energy-momentum tensor $T^{\mu\nu}$ calculated with the approximate solution to Einstein's equations, will be a function of $\beta^\mu(x)$ and its derivatives up to our order of approximation. Furthermore, one of Einstein's equations in the bulk ensures that $T^{\mu\nu}$ is conserved. A conserved $T^{\mu\nu}$ expressed as a function of $\beta^\mu(x)$ and its derivatives is precisely what we defined as the constitutive relations for a fluid. This short discussion shows that the bulk gravity solution can be used to derive the boundary-fluid constitutive relations. This is the fluid/gravity correspondence.

We can apply the fluid/gravity correspondence to calculate the constitutive relations for a fluid moving in a metric affine spacetime. In order to do so, we first need to specify the dynamics, i.e. the Lagrangian of metric affine gravity $\mathcal{L}_{\text{MAG}}$. Thankfully, this has already been done in [183] up to second order in curvature, torsion and non-metricity, although the precise form of the Lagrangian is not that illuminating. In order then to apply the fluid/gravity correspondence we must find an exact black hole solution for MAG with a non-trivial torsion and non-metricity tensor. Luckily for us, there is already a whole zoo of such black hole solutions in the literature [205]. Of these, the solution of [206] is of particular interest, since it is a generalization of the Reissner-Nordström solution including torsion and non-metricity[4]. The remaining tasks, then, for holographers is first to perturb this black hole solution and find an approximate solution after the perturbation. Second, to substitute the solution back to $\mathcal{L}_{\text{MAG}}$ and use the on-shell action to derive the constitutive relations. The second step, might sound trivial, but is far from so. Recall that the on-shell action exhibits divergences near the AdS boundary, which are dual to the UV divergences in a QFT. To use the on-shell action as a generating functional, these divergences must be renormalized by adding the appropriate boundary counterterms to $\mathcal{L}_{\text{MAG}}$ [207]. Working out the details of this renormalization procedure for MAG is current work in progress [188].

[4]Note that due to the high symmetry of this solution, if torsion vanishes so does non-metricity and vice-versa.

Torsional anomalies

Finally, let us discuss a purely QFT project. To this end, we note that spin-hydrodynamics is not the first time torsion has reared its head in condensed matter physics. Namely, torsion is the source of the most controversial anomaly of all, the Nie-Yah anomaly for the chiral current J_5^μ in $3+1$ spacetime dimensions [208, 209]

$$\partial_\mu J_5^\mu = \frac{e}{16\pi^2 l^2}\epsilon^{\mu\nu\rho\lambda}\eta_{ab}T^a_{\mu\nu}T^b_{\rho\lambda} \ . \tag{8.6}$$

On the RHS of (8.6) we see the torsion tensor $T^a_{\mu\nu}$ and the electron charge e. Most important of all, the length scale l also appears. l is the reason this anomaly is so controversial, since it is nothing more than the cutoff scale used to regularize the UV divergence appearing in the calculation. The appearance of l in Eq. (8.6) is troubling for two reasons: First of all it appears in the one-point function of a hermitian and, hence, observable operator. Therefore, the RHS of Eq. (8.6) has zero predictive power since it can be adjusted at will to match the experiments. Second, chiral anomalies are by and large topological beasts, i.e. the anomaly coefficients depend only on the properties of the manifold the fermions are propagating upon(including the spin structure) [112].

It is interesting then to understand what is the true nature of the length scale and why it should appear in the torsional anomaly. Several proposed answers exist: First, the cutoff is simply the cutoff [210]: In condensed matter systems the cutoff is not an arbitrary scale, but is set by the underlying lattice. So l cannot be altered at will and (8.6) has predictive power. This is a perfectly valid answer for condensed matter systems, but not so for high energy physics. This is because the natural cutoff scale in high energy physics is at the Planck scale, where quantum gravity effects also become non-negligible. Therefore, the torsion tensor on RHS of (8.6) cannot be considered an external field, but must be replaced by its quantized counterpart, whatever that may look like.

Another approach suggests that l is proportional to the temperature of the system [211, 212]. While this gives a precise physical meaning and a way to measure l, it is not an appealing solution. This is because anomalies are effects which stem from purely quantum, and not thermal, fluctuations. The modification of the anomaly coefficient due to temperature, does however suggest an interpretation for l: Recall that the temperature of the QFT is encoded in the background geometry. Therefore, l should have a similar geometric origin. We believe this geometric origin can be gleaned from the Ehresmann connection A_M of Eq. (8.4). More precisely, in Eq. (8.4) we have split the connection into a translational and rotational part. However, we can extend A_M to a connection of their product group and write

$$A_M \to \mathcal{A}_M = \begin{pmatrix} \Gamma^a_{\mu b} & \Lambda e^a_\mu \\ -\Lambda e^a_\mu & 0 \end{pmatrix} . \tag{8.7}$$

Physically, the inverse length scale Λ is the cosmological constant of the spacetime we are considering[5] [213]. Given $\mathcal{A}_M$, the translation part of its curvature tensor, $\Omega^{T\ a}_{\mu\nu}$, is proportional to the torsion tensor

$$\Omega^{T\ a}_{\mu\nu} = \Lambda T^a_{\mu\nu} \ . \tag{8.8}$$

Contrasting Eq. (8.8) with Eq. (8.6), it should be clear what we think the origin of l is. We believe that $l = \Lambda^{-1}$ and so we can write

$$\partial_\mu J^\mu_5 = \frac{e}{16\pi^2} \epsilon^{\mu\nu\rho\lambda} \eta_{ab} \Omega^{T\ a}_{\mu\nu} \Omega^{T\ b}_{\rho\lambda} \ . \tag{8.9}$$

Expressing the anomaly in terms of $\Omega^{T\ a}_{\mu\nu}$ brings the anomaly into a *topologically invariant* form. Furthermore, we now know why l must be taken to infinity: The calculation leading to Eq. (8.9) was performed around a flat Minkowski space background with a vanishing cosmological constant. Further motivation for our conjecture stems from the explicit calculation of the anomaly in condensed matter. This calculation shows that l stems from the vacuum energy of the material. In QFT models, the very same vacuum energy also contributes to the cosmological constant of the spacetime (and leads to the "worst prediction of particle physics") [214]. In order to confirm our conjecture $l = \Lambda^{-1}$, we must calculate the anomaly around a De Sitter or AdS background. Furthermore, we should extend the formalism leading to $\mathcal{A}_\mu$ to a non-relativistic, thermal geometry in order to check whether the temperature dependence found in [211, 212] has a similar geometric origin. Finally, if our conjecture is correct, then the *same* length scale l should appear in all anomalies involving torsion. Therefore, it is necessary to construct theories where operators other than J^μ_5 become anomalous in the presence of torsion. This amounts to constructing all possible topological QFTs involving $\mathcal{A}_\mu$ and the gauge fields which couple to the anomalous operators [112].

To conclude, we want to note that the conjunction of hydrodynamics, high-energy and condensed matter physics has given us access to a plethora of new and interesting phenomena, some of which were presented in this thesis. More importantly the ideas for further research we discussed, showcase that more of these phenomena and their far-reaching consequences on theoretical expectations and technical applications are there to explore.

[5] This identification works even for Minkowski spacetime [213].

Acknowledgements

It is my honour to conclude this thesis with acknowledging the support of everyone that made it possible. First, let me thank both my official and unofficial supervisors Prof. Dr. Johanna Erdmenger and Dr. René Meyer, respectively. Without their guidance and their inquisitive comments and questions, this thesis as well as my abilities as a researcher would have been but a mere shadow of what they are today.

Moreover, I would like to thank my collaborators at the university including in no particular order Dr. David Rodríguez Fernández, Dr. Christian Tutschku, Bastian Heß, Pablo Basteiro, Prof. Dr. Ewelina M. Hankiewicz, Prof. Dr. Ronny Thomale, Prof. Dr. Martin Greiter, Prof. Dr. Domenico Di Sante and Sven Danz for the hours of fruitful physics discussions, which always managed to expand my understanding on a given topic.

I would be remissed if I did not also acknowledge the valuable emotional support provided by my friends and family, which made bearable even the more stressful times of completing my PhD.

Finally, I want to thank the SFB - 1170 for funding my PhD research.

Appendix

Appendix

A Hydrostatic constraints

In this appendix we prove formulae (3.46) used to construct the hydrostatic effective action of section 3.2. For ease of reference, we quote (3.46) below

$$\partial_\mu T = -T a_\mu \quad , \quad \partial_\nu \mu = -\mu a_\nu + E_\nu \quad , \quad \partial_\mu u_\nu = -u_\mu a_\nu + \omega_{\mu\nu} \quad . \tag{10}$$

We star-off simple, by examining the gradient of temperature. We have

$$\partial_\mu T = \partial\mu(-\beta^2)^{-1/2} = (-\beta^2)^{-3/2}\partial_\mu\beta = -T\partial_\mu \log\beta \ . \tag{11}$$

In static equilibrium, we can re-express $\partial_\mu \log\beta$ in terms of the velocity profile u_μ. To see this, recall that u_μ is also static, i.e.

$$\begin{aligned} 0 = \mathcal{L}_\beta u_\mu &= \beta^\nu \partial_\mu u_\nu + u_\nu \partial_\mu \beta^\nu = \beta u^\nu \partial_\nu u_\mu + u_\nu \partial_\mu(\beta) u^\nu + \beta u^\nu \partial_\mu u_\nu \\ &= \beta a_\mu - \partial_\mu \beta \Rightarrow a_\mu = \partial_\mu \log\beta \ . \end{aligned} \tag{12}$$

To prove Eq. (12), we used $\beta_\mu = \beta u_\mu$, $u^2 = -1$ and defined the acceleration vector $a_\mu = u^\nu \partial_\nu u_\mu$. So, we can re-write Eq. (11) as

$$\partial_\mu T = -T a_\mu \tag{13}$$

and the first part of (10) is complete. As a consistency check, note that $\mathcal{L}_\beta T = \beta^\mu \partial_\mu T = 0$ is automatically satisfied because $a_\mu u^\mu = 0$.

Let's proceed now to how statisticity constraints $\partial_\mu \mu$. Again we begin with the definition of the chemical potential $\beta^\mu A_\mu = \mu/T$. We take the gradient of this definition to find

$$\begin{aligned} \partial_\mu(\mu/T) &= \partial_\mu(\beta^\nu) A_\nu + \beta^\nu \partial_\mu A_\nu = \beta^\nu \partial_\nu A_\mu - \beta^\nu \partial_\nu A_\mu + \partial_\mu(\beta^\nu) A_\nu + \beta^\nu \partial_\mu A_\nu \\ &= \beta^\nu \left(\partial_\mu A_\nu - \partial_\nu A_\mu\right) + \mathcal{L}_\beta A_\mu = \beta^\nu F_{\nu\mu} \equiv \beta E_\mu \ . \end{aligned} \tag{14}$$

In the above derivation, we have added and subtracted $\beta^\nu \partial_\mu A_\nu$ to construct the Lie derivative of A_μ with respect to β^μ, $\mathcal{L}_\beta A_\mu$. Then, in the last equality we enforced $\mathcal{L}_\beta A_\mu = 0$ and introduced the electric field $E_\mu = F_{\mu\nu}u^\nu$. Now we can use Eq. (14) in conjunction with Eq. (13) to find for the gradient of the chemical potential

$$\partial_\mu \mu = -\mu a_\mu + E_\mu \tag{15}$$

as promised. Again, we see that Eq. (15) satisfies $\mathcal{L}_\beta \mu = 0$ identically.

Finally, we will write down the expansion of $\partial_\mu u_\nu$ in terms of first order static data. To do so, let us first choose a co-ordinate system with one of its axes parallel to u^μ.[6] In this co-ordinate system, we can expand any tensor as

$$A_{\mu\nu} = a u_\mu u_\nu + q_\mu u_\nu + u_\mu h_\nu + \tilde{A}_{\mu\nu} \ , \tag{16}$$

with

$$a = u^\mu A_{\mu\nu} u^\nu \quad , \quad q_\mu = -\Delta^a_\mu A_{ab} u^b \quad , \quad h_\mu = -u^a A_{ab} \Delta^b_\mu \quad , \quad \tilde{A}_{\mu\nu} = \Delta_{\mu a} A^{ab} \Delta_{b\nu} \tag{17}$$

and $\Delta^{\mu\nu} = g^{\mu\nu} + u^\mu u^\nu$ the projector in the directions normal to u^μ. Expanding $\partial_\mu u_\nu$ as in Eq. (16), we find $a = 0 = q_\mu$ and $h_\mu = -a_\mu$. Thus,

$$\partial_\mu u_\nu = -u_\mu a_\nu + \tilde{\partial u}_{\mu\nu} \ . \tag{18}$$

Further, we can decompose $\tilde{\partial u}_{\mu\nu}$ in terms a symmetric-traceless, anti-symmetric and trace part simply by writing

$$\begin{aligned} \tilde{\partial u}_{\mu\nu} &= \frac{1}{2}\Delta_{\mu a}\left(\partial^a u^b + \partial^b u^a - g^{ab}\partial_\lambda u^\lambda\right)\Delta_{\nu b} + \frac{1}{2}\Delta_{\mu a}\left(\partial^a u^b - \partial^b u^a\right)\Delta_{\nu b} \\ &\quad + \frac{1}{2}\Delta_{\mu a} g^{ab} \Delta_{b\nu} \partial_\lambda u^\lambda \equiv \sigma_{\mu\nu} + \omega_{\mu\nu} + \frac{1}{2}\Delta_{\mu\nu}\partial_\lambda u^\lambda \ . \end{aligned} \tag{19}$$

For brevity, we have defined the shear and vorticity tensors, $\sigma_{\mu\nu}$, $\omega_{\mu\nu}$ respectively as

$$\begin{aligned} \sigma_{\mu\nu} &= \frac{1}{2}\Delta_{\mu a}\left(\partial^a u^b + \partial^b u^a - g^{ab}\partial_\lambda u^\lambda\right)\Delta_{\nu b} \quad , \\ \omega_{\mu\nu} &= \frac{1}{2}\Delta_{\mu a}\left(\partial^a u^b - \partial^b u^a\right)\Delta_{\nu b} \ . \end{aligned} \tag{20}$$

[6] The physical reason for this choice of co-ordinate system is that the functional W is invariant under diffeomoprhisms only in the directions normal to u^μ when we are out of equilibrium. See discussion around Eq. (3.25).

Given the expansion Eq. (19), we can easily impose the staticity constraint $\mathcal{L}_\beta = 0$. Indeed note that the trace of $\partial_\mu u_\nu$ is a pure time-derivative and so must vanish in equilibrium. Similarly, $\sigma_{\mu\nu}$ contains the trace of $\partial_\mu u_\nu$ so it must also vanish in equilibrium. On the other hand, $\omega_{\mu\nu}$ does not contain any time-derivatives[7] because of the transverse projectors $\Delta_{\mu\nu}$. Therefore, we find that $\partial_\mu u_\nu$ in equilibrium is simply given by

$$\partial_\mu u_\nu = -u_\mu a_\nu + \omega_{\mu\nu} \ , \tag{21}$$

thus concluding the derivation of Eq. (10).

B Variation of equilibrium effective action

In this appendix, we give an explicit derivation of the constitutive relations Eq. (3.43) and Eq. (3.51) which stem from the equilibrium effective action

$$W = \int d^3x\sqrt{-g}\,[\ P(T,\mu) + \alpha_1 B + \alpha_2\omega] \equiv \int d^3x\sqrt{-g}\mathcal{P} \ . \tag{22}$$

Where

$$\begin{aligned} T &= \sqrt{-\beta^2} \quad , \quad \mu = \frac{\beta^\mu}{\sqrt{-\beta^2}} A_\mu = u^\mu A_\mu \quad , \\ B &= \frac{1}{2}\varepsilon_{\mu\nu\rho} u^\mu F^{\nu\rho} \quad , \quad \omega = \frac{1}{2}\varepsilon_{\mu\nu\rho} u^\mu \omega^{\nu\rho} \end{aligned} \tag{23}$$

and $\alpha_1,\ \alpha_2$ are functions of μ and T.

The constitutive relations are defined in terms of the variation of W and more precisely

$$\delta W = \int d^3x\sqrt{-g}\left[\frac{1}{2}T^{\mu\nu}\delta g_{\mu\nu} + J^\mu \delta A_\mu\right] \ . \tag{24}$$

To derive these variations, we will first derive simpler variations that can be used to construct more complicated ones. To commence the derivation, we consider the variation of the temperature

$$\begin{aligned} \delta T &= \delta(-\beta^2)^{-1/2} = \frac{-1}{2}(-\beta^2)^{-3/2}\delta(-\beta^2) \\ &= \frac{1}{2}(-\beta^2)^{-3/2}\beta^\mu\beta^\nu\delta g_{\mu\nu} = \frac{1}{2}T u^\mu u^\nu \delta g_{\mu\nu} \ . \end{aligned} \tag{25}$$

One very important assumption that entered the derivation of Eq. (25) was the non-variation of the thermal vector, $\delta\beta^\mu = 0$. This is natural assumption

[7] In the co-ordinate system where the time-direction is parallel to u^μ.

for the following reason: In order for a system to be in static equilibrium one needs to define time, which in a relativistic theory is defined through a timelike Lorentz vector. The thermal vector β^μ plays precisely this role in our construction. We can use this property of β^μ to find

$$\delta u^\mu = \delta[\beta^\mu(-\beta^2)^{-1/2}] = \beta^\mu\delta(-\beta^2)^{-1/2} = \frac{1}{2}u^\mu u^\nu u^\rho \delta g_{\nu\rho} \ . \tag{26}$$

We can also easily find the variation of the chemical potential

$$\delta\mu = \delta(u^\mu A_\mu) = \frac{1}{2}u^\mu A_\mu u^\nu u^\rho \delta g_{\nu\rho} + u^\mu \delta A_\mu = \frac{1}{2}\mu u^\nu u^\rho \delta g_{\nu\rho} + u^\mu \delta A_\mu \ . \tag{27}$$

Given the variation of μ and T, we have for any function f of μ and T

$$\delta f(\mu,T) = \frac{\partial f}{\partial \mu}\delta\mu + \frac{\partial f}{\partial T}\delta T = \frac{1}{2}u^\mu u^\nu \left(T\frac{\partial f}{\partial T} + \mu\frac{\partial f}{\partial \mu}\right)\delta g_{\mu\nu} + \frac{\partial f}{\partial \mu}u^\mu \delta A_\mu \ . \tag{28}$$

We can apply this result when we consider the variation of W, keeping B and ω, fixed to find

$$\begin{aligned}\tilde{\delta}W &= \int \left[\tilde{\delta}(\sqrt{-g})\mathcal{P} + \sqrt{-g}\tilde{\delta}\mathcal{P}\right] \\ &= \int dV \left[\ \frac{1}{2}\left(g^{\mu\nu}\mathcal{P} + u^\mu u^\nu\left(T\frac{\partial \mathcal{P}}{\partial T} + \mu\frac{\partial \mathcal{P}}{\partial \mu}\right)\right)\delta g_{\mu\nu} + \frac{\partial \mathcal{P}}{\partial \mu}u^\mu \delta A_\mu\right] ,\end{aligned} \tag{29}$$

where $\tilde{\delta}B = 0 = \tilde{\delta}\omega$ and we have made use of well-known formula for the variation of the metric determinant [122]

$$\delta\sqrt{-g} = \frac{1}{2}\sqrt{-g}g^{\mu\nu}\delta g_{\mu\nu}. \tag{30}$$

We are now in position to write down the zeroth order constitutive relations by simply setting $B = 0 = \omega$ in $\tilde{\delta}W$. The result is that quoted in Eq. (3.43) and which we repeat below for ease of reference

$$T^{\mu\nu} = \epsilon u^\mu u^\nu + P\Delta^{\mu\nu} \quad , \quad J^\mu = \rho u^\mu \ , \tag{31}$$

$$\epsilon = T\frac{\partial P}{\partial T} + \mu\rho - P \quad , \quad u^\mu = \frac{\beta^\mu}{\sqrt{-\beta^2}} \quad , \quad \Delta^{\mu\nu} = g^{\mu\nu} + u^\mu u^\nu \quad , \quad \rho = \frac{\partial P}{\partial \mu} \ . \tag{32}$$

To complete the derivation of the constitutive relations we need to derive the variations of B and ω and use

$$\delta W = \tilde{\delta} W + \int d^3x \sqrt{-g} \left[\alpha_1 \delta B + \alpha_2 \delta \omega \right], \tag{33}$$

which stems directly from the definitions of W and $\tilde{\delta}$.

To take the variation of B we re-express it as

$$B = \frac{1}{2} \varepsilon^{\mu\nu\rho} u_\mu F_{\nu\rho} = \frac{1}{2} \varepsilon^{\mu\nu\rho} u_\mu F_{\nu\rho} \ . \tag{34}$$

This way we simplify the calculation since we wont have to deal with expressing the variation of $\partial^\nu A^\rho$ in terms of the variation of $\partial_\nu A_\rho$. Then to compute δB, we need

$$\delta \varepsilon^{\mu\nu\rho} = -\delta \left(\frac{1}{\sqrt{-g}} \right) \epsilon^{\mu\nu\rho} = -\frac{1}{2} \varepsilon^{\mu\nu\rho} \ , \tag{35}$$

$$\delta u_\mu = \delta \left(g_{\mu\nu} u^\nu \right) = \delta g_{\mu\nu} u^\nu + \frac{1}{2} u_\mu u^\kappa u^\lambda \delta g_{\kappa\lambda} \ , \tag{36}$$

where $\epsilon^{\mu\nu\rho}$ the Levi-Civita symbol. The final identity we need is the the e/m decomposition of $F_{\mu\nu}$,

$$F_{\mu\nu} = u_\mu E_\nu - u_\nu E_\mu + u^\lambda \varepsilon_{\lambda\mu\nu} B \ , \tag{37}$$

which can be confirmed directly by contracting $F_{\mu\nu}$ with u_μ, u_ν and $\varepsilon^{\mu\nu\rho}$.

Putting everything together we find for δB

$$\delta B = \frac{1}{2} \delta \left(\varepsilon^{\mu\nu\rho} u_\mu F_{\nu\rho} \right) = \frac{1}{2} \left[(u \times E)^{(\mu} u^{\nu)} - B \Delta^{\mu\nu} \right] \delta g_{\mu\nu} + \varepsilon^{\mu\nu\rho} u_\mu \partial_\nu \delta A_\rho \ , \tag{38}$$

with $\Delta^{\mu\nu} = g^{\mu\nu} + u^\mu u^\nu$. Note that the partial derivative found in Eq. (38) can be replaced by covariant derivative with a symmetric Christoffel connection. We will use this derivative substitution in the following to simplify our calculation.

Finally, we consider the variation of ω. In this case, we will use the definition of ω as in (23) with the Levi-Civita tensor with all lower indices. Because of this, we need the variation of the Levi-civita tensor $\varepsilon_{\mu\nu\rho} = \sqrt{-g} \epsilon_{\mu\nu\rho}$ and of the inverse metric

$$\delta \varepsilon_{\mu\nu\rho} = \frac{1}{2} \varepsilon_{\mu\nu\rho} g^{\kappa\lambda} \delta g_{\kappa\lambda} \ , \ \delta g^{\mu\nu} = -g^{\mu\kappa} g^{\nu\lambda} \delta g_{\kappa\lambda}. \tag{39}$$

We will need $\delta g^{\mu\nu}$ during the variation of $\omega^{\mu\nu}$ since δ does not commute with ∂^μ, but instead

$$[\delta, \partial^\nu] = \delta g^{\nu\mu}\partial_\mu \ . \tag{40}$$

The last identity we will make use of in our derivation is the decomposition of $\partial_\mu u_\nu$ similar to the e/m decomposition of $F_{\mu\nu}$

$$\partial_\mu u_\nu = -u_\mu a_\nu + \omega_{\mu\nu} = -u_\mu a_\mu - \varepsilon_{\mu\nu\rho}\omega^\rho = -u_\mu a_\nu + u^\lambda \varepsilon_{\lambda\mu\nu}\omega \ . \tag{41}$$

In the above decomposition ω_ρ is the angular velocity vector

$$\omega_\mu = \frac{1}{2}\varepsilon_{\mu\nu\rho}\omega^{\nu\rho} \ . \tag{42}$$

The angular velocity vector is purely timelike, since $\omega_{\mu\nu}$ is purely spacelike. Therefore, $\omega_\mu = cu_\mu$ with $c = -u^\mu\omega_\mu = \omega$. We have, thus, all the ingredients necessary to calculate $\delta\omega$ to find

$$\delta\omega = \frac{1}{2}\delta\left(\varepsilon_{\mu\nu\rho}u^\mu\omega^{\nu\rho}\right) = \frac{1}{2}\omega\left[u^\mu u^\nu - \Delta^{\mu\nu}\right]\delta g_{\mu\nu} - \frac{1}{2}(u\times a)^{(\mu}u^{\nu)}\delta g_{\mu\nu} \ . \tag{43}$$

We are now ready to piece everything together and calculate the variation of W. To aid our understanding let's focus first on the variation with respect to the metric

$$\begin{aligned}
\delta W &= \tilde{\delta}W + \int d^3x\sqrt{-g}\left[\alpha_1\delta B + \alpha_2\delta\omega\right] \\
&= \int d^3x\sqrt{-g}\ \frac{1}{2}\delta g_{\mu\nu}\Bigg[g^{\mu\nu}\mathcal{P} + u^\mu u^\nu\left(T\frac{\partial\mathcal{P}}{\partial T} + \mu\frac{\partial\mathcal{P}}{\partial\mu} + \alpha_2\omega\right) \\
&\quad - \left(\alpha_1 B + \alpha_2\omega\right)\Delta^{\mu\nu} + \alpha_1(u\times E)^{(\mu}u^{\nu)} - \alpha_2(u\times a)^{(\mu}u^{\nu)}\Bigg] \\
&= \int d^3x\sqrt{-g}\ \frac{1}{2}\delta g_{\mu\nu}\Bigg[u^\mu u^\nu\left(T\frac{\partial\mathcal{P}}{\partial T} + \mu\frac{\partial\mathcal{P}}{\partial\mu} + \alpha_2\omega - \mathcal{P}\right) \\
&\quad + \Delta^{\mu\nu}\left(\mathcal{P} - \alpha_1 B - \alpha_2\omega\right) + \alpha_1(u\times E)^{(\mu}u^{\nu)} + \alpha_2(u\times a)^{(\mu}u^{\nu)}\Bigg] \\
&\equiv \int d^3x\sqrt{-g}\ \frac{1}{2}\delta g_{\mu\nu}T^{\mu\nu} = \int dV\ \frac{1}{2}\delta g_{\mu\nu}T^{\mu\nu}.
\end{aligned} \tag{44}$$

Before we write down the explicit result for $T^{\mu\nu}$, let us also take the variation of W with respect to A_μ

$$
\begin{aligned}
\delta W &= \tilde{\delta} W + \int d^3x\sqrt{-g}\ \alpha_1 \delta B \\
&= \int d^3x \left[\tilde{\delta}\left(\sqrt{-g}\mathcal{P}\right) + \sqrt{-g}\left(\alpha_1\delta B + \alpha_2\delta\omega\right)\right] \\
&= \int d^3x\sqrt{-g}\left(\frac{\partial\mathcal{P}}{\partial\mu}u^\mu + \alpha_1\epsilon^{\mu\nu\rho}u_\nu\nabla_\rho\right)\delta A_\mu \\
&= \int d^3x\sqrt{-g}\left[\frac{\partial\mathcal{P}}{\partial\mu}u^\mu - \nabla_\rho(\alpha_1\epsilon^{\mu\nu\rho}u_\nu)\right]\delta A_\mu \\
&= \int d^3x\sqrt{-g}\left[\frac{\partial\mathcal{P}}{\partial\mu}u^\mu - \varepsilon^{\mu\nu\rho}\left(\frac{\partial\alpha_1}{\partial T}\nabla_\rho T + \frac{\partial\alpha_1}{\partial\mu}\nabla_\rho\mu + \alpha_1\nabla_\rho u_\nu\right)\right]\delta A_\mu \\
&= \int d^3x\sqrt{-g}\Bigg[\frac{\partial\mathcal{P}}{\partial\mu}u^\mu + (u\times a)^\mu\left(T\frac{\partial\alpha_1}{\partial T} + \mu\frac{\partial a_1}{\partial\mu} - \alpha_1\right) \\
&\qquad\qquad + (u\times E)^\mu\frac{\partial\alpha_1}{\partial\mu} + \alpha_1\omega^\mu\Bigg]\delta A_\mu \\
&= \int d^3x\sqrt{-g}\Bigg[\left(\frac{\partial\mathcal{P}}{\partial\mu} - \alpha_1\omega\right)u^\mu(u\times a)^\mu\left(T\frac{\partial\alpha_1}{\partial T} + \mu\frac{\partial a_1}{\partial\mu} - \alpha_1\right) \\
&\qquad\qquad + (u\times E)^\mu\frac{\partial\alpha_1}{\partial\mu}\Bigg]\delta A_\mu \\
&\equiv \int d^3x\sqrt{-g}\ J^\mu\delta A_\mu = \int dV\ J^\mu\delta A_\mu\ .
\end{aligned}
\tag{45}
$$

Some comments on the last calculation: In the 4th line of the δA_μ variation we substituted the gradients of the temperature, chemical potential and velocity profile via Eq. (3.46) in terms of the acceleration vector a_μ and the electric field $E^\mu = F^{\mu\nu}u_\nu$. We also used the angular velocity vector ω_μ Eq. (42) and its expansion in terms of u_μ in the 4th and 5th lines of the derivation respectively.

Thus we are ready, after a long dance with algebra, to write down the energy-momentum tensor and charge current derived from the equilibrium partition function at first order in the derivative expansion. We have

$$
\begin{aligned}
T^{\mu\nu} &= \mathcal{E}u^\mu u^\nu + \Pi\Delta^{\mu\nu} + \alpha_1(u\times E)^{(\mu}u^{\nu)} - \alpha_2(u\times a)^{(\mu}u^{\nu)}\ , \\
J^\mu &= Ru^\mu + c_a(u\times a)^\mu + c_E(u\times E)^\mu\ ,
\end{aligned}
\tag{46}
$$

with

$$\mathcal{E} = T\frac{\partial \mathcal{P}}{\partial T} + \mu\frac{\partial \mathcal{P}}{\partial \mu} + \alpha_2\omega - \mathcal{P} \quad , \quad \Pi = \mathcal{P} - \alpha_1 B - \alpha_2\omega$$
$$R = \frac{\partial \mathcal{P}}{\partial \mu} - \alpha_1\omega \quad , \quad c_a = T\frac{\partial \alpha_1}{\partial T} + \mu\frac{\partial a_1}{\partial \mu} - \alpha_1 \quad , \quad c_E = \frac{\partial \alpha_1}{\partial \mu} \ . \tag{47}$$

C Linearised hEOM

Below we reprint the code that we used to calculate the linearised equations of motion (3.111).

General definitions

In[ ]:=
```
ClearAll;
coord = {t, x, y};
Assumptions[ϵ > 0]
h [t_, x_, y_] =
  ϵ {{h00[t, x, y], h01[t, x, y], h02[t, x, y]}, {h01[t, x, y], h11[t, x, y], h12[t, x, y]},
    {h02[t, x, y], h12[t, x, y], h22[t, x, y]}};(*Metric perturbation *)
metric = DiagonalMatrix[{-1, 1, 1}] + h[t, x, y];
metricsign = -1;
$Assumptions = And[t ∈ Reals, x ∈ Reals, y ∈ Reals];
SetDirectory["C://Users//iom06dg//Desktop//PhD//Wolfram Mathematica"];
(* Set directory where diffgeo.m is located *)
<< diffgeo.m
T[t_, x_, y_] =  T0 + ϵ * δT[t, x, y];
(* temperature in terms of background, T0, and fluct field δT *)
μ[t_, x_, y_] = μ0 + ϵ * δμ[t, x, y];
(* same as temperature but with the chemical potential *)
u[t_, x_, y_] = {1, ϵ * v1[t, x, y], ϵ * v2[t, x, y]}; (*Velocity profile around,
equilibrium {1,0,0} and fluctuations propto ϵ. Index up *)
Delta[t_, x_, y_] = Normal[Series[inverse + u[t, x, y] ** u[t, x, y], {ϵ, 0, 1}]];
(* Projector normal to u up to order ϵ. Both upper indices *)
MatrixForm[Delta[t, x, y]];
En[t_, x_, y_] = ϵ0 + ϵ * (ϵ0T * δT[t, x, y] + ϵ0m * δμ[t, x, y]);
(* Definitions of energy, pressure and density up to first order in ϵ *)
P[t_, x_, y_] = P0 + ϵ * (P0T * δT[t, x, y] + P0m * δμ[t, x, y]);
ρ[t_, x_, y_] = ρ0 + ϵ * (ρ0T * δT[t, x, y] + ρ0m * δμ[t, x, y]);
Efield[t_, x_, y_] = ϵ * {0, Ex[t, x, y], Ey[t, x, y]};
(* Electric field, upper index*)
Fmn[t_, x_, y_] = Normal[Series[2 antisymmetrize[u[t, x, y] ** Efield[t, x, y]] +
     raise[u[t, x, y].LeviCivita] * ϵ * B[t, x, y], {ϵ, 0, 1}]];
 (* E/M decomposition of Maxwell's tensor, upper indices *)
Σ[t_, x_, y_] = Normal[Series[u[t, x, y].LeviCivita, {ϵ, 0, 1}]];
(* parity-odd projector, both indices down *)
(* Up to order ϵ,
all indices are raised and lowered by the Minkowski metric. So for spatial tensors,
one does not need to keep track of the index
 position. This fails for any other background spatial metric*)
```

Out[ ]=
```
Assumptions[ϵ > 0]
```

Current – specific definitions

In[ ]:=

```
U[t_, x_, y_] =
  Normal[Series[Efield[t, x, y] - T[t, x, y] Delta[t, x, y].partial[μ[t, x, y] / T[t, x, y]],
    {ϵ, 0, 1}]];(* Einstein vector, upper index *)
ΣU[t_, x_, y_] = -Normal[Series[raise[Σ[t, x, y].U[t, x, y]], {ϵ, 0, 1}]];
(* parity-odd U, E and gradT, index up*)
ΣE[t_, x_, y_] = -Normal[Series[raise[Σ[t, x, y].Efield[t, x, y]], {ϵ, 0, 1}]];
ΣT[t_, x_, y_] = -Normal[Series[raise[Σ[t, x, y].raise[partial[T[t, x, y]]]], {ϵ, 0, 1}]];
```

```
Jm[t_, x_, y_] =
 Normal[Series[ρ[t, x, y] * u[t, x, y] + σ * U[t, x, y] + σp * ΣU[t, x, y] + χpT * ΣT[t, x, y] +
    χpE * ΣE[t, x, y], {ϵ, 0, 1}]] (* Current, upper index *)
MatrixForm[Jm[t, x, y]];
FJ[t_, x_, y_] = Normal[Series[Fmn[t, x, y].lower[Jm[t, x, y]], {ϵ, 0, 1}]];
(* Right-hand side of energy-momentum conservation, upper index *)
```

```
```

Tensor – specific definitions

```
Gradu[t_, x_, y_] = Normal[Series[covariant[lower[u[t, x, y]], {down}], {ϵ, 0, 1}]];
(*Definition of the gradient of u, both lower indices *)
ω[t_, x_, y_] =
  Normal[Series[ contract[u[t, x, y].LeviCivita ** Gradu[t, x, y], {1, 3}, {2, 4}],
    {ϵ, 0, 1}]]; (* vorticity *)
σt[t_, x_, y_] = 2 * Normal[Series[Delta[t, x, y].symmetrize[Gradu[t, x, y]].Delta[t, x, y],
     {ϵ, 0, 1}]]; (* Shear tensor, both indices up*)
σpt[t_, x_, y_] = -Normal[Series[raise[symmetrize[
       contract[Σ[t, x, y] ** lower[σt[t, x, y]], {2, 3}]]], {ϵ, 0, 1}]];
(* parity-odd shear tensor, upper indices *)
Π[t_, x_, y_] =
  Normal[Series[P[t, x, y] - ζ * divergence[u[t, x, y]] + χo * ω[t, x, y] - ϵ * χB * B[t, x, y],
    {ϵ, 0, 1}]]; (* Pressure term *)
```

```
Clear[Tmn]
Tmn[t_, x_, y_] =
  Normal[Series[ En[t, x, y] * u[t, x, y] ** u[t, x, y] + Π[t, x, y] * Delta[t, x, y],
     {ϵ, 0, 1}]] - η * σt[t, x, y] - ηH * σpt[t, x, y];
MatrixForm[Tmn[t, x, y]];
DTmn[t_, x_, y_] =
  Normal[Series[lower[covariant[Tmn[t, x, y], {up, up}], {2, 3}], {ϵ, 0, 1}]];
(* Covariant derivative of the energy momentum tensor, all indices down *)
```

Equations of motion

```
EOMvector = FullSimplify[TraditionalForm[
   Normal[Series[raise[contract[DTmn[t, x, y], {1, 2}]] == FJ[t, x, y], {ϵ, 0, 1}]]]]
```

```
EOMscalar =
 FullSimplify[TraditionalForm[Normal[Series[divergence[Jm[t, x, y]] == 0, {ϵ, 0, 1}]]]]
```

Appendix

Bibliography

[1] J. Erdmenger, I. Matthaiakakis, R. Meyer, and D. Rodríguez Fernández, "Strongly coupled electron fluids in the Poiseuille regime," *Phys. Rev. B*, vol. 98, no. 19, p. 195143, 2018.

[2] D. Di Sante, J. Erdmenger, M. Greiter, I. Matthaiakakis, R. Meyer, D. Rodríguez Fernández, R. Thomale, E. van Loon, and T. Wehling, "Turbulent hydrodynamics in strongly correlated Kagome metals," *Nature Commun.*, vol. 11, no. 1, p. 3997, 2020.

[3] I. Matthaiakakis, D. Rodríguez Fernández, C. Tutschku, E. M. Hankiewicz, J. Erdmenger, and R. Meyer, "Functional dependence of Hall viscosity induced transverse voltage in two-dimensional Fermi liquids," *Phys. Rev. B*, vol. 101, no. 4, p. 045423, 2020.

[4] O. Dariggol, *Worlds of Flow: A history of hydrodynamics from the Bernoullis to Prandtl*. Oxford University Press, February 2005.

[5] L. Euler, "Principes généraux du mouvement des fluides," *Mémoires de l'académie des sciences de Berlin*, vol. 11, pp. 274–315, 1757.

[6] J. C. Maxwell, *On Faraday's Lines of Force*, vol. 1 of *Cambridge Library Collection - Physical Sciences*, p. 155–229. Cambridge University Press, 2011.

[7] D. T. Son and P. Surowka, "Hydrodynamics with Triangle Anomalies," *Phys. Rev. Lett.*, vol. 103, p. 191601, 2009.

[8] J. Bhattacharya, S. Bhattacharyya, S. Minwalla, and A. Yarom, "A Theory of first order dissipative superfluid dynamics," *JHEP*, vol. 05, p. 147, 2014.

[9] K. Jensen, M. Kaminski, P. Kovtun, R. Meyer, A. Ritz, and A. Yarom, "Parity-Violating Hydrodynamics in 2+1 Dimensions," *JHEP*, vol. 05, p. 102, 2012.

[10] S. Weinberg, "On the development of effective field theory," *The European Physical Journal H*, vol. 46, p. 6, Mar 2021.

[11] E. Noether, "Invariant variation problems," *Transport Theory and Statistical Physics*, vol. 1, no. 3, pp. 186–207, 1971.

[12] G. Stokes, "On the theories of the internal friction of fluids in motion and of the equilibrium and motion of elastic solids.," *Trans. Cambridge Philos. Soc.*, vol. 8, pp. 287–319, 1845.

[13] R. N. Gurzhi, "Minimum of resistance in impurity-free conductors," *Journal of Experimental and Theoretical Physics*, vol. 17, p. 521, August 1963.

[14] R. N. Gurzhi, "HYDRODYNAMIC EFFECTS IN SOLIDS AT LOW TEMPERATURE," *Soviet Physics Uspekhi*, vol. 11, pp. 255–270, feb 1968.

[15] D. T. Son, "Newton-Cartan Geometry and the Quantum Hall Effect," 6 2013.

[16] L. W. Molenkamp and M. J. M. de Jong, "Electron-electron-scattering-induced size effects in a two-dimensional wire," *Phys. Rev. B*, vol. 49, pp. 5038–5041, Feb 1994.

[17] M. J. M. de Jong and L. W. Molenkamp, "Hydrodynamic electron flow in high-mobility wires," *Phys. Rev. B*, vol. 51, pp. 13389–13402, May 1995.

[18] R. N. Gurzhi, A. N. Kalinenko, and A. I. Kopeliovich, "Electron-electron collisions and a new hydrodynamic effect in two-dimensional electron gas," *Phys. Rev. Lett.*, vol. 74, pp. 3872–3875, May 1995.

[19] D. A. Bandurin, I. Torre, R. K. Kumar, M. Ben Shalom, A. Tomadin, A. Principi, G. H. Auton, E. Khestanova, K. S. Novoselov, I. V. Grigorieva, L. A. Ponomarenko, A. K. Geim, and M. Polini, "Negative local resistance caused by viscous electron backflow in graphene," *Science*, vol. 351, no. 6277, pp. 1055–1058, 2016.

[20] P. J. W. Moll, P. Kushwaha, N. Nandi, B. Schmidt, and A. P. Mackenzie, "Evidence for hydrodynamic electron flow in pdcoo2," *Science*, vol. 351, no. 6277, pp. 1061–1064, 2016.

[21] J. Gooth, F. Menges, N. Kumar, V. Süβ, C. Shekhar, Y. Sun, U. Drechsler, R. Zierold, C. Felser, and B. Gotsmann, "Thermal and electrical signatures of a hydrodynamic electron fluid in tungsten diphosphide," *Nature Communications*, vol. 9, p. 4093, Oct 2018.

[22] J. A. Sulpizio, L. Ella, A. Rozen, J. Birkbeck, D. J. Perello, D. Dutta, M. Ben-Shalom, T. Taniguchi, K. Watanabe, T. Holder, R. Queiroz, A. Principi, A. Stern, T. Scaffidi, A. K. Geim, and S. Ilani, "Visualizing poiseuille flow of hydrodynamic electrons," *Nature*, vol. 576, pp. 75–79, Dec 2019.

[23] M. J. H. Ku, T. X. Zhou, Q. Li, Y. J. Shin, J. K. Shi, C. Burch, L. E. Anderson, A. T. Pierce, Y. Xie, A. Hamo, U. Vool, H. Zhang, F. Casola, T. Taniguchi, K. Watanabe, M. M. Fogler, P. Kim, A. Yacoby, and R. L. Walsworth, "Imaging viscous flow of the dirac fluid in graphene," *Nature*, vol. 583, pp. 537–541, Jul 2020.

[24] R. Kubo, "Statistical-mechanical theory of irreversible processes. i. general theory and simple applications to magnetic and conduction problems," *Journal of the Physical Society of Japan*, vol. 12, no. 6, pp. 570–586, 1957.

[25] R. Kubo, M. Yokota, and S. Nakajima, "Statistical-mechanical theory of irreversible processes. ii. response to thermal disturbance," *Journal of the Physical Society of Japan*, vol. 12, no. 11, pp. 1203–1211, 1957.

[26] J. Maldacena, "The large-n limit of superconformal field theories and supergravity," *International Journal of Theoretical Physics*, vol. 38, pp. 1113–1133, Apr 1999.

[27] A. M. Polyakov, "String theory and quark confinement," *Nuclear Physics B - Proceedings Supplements*, vol. 68, no. 1, pp. 1–8, 1998. Strings '97.

[28] S. Sachdev, *Quantum Phase Transitions*. Cambridge University Press, 2 ed., 2011.

[29] P. K. Kovtun, D. T. Son, and A. O. Starinets, "Viscosity in strongly interacting quantum field theories from black hole physics," *Phys. Rev. Lett.*, vol. 94, p. 111601, Mar 2005.

[30] M. Ammon and J. Erdmenger, *Gauge/Gravity Duality: Foundations and Applications*. Cambridge University Press, 2015.

[31] M. Müller, J. Schmalian, and L. Fritz, "Graphene: A nearly perfect fluid," *Phys. Rev. Lett.*, vol. 103, p. 025301, Jul 2009.

[32] B. N. Narozhny, I. V. Gornyi, A. D. Mirlin, and J. Schmalian, "Hydrodynamic approach to electronic transport in graphene," *Annalen Phys.*, vol. 529, no. 11, p. 1700043, 2017.

[33] B. N. Narozhny, "Electronic hydrodynamics in graphene," *Annals Phys.*, vol. 411, p. 167979, 2019.

[34] B. N. Narozhny and M. Schütt, "Magnetohydrodynamics in graphene: shear and Hall viscosities," *Phys. Rev. B*, vol. 100, no. 3, p. 035125, 2019.

[35] C. P. Herzog, P. Kovtun, S. Sachdev, and D. T. Son, "Quantum critical transport, duality, and m theory," *Phys. Rev. D*, vol. 75, p. 085020, Apr 2007.

[36] L. Fritz, J. Schmalian, M. Müller, and S. Sachdev, "Quantum critical transport in clean graphene," *Physical Review B*, vol. 78, Aug 2008.

[37] R. A. Davison, K. Schalm, and J. Zaanen, "Holographic duality and the resistivity of strange metals," *Physical Review B*, vol. 89, Jun 2014.

[38] A. Lucas, S. Sachdev, and K. Schalm, "Scale-invariant hyperscaling-violating holographic theories and the resistivity of strange metals with random-field disorder," *Phys. Rev. D*, vol. 89, no. 6, p. 066018, 2014.

[39] K. Landsteiner, "Notes on Anomaly Induced Transport," *Acta Phys. Polon. B*, vol. 47, p. 2617, 2016.

[40] S. L. Adler, "Axial-vector vertex in spinor electrodynamics," *Phys. Rev.*, vol. 177, pp. 2426–2438, Jan 1969.

[41] J. S. Bell and R. Jackiw, "A pcac puzzle: $\pi 0 \to \gamma\gamma$ in the σ-model," *Il Nuovo Cimento A (1965-1970)*, vol. 60, pp. 47–61, Mar 1969.

[42] H. B. Nielsen and M. Ninomiya, "ADLER-BELL-JACKIW ANOMALY AND WEYL FERMIONS IN CRYSTAL," *Phys. Lett. B*, vol. 130, pp. 389–396, 1983.

[43] K. Fukushima, D. E. Kharzeev, and H. J. Warringa, "The Chiral Magnetic Effect," *Phys. Rev. D*, vol. 78, p. 074033, 2008.

[44] Q. Li and D. E. Kharzeev, "Chiral magnetic effect in condensed matter systems," *Nucl. Phys. A*, vol. 956, pp. 107–111, 2016.

[45] E. A. Abbott, *Flatland: A Romance of Many Dimensions*. Seeley & Co, 1884.

[46] A. N. Redlich, "Gauge Noninvariance and Parity Violation of Three-Dimensional Fermions," *Phys. Rev. Lett.*, vol. 52, p. 18, 1984.

[47] A. J. Niemi and G. W. Semenoff, "Axial Anomaly Induced Fermion Fractionization and Effective Gauge Theory Actions in Odd Dimensional Space-Times," *Phys. Rev. Lett.*, vol. 51, p. 2077, 1983.

[48] A. N. Redlich, "Parity Violation and Gauge Noninvariance of the Effective Gauge Field Action in Three-Dimensions," *Phys. Rev. D*, vol. 29, pp. 2366–2374, 1984.

[49] G. W. Semenoff, "Condensed Matter Simulation of a Three-dimensional Anomaly," *Phys. Rev. Lett.*, vol. 53, p. 2449, 1984.

[50] A. K. Geim, "Graphene: Status and prospects," *Science*, vol. 324, no. 5934, pp. 1530–1534, 2009.

[51] J. Böttcher, C. Tutschku, L. W. Molenkamp, and E. M. Hankiewicz, "Survival of the Quantum Anomalous Hall Effect in Orbital Magnetic Fields as a Consequence of the Parity Anomaly," *Phys. Rev. Lett.*, vol. 123, no. 22, p. 226602, 2019.

[52] J. Böttcher, C. Tutschku, and E. M. Hankiewicz, "Fate of quantum anomalous Hall effect in the presence of external magnetic fields and particle-hole asymmetry," *Phys. Rev. B*, vol. 101, no. 19, p. 195433, 2020.

[53] C. Tutschku, J. Böttcher, R. Meyer, and E. M. Hankiewicz, "Momentum-Dependent Mass and AC Hall Conductivity of Quantum Anomalous Hall Insulators and Their Relation to the Parity Anomaly," *Phys. Rev. Res.*, vol. 2, no. 3, p. 033193, 2020.

[54] C. Tutschku, F. S. Nogueira, C. Northe, J. van den Brink, and E. M. Hankiewicz, "Temperature and chemical potential dependence of the parity anomaly in quantum anomalous Hall insulators," *Phys. Rev. B*, vol. 102, no. 20, p. 205407, 2020.

[55] T. L. Hughes, R. G. Leigh, and O. Parrikar, "Torsional Anomalies, Hall Viscosity, and Bulk-boundary Correspondence in Topological States," *Phys. Rev. D*, vol. 88, no. 2, p. 025040, 2013.

[56] C. Hoyos, "Hall viscosity, topological states and effective theories," *Int. J. Mod. Phys. B*, vol. 28, p. 1430007, 2014.

[57] N. W. Ashcroft and N. D. Mermin, *Solid State Physics*. Holt-Saunders, 1976.

[58] A. Lucas and K. C. Fong, "Hydrodynamics of electrons in graphene," *Journal of Physics: Condensed Matter*, vol. 30, p. 053001, Jan 2018.

[59] M. Polini and A. K. Geim, "Viscous electron fluids," *Physics Today*, vol. 73, no. 6, pp. 28–34, 2020.

[60] A. Hirohata, K. Yamada, Y. Nakatani, I.-L. Prejbeanu, B. Diény, P. Pirro, and B. Hillebrands, "Review on spintronics: Principles and device applications," *Journal of Magnetism and Magnetic Materials*, vol. 509, p. 166711, 2020.

[61] S. J. Barnett, "Magnetization by rotation," *Phys. Rev.*, vol. 6, pp. 239–270, Oct 1915.

[62] E. Witten, "Anti-de Sitter space and holography," *Adv. Theor. Math. Phys.*, vol. 2, pp. 253–291, 1998.

[63] S. S. Gubser, I. R. Klebanov, and A. M. Polyakov, "Gauge theory correlators from noncritical string theory," *Phys. Lett. B*, vol. 428, pp. 105–114, 1998.

[64] E. Kiritsis, *String theory in a nutshell*. USA: Princeton University Press, 2019.

[65] J. Polchinski, "Introduction to Gauge/Gravity Duality," in *Theoretical Advanced Study Institute in Elementary Particle Physics: String theory and its Applications: From meV to the Planck Scale*, 10 2010.

[66] S. A. Hartnoll, A. Lucas, and S. Sachdev, "Holographic quantum matter," 12 2016.

[67] D. Z. Freedman and A. Van Proeyen, *Supergravity*. Cambridge, UK: Cambridge Univ. Press, 5 2012.

[68] H. J. Kim, L. J. Romans, and P. van Nieuwenhuizen, "Mass spectrum of chiral ten-dimensional n=2 supergravity on S^5," *Phys. Rev. D*, vol. 32, pp. 389–399, Jul 1985.

[69] M. Gunaydin and N. Marcus, "The spectrum of the s5 compactification of the chiral n=2, d=10 supergravity and the unitary supermultiplets of u(2,2/4)," *Classical and Quantum Gravity*, vol. 2, no. 2, pp. L11–L17, 1985.

[70] K. Skenderis and M. Taylor, "Kaluza-Klein holography," *JHEP*, vol. 05, p. 057, 2006.

[71] J. V. José and E. J. Saletan, *Classical Dynamics: A Contemporary Approach*. Cambridge University Press, 1998.

[72] M. E. Peskin and D. V. Schroeder, *An Introduction to quantum field theory*. Reading, USA: Addison-Wesley, 1995.

[73] J. W. York, "Role of conformal three-geometry in the dynamics of gravitation," *Phys. Rev. Lett.*, vol. 28, pp. 1082–1085, Apr 1972.

[74] G. W. Gibbons and S. W. Hawking, "Action integrals and partition functions in quantum gravity," *Phys. Rev. D*, vol. 15, pp. 2752–2756, May 1977.

[75] S. Weinberg, *The quantum theory of fields. Vol. 2: Modern applications*. Cambridge University Press, 8 2013.

[76] J. D. Bekenstein, "Black holes and entropy," *Phys. Rev. D*, vol. 7, pp. 2333–2346, Apr 1973.

[77] S. W. Hawking, "Particle creation by black holes," *Communications in Mathematical Physics*, vol. 43, pp. 199–220, Aug 1975.

[78] T. Jacobson and R. C. Myers, "Black hole entropy and higher curvature interactions," *Phys. Rev. Lett.*, vol. 70, pp. 3684–3687, Jun 1993.

[79] T. Jacobson, G. Kang, and R. C. Myers, "On black hole entropy," *Phys. Rev. D*, vol. 49, pp. 6587–6598, Jun 1994.

[80] G. C. Psaltakis, *Quantum Many-Particle Systems*. Crete University Press, 2008.

[81] D. T. Son and A. O. Starinets, "Minkowski space correlators in AdS / CFT correspondence: Recipe and applications," *JHEP*, vol. 09, p. 042, 2002.

[82] N. Iqbal and H. Liu, "Real-time response in AdS/CFT with application to spinors," *Fortsch. Phys.*, vol. 57, pp. 367–384, 2009.

[83] A. Kamenev, *Field Theory of Non-Equilibrium Systems*. Cambridge University Press, 2011.

[84] J. S. Schwinger, "Brownian motion of a quantum oscillator," *J. Math. Phys.*, vol. 2, pp. 407–432, 1961.

[85] L. V. Keldysh, "Diagram technique for nonequilibrium processes," *Zh. Eksp. Teor. Fiz.*, vol. 47, pp. 1515–1527, 1964. [Sov. Phys. JETP20,1018(1965)].

[86] C. P. Herzog and D. T. Son, "Schwinger-Keldysh propagators from AdS/CFT correspondence," *JHEP*, vol. 03, p. 046, 2003.

[87] D. Marolf, "States and boundary terms: Subtleties of Lorentzian AdS / CFT," *JHEP*, vol. 05, p. 042, 2005.

[88] K. Skenderis and B. C. van Rees, "Real-time gauge/gravity duality," *Phys. Rev. Lett.*, vol. 101, p. 081601, 2008.

[89] K. Skenderis and B. C. van Rees, "Real-time gauge/gravity duality: Prescription, Renormalization and Examples," *JHEP*, vol. 05, p. 085, 2009.

[90] E. Barnes, D. Vaman, C. Wu, and P. Arnold, "Real-time finite-temperature correlators from AdS/CFT," *Phys. Rev. D*, vol. 82, p. 025019, 2010.

[91] N. Iqbal and H. Liu, "Universality of the hydrodynamic limit in AdS/CFT and the membrane paradigm," *Phys. Rev. D*, vol. 79, p. 025023, 2009.

[92] N. Itzhaki, J. M. Maldacena, J. Sonnenschein, and S. Yankielowicz, "Supergravity and the large N limit of theories with sixteen supercharges," *Phys. Rev. D*, vol. 58, p. 046004, 1998.

[93] S. Cremonini, "The Shear Viscosity to Entropy Ratio: A Status Report," *Mod. Phys. Lett. B*, vol. 25, pp. 1867–1888, 2011.

[94] R. C. Myers, M. F. Paulos, and A. Sinha, "Holographic Hydrodynamics with a Chemical Potential," *JHEP*, vol. 06, p. 006, 2009.

[95] R. P. Woodard, "Avoiding dark energy with 1/r modifications of gravity," *Lect. Notes Phys.*, vol. 720, pp. 403–433, 2007.

[96] R. P. Woodard, "Ostrogradsky's theorem on Hamiltonian instability," *Scholarpedia*, vol. 10, no. 8, p. 32243, 2015.

[97] M. Brigante, H. Liu, R. C. Myers, S. Shenker, and S. Yaida, "Viscosity Bound Violation in Higher Derivative Gravity," *Phys. Rev. D*, vol. 77, p. 126006, 2008.

[98] A. Buchel, R. C. Myers, and A. Sinha, "Beyond eta/s = 1/4 pi," *JHEP*, vol. 03, p. 084, 2009.

[99] Y. Kats and P. Petrov, "Effect of curvature squared corrections in AdS on the viscosity of the dual gauge theory," *JHEP*, vol. 01, p. 044, 2009.

[100] X. O. Camanho, J. D. Edelstein, J. Maldacena, and A. Zhiboedov, "Causality constraints on corrections to the graviton three-point coupling," *Journal of High Energy Physics*, vol. 2016, p. 20, Feb 2016.

[101] S. Aaronson and J. Watrous, "Closed timelike curves make quantum and classical computing equivalent," *Proceedings of the Royal Society A: Mathematical, Physical and Engineering Sciences*, vol. 465, p. 631–647, Nov 2008.

[102] R. Metsaev and A. Tseytlin, "Curvature cubed terms in string theory effective actions," *Physics Letters B*, vol. 185, no. 1, pp. 52–58, 1987.

[103] A. Buchel, J. T. Liu, and A. O. Starinets, "Coupling constant dependence of the shear viscosity in n=4 supersymmetric yang–mills theory," *Nuclear Physics B*, vol. 707, no. 1, pp. 56–68, 2005.

[104] P. Benincasa and A. Buchel, "Transport properties of N=4 supersymmetric Yang-Mills theory at finite coupling," *JHEP*, vol. 01, p. 103, 2006.

[105] K. Jensen, M. Kaminski, P. Kovtun, R. Meyer, A. Ritz, and A. Yarom, "Towards hydrodynamics without an entropy current," *Phys. Rev. Lett.*, vol. 109, p. 101601, 2012.

[106] N. Banerjee, J. Bhattacharya, S. Bhattacharyya, S. Jain, S. Minwalla, and T. Sharma, "Constraints on fluid dynamics from equilibrium partition functions," *Journal of High Energy Physics*, vol. 2012, Sep 2012.

[107] J. Bhattacharya, S. Bhattacharyya, and M. Rangamani, "Non-dissipative hydrodynamics: Effective actions versus entropy current," *JHEP*, vol. 02, p. 153, 2013.

[108] S. Bhattacharyya, S. Jain, S. Minwalla, and T. Sharma, "Constraints on Superfluid Hydrodynamics from Equilibrium Partition Functions," *JHEP*, vol. 01, p. 040, 2013.

[109] E. Gourgoulhon, "3+1 formalism and bases of numerical relativity," 3 2007.

[110] L. Landau and E. Lifshitz, *Statistical Physics: Volume 5*. No. τ. 5, Elsevier Science, 2013.

[111] K. Jensen, R. Loganayagam, and A. Yarom, "Anomaly inflow and thermal equilibrium," *Journal of High Energy Physics*, vol. 2014, May 2014.

[112] R. A. Bertlmann, *Anomalies in quantum field theory*. Oxford University Press, 1996.

[113] A. A. Petrov and A. E. Blechman, *Effective Field Theories*. WORLD SCIENTIFIC, 2016.

[114] H. Liu and P. Glorioso, "Lectures on non-equilibrium effective field theories and fluctuating hydrodynamics," *PoS*, vol. TASI2017, p. 008, 2018.

[115] R. Feynman and F. Vernon, "The theory of a general quantum system interacting with a linear dissipative system," *Annals of Physics*, vol. 24, pp. 118–173, 1963.

[116] S. R. Coleman, J. Wess, and B. Zumino, "Structure of phenomenological Lagrangians. 1.," *Phys. Rev.*, vol. 177, pp. 2239–2247, 1969.

[117] C. G. Callan, Jr., S. R. Coleman, J. Wess, and B. Zumino, "Structure of phenomenological Lagrangians. 2.," *Phys. Rev.*, vol. 177, pp. 2247–2250, 1969.

[118] M. J. Landry, "The coset construction for non-equilibrium systems," *JHEP*, vol. 07, p. 200, 2020.

[119] L. D. Landau and E. M. Lifshitz, *Fluid Mechanics, Second Edition: Volume 6 (Course of Theoretical Physics)*. Course of theoretical physics / by L. D. Landau and E. M. Lifshitz, Vol. 6, Butterworth-Heinemann, 2 ed., 1987.

[120] P. Kovtun, "Lectures on hydrodynamic fluctuations in relativistic theories," *J. Phys. A*, vol. 45, p. 473001, 2012.

[121] C. Eckart, "The thermodynamics of irreversible processes. iii. relativistic theory of the simple fluid," *Phys. Rev.*, vol. 58, pp. 919–924, Nov 1940.

[122] S. Weinberg, *Gravitation and Cosmology: Principles and Applications of the General Theory of Relativity*. New York, NY: Wiley, 1972.

[123] F. S. Bemfica, M. M. Disconzi, and J. Noronha, "Causality and existence of solutions of relativistic viscous fluid dynamics with gravity," *Phys. Rev. D*, vol. 98, no. 10, p. 104064, 2018.

[124] P. Kovtun, "First-order relativistic hydrodynamics is stable," *JHEP*, vol. 10, p. 034, 2019.

[125] N. Poovuttikul and W. Sybesma, "First order non-Lorentzian fluids, entropy production and linear instabilities," *Phys. Rev. D*, vol. 102, no. 6, p. 065007, 2020.

[126] W. Israel, "Nonstationary irreversible thermodynamics: A causal relativistic theory," *Annals of Physics*, vol. 100, no. 1, pp. 310–331, 1976.

[127] W. Israel and J. Stewart, "Transient relativistic thermodynamics and kinetic theory," *Annals of Physics*, vol. 118, no. 2, pp. 341–372, 1979.

[128] W. A. Hiscock and L. Lindblom, "Generic instabilities in first-order dissipative relativistic fluid theories," *Phys. Rev. D*, vol. 31, pp. 725–733, Feb 1985.

[129] D. Gallegos, U. Gursoy, and A. Yarom, "Hydrodynamics of spin currents," 2021.

[130] G. Rizzi and M. L. Ruggiero, eds., *Relativity in Rotating Frames*. Springer Netherlands, 2004.

[131] R. D. Klauber, "Relativistic rotation: A comparison of theories," *Foundations of Physics*, vol. 37, p. 198–252, Feb 2007.

[132] F. M. Haehl, R. Loganayagam, and M. Rangamani, "Schwinger-Keldysh formalism. Part I: BRST symmetries and superspace," *JHEP*, vol. 06, p. 069, 2017.

[133] F. M. Haehl, R. Loganayagam, and M. Rangamani, "Schwinger-Keldysh formalism. Part II: thermal equivariant cohomology," *JHEP*, vol. 06, p. 070, 2017.

[134] K. Jensen, R. Marjieh, N. Pinzani-Fokeeva, and A. Yarom, "A panoply of Schwinger-Keldysh transport," *SciPost Phys.*, vol. 5, no. 5, p. 053, 2018.

[135] F. M. Haehl, R. Loganayagam, and M. Rangamani, "Effective Action for Relativistic Hydrodynamics: Fluctuations, Dissipation, and Entropy Inflow," *JHEP*, vol. 10, p. 194, 2018.

[136] L. P. Kadanoff and P. C. Martin, "Hydrodynamic equations and correlation functions," *Annals of Physics*, vol. 24, pp. 419–469, 1963.

[137] G. D. Moore and K. A. Sohrabi, "Kubo formulas for second-order hydrodynamic coefficients," *Physical Review Letters*, vol. 106, Mar 2011.

[138] C. P. Herzog, "Lectures on holographic superfluidity and superconductivity," *Journal of Physics A: Mathematical and Theoretical*, vol. 42, p. 343001, Aug 2009.

[139] L. V. Delacretaz, "Heavy Operators and Hydrodynamic Tails," *SciPost Phys.*, vol. 9, no. 3, p. 034, 2020.

[140] A. Jain and P. Kovtun, "Non-universality of hydrodynamics," 9 2020.

[141] W. K. George, "Lectures in turbulence for the 21st century," 2013.

[142] N. Flytzanis, *Introduction to fluid mechanics*. Kallipos Publications, 2015.

[143] G. G. Stokes, "On the Effect of the Internal Friction of Fluids on the Motion of Pendulums," *Transactions of the Cambridge Philosophical Society*, vol. 9, p. 8, Jan. 1851.

[144] O. Reynolds, "Xxix. an experimental investigation of the circumstances which determine whether the motion of water shall be direct or sinuous, and of the law of resistance in parallel channels," *Philosophical Transactions of the Royal Society of London*, vol. 174, pp. 935–982, 1883.

[145] J. D. Jackson, *Classical electrodynamics; 2nd ed.* New York, NY: Wiley, 1975.

[146] T. Andrade and B. Withers, "A simple holographic model of momentum relaxation," *Journal of High Energy Physics*, vol. 2014, May 2014.

[147] S. A. Hartnoll and C. P. Herzog, "Ohm's law at strong coupling:sduality and the cyclotron resonance," *Physical Review D*, vol. 76, Nov 2007.

[148] S. A. Hartnoll, P. K. Kovtun, M. Müller, and S. Sachdev, "Theory of the nernst effect near quantum phase transitions in condensed matter and in dyonic black holes," *Physical Review B*, vol. 76, Oct 2007.

[149] C. P. Herzog, P. Kovtun, S. Sachdev, and D. T. Son, "Quantum critical transport, duality, and m theory," *Physical Review D*, vol. 75, Apr 2007.

[150] C. Brüne, C. Thienel, M. Stuiber, J. Böttcher, H. Buhmann, E. G. Novik, C.-X. Liu, E. M. Hankiewicz, and L. W. Molenkamp, "Dirac-screening stabilized surface-state transport in a topological insulator," *Phys. Rev. X*, vol. 4, p. 041045, Dec 2014.

[151] M. Mendoza, H. J. Herrmann, and S. Succi, "Preturbulent regimes in graphene flow," *Phys. Rev. Lett.*, vol. 106, p. 156601, Apr 2011.

[152] L. Fritz, J. Schmalian, M. Müller, and S. Sachdev, "Quantum critical transport in clean graphene," *Phys. Rev. B*, vol. 78, p. 085416, Aug 2008.

[153] I. Syôzi, "Statistics of Kagomé Lattice," *Progress of Theoretical Physics*, vol. 6, pp. 306–308, 06 1951.

[154] M. Mekata, "Kagome: The story of the basketweave lattice," *Physics Today*, vol. 56, no. 2, pp. 12–13, 2003.

[155] C. H. Redder and G. S. Uhrig, "Topologically nontrivial hofstadter bands on the kagome lattice," *Phys. Rev. A*, vol. 93, p. 033654, Mar 2016.

[156] J. Zak, "Topologically unavoidable points and lines of crossings in the band structure of solids," *Journal of Physics A: Mathematical and General*, vol. 35, pp. 6509–6516, jul 2002.

[157] M. L. Kiesel, C. Platt, and R. Thomale, "Unconventional fermi surface instabilities in the kagome hubbard model," *Phys. Rev. Lett.*, vol. 110, p. 126405, Mar 2013.

[158] M. Indergand, A. Läuchli, S. Capponi, and M. Sigrist, "Modeling bond-order wave instabilities in doped frustrated antiferromagnets: Valence bond solids at fractional filling," *Phys. Rev. B*, vol. 74, p. 064429, Aug 2006.

[159] M. L. Kiesel and R. Thomale, "Sublattice interference in the kagome hubbard model," *Phys. Rev. B*, vol. 86, p. 121105, Sep 2012.

[160] I. I. Mazin, H. O. Jeschke, F. Lechermann, H. Lee, M. Fink, R. Thomale, and R. Valentí, "Theoretical prediction of a strongly correlated dirac metal," *Nature Communications*, vol. 5, p. 4261, Jul 2014.

[161] R. C. Myers, M. F. Paulos, and A. Sinha, "Holographic hydrodynamics with a chemical potential," *Journal of High Energy Physics*, vol. 2009, pp. 006–006, jun 2009.

[162] L. S. Tuckerman, M. Chantry, and D. Barkley, "Patterns in wall-bounded shear flows," in *Annual review of fluid mechanics. Vol. 52*, pp. 343–367, Palo Alto, CA: Annual Reviews, 2020.

[163] A. Gabbana, M. Polini, S. Succi, R. Tripiccione, and F. M. D. Pellegrino, "Prospects for the detection of electronic preturbulence in graphene," *Phys. Rev. Lett.*, vol. 121, p. 236602, Dec 2018.

[164] P. S. Alekseev, "Negative magnetoresistance in viscous flow of two-dimensional electrons," *Phys. Rev. Lett.*, vol. 117, p. 166601, Oct 2016.

[165] T. Scaffidi, N. Nandi, B. Schmidt, A. P. Mackenzie, and J. E. Moore, "Hydrodynamic electron flow and hall viscosity," *Phys. Rev. Lett.*, vol. 118, p. 226601, Jun 2017.

[166] E. I. Kiselev and J. Schmalian, "Boundary conditions of viscous electron flow," *Phys. Rev. B*, vol. 99, p. 035430, Jan 2019.

[167] R. Moessner, N. Morales-Durán, P. Surówka, and P. Witkowski, "Boundary-condition and geometry engineering in electronic hydrodynamics," *Phys. Rev. B*, vol. 100, p. 155115, Oct 2019.

[168] G. F. Giuliani and J. J. Quinn, "Lifetime of a quasiparticle in a two-dimensional electron gas," *Phys. Rev. B*, vol. 26, pp. 4421–4428, Oct 1982.

[169] Z. Qian and G. Vignale, "Lifetime of a quasiparticle in an electron liquid," *Phys. Rev. B*, vol. 71, p. 075112, Feb 2005.

[170] D. S. Novikov, "Viscosity of a two-dimensional Fermi liquid," *arXiv e-prints*, pp. cond–mat/0603184, Mar. 2006.

[171] G. Czycholl, *Theoretische Festkörperphysik Band 1*. Springer Berlin Heidelberg, 2016.

[172] A. D. Gallegos, U. Gürsoy, and A. Yarom, "Hydrodynamics of spin currents," 1 2021.

[173] S. A. Fulling, "Nonuniqueness of canonical field quantization in riemannian space-time," *Phys. Rev. D*, vol. 7, pp. 2850–2862, May 1973.

[174] P. C. W. Davies, "Scalar production in schwarzschild and rindler metrics," *Journal of Physics A: Mathematical and General*, vol. 8, pp. 609–616, apr 1975.

[175] W. G. Unruh, "Notes on black-hole evaporation," *Phys. Rev. D*, vol. 14, pp. 870–892, Aug 1976.

[176] J. I. Korsbakken and J. M. Leinaas, "Fulling-unruh effect in general stationary accelerated frames," *Phys. Rev. D*, vol. 70, p. 084016, Oct 2004.

[177] P. C. W. Davies, T. Dray, and C. A. Manogue, "The Rotating quantum vacuum," *Phys. Rev. D*, vol. 53, pp. 4382–4387, 1996.

[178] S. Weinberg, *The Quantum theory of fields. Vol. 1: Foundations*. Cambridge University Press, 6 2005.

[179] S. Floerchinger and E. Grossi, "Conserved and non-conserved noether currents from the quantum effective action," 2021.

[180] A. Trautman, "Einstein-Cartan theory," 6 2006.

[181] F. W. Hehl, P. von der Heyde, G. D. Kerlick, and J. M. Nester, "General relativity with spin and torsion: Foundations and prospects," *Rev. Mod. Phys.*, vol. 48, pp. 393–416, Jul 1976.

[182] B. O'Neill, *Elementary Differential Geometry*. Academic Press, 2nd ed., 2006.

[183] F. W. Hehl, J. McCrea, E. W. Mielke, and Y. Ne'eman, "Metric-affine gauge theory of gravity: field equations, noether identities, world spinors, and breaking of dilation invariance," *Physics Reports*, vol. 258, no. 1, pp. 1–171, 1995.

[184] J. E. Hirsch, "Spin hall effect," *Phys. Rev. Lett.*, vol. 83, pp. 1834–1837, Aug 1999.

[185] S. D. Brechet, M. P. Hobson, and A. N. Lasenby, "Weyssenhoff fluid dynamics in general relativity using a 1 + 3 covariant approach," *Classical and Quantum Gravity*, vol. 24, p. 6329–6348, Nov 2007.

[186] D. A. Roberts, "Why is AI hard and Physics simple?," 3 2021.

[187] G. T. Horowitz, "Exactly soluble diffeomorphism invariant theories," *Communications in Mathematical Physics*, vol. 125, no. 3, pp. 417 – 437, 1989.

[188] B. Hess, "Fluid/gravity correspondence for post-riemannian spacetimes: Metric-affine black holes for hydrodynamics," Master's thesis, Julius-Maximilians-Universität Würzburg, 2020.

[189] T. Holder, R. Queiroz, and A. Stern, "Unified description of the classical hall viscosity," *Phys. Rev. Lett.*, vol. 123, p. 106801, Sep 2019.

[190] A. v. Ettingshausen and W. Nernst, "Ueber das auftreten electromotorischer kräfte in metallplatten, welche von einem wärmestrome durchflossen werden und sich im magnetischen felde befinden," *Annalen der Physik*, vol. 265, no. 10, pp. 343–347, 1886.

[191] M. Fuchs, P. Liu, T. Schwemmer, G. Sangiovanni, R. Thomale, C. Franchini, and D. D. Sante, "Kagome metal-organic frameworks as a platform for strongly correlated electrons," *Journal of Physics: Materials*, vol. 3, p. 025001, feb 2020.

[192] A. Adams, P. M. Chesler, and H. Liu, "Holographic turbulence," *Phys. Rev. Lett.*, vol. 112, p. 151602, Apr 2014.

[193] T. Andrade, C. Pantelidou, J. Sonner, and B. Withers, "Driven black holes: from Kolmogorov scaling to turbulent wakes," 11 2019.

[194] S. Waeber and A. Yarom, "Stochastic gravity and turbulence," 5 2021.

[195] G.-Y. Qin and X.-N. Wang, "Jet quenching in high-energy heavy-ion collisions," *Int. J. Mod. Phys. E*, vol. 24, no. 11, p. 1530014, 2015.

[196] H. Liu, K. Rajagopal, and U. A. Wiedemann, "Calculating the jet quenching parameter from AdS/CFT," *Phys. Rev. Lett.*, vol. 97, p. 182301, 2006.

[197] S. S. Gubser, "Drag force in ads/cft," *Physical Review D*, vol. 74, Dec 2006.

[198] M. Nakahara, *Geometry, topology and physics. 2nd ed.* Bristol: Institute of Physics (IOP), 2nd ed. ed., 2003.

[199] E. Witten, "(2+1)-Dimensional Gravity as an Exactly Soluble System," *Nucl. Phys. B*, vol. 311, p. 46, 1988.

[200] E. Witten, "Three-Dimensional Gravity Revisited," 6 2007.

[201] M. P. Blencowe, "A consistent interacting massless higher-spin field theory in d=2+1," *Classical and Quantum Gravity*, vol. 6, pp. 443–452, apr 1989.

[202] H. F. Westman and T. G. Zlosnik, "Gravity, Cartan geometry, and idealized waywisers," 3 2012.

[203] H. F. Westman and T. G. Zlosnik, "Cartan gravity, matter fields, and the gauge principle," *Annals Phys.*, vol. 334, pp. 157–197, 2013.

[204] V. E. Hubeny, S. Minwalla, and M. Rangamani, "The fluid/gravity correspondence," in *Theoretical Advanced Study Institute in Elementary Particle Physics: String theory and its Applications: From meV to the Planck Scale*, 7 2011.

[205] F. W. Hehl and A. Macias, "Metric affine gauge theory of gravity. 2. Exact solutions," *Int. J. Mod. Phys. D*, vol. 8, pp. 399–416, 1999.

[206] M. Alfredo and S. José, "Generalized reissner-nordström solution in metric-affine gravity," *Classical and Quantum Gravity*, vol. 16, pp. 2323–2333, jan 1999.

[207] K. Skenderis, "Lecture notes on holographic renormalization," *Class. Quant. Grav.*, vol. 19, pp. 5849–5876, 2002.

[208] H. Nieh and M. Yan, "Quantized dirac field in curved riemann-cartan background. i. symmetry properties, green's function," *Annals of Physics*, vol. 138, no. 2, pp. 237–259, 1982.

[209] H. T. Nieh and M. L. Yan, "An identity in riemann–cartan geometry," *Journal of Mathematical Physics*, vol. 23, no. 3, pp. 373–374, 1982.

[210] O. Parrikar, T. L. Hughes, and R. G. Leigh, "Torsion, Parity-odd Response and Anomalies in Topological States," *Phys. Rev. D*, vol. 90, no. 10, p. 105004, 2014.

[211] J. Nissinen and G. E. Volovik, "Thermal Nieh-Yan anomaly in Weyl superfluids," *Phys. Rev. Res.*, vol. 2, no. 3, p. 033269, 2020.

[212] Z.-M. Huang, B. Han, and M. Stone, "Nieh-yan anomaly: Torsional landau levels, central charge, and anomalous thermal hall effect," *Phys. Rev. B*, vol. 101, p. 125201, Mar 2020.

[213] D. K. Wise, "MacDowell-Mansouri gravity and Cartan geometry," *Class. Quant. Grav.*, vol. 27, p. 155010, 2010.

[214] S. Weinberg, "The cosmological constant problem," *Rev. Mod. Phys.*, vol. 61, pp. 1–23, Jan 1989.